CHEMICAL AND ELECTROCHEMICAL STUDIES OF BORANE ANIONS AND METALLABORANES

by

DOMINIC G. MEINA B.Sc.

Thesis submitted to the Department of Pure and Applied Chemistry, University of Strathclyde, in part fulfilment of the requirements for the Degree of Doctor of Philosophy

May, 1985.

TO MY WIFE AND FAMILY

ACKNOWLEDGEMENTS

The author would like to express his sincerest gratitude to his supervisor, Dr. J.H. Morris, whose constant enthusiastic help, guidance and encouragement was an inspiration throughout. He would also like to thank Dr. D. Reed, of the University of Edinburgh, for running n.m.r. spectra and for many helpful discussions.

Thanks are also due to Miss A. Drummond for assistance throughout the course of this work.

In addition, thanks are due to Mrs. J. Mitchell for typing. Finally, financial support by the S.E.R.C. is gratefully acknowledged.

Abstract

Several new monosubstituted anionic derivatives of $[B_3H_8]^-$ of the type $[B_3H_7(X)]^-$(X = NCSe, $NCBPh_3$, $NCBH_2NCBH_3$, NCB_3H_7, $NCBH_2CN$ and $NCBH_2CNB_3H_7$) have been prepared. The disubstituted anions $[B_3H_6(Cl)(X)]^-$(X = $NCBH_2NCBH_3$, $NCBH_2CN$ and NCB_3H_7) and $[B_3H_6(Br)NCB_3H_6(Br)]^-$ have also been prepared and studied by various spectroscopic techniques. Two-dimensional n.m.r. spectroscopy was shown to be useful in the qualitative determination of the bonding employed in these anions.

The electrochemical properties of these anions have been investigated by various techniques. It was found that when the substituent was varied the oxidative stability of the anions varied. Metallaboranes of some of these anions have been prepared by anodic dissolution of a suitable metal in a solution of the anion.

The structures and dynamics of substituted derivatives of the $[B_9H_{14}]^-$ ion have been studied. The anions $[B_9H_{13}(X)]^-$(X = Cl,NCSe,$NCBPh_3$, $NCBH_2NCBH_3$, $NCBH_2CN$, $NCBH_2CNB_9H_{13}$, CN, and $NCAgCNB_9H_{13}$) and $[B_9H_{12}(CN)_2]^-$ have been prepared. ^{11}B and ^1H n.m.r. spectroscopy indicated that when the substituent contained electron withdrawing groups (e.g. the hydrogen atoms on $NCBH_2NCBH_3$) the anion was static at room temperature on the n.m.r. time scale. If no electron withdrawing groups were present on the substituent then the molecule was fluxional at room temperature on the n.m.r. time scale.

The electrochemistry of these anions was also studied and it was found that, in some cases, oxidation resulted in cage closure to give substituted nido-derivatives. Anodic dissolution of Cu or Ag in solutions of some of the anions produced metallaboranes.

The chemistry and electrochemistry of $[B_9H_{12}]^-$ was also studied and the crystal structure of the $[N(PPh_3)_2]^+$ salt was obtained.

Several new substituted metallaboranes have been prepared by reaction of the substituted octahydrotriborate (1-) or substituted tetradecahydro-nonaborate (1-) anions with $Cu(PPh_3)_2(BH_4)$. The reactions of $Mn(CO)_5Br$ with $[B_9H_{13}(X)]^-$(X = NCSe, $NCBH_2NCBH_3$ and $NCBPh_3$) have also been investigated.

CONTENTS

Correction: MH_z should read MHz throughout.

F I G U R E S

TABLES

CHAPTER ONE

INTRODUCTORY SURVEY

1.1 Introduction

In this chapter the general chemistry of the octahydrotriborate (1-) ion, $[B_3H_8]^-$, the tetradecahydrononaborate (1-) ion, $[B_9H_{14}]^-$, and the tri-μ-hydro-nonahydro-nido-nonaborate (1-) ion, $[B_9H_{12}]^-$, and their derivatives are surveyed. This review is limited to general chemical, physical and spectroscopic properties, with emphasis on areas which are important with respect to subsequent work described in later chapters. In addition, the electrochemical and nuclear magnetic resonance (n.m.r.) of these derivatives are also reviewed, but are limited to studies of boranes, borane anions and metallaboranes and neglect carbaboranes and metallacarbaboranes.

1.2 The Octahydrotriborate (1-) ion, $[B_3H_8]^-$, and Related Compounds

1.2.1 Introduction

The arachno-octahydrotriborate (1-) ion, $[B_3H_8]^-$, has been shown to be a useful precursor in the synthesis of higher boranes,[1] polyhedral borane anions[2] and transition metal complexes.[3] In this section the preparation, structure and reactions of the $[B_3H_8]^-$ ion and its derivatives are reviewed.

1.2.2 Preparations

(a) Condensation of Smaller Species

Originally $Na[B_3H_8]$ was prepared in 80% yield by the reaction of diborane and sodium amalgam in an ethereal medium.[4]

$$2Na(amalgam) + 2B_2H_6 \rightarrow Na[B_3H_8] + NaBH_4 \qquad (1\text{-}1)$$

A large scale preparation of $Na[B_3H_8]$ has been developed[5] from the reaction of $NaBH_4$ with I_2 in diglyme at 100°C

$$3NaBH_4 + I_2 \rightarrow Na[B_3H_8] + 2H_2 + 2NaI \qquad (1\text{-}2)$$

The reaction of B_2H_6 with $NaBH_4$ in diglyme at 200°C[6,7] and reactions (1-3) and (1-4) in diglyme[6,8] have also been used for the large scale preparation of $Na[B_3H_8]$.

$$7NaBH_4 + 4BF_3 \rightarrow 3NaBF_4 + 4Na[B_2H_7] \qquad (1\text{-}3)$$

$$2Na[B_2H_7] \xrightarrow{100°C} NaBH_4 + Na[B_3H_8] + H_2 \qquad (1\text{-}4)$$

The sodium salt $Na[B_2H_7]$ is so strongly solvated by diglyme that it cannot be isolated free of the solvent[9] in which it slowly decomposes to $[B_3H_8]^-$ and $[BH_4]^-$ at room temperature.[10]

(b) Cleavage of Tetraborane (10)

The $[B_3H_8]^-$ ion can be considered as a fragment of tetraborane (10) with one vertex removed and, indeed, may be prepared by unsymmetrical cleavage of B_4H_{10} by ammonia[11]

$$B_4H_{10} + 2NH_3 \longrightarrow [(H_3N)_2BH_2][B_3H_8] \qquad (1\text{-}5)$$

Tetraborane also yields $[B_3H_8]^-$ in the following reactions;[12]

$$B_4H_{10} + NaH \xrightarrow{ether} Na[B_3H_8] + 1/2B_2H_6 \qquad (1\text{-}6)$$

$$B_4H_{10} + NaBH_4 \rightarrow Na[B_3H_8] + B_2H_6 \qquad (1\text{-}7)$$

(c) Cleavage/Degradation of Higher Boranes

The methanolysis of $B_{10}H_{12}(SEt_2)_2$[13] and B_5H_9[14] both yield the $[B_3H_8]^-$ ion.

$$B_5H_9 + 6CH_3OH + [N(CH_3)_4][OH] \longrightarrow$$
$$[N(CH_3)_4][B_3H_8] + 2B(OCH_3)_3 + 3H_2 + H_2O \qquad (1\text{-}8)$$

(d) Various Salts by Metathesis

The tetramethylammonium salt, $[N(CH_3)_4][B_3H_8]$, has been prepared by the metathesis of $Na[B_3H_8]$ and $[N(CH_3)_4][OH]$.[5] Similarly salts of the large cations tetra-n-butylammonium and μ-nitrido-bis[triphenyl-phosphorus] have been prepared.[5] The cesium salt, $Cs[B_3H_8]$, has also been obtained from the reaction.

$$CsBr + Na[B_3H_8].3(C_4H_8O_2) \rightarrow NaBr + Cs[B_3H_8] + 2C_4H_8O_2 \qquad (1\text{-}9)$$

1.2.3 Structure and Dynamics

(b) X-ray Structure

An X-ray crystallographic study carried out by Peters and Nordmann[15] on $[(H_3N)_2BH_2][B_3H_8]$ has shown the $[B_3H_8]^-$ ion to have a 2013 styx[16] structure as in (I).

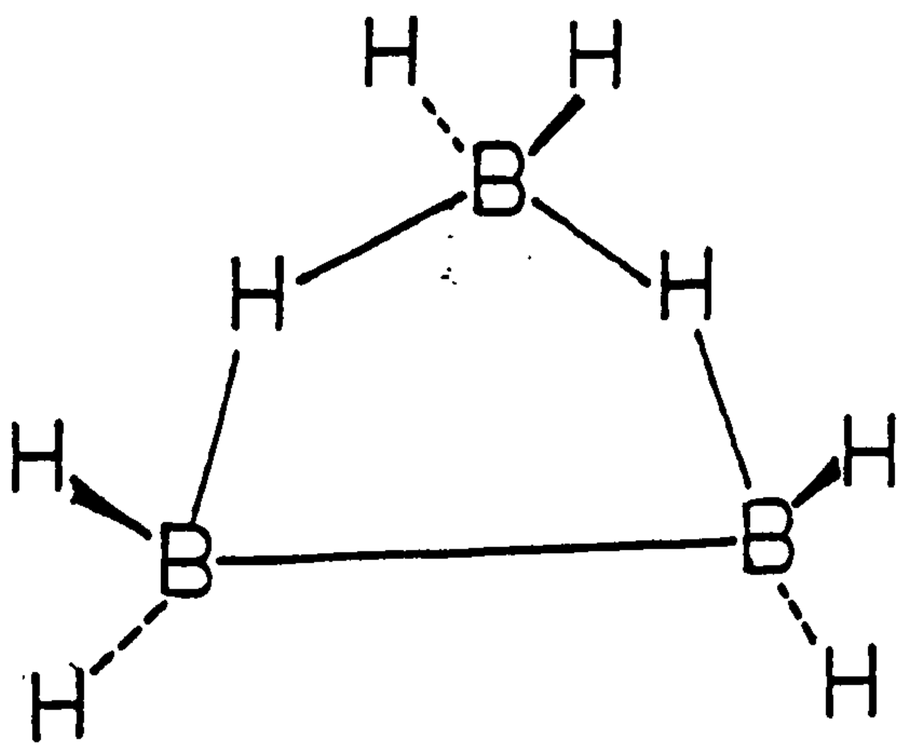

I

(b) Nuclear Magnetic Resonance Studies

Nuclear magnetic resonance studies[17] have shown that in solution a species of higher symmetry than (I) exists on the n.m.r. time scale All eight hydrogen atoms are rapidly undergoing intramolecular hydrogen exchange so that they spin couple equally to all three boron atoms; this results in a nonet being observed in the ^{11}B n.m.r. spectrum and a complex decet in the ^{1}H n.m.r. spectrum..

Studies of various $[B_3H_8]^-$ salts revealed changes in the ^{1}H n.m.r. spectrum consistent with both quadrupole-induced spin decoupling and variable rates of $[B_3H_8]^-$ internal exchange depending on structure. Upon lowering the temperature of $Tl[B_3H_8]$ in a 50% CD_3OD - 50% CD_3COCD_3 (V/V) to -127°C the ten line multiplet ($J_{^{1}H-^{11}B}$ = 33Hz) coalesced and the ^{1}H n.m.r. spectrum sharpened into a singlet resonance.[17(e),(f)] The loss of ^{10}B, ^{11}B — ^{1}H spin-spin coupling at lower temperatures is consistent with more efficient boron quadrupolar relaxation effectively decoupling boron from hydrogen. The singlet proton resonance which appears at low temperatures is best rationalized on the basis of fast $[B_3H_8]^-$ scrambling or "pseudorotation".

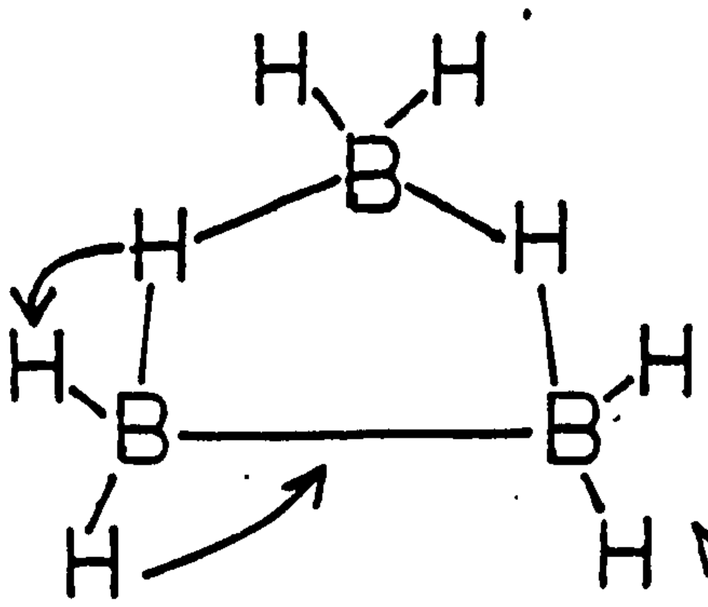

II

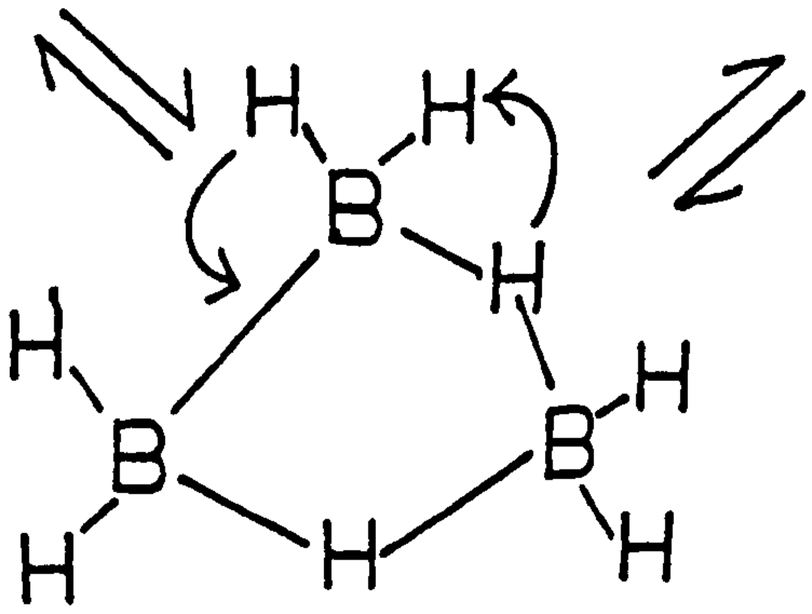

III

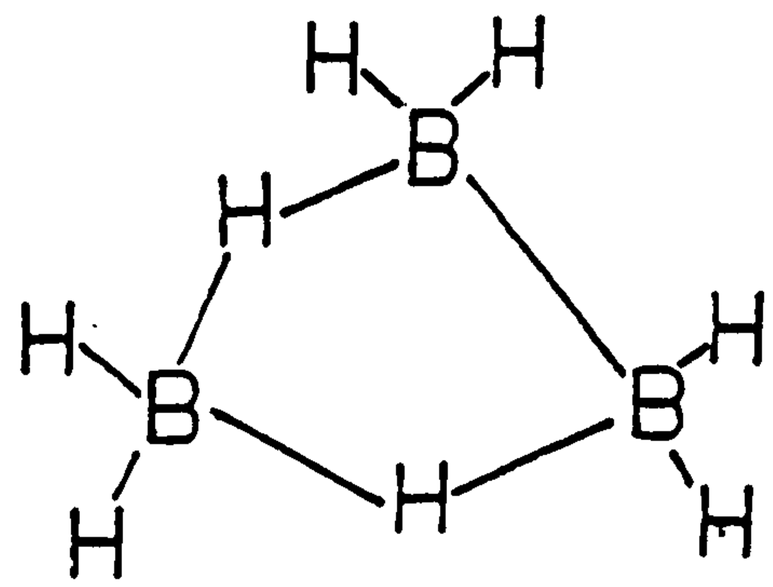

IV

1.2.4 Chemical Properties

(a) Stability

The relative stability of salts of the $[B_3H_8]^-$ ion are dependent on the nature of the cation and the degree of solvation. In contrast to $Na[B_3H_8]$ the tetramethylammonium salt, $[N(CH_3)_4]$ $[B_3H_8]$ is not strongly solvated by glycol ethers.[5] The sodium salt is stable to at least 200°C[4(a)] when freed of solvent while the tetramethylammonium salt is stable to at least 275°C[13] in an inert atmosphere.

(b) Preparation of Base Adducts of Triborane (7)

(i) Cleavage of Tetraborane (10)

A large number of neutral substituted derivatives of the $[B_3H_8]^-$ ion of the type B_3H_7L are known. The $[B_3H_7]$ moiety can be considered to be a relatively strong Lewis acid and therefore many adducts are formed with Lewis bases. Many molecular fragments of the type B_3H_7L have been prepared by the symmetrical bridge hydrogen cleavage of B_4H_{10} with a Lewis base. Common Lewis base donor atoms are N, O, P and S.[18]

$$B_4H_{10} + 2L \rightarrow B_3H_7L + BH_3L \qquad (1\text{-}10)$$

where L = $N(CH_3)_3$ [18(c),(d),(e)], Py [18(c)(d)(e)], $PF_2N(CH_3)_2$ [19,20]

Since the $[B_3H_7]$ moiety is a stronger Lewis acid than the $[BH_3]$ moiety[18(3),21] Lewis bases which contain oxygen or sulphur as the donor atom form such weak adducts with $[BH_3]$ that B_2H_6 can be pumped from the system leaving behind B_3H_7L.[18,22]

$$B_4H_{10} + L \rightarrow B_3H_7L + 1/2B_2H_6 \qquad (1\text{-}11)$$

where L = $(CH_3)_2O$[22(a)], T.H.F.,[18] diglyme[22(b)], Me_2S[18]

(ii) Ligand Substitution

Base displacement reactions where a more basic substituent is used to displace a weaker base have proved useful for the preparation of certain adducts of $[B_3H_7]$[18,19,23,24].

$$B_3H_7[THF] + P(C_6H_5)_3 \rightarrow B_3H_7[P(C_6H_5)_3] + T.H.F. \qquad (1\text{-}12)$$

$$B_3H_7[THP] + NH_3 \rightarrow B_3H_7[NH_3] + THP \qquad (1\text{-}13)$$

where THP = tetrahydropyran.

Ammonia triborane has been prepared in 75% yield in this way.[24(a)]

Attempts to cleave B_4H_{10} symmetrically with CO and PF_3 to produce B_3H_7CO and $B_3H_7PF_3$ have failed. The products obtained from these reactions were B_4H_8CO[25] and $B_2H_4[PF_3]_2$.[26] However, using "acid assisted base displacement reactions" the triborane adducts have been prepared.[27]

$$B_3H_7[O(CH_3)_2] + CO + BF_3 \rightarrow B_3H_7[CO] + BF_3O(CH_3)_2 \qquad (1\text{-}14)$$

$$B_3H_7[O(CH_3)_2] + PF_2X + BF_3 \rightarrow B_3H_7[PF_2X] + BF_3O(CH_3)_2 \qquad (1\text{-}15)$$

where X = F, Cl, Br

The relative basicity of PF_2X ligands with respect to $[B_3H_7]$ as a reference acid has been determined.[27]

(iii) $[B_3H_8]^- + [LH]^+[X]^-$

The $[B_3H_8]^-$ ion is sufficiently hydridic in character to react with weak acids to evolve hydrogen[24(a)]

$$[N(CH_3)_3H]Cl + Na[B_3H_8] \longrightarrow B_3H_7[N(CH_3)_3] + H_2 + NaCl \quad (1\text{-}16)$$

This is a potentially useful reaction which obviates the use of the hazardous B_4H_{10} and which can be extended to other amines.[13]

(c) Structure and Dynamics of B_3H_7L Adducts

(i) X-ray Studies

An X-ray crystallographic study has shown that triborane (7)-carbonyl, $B_3H_7[CO]$,[27(b)] adopts a 1104 styx* structure with the geometry shown below (V)

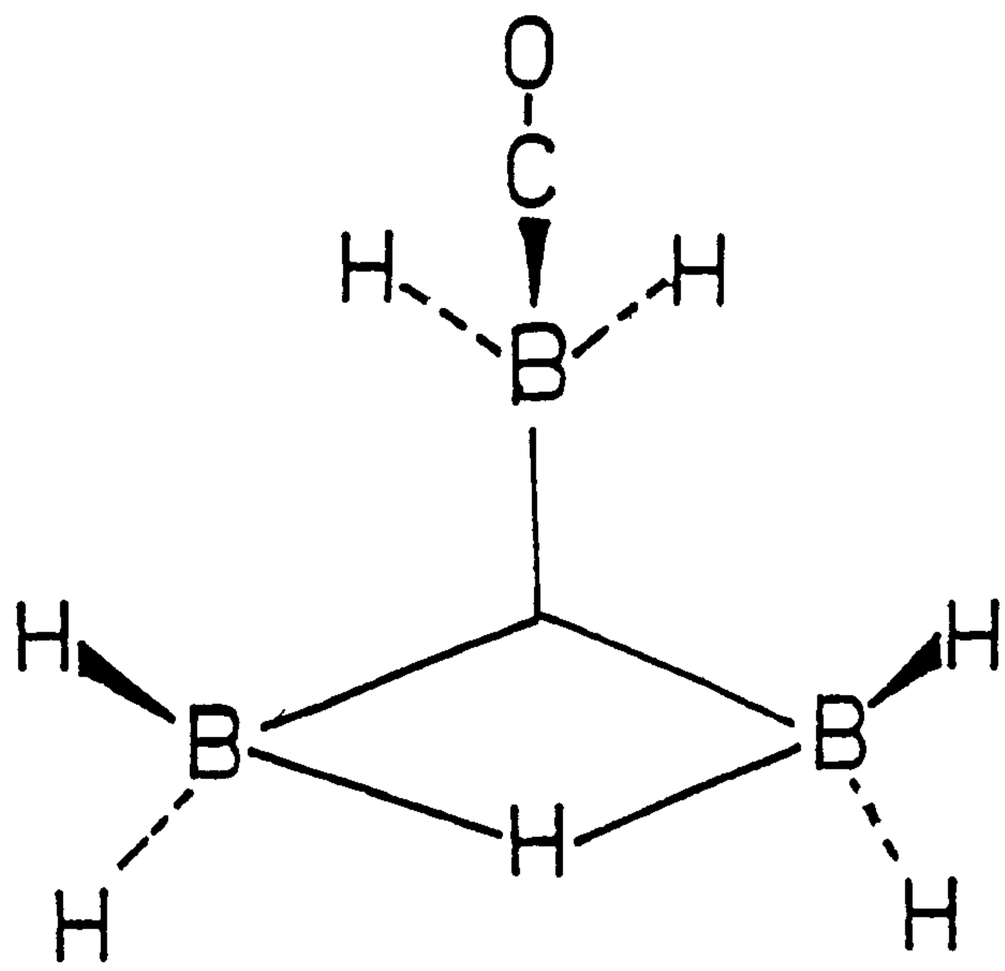

V

* treating CO as H^- in the styx notation.

In contrast the crystal structure of ammonia triborane (7), $B_3H_7[NH_3]$[39] has shown that triborane framework is asymmetric and that the structure is an intermediate between the 1104 and the 2013 structures described by the styx notation

(ii) N.m.r. Studies

The ^{11}B n.m.r. spectra show that B_3H_7L adducts can be divided into two general groups. The ^{11}B n.m.r. spectrum of $B_3H_7[CO]$[27] displays a downfield triplet of relative area two and a second triplet of relative area one at higher field indicating that this adduct is static on the n.m.r. time scale. The n.m.r. spectrum is consistent with the determined crystal structure. Other adducts of weak bases such as PF_2X (X = Cl, Br)[27] display ^{11}B n.m.r. spectra similar to $B_3H_7[CO]$ indicating that they too are static and have a rigid structure similar to $B_3H_7[CO]$, i.e. 1104 in the styx notation.

In contrast the reported ^{11}B n.m.r. spectra of $B_3H_7[PF_2H]$[19] and $B_3H_7[PF_2N(CH_3)_2]$[19] seem consistent with a rigid structure in the 2013 mode. (VI).

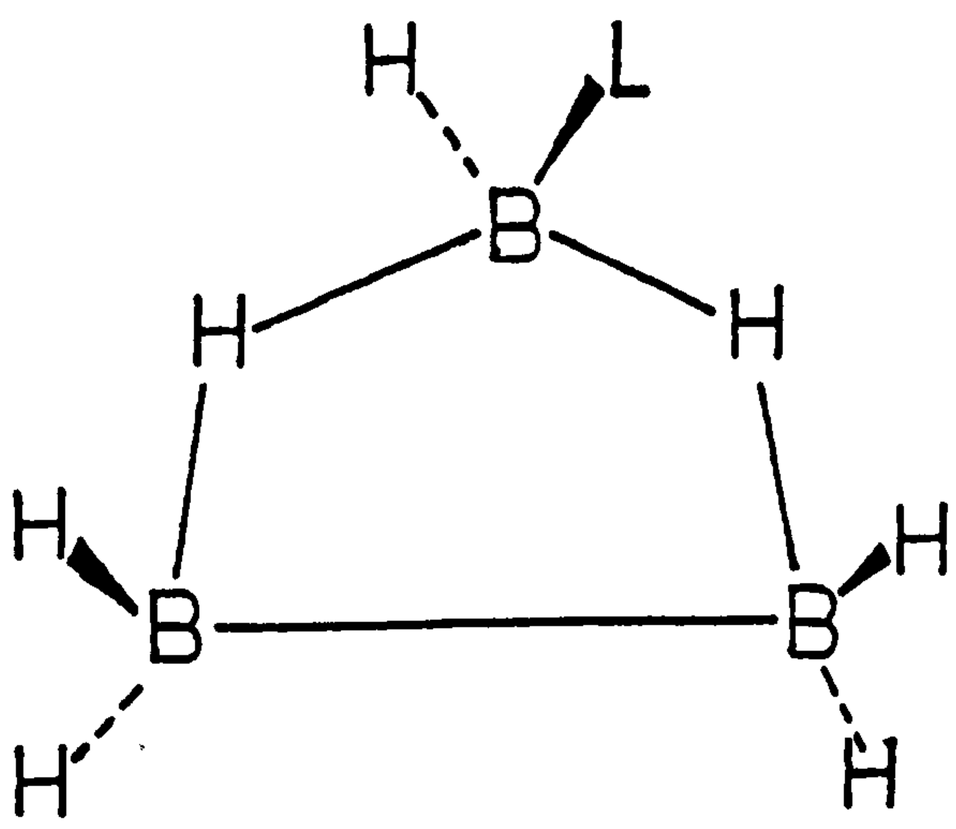

VI

The second group of neutral B_3H_7L adducts are distinguished from the first in that the ^{11}B n.m.r. spectra indicated that intramolecular hydrogen migration takes place on boron on the n.m.r. time scale, as in the parent $[B_3H_8]^-$ ion. Fluxional behaviour has been observed in amine triboranes,[28] phosphine triboranes[29] and ether triboranes.[30]

Variable temperature ^1H and ^{11}B n.m.r. studies of phosphine and methylphosphine adducts of triborane (7) show that on lowering the temperature the tautomeric motion of the hydrogen on boron is "frozen out" relative to the n.m.r. time scale. The spectra now reflected a structure analogous to that of triborane (7) - carbonyl in the 1104 styx mode. It was found that the static structure became recognisable at relatively high temperatures (-50°C) for phosphine triborane, $B_3H_7[PH_3]$, and decreased on increasing the number of methyl substituents in the phosphine ligand. The adducts $B_3H_7[PH_2(CH_3)]$ and $B_3H_7[PH(CH_3)_2]$ became static at -70°C and -85°C respectively. Trimethylphosphine triborane (7), $B_3H_7[P(CH_3)_3]$ remained fluxional even at -90°C. These results show that the ease of hydrogen tautomerism for the triborane (7) adducts discussed is directly related to the base strength of the phosphine ligands. The observed trend is in accord with the theoretical predictions of Brown and Lipscomb. Slowing of intramolecular hydrogen exchange has also been observed in the low temperature ^1H n.m.r. spectrum of $B_3H_7[N(CH_2C_6H_5)_2CH_3]$.[28(b)]

(iii) Theoretical Studies

A detailed theoretical study[31] of the Lewis base adducts of triborane (7) indicated that adducts of strong bases (amines and ethers) tended

to show fluxional character on the n.m.r. time scale, whereas adducts of weak bases (CO and PF_3) tended to show non-fluxional behaviour. It was proposed that, in general, with the exception of $B_3H_7[PF_2X]$ (X=H or $N(CH_3)_2$), that the preferred geometry was that of triborane (7) carbonyl, i.e., 1104 in the styx mode, rather than the 2013 mode of the parent $[B_3H_8]^-$ anion, the preference being stronger with weaker bases.

(d) Mono and Disubstituted Anionic Derivatives of $[B_3H_8]^-$

In comparison with the neutral adducts of triborane (7), B_3H_7L, there have been relatively few reports of substituted octahydrotriborate (1-) anions. The monosubstituted arachno-octahydrotriborate anions, $[B_3H_7(X)]^-$ (X=Cl,Br,I) have been prepared by treating $[B_3H_8]^-$ with the appropriate hydrogen halide in a non-coordinating solvent, the relative stability of the anions decreases going from the Cl^- to the I substituted derivatives. The structures of the chloro- and the bromo-substituted anions have been determined by infra-red spectroscopy and have structures consistent with a 2013 styx structure. The anion, $[B_3H_7(Br)]^-$ has been used in a convenient synthesis of pentaborane (9).[32,33]

It has been reported that [34] cyanide, $[CN]^-$, cleaves tetraborane (1) symmetrically to yield the triborane anion.

$$B_4H_{10} + 2[CN]^- \rightarrow [B_3H_7(CN)]^- + [BH_3(CN)]^- \qquad (1.17)$$

The hydroxyheptahydrotriborate. $[B_3H_7(OH)]^-$, ion has been prepared

by treating $B_3H_7(OH)_2$ with hydroxide at -78°C.[35] Above -65°C the $[B_3H_7(OH)]^-$ ion undergoes quantitative base-catalysed disproportionation to borate, $[B(OH)_4]^-$, and borohydride,$[BH_4]^-$.

It has recently been reported that a series of halogenated octahydrotriborate (1-) derivatives was prepared by treating $[B_3H_8]^-$ with the respective mercurous halide.[36]

$$[B_3H_8]^- + 1/2\ Hg_2X_2 \rightarrow [B_3H_7(X)]^- + 1/2\ H_2 + Hg^\circ \qquad (1.18)$$

where X = F, Cl, Br.

The disubstituted octahydrotriborate (1-) derivative, $[B_3H_6(Cl)_2]^-$, was produced by reaction of $[B_3H_8]^-$ ion and one equivalent of Hg_2Cl_2.

$$[B_3H_8]^- + Hg_2Cl_2 \rightarrow [B_3H_6(Cl)_2]^- + H_2 + 2Hg^\circ \qquad (1-19)$$

It was found that the chloride substituent of $[B_3H_7(Cl)]^-$ was labile and could be replaced by more nucleophilic bases.

$$[B_3H_7(Cl)]^- + [X]^- \rightarrow [B_3H_7(X)]^- + [Cl]^- \qquad (1.20)$$

where X = NCS,[36] $NCBH_3$.[36] NC[37] and NCO.[37]

The crystal structure determination of $[N(PPh_3)_2][B_3H_7(NCS)]$ at room temperature appeared to exhibit asymmetric hydrogen bridging of the triborane face,[38] whereas at low temperatures only one edge bridging hydrogen atom was observed as in the structure of $B_3H_7[NH_3]$.[39]

By treating the monosubstituted octahydrotriborate (1-) derivatives, $[B_3H_7(X)]^-$ (X=Cl, NCS, $NCBH_3$ and $NCBH_2Cl$), with gaseous HCl in a non-coordinating solvent it was possible to prepare[37] disubstituted derivatives of the octahydrotriborate (1-) ion, $[B_3H_6(Cl)(X)]^-$ (X=Cl, NCS, $NCBH_3$ and $NCBH_2Cl$). X-ray diffraction studies have shown the $[B_3H_6(Cl)_2]^-$ ion to have two μ-H atoms in a structure resembling that of the $[B_3H_8]^-$ ion.[15] The two chloride substituents were found to be in a trans-configuration to each other and the two substituted boron atoms were connected via a B-B single bond. It was originally postulated that the reaction of AgCN with $[B_3H_7(Cl)]^-$ resulted in cyanide displacement of the facile chloride to give $[B_3H_7(CN)]^-$.[36] However, X-ray diffraction studies have shown that the product obtained is $[Ag\{B_3H_7(NC)\}_2]^-$[36] in which two triborane (7) cages are linked via an essentially linear NC-Ag-CN bridge. A disubstituted derivative of this anion could also be produced by reaction of AgCN with $[B_3H_6(Cl)_2]^-$ to give $[Ag\{B_3H_6(Cl)(CN)\}_2]^-$.[37]

1.2.5 Metallaborane Derivatives of the $[B_3H_8]^-$ Ion

(a) Preparation

Metal complexes of the octahydrotriborate (1-) ion have usually been prepared by displacement of co-ordinated ligands by $[B_3H_8]^-$.[3,40]

$$M(CO)_6 + [B_3H_8]^- \longrightarrow [(CO)_4M(B_3H_8)]^- + 2CO \qquad (1\text{-}21)$$

M = Cr, Mo, W.[3b]

$$(CH_3)_2MCl + [B_3H_8]^- \longrightarrow [(CH_3)_2MB_3H_8]^- + Cl^- \qquad (1\text{-}22)$$

M = Al, Ga.[40]

$$[(C_6H_5)_3Y]_mCuCl + Cs[B_3H_8] \rightarrow [(C_6H_5)_3Y]_nCu[B_3H_8] \qquad (1\text{-}23)$$

When Y=P (n=2), As (n=2) and Sb (n=3).

(b) Structures and Dynamics

The bidentate metal derivatives of $[B_3H_8]^-$ have been likened to B_4H_{10} in which the metal centre has formally replaced a "wing tip" BH_2^+ in the borane butterfly.[41] The bidentate co-ordination between the metal fragment and the borane ligand was first shown to be via two M-H-B hydrogen bridge bonds by Guggenberger[42,43] in the crystal structure determination of $[(CO)_4CrB_3H_8]^-$. This complex, and the molybdenum and tungsten analogues, have pseudooctahedral co-ordination about the metal centre. In derivatives of main group elements and in certain transition metal derivatives the exo-endo geometry of the BH_2^+ fragment that has been replaced by the metal centre is retained. This is reflected in the crystal structure determination of $[Cu(PPh_3)_2B_3H_8]$[44], (VII) the exo-endo geometry of the phosphine ligands is similar to that of the hydrogen atoms in the BH_2^+ unit (VII).

VII

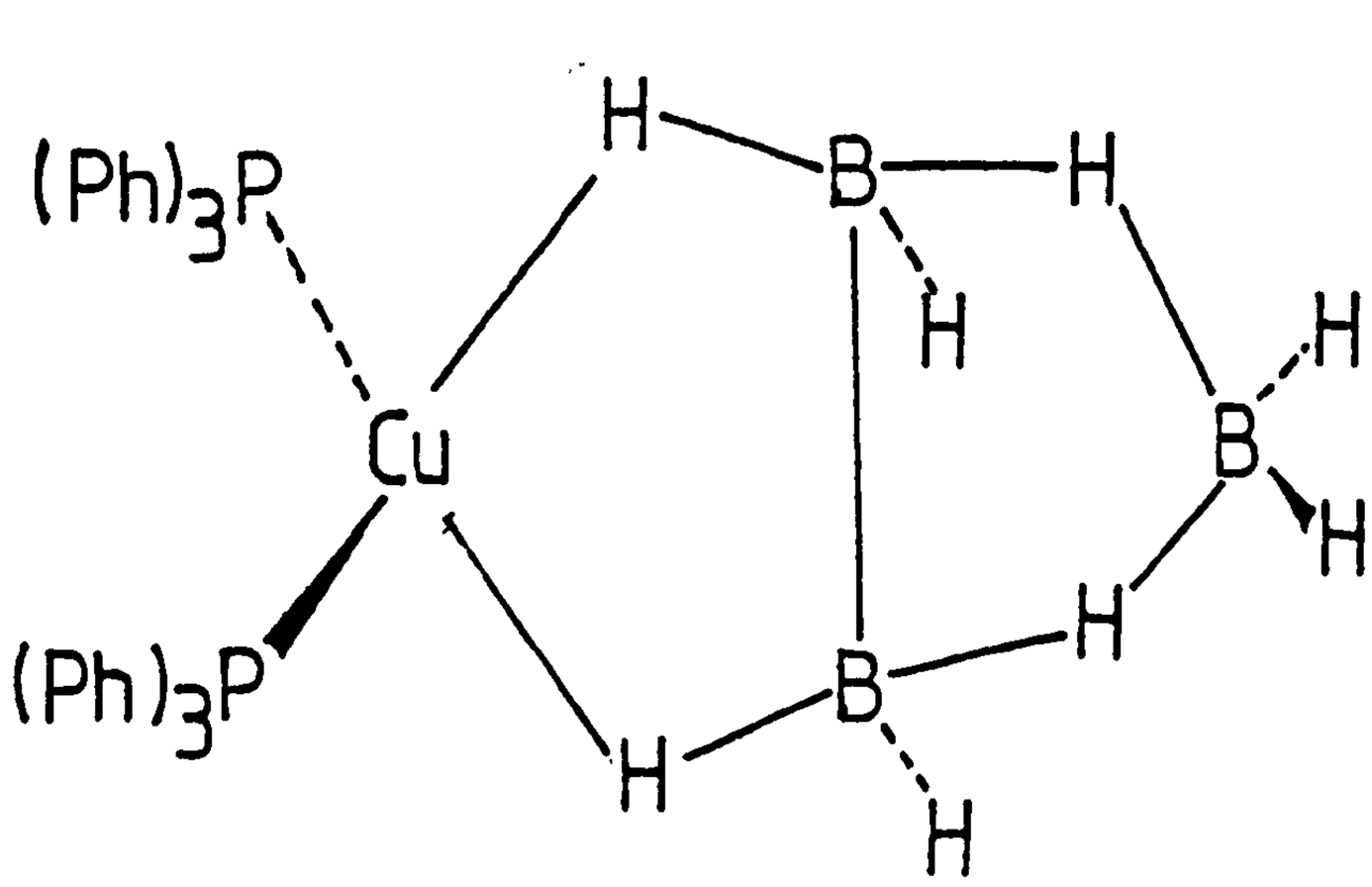

The majority of metal complexes of $[B_3H_8]^-$ have been shown to be fluxional by extensive n.m.r. studies.[45,46] In contrast to $Tl[B_3H_8]$ and $[(CH_3)_4N][B_3H_8]$[17(c),(d),(e),(f)] the ^1H n.m.r. spectrum of $[Cu(PPh_3)_2B_3H_8]$ in 50% $CDCl_3$ - 50% CD_2Cl_2 was a broad featureless singlet. However, it was found that upon lowering the temperature the bridge hydrogen resonance of the $[B_3H_8]$ moiety sharpened due to quadrupole induced spin decoupling, reducing the temperature further to -90°C caused the resonance to broaden in an asymmetric fashion and separate into several resonances. This behaviour is consistent with a slowing of $[B_3H_8]$ pseudorotation at low temperatures; a static system is observed at -97°C.

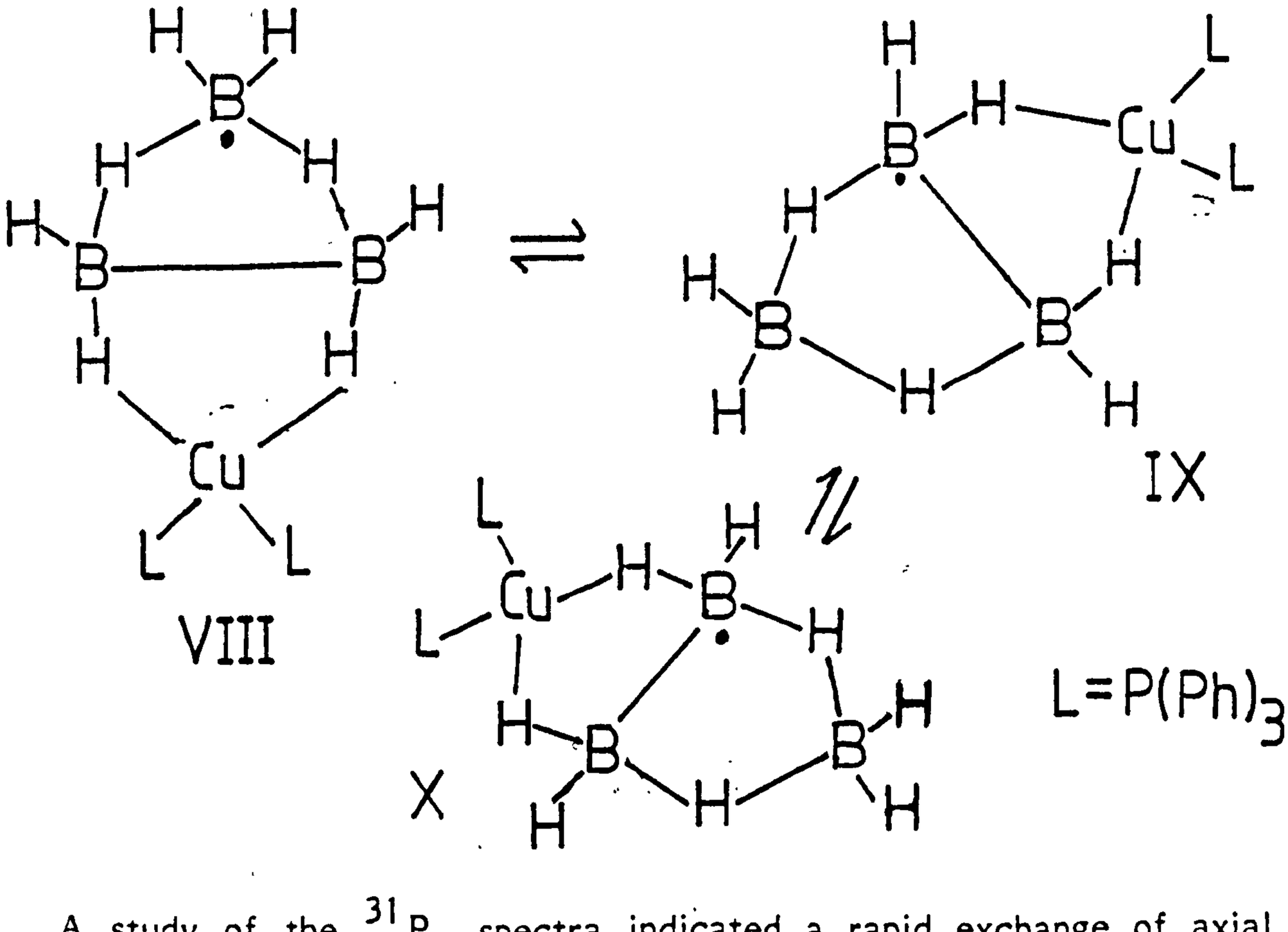

A study of the ^{31}P spectra indicated a rapid exchange of axial and equatorial phosphine environments[45] at room temperature which were distinguishable at -80°C in $[Cu\{(pCH_3C_6H_5)_3P\}_2B_3H_8]$. Addition of an

excess of tri-p-tolylphosphine ligand below -20°C to [Cu{ ($pCH_3C_6H_5)_3$ P }$_2B_3H_8$] resulted in two ^{31}P n.m.r. resonances due to the free and complexed ligand being observed. However, above -20°C the free and complexed ligand resonances coalesced to a single resonance indicating that above -20°C intermolecular ligand exchange may take place.

The ^{11}B n.m.r. spectra of $[(CO)_4MB_3H_8]^-$ (where M=Cr,Mo,W) in CH_3CN at room temperature showed two broad resonances at δ 23.0p.p.m. and δ61.3p.p.m. (relative to $B(OCH_3)_3$) of relative intensity 1:2,consistent with slow pseudorotation of $[B_3H_8]$ on the n.m.r. time scale at room temperature. These complexes represent a more static $[B_3H_8]$ ligand than the [(triarylphosphine)$_2CuB_3H_8$] complexes.

It is evident that complexation of the $[B_3H_8]^-$ ion by a metal via hydrogen bridge bonds results in a slowing of the pseudorotatory process of the $[B_3H_8]$ ligand compared with that of the free ion.

In addition to the fluxional complexes several static complexes have been reported,[47] $[(CO)_4MB_3H_8]$ where (M=Mn,Re),$[(\eta^5\text{-}C_5H_5)(CO)_2MB_3H_8]$, (where M=Mo,W), $[(\eta^5\text{-}C_5H_5)(CO)FeB_3H_8]$ and $[H(CO)_3FeB_3H_8]$, in which the metal centre completely "locks" the pseudorotary mechanism of the $[B_3H_8]$ ligand. This results in the resolution of five distinct hydrogen environments in the ^1H n.m.r. spectrum for the $[B_3H_8]$ hydrogen atoms in these static bidentate complexes. The ferraborane $[H(CO)_3FeB_3H_8]$ is formulated as the mer isomer since all nine hydrogen atoms have different chemical shifts in the 270 MH_z ^1H n.m.r. spectrum.

The preparation of $[Be(B_3H_8)_2]$ has been reported[48] and is the first example of a metal centre co-ordinated to two $[B_3H_8]$ ligands. An X-ray crystal structure determination[49] showed that the central beryllium atom is attached to each $[B_3H_8]$ ligand via two Be-H-B hydrogen bridge bonds. Three basic solution structures were shown to exist by n.m.r. spectroscopy, one which was static at low temperatures (-10°C) and two which were fluxional at higher temperatures.

(c) Chemical Properties of Metallaboranes Derived from $[B_3H_8]^-$

The derivative $[(CO)_4MnB_3H_8]$ has been shown to display unusual reactivity in that it undergoes reversible decarbonylation[47] on U.V. irradiation or heating to produce the tridentate $[(CO)_3MnB_3H_8]$. This species is unusual in that the manganese is bonded to the borane fragment via three Mn-H-B hydrogen bridge bonds (XI).[50]

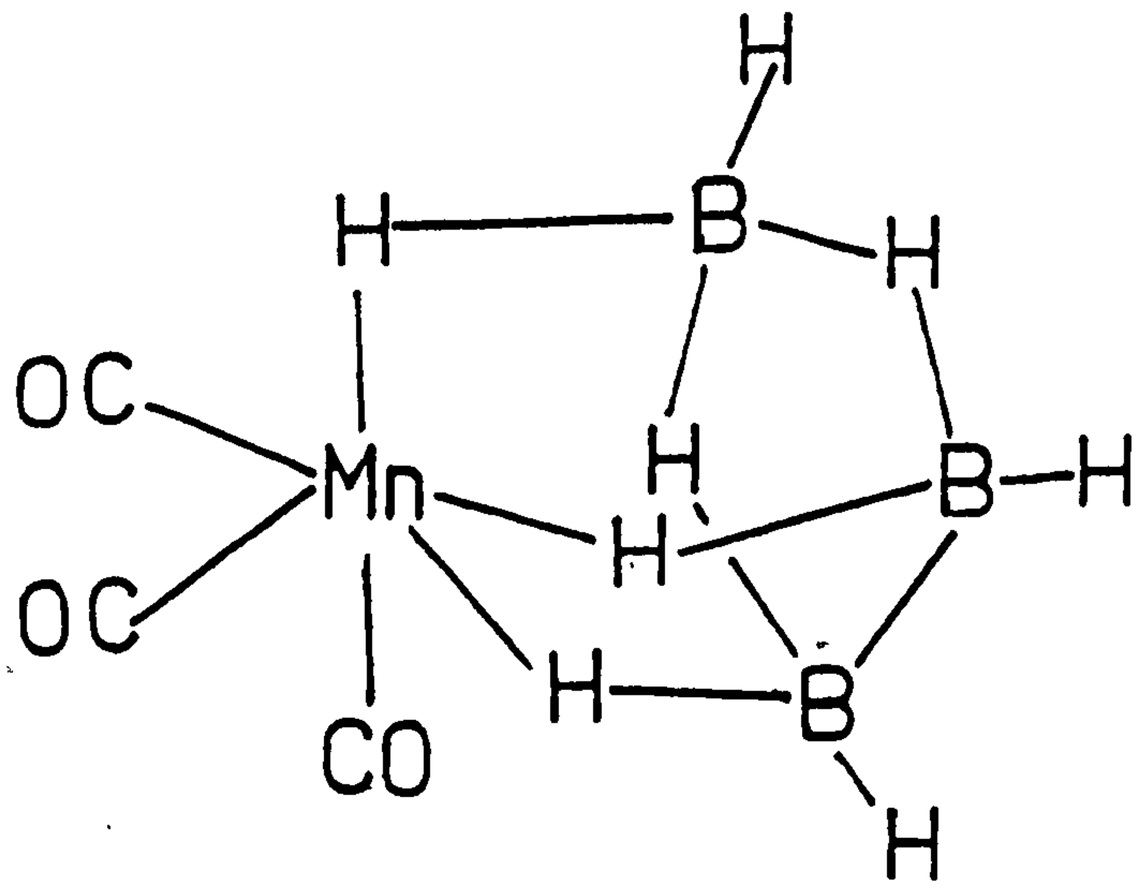

XI

The tridentate $[(CO)_3MnB_3H_8]$ is partially fluxional on the n.m.r. time scale down to -80°C. The ^1H n.m.r. spectrum indicates that the hydrogen atoms of the Mn-H-B bridge bonds are static, whereas the hydrogen atoms not involved in hydrogen bridge bonds are equivalent due to rapid intramolecular exchange on the n.m.r time scale around the periphery of the borane triangle. This results in all three boron atoms being equivalent in the ^{11}B n.m.r. spectrum. A higher homologue of this tridentate complex is $[(CO)_3MnB_8H_{13}]$[51] in which the $[B_8H_{13}]$ fragment acts as a tridentate ligand, this compound has been described as a polyhedral borane with a face bridging $Mn(CO)_3$ fragment. As such, the metal fragment is an exo-polyhedral substituent.

$[(CO)_3MnB_3H_8]$ reacted quantitatively with PF_3 or NH_3 to produce $[(L)(CO)_3MnB_3H_8]$ (where L=PF_3 or NH_3). In both cases the octahedral co-ordination of the metal atom is retained by conversion of the $[B_3H_8]$ fragment from a tridentate ligand to a bidentate ligand on addition of PF_3 or NH_3.

Halogenation of $[(CO)_4MnB_3H_8]$ with Cl_2 or Br_2 affords the substituted derivatives $[(CO)_4MnB_3H_7X]$ (X=Cl or Br), halogen substitution was shown to be at the boron atom not hydrogen bridge bonded to the metal centre.[47] At low temperatures the ^{11}B n.m.r. spectra suggest a static structure in which the halogen occupies a terminal site on the unbridged atom. At higher temperatures the M-H-B hydrogen atoms are static, whereas, the protons of the triborane fragment are fluxional. Therefore, this complex exhibits partial fluxionality

similar to the $[(CO)_3MnB_3H_8]$ complex.

The reaction of halogens with $[(CO)_3MnB_3H_8]$ in the presence of aluminium chloride yields $[(\mu\text{-}X)(CO)_6Mn_2B_3H_8]$ (X=Cl or Br) in which the $[B_3H_8]$ fragment acts as a bridge between the two manganese atoms by supplying two Mn-H-B bridge hydrogen bonds to each manganese atom.[52] These complexes appear to be static on the n.m.r. time scale. The dimanganoborane complexes can be considered as being analogous to $[(CO)_{10}HMn_3B_2H_6]$[53] by formally replacing BH_2 with $Mn(CO)_4$.

It has been shown that treating bis(triphenylphosphine) copper (1) triborane with $[B_2H_6]$ results in ligand abstraction by formation of $[P(C_6H_5)_3BH_3]$ and formation of the complex $[CuB_3H_8]$.[54]

$$[Cu(PPh_3)_2B_3H_8] + B_2H_6 \rightarrow [CuB_3H_8] + 2[PPh_3BH_3] \qquad (1\text{-}24)$$

The $[CuB_3H_8]$ complex is assumed to be polymeric in the solid state with each copper atom being bound to more than one $[B_3H_8]$fragment by Cu-H-B bridge bonds.

(d) Π - Borallyl Complexes

A unique series of complexes of general formula $[(R_3P)_2 MB_3H_7]$. (M=Ni,Pd,Pt) have been reported.[55,56] Proton n.m.r. studies of these complexes indicated a metal-boron interaction analagous to a Π-allyl system, which was confirmed by X-ray crystallography.

1.3 The Tetradecahydrononaborate (1-) Ion, $[B_9H_{14}]^-$ and Related Compounds.

1.3.1 Preparation

The $[B_9H_{14}]^-$ ion was first prepared[57] by the aqueous base degradation of decaborane(14). Reaction of two molar equivalents of hydroxide ion with one of decaborane(14) produced a colourless intermediate which slowly hydrolysed to $[B_9H_{14}]^-$. On acidification $[B_9H_{14}]^-$ was obtained in high yield.

$$B_{10}H_{14} + [OH]^- \rightarrow [B_{10}H_{13}]^- + H_2O \qquad (1\text{-}25)$$

$$[B_{10}H_{13}]^- + [OH]^- \rightarrow [B_{10}H_{13}(OH)]^{2-} \qquad (1\text{-}26)$$

$$[B_{10}H_{13}(OH)]^{2-} + H_3O^+ + H_2O \rightarrow [B_9H_{14}]^- + B(OH)_3 + H_2 \qquad (1\text{-}27)$$

Base degradation of decaborane(14) in methanol also produces $[B_9H_{14}]^-$.[58] The reaction of B_5H_9 with $[BH_4]^-$[59] or NaH[60] also produced $[B_9H_{14}]^-$.

1.3.2 Structure and Dynamics

(a) The structure of $Cs[B_9H_{14}]$ has been determined crystallographically[61,62] and has been shown to be an arachno- fragment with the overall arrangement of boron atoms similar to that found in iso-B_9H_{15}.[63,64] Although the boron atom arrangement of $[B_9H_{14}]^-$ is the same as that of its isoelectronic substituted analogue, $B_9H_{13}[NCCH_3]$ the two structures clearly differ in the position of the hydrogen bridge bonds, (Figure 1.1).

(b) N.m.r. Studies

In solution, ^{11}B[62,63] and ^{1}H[62] n.m.r. spectra are consistent with a structure of higher symmetry (C_{3v}) than that observed in the solid state (C_s). These observations indicate that $[B_9H_{14}]^-$ ion is fluxional in solution on the n.m.r. time scale with rapid intramolecular hydrogen exchange involving two bridge hydrogen atoms and one hydrogen atom from each BH_2 unit.

1.3.3 Substituted Derivatives of the $[B_9H_{14}]^-$ Ion

(a) Preparation

(i) Acidolysis and Alcoholysis Reactions

Two general methods have been employed in degrading a B_{10} framework to $B_9H_{13}L$. These involve either acidolysis[66] or alcoholysis[13,66(b),67] reactions.

$$[B_{10}H_{13}L]+H_3O^+ +2H_2O \rightarrow B_9H_{13}L+B(OH)_3+2H_2 \qquad (1\text{-}28)$$

$$B_{10}H_{12}L_2+3ROH \rightarrow B_9H_{13}L+B(OR)_3+L+H_2 \qquad (1\text{-}29)$$

$$B_{10}H_{14}+L+ROH \rightarrow B_9H_{13}L+B(OR)_3+2H_2 \qquad (1\text{-}30)$$

The alcoholysis of $B_{10}H_{14}$ in the presence of a ligand has been studied in some detail[67] with respect to the effect of base strength of the ligand and the mechanism of the degradation reaction. In aqueous dioxan solution $K[B_9H_{13}(NCS)]$ has been prepared from $B_{10}H_{14}$ with KSCN.[68]

(ii) Base Displacement Reactions

Base displacement reactions have been widely used in the preparation of the base adducts of $[B_9H_{13}]$.[66(b)]

This method is particularly useful for the preparation of $B_9H_{13}[NCCH_3]$ from $B_9H_{13}[SEt_2]$ since alcoholic degradation of $B_{10}H_{12}[NCCH_3]_2$ yields $B_9H_{13}[NH=C(OC_2H_5)CH_3]$.[66(b)]

(iii) Other Reactions

The bromo derivatives $BrB_9H_{12}[P(C_6H_5)_2H]$[69] and $BrB_9H_{12}[SMe_2]$[70] have been prepared through bromination of $B_9H_{13}[P(C_6H_5)_2H]$ and $B_9H_{13}[SMe_2]$ respectively. It has been shown that ethanolysis[71] of 2-$BrB_{10}H_{11}[SMe_2]$ yields 1-$BrB_9H_{12}[SMe_2]$ and methanolysis[72] yields 7-$CH_3OB_9H_{12}[SMe_2]$.

Pyrolysis of $B_9H_{13}[SMe_2]$ gave n-$B_{18}H_{22}$[73] and in much smaller yields $B_{16}H_{20}$.[74] Pyrolysis of $B_9H_{13}[O(n\text{-}C_4H_9)_2]$ also gave n-$B_{18}H_{22}$[64]

$B_9H_{13}[CO]$ has been prepared[75] by the decomposition of iso-B_9H_{15} in pentane under 25atm. of carbon monoxide.

(b) Structure and Dynamics

(i) X-ray Studies

The structure of $B_9H_{13}[CH_3CN]$ is illustrated in Fig.1.1.(b).[65] The nonaborane framework is clearly similar to that of $[B_9H_{14}]^-$ but differs in position of bridge hydrogen atoms.

(a)

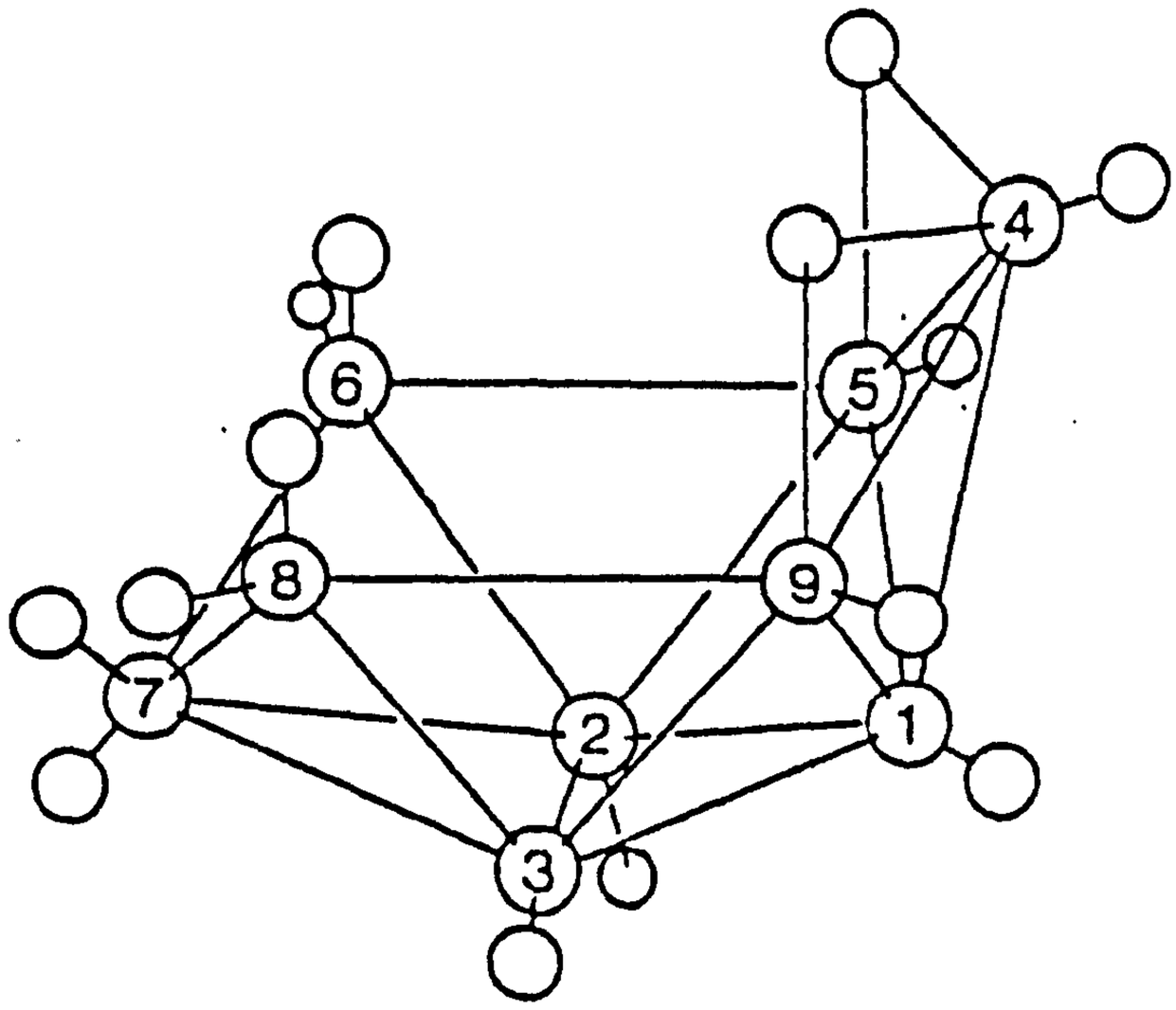

(b)

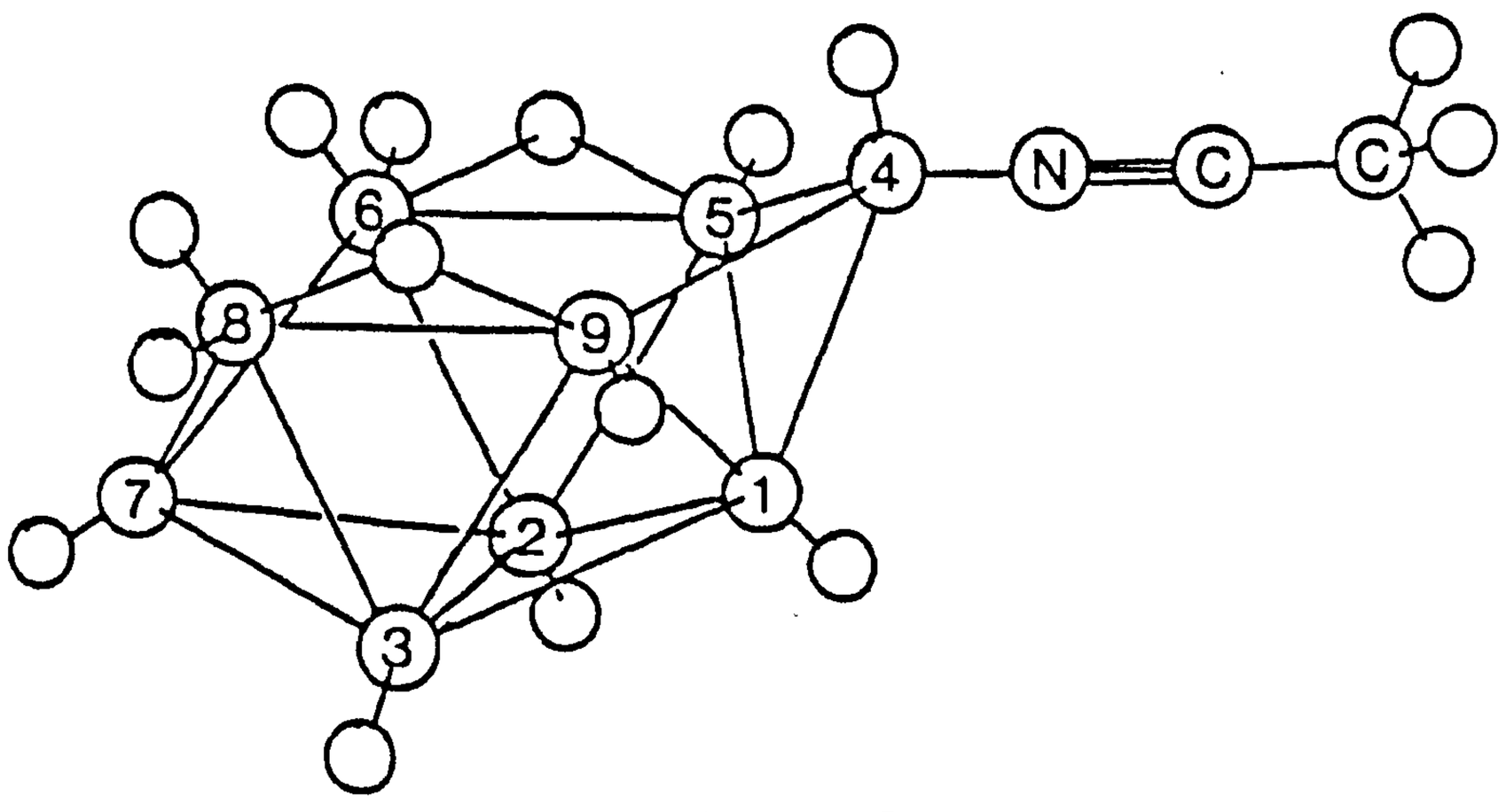

Figure 1.1 (a) The structure of $[B_9H_{14}]^-$ and (b) the structure of $B_9H_{13}[NCCH_3]$

(ii) N.m.r. Studies

^{11}B n.m.r. studies[71] of $B_9H_{13}L$ compounds indicate six individual boron resonances consistent with the C_s symmetry of $B_9H_{13}[NCCH_3]$. The ^{11}B and ^{1}H n.m.r. spectra of $B_9H_{13}[CO]$[75] showed evidence of two bridge hydrogen atoms in the molecule. It was suggested that, in this case, there were BH_2 groups comparable to the unusual BH_2 group found in B_5H_{11}[76] present.

1.3.4 Metallaboranes Derived from the $[B_9H_{14}]^-$ Ion

Metallaboranes of general formula $L_nMB_9H_{14}$ have been prepared[3(b),45] where L is a triarylphosphine or triarylarsine ligand, n=2,3 or 4 and M=Cu,Ag,Au. Reactions of simple salts of copper (II), silver (I) and gold (III) with $Cs[B_9H_{14}]$ in aqueous ethanol with excess triphenylphosphine yields complexes of general stoichiometry $[(Ph_3P)_3MB_9H_{14}]$.[3(b)] When tri-p-tolylphosphine is used as a ligand only ionic $[L_4M]^+$ salts of $[B_9H_{14}]^-$ are isolated.[45] The ^{31}P n.m.r. of the $[L_4Cu][B_9H_{14}]$ salt below -100°C showed resonances attributable to L_4Cu-borane and L_3Cu-borane species.[45] The equilibrium that exists between these species at low temperature could be completely shifted to the L_4Cu-borane species by addition of excess ligand. Above -95°C, ligand exchange between the L_4Cu-borane and the L_3 Cu-borane was sufficiently fast on the n.m.r. time scale to give only a single ^{31}P n.m.r. resonance.[45] The ^{31}P n.m.r. spectra of $L_4AuB_9H_{14}$ and $L_4AgB_9H_{14}$ indicated that at high temperatures (above -50°C) there was rapid intermolecular ligand exchange on the n.m.r time scale.

Metallaboranes which have the basic heavy atom structure of decaborane(14) including bridge hydrogen positions, have been prepared (Fig.1.2). Metallaboranes of the type nido-$[6\text{-}(CO)_3\text{-}6\text{-}MB_9H_{13}]^-$ (M=Mn,Re) have been prepared from $[B_9H_{14}]^-$ and $BrM(CO)_5$.[77] A neutral complex, $5\text{-}(C_4H_8O)\text{-}6\text{-}(CO)_3\text{-}6\text{-}MnB_9H_{12}$ was isolated from a reaction between $K[B_9H_{14}]$ and $BrMn(CO)_5$ in refluxing tetrahydrofuran. Oxidation of $[6\text{-}(CO)_3\text{-}6\text{-}MnB_9H_{13}]^-$ in the presence of THF produces the isomeric $2\text{-THF-}6\text{-}(CO)_3\text{-}6\text{-}MnB_9H_{13}$. In these complexes a $Mn(CO)_3^+$ unit formally replaces a BH^{2+} unit at the six position in $B_{10}H_{14}$. The borane ligands can be regarded as $[B_9H_{13}]^{2-}$ in the anionic complex and $[B_9H_{13}L]^-$ in the neutral complex. The manganese is bonded to the borane cages via two Mn-H-B hydrogen bridge bonds and a direct Mn-B single bond. Low yields of the arachno-complex, $[(CO)_3MnB_8H_{13}]$ have also been obtained, in this case the borane ligand is bound to the metal fragment via three M-H-B bridge bonds.[51]

Line-narrowed $70.6MH_z$ ^{11}B n.m.r. spectra of these THF derivatives show fine structure due to coupling of boron with the Mn-H-B bridge hydrogen atoms.[77] The proposed assignments of individual resonances are based on the similarity between the metallaborane and $B_{10}H_{14}$, and the belief that when the $B_{10}H_{14}$ cage is modified by replacing the BH^{2+} unit at the six position in decaborane(14) by the $Mn(CO)_3^+$ moiety, the boron nuclei nearest the metal centre will suffer the greatest change in chemical shift.

Reaction of $2\text{-THF-}6\text{-}(CO)_3\text{-}6\text{-}MnB_9H_{12}$ with triethylamine results in the novel rearrangement product $8\text{-}[Et_3N.THF]\text{-}6\text{-}(CO)_3\text{-}6\text{-}MnB_9H_{12}$[78] whose structure has been determined crystallographically.

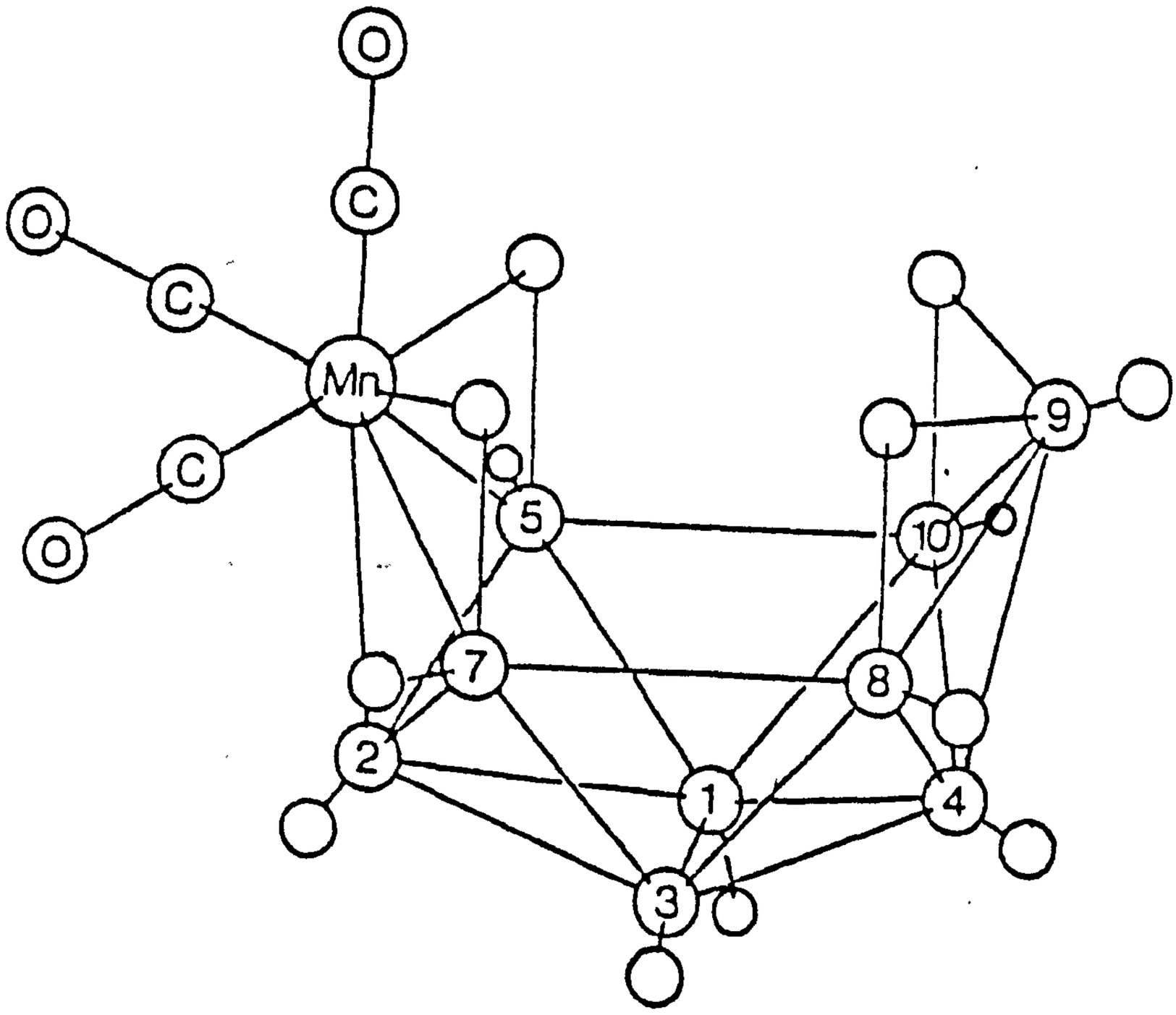

Figure 1.2 The structure of $[6\text{-}(CO)_3\text{-}6MnB_9H_{13}]^-$

Condensation of $Na[B_5H_8]$, $Na[C_5H_5]$ and cobalt chloride yields a variety of cobaltaboranes one of which, nido-5-$[C_5H_5]CoB_9H_{13}$ is obtained in low yield. This compound is isoelectronic and isostructural with $B_{10}H_{14}$, with a $Co[C_5H_5]^{2+}$ moiety formally replacing a BH^{2+} unit at the five position in $B_{10}H_{14}$. The B-B bond lengths in the complex differ from those of $B_{10}H_{14}$ by only 0.019 Å on average. The ^{11}B n.m.r. spectra of the cobaltaborane and decaborane are similar considering the gross electronic changes involved when replacing the boron atom at the five position by cobalt.

1.4 The Tri- μ-hydro-nonahydro-nido-nonaborate (1-)Anion, $[B_9H_{12}]^-$.

1.4.1 Preparation

In the presence of strong bases $B_9H_{13}[SEt_2]$ is deprotonated with loss of ligand to yield nido -$[B_9H_{12}]^-$[113,66(b)]

$$B_9H_{13}[SEt_2]+[N(CH_3)_4]OH] \rightarrow [N(CH_3)_4]B_9H_{12}]+SEt_2 + H_2O \quad (1\text{-}32)$$

1.4.2 Structure and Dynamics

(a) X-ray Structure

X-ray diffraction studies[80] of $[NMe_4]^+$ and $[NMe_2Et_2]^+$ salts of $[B_9H_{12}]^-$ were inconclusive because of disorder problems but did suggest that the anion was monomeric.

(b) N.m.r. Spectra

Todd, et al[81,82] have suggested from the ^{11}B n.m.r. spectrum of $[B_9H_{12}]^-$ that the gross arrangement of boron atoms is similar to

that found in <u>arachno-</u> $B_9H_{13}[NCCH_3]$,[65]

(c) <u>Chemical Reactions</u>

Previously $[B_9H_{12}]^-$ has been shown to react with HCl in ethereal media to yield $B_9H_{13}[OR_2]$[64] or in diethylsulphide to give $B_9H_{13}[SEt_2]$.[82] The $[B_9H_{12}]^-$ anion has recently been shown to react with mercury halides to give $B_{18}H_{22}$, $[B_9H_{10}Cl_2]^-$, $[B_9H_{11}Cl]^-$ and $[B_9H_{10}Br_2]^-$.[83]

1.5 Electrochemistry of Boron Hydrides

1.5.1 Electrochemical Techniques

In this section, a brief summary of the electrochemical techniques employed in studies of boron hydrides are described. The techniques described are based on potential sweep methods; linear potential sweep chronoamperometry and cyclic voltammetry, and impedance methods; a.c. voltammetry and cyclic a.c. voltammetry. Detailed descriptions of these techniques can be found in the literature.[84]

(a) <u>Controlled Potential Techniques - Potential Sweep Methods</u>

(i) <u>Linear Potential Sweep Chronoamperometry</u>

Linear potential sweep chronoamperometry or linear sweep voltammetry (L.S.V.), is an experiment in which the potential is swept linearly at $vV\ sec^{-1}$ as shown in Figure 1.3.

Generally current is recorded as a function of potential which is equivalent to recording current against time. A typical L.S.V. curve is shown in Figure 1.4.

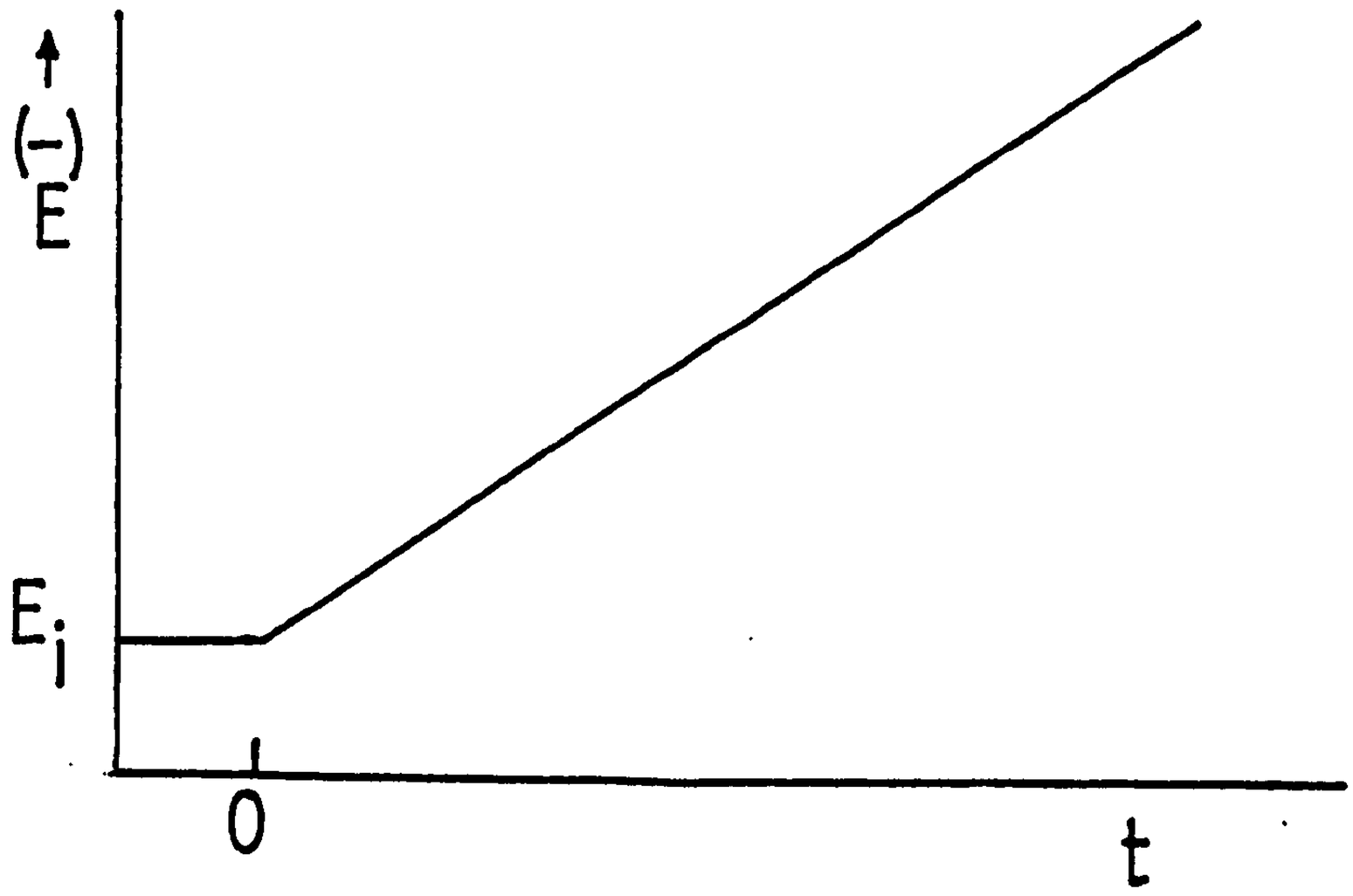

Figure 1.3 Linear potential sweep or ramp starting at E_i

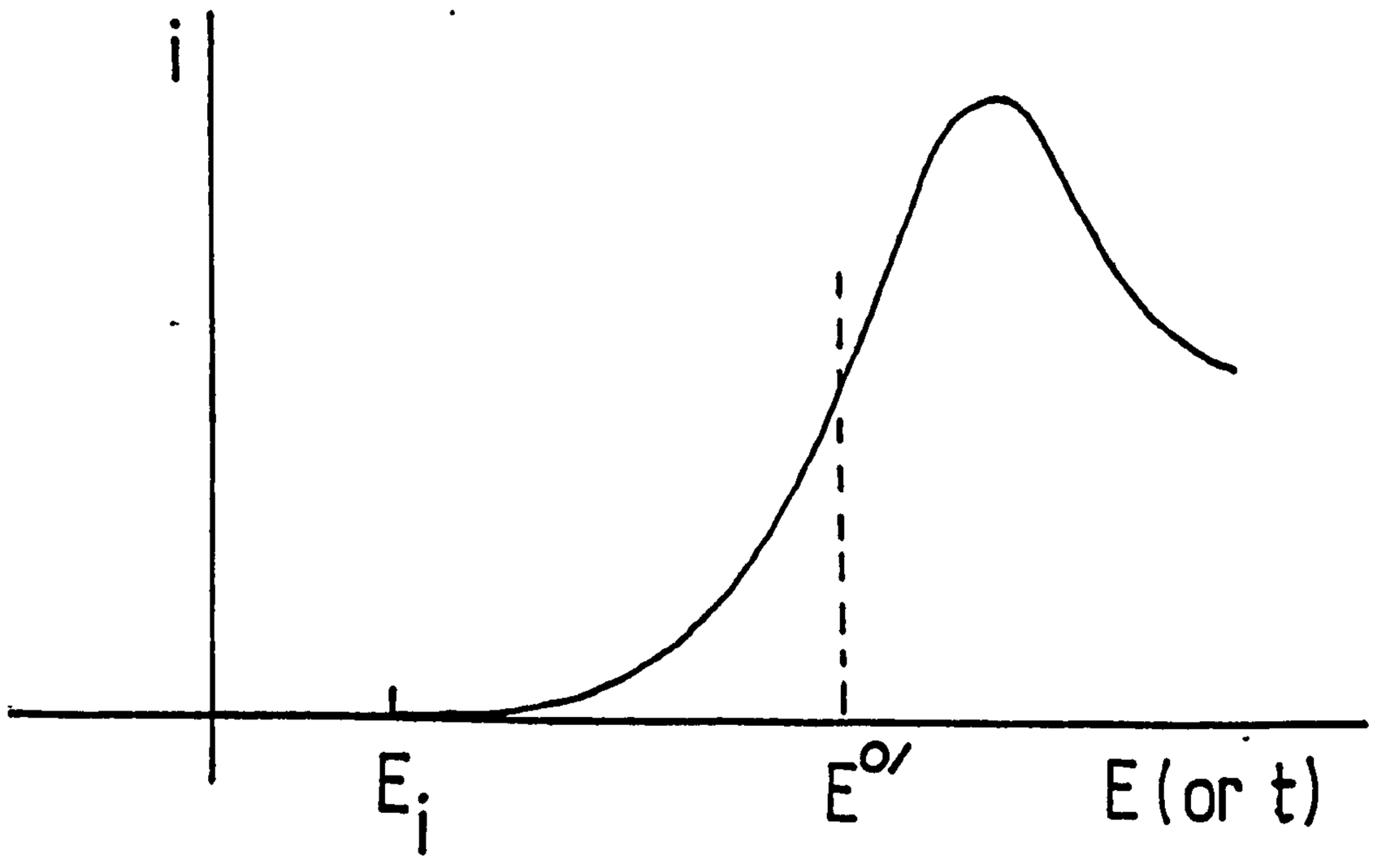

Figure 1.4 Resulting i-E curve

This curve represents a scan began at a positive potential well before the formal potential for the reduction $E^{0\prime}$, where only faradaic currents flow. When the electrode potential approaches $E^{0\prime}$ the reduction begins and a current starts to flow. As the reduction continues,

i.e. as the potential becomes more negative, the surface concentration of the oxidant drops, this concentration gradient results in a flux to the electrode surface and a current increase. As the potential increases beyond $E^{0\prime}$ the surface concentration of oxidant drops almost to zero, mass transfer of the oxidant to the surface reaches a maximum and is rate limiting, then declines as the depletion effect becomes dominant resulting in the current falling.

(ii) Cyclic Voltammetry (C.V.)

In cyclic voltammetry the potential is swept linearly at ν $Vsec^{-1}$ and the direction of the scan is reversed at the switching time, λ, (or the switching potential E_λ) as shown in Figure 1.5.

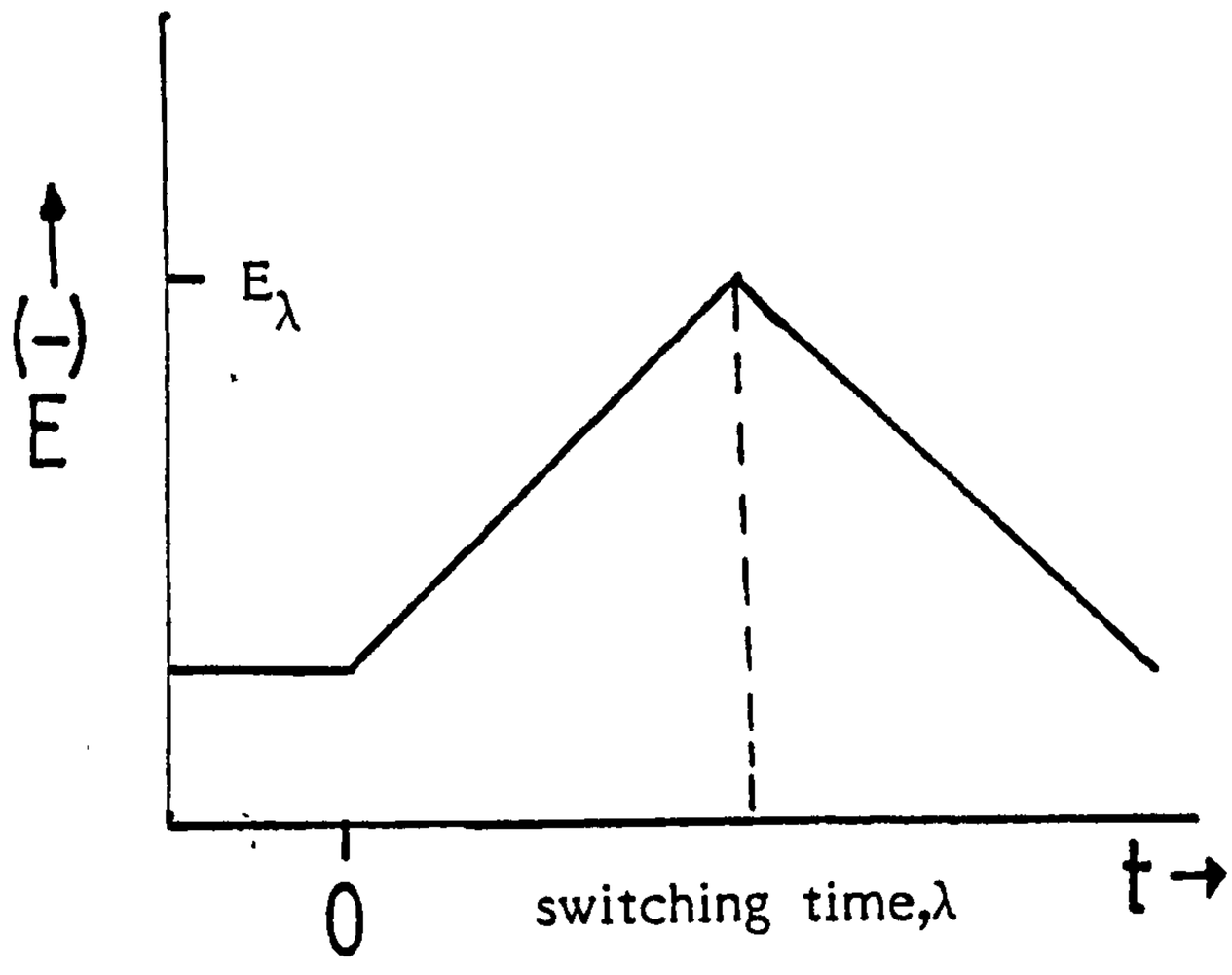

Figure 1.5 Cyclic potential sweep

Consider the electrode reaction:

$$Ox + ne^- \underset{k_r}{\overset{k_f}{\rightleftharpoons}} Red$$

If the electrode reaction is reversible, that is, if k_f and k_r are fast enough to maintain [Ox] and [Red] in equilibrium at the electrode surface then the current vs. voltage curve obtained is as shown in Figure 1.6.

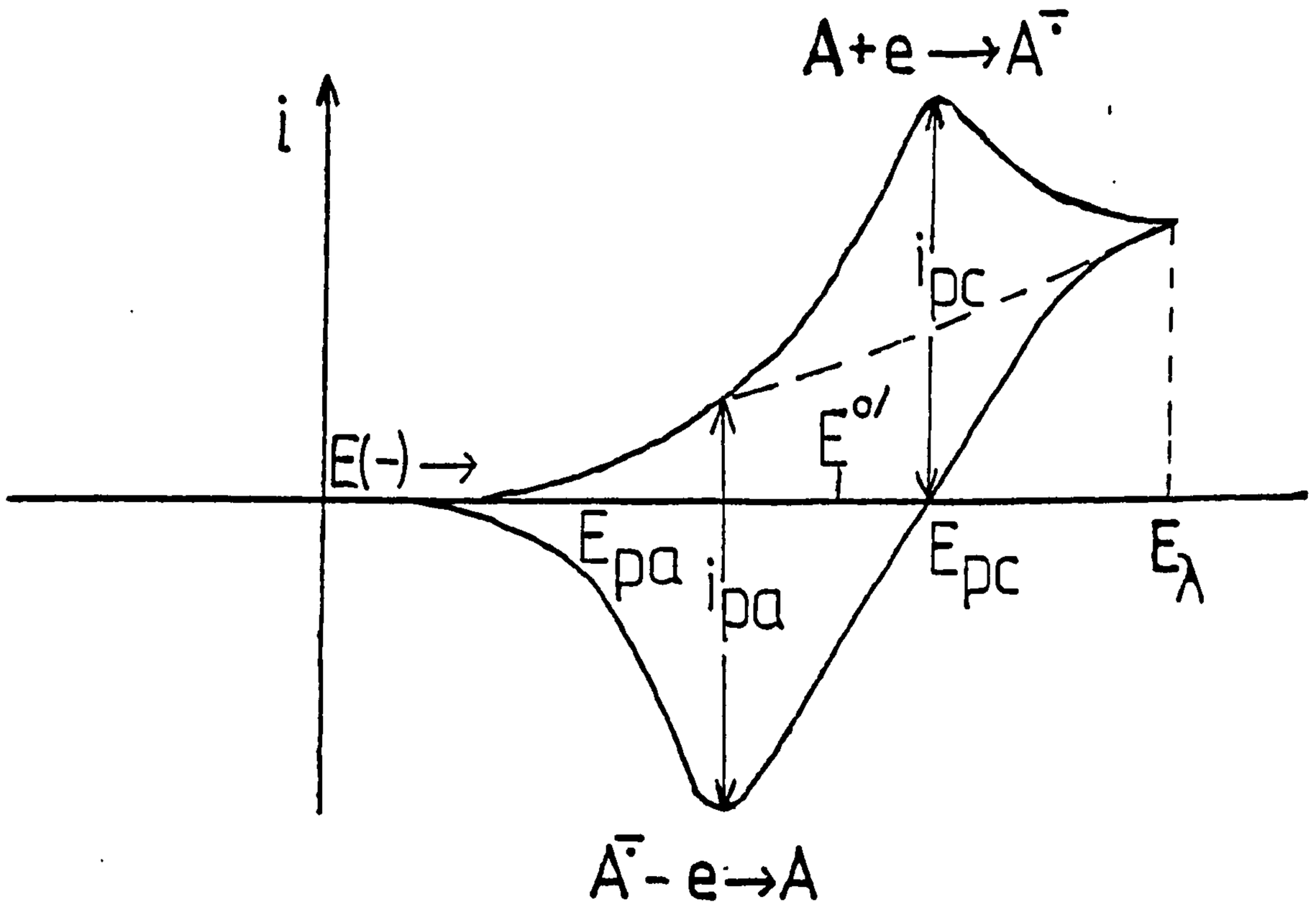

Figure 1.6 Cyclic voltammogram

If the electrochemical reaction is reversible then a concentration of product will be built up at the electrode surface, if the scan is fast enough this is essentially equal to the original concentration of reactant. Reversing the direction of the scan then reconverts product to reactant with an equal current.

The shape of the curve on reversal depends on the switching potential, E_λ, or how far beyond the cathodic peak the scan is allowed to proceed before reversal. If E_λ is at least $\frac{35}{n}$ mV beyond the cathodic peak, the reversal peaks all have the same general shape, basically consisting of a curve shaped like the forward i-E curve plotted in the opposite

direction on the current axis, with the decaying current of the cathodic wave used as a baseline and $i_{pa} = i_{pc}$. The measured parameters of interest in cyclic voltammograms are i_{pa}/i_{pc}, the ratio of peak currents, and $E_{pa} - E_{pc}$, the separation of peak potentials. For a nernstian wave with a stable product the ratio $i_{pa}/i_{pc} = 1$ regardless of scan rate, E_λ (for $E_\lambda > \frac{35}{n}$ mV past E_{pc}) and diffusion coefficients. The separation of peak potentials ΔE_p is a useful diagnostic test of a nernstian (reversible) reaction. Although ΔE_p is a function of E_λ it is always close to 2.3RT/nF. For an irreversible reaction the charge transfer rate constant, k°, is $< 2\times10^{-5}V^{\frac{1}{2}}$ cms^{-1} and ΔE_p is $> 2.3RT/nF$.

(b) Techniques Based on Concepts of Impedance

(i) A.C. Voltammetry

A.c. voltammetry is basically a faradaic impedance technique in which the mean d.c. potential (E_{dc}) is imposed potentiostatically at arbitrary values that usually differ from the equilibrium value. Ordinarily it is varied systematically (e.g. linearly) on a long time scale compared to that of the superimposed a.c. variation ($E_{a.c.} \approx$ 10mV peak to peak). The output is a plot of the magnitude of the a.c. component of the curret vs E_{dc}. The phase angle between the alternating current and E_{dc} is also of interest. A typical voltammogram is shown in Figure 1.7.

Figure 1.7 Shape of a reversible a.c. voltammetric peak when n=1.

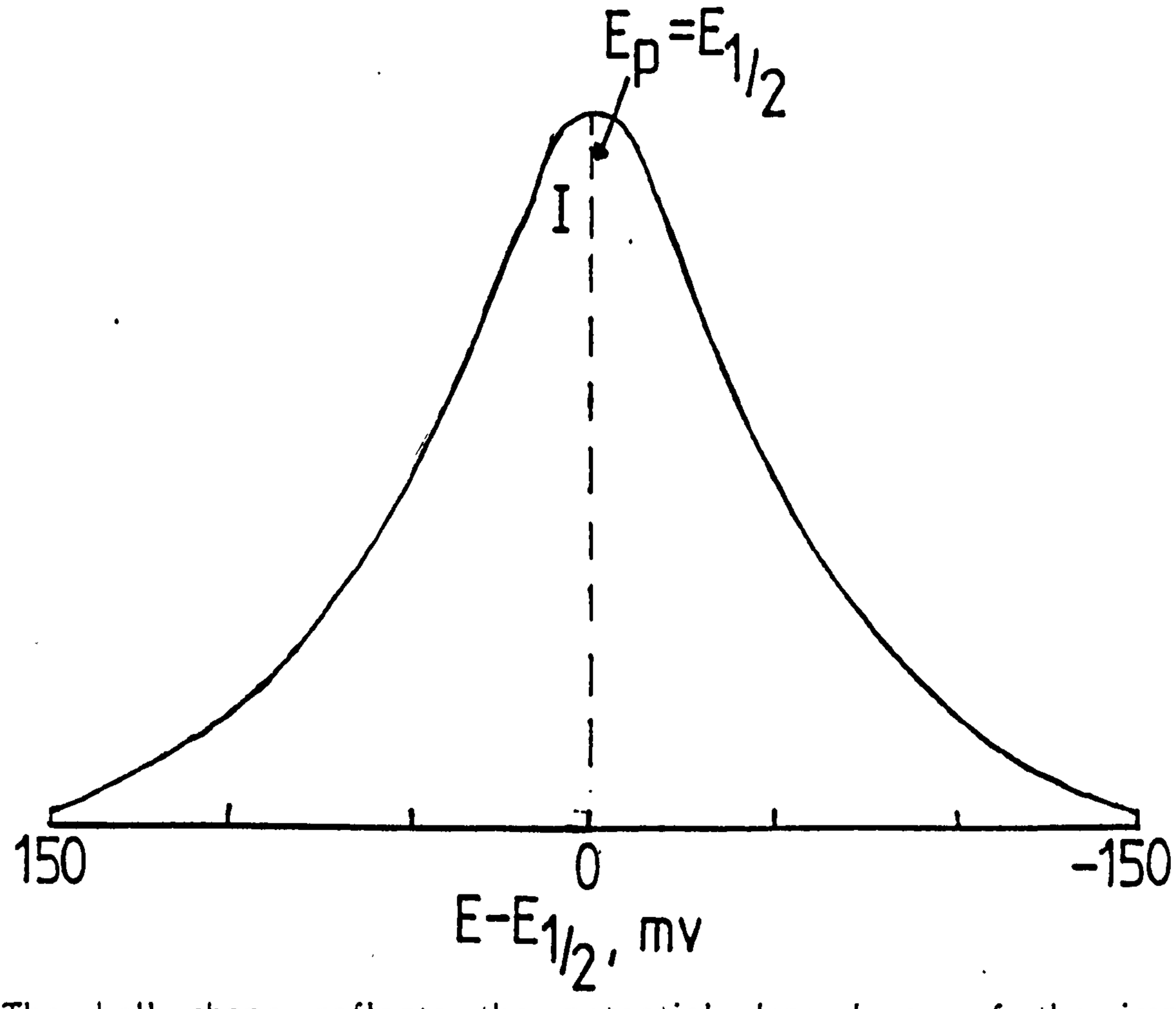

The bell shape reflects the potential dependence of the impedance Zf. The current maximum occurs when $E_{dc} = E_{1/2}$ which is near $E^{0\prime}$. Moving away from $E^{0\prime}$, either positively or negatively, the impedance rises sharply and the current falls off. At $E^{0\prime}$ the mass transfer impedance is small and both electroreactants are present in comparable concentrations, i.e. [Ox]/[Red] = 1, large and small ratios of [Ox]/[Red] imply that one of the concentrations is small, hence the mass transfer impedance is large and the current is small. The width of the peak at half height depends on ΔE if large values are used. If it is kept below 10/n mV there is a constant width of 90.4/n mV at 25°C. At larger values of ΔE the peaks are broader.

(ii) Cyclic A.C. Voltammetry

Cyclic a.c. voltammetry is a simple extension of the linear sweep

technique; one simply adds the reversal scan in E_{dc}. Cyclic a.c. voltammetry is a more attractive technique than cyclic voltammetry in that it retains the diagnostic information about the qualitative aspects of an electrode process, but does so with an improved response function that permits quantitative evaluations as precise as those obtained by usual a.c. methods.

For a completely nernstian system (i.e. reversible) the cyclic a.c. voltammogram shows superimposed forward and reverse traces of a.c. current amplitude vs E_{dc}. (Figure 1.8).

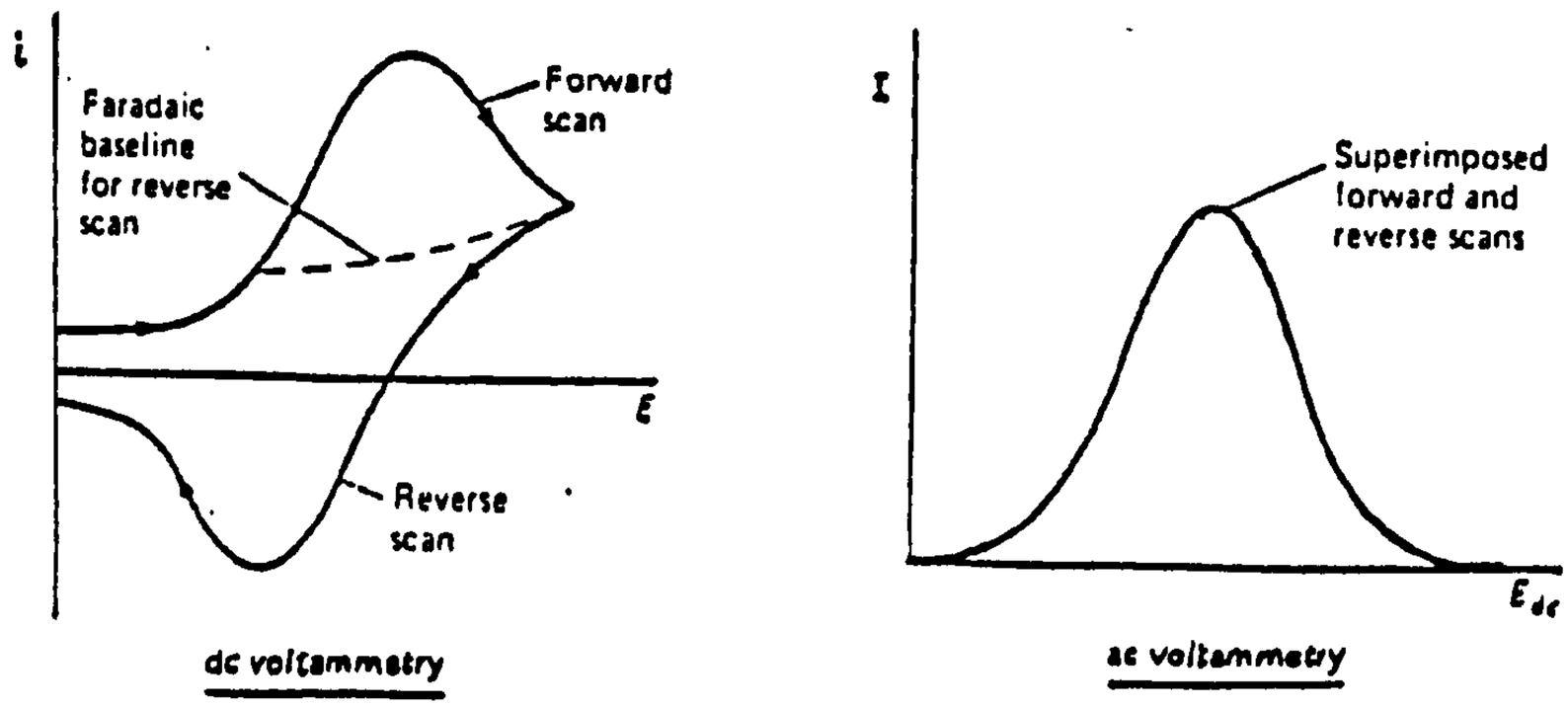

Figure 1.8 Comparison of the response waveforms for cyclic d.c. and cyclic a.c. voltammetry for a reversible system.

Figure 1.8 contrasts the response from a.c. and d.c. cyclic voltammetry for a purely nernstian case. Kinetic reversibility is shown in the d.c. experiment by a peak separation approximately 60/n mV regardless of scan rate. In the a.c. experiment kinetic reversibility is shown by identical forward and reverse peak potentials and by peak widths

of 90/n mV, also regardless of scan rate. The advantage in the a.c. experiment is that the reversal response has an obvious baseline for quantitative measurements, whereas the baseline for reversal currents in the d.c. response is more difficult to fix.

1.5.2 Electrochemistry of Boron Hydrides

The electrochemical behaviour of boron hydrides has received relatively little attention, therefore several boron hydride systems are reviewed in some detail in this section.

1.5.3 $[BH_4]^-$

The reported electrochemical studies of $[BH_4]^-$ have principally been carried out in the melt or aqueous phase to produce diborane.[85]

$$2[BH_4]^- \xrightarrow{\text{anode}} B_2H_6 + H_2 + 2e^- \qquad (1\text{-}33)$$

The electrolysis of $Na[BH_4]$ in polyethylene glycol dimethyl ethers with a mercury cathode gave diborane in good yield. The formation of sodium heptahydrotriborate is indicated by a time lapse in the release of diborane.[86]

$$2[BH_4]^- \rightarrow [B_2H_7]^- + e^- + 1/2H_2 \qquad (1\text{-}34)$$

$$[B_2H_7]^- \longrightarrow B_2H_6 + e^- + 1/2H_2 \qquad (1\text{-}35)$$

Diborane has also been produced by electrolysis of $[BH_4]^-$ in DMF[87] whereas in dimethylamine the product obtained is dimethylamine borane.[88] Ethylamine borane has been obtained from a similar reaction[89] at an inert electrode such as platinum.

1.5.4 $[BH_3(CN)]^-$

The cyclic voltammetry of $[BH_3(CN)]^-$ has been examined at various metal electrodes in acetonitrile.[90,91,92] No oxidation was observed at inert electrodes (e.g. Pt), whereas several "reactive" electrodes (e.g. Fe, Cu, Co, Ni) led to the formation of metallacyanoborane derivatives. However, Mo or V electrodes resulted in oxidation of the $[BH_3(CN)]^-$ ion at Ep ca. + 0.9V $(Ag/AgNO_3)^*$ to give the anion $[BH_3(CN)BH_2(CN)]^-$ by the process:

$$[BH_3(CN)]^- \rightarrow [BH_2(CN)] + e^- + H^\bullet \qquad (1\text{-}36)$$

$$[BH_2(CN)] + [BH_3(CN)]^- \rightarrow [BH_3(CN)BH_2(CN)]^- \qquad (1\text{-}37)$$

$$H^\bullet \rightarrow 1/2\ H_2 \qquad (1\text{-}38)$$

The $[BH_3(CN)BH_2(CN)]^-$ ion has also been prepared by chemical oxidation with Hg_2Cl_2[93] or HCl[94] in THF. Dissolution of Fe with $Na[BH_3(CN)]$ in the presence of $(CH_3)_3P$ or $(CH_3CH_2O)_3P$ ligand gave cis-trans mixtures of $\{Fe[(RO)_3P]_4[BH_3(CN)]\}$[91] Similarly anodic dissolution of Co or Ni in acetonitrile solutions of $Na[BH_3(CN)]$ yielded octahedral and tetrahedral metallacyanoborane complexes.

1.5.5 $[B_3H_8]^-$

Chronopotentiometry and exhaustive controlled potential electrolysis[95] experiments have shown that $[B_3H_8]^-$ undergoes a one electron oxidation in acetonitrile and dimethylformamide at a platinum or gold anode to yield $B_3H_7[CH_3CN]$ or $B_3H_7[DMF]$.

$$[B_3H_8]^- \xrightarrow{CH_3CN} B_3H_7[CH_3CN] + 1/2H_2 + e^- \qquad (1\text{-}39)$$

* + 0.34V vs S.C.E.

The chronopotentiometric oxidation wave occurred near +0.4V (Ag/Ag Cl/LiCl).*

Anodic dissolution of Cu or Ag in an acetonitrile solution of $[B_3H_8]^-$ with added triphenylphosphine ligand produced the metallaboranes $[Cu(PPh_3)_2B_3H_8]$ and $[Ag(PPh_3)_2B_3H_8]$.[96] However, at Zn or Cd anodes electrolysis of $[B_3H_8]^-$ led to metal dissolution but the only products isolated were $B_3H_7[Ph_3P]$, $[Ph_3P]BH_3$ and $[Ph_3P]B_2H_4$.

It has been shown that substitution of $[B_3H_8]^-$ ion with $[NCS]^-$ and $[NCBH_3]^-$ results in an increased oxidative stability.[97] It has also been shown that copper dissolution in an acetonitrile solution of $[B_3H_7(NCBH_3)]^-$ with two equivalents of added triphenylphosphine ligand yields the metallaborane $[Cu(PPh_3)_2B_3H_7NCBH_3]$ in which the Cu is in a tetrahedral environment and is bonded via two Cu-H-B bridge bonds to the BH_3 moiety of the cyano substituent.

1.5.6 $[B_9H_{14}]^-$

Oxidation of $Cs[B_9H_{14}]$ in acetonitrile (0.1M $LiBF_4$) at a platinum electrode at low current density was shown to yield crystals identified as $B_9H_{13}[NCCH_3]$ by x-ray crystallography.[98]

The derivatives $[B_9H_{13}(NCS)]^-$ and $B_9H_{13}[SMe_2]$ both showed two electron oxidations at +0.99V and +1.42V respectively (Ag/0.1M$AgNO_3$; +0.34V vs S.C.E.) although the products from potential electrolysis were not characterised.[99]

* +0.19V vs S.C.E.

1.5.7 $B_{10}H_{14}$

The electrochemical behaviour of decaborane (14) has been studied in great detail. The chemical reduction of $B_{10}H_{14}$ was shown to be both solvent and time dependent.[103,104] Detailed electrochemical studies in acetonitrile and glyme have shown[100-102] that the reduction of $B_{10}H_{14}$ is mechanistically complex. In glyme solution (0.1MBu_4NClO_4) decaborane gave two polarographic reduction waves at $E_{1/2}$ = -1.54 V and -2.75V (Ag/$AgNO_3$ satd.) and no apparent oxidation waves.[100] Under the conditions studied, at the first wave, plots of instantaneous limiting current vs. (mercury column height)$^{1/2}$ were linear with intercepts at or near the origin indicating a diffusion controlled process. A plot of log [(id-i)/i] vs potential was also linear with a slope of 0.06V. These data are indicative of a primary reduction step of $B_{10}H_{14}$ involving one electron.

$$B_{10}H_{14} + e^- \rightarrow B_{10}H_{14}^{\cdot -} \qquad (1\text{-}40)$$

The total absence of kinetic character and the diffusion controlled character of the limiting current first wave indicates that there is no preceding chemical reaction such as:

$$B_{10}H_{14} \underset{k_r}{\overset{k_f}{\rightleftharpoons}} H^+ + B_{10}H_{13}^- \qquad (1\text{-}41)$$

where the electroactive species is H^+ or $B_{10}H_{13}^-$. The cyclic voltammograms for $B_{10}H_{14}$ in glyme[100] after the application of several triangular wave cycles in a multicycle experiment (ie. approximately steady state) in which the potential sweep did not encompass the second reduction wave are shown in Figure 1.9.

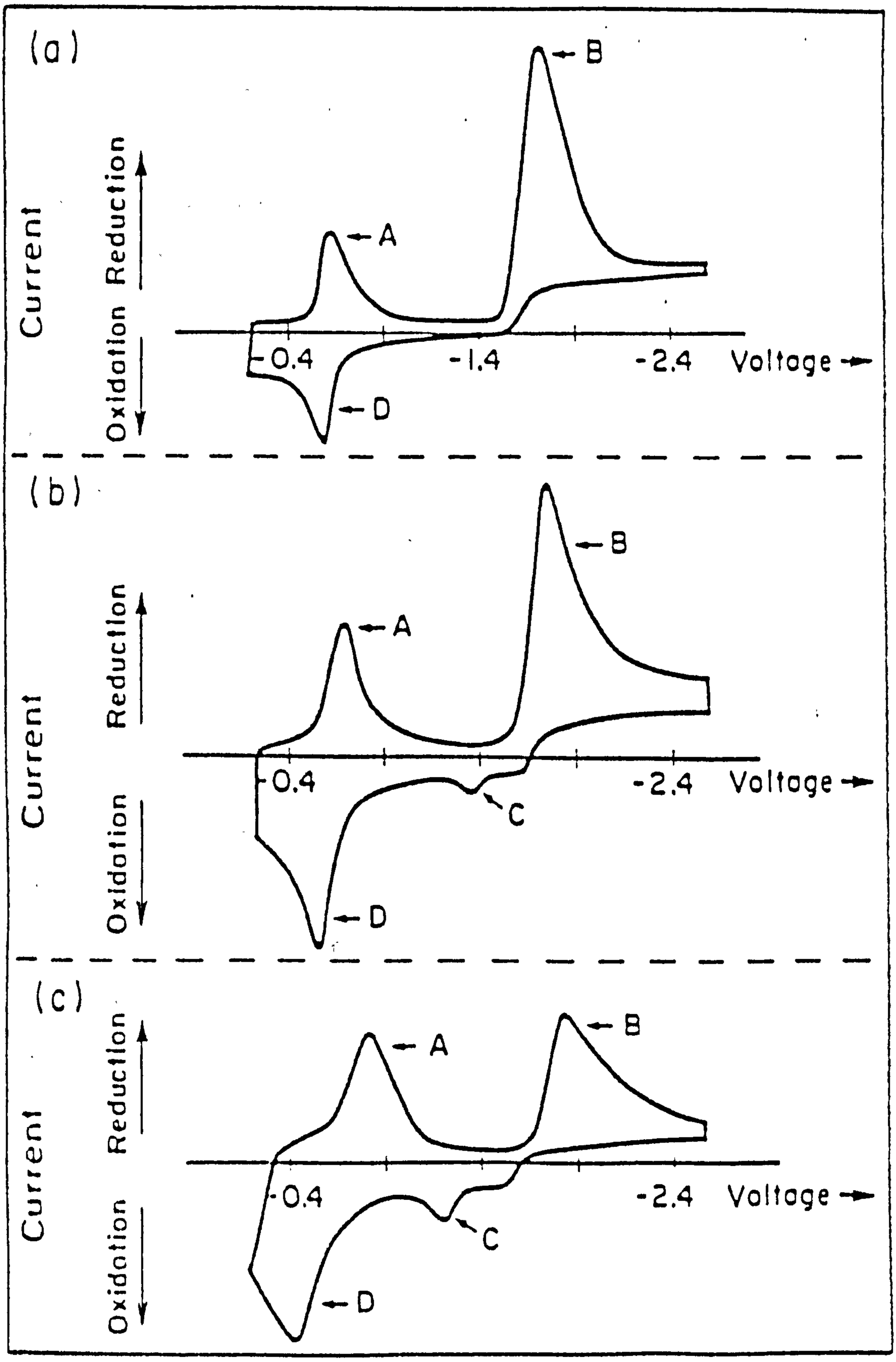

Figure 1.9 Cyclic voltammograms of $B_{10}H_{14}$ (0.99×10^{-3}M; 0.1 M Bu_4NClO_4 in 1,2-dimethoxyethane) with scan rates (a) 0.88 Vs^{-1} (b) 1.9Vs^{-1} and (c) 5.5Vs^{-1}

Wave B corresponded to the first reduction wave of $B_{10}H_{14}$. Waves A, C and D were not observed unless wave B was included in the potential sweep, indicating that these waves were related to, and subsequent to the initial reduction step (wave B). The magnitude of wave C decreased as scan rate decreased and temperature increased indicating that wave C represents the oxidation of a transient intermediate. The magnitude of wave C decreased relative to other waves as the concentration of $B_{10}H_{14}$ was increased, suggesting that this species decomposed by a second order (or higher) reaction. The characteristics of wave C were not significantly influenced by whether or not waves A and D were included in the potential sweep. This shows that the electrode reaction associated with the reversible couple A and D neither served as the origin nor influenced the depletion of the transient species produced at C. From this evidence the wave at C has been assigned to the oxidation of the radical anion $[B_{10}H_{14}]^{\cdot -}$ However, the substantial overvoltage separating the reduction step (B) and the oxidation step (C) suggested that the species which produced wave C was not the product of the initial electron transfer step, $[B_{10}H_{14}]^{\cdot -}$, but was due to a species resulting from a unimolecular transformation of the primary electrolysis product. Unlike wave C, the sweep-rate dependence of waves A and D suggested that they arose from a product of $B_{10}H_{14}$ reduction that was stable during the cyclic voltammetric experiment. These waves were assigned to the redox processes of $[B_{10}H_{13}]^{\cdot -}$ The presence of $[B_{10}H_{15}]^{-}$ in the solution was deduced from the overall stoichiometry of the electrode reaction. Constant potential electrolysis at the first reduction wave (B) gave a solution whose U.V. spectrum and polarogram supported

the presence of equimolar quantities of $[B_{10}H_{13}]^-$ and $[B_{10}H_{15}]^-$. The overall proposed mechanism was:[100]

$$B_{10}H_{14} + e^- \rightleftharpoons \{[B_{10}H_{14}]^-\} \qquad (1\text{-}42)$$

$$\{[B_{10}H_{14}]^-\} \rightleftharpoons [B_{10}H_{14}]^- \qquad (1.43)$$

$$2[B_{10}H_{14}]^- \rightleftharpoons [B_{10}H_{13}]^- + [B_{10}H_{15}]^- \qquad (1\text{-}44)$$

$$2B_{10}H_{14} + 2e^- \rightarrow [B_{10}H_{13}]^- + [B_{10}H_{15}]^- \qquad (1\text{-}45)$$

The oxidation wave due to the postulated $[B_{10}H_{14}]^-$ was not observed up to the limit of the instrumentation used, however, polarographic data supports such a unimolecular decomposition after the one electron charge transfer step. A plot of log $[(i_d-i)/i]^{2/3}$ vs. potential was not linear with a slope of 0.06V indicating that the second order decomposition (e.g. 1-45) was not directly coupled to a reversible one electron charge transfer step (wave B).

The second reduction step has also been studied in detail with glyme solutions.[101] It was assigned to the one electron reduction of $[B_{10}H_{13}]^-$ forming the dianion $[B_{10}H_{13}]^{2-}$ which rapidly disproportionates forming $[B_{10}H_{14}]^{2-}$. The $[B_{10}H_{14}]^{2-}$ in turn reacts rapidly with bulk $B_{10}H_{14}$ to generate more electroactive $[B_{10}H_{13}]^-$. The overall reaction at the second reduction wave corresponded to:

$$4B_{10}H_{14} + 6e^- \rightarrow [B_{10}H_{12}]^{2-} + [B_{10}H_{14}]^{2-} + 2[B_{10}H_{15}]^- \qquad (1\text{-}46)$$

A reaction between $[B_{10}H_{15}]^-$ and $[B_{10}H_{12}]^{2-}$ generating $[B_{10}H_{13}]^-$ appeared to contribute to the electrode reaction over the longer times

of constant potential electrolysis experiments (1-2hr.), so that the net reaction under these conditions was:

$$B_{10}H_{14} + 2e^- \rightarrow [B_{10}H_{14}]^{2-} \qquad (1\text{-}47)$$

Constant potential coulometry at the first reduction wave of $B_{10}H_{14}$ in acetonitrile and dichloromethane solutions[102] gave an n value of about one electron per $B_{10}H_{14}$ molecule. ^{11}B n.m.r. showed that the electrolysis product was an equimolar mixture of $[B_{10}H_{13}]^-$ and $[B_{10}H_{15}]^-$. The reduction in these solvents has however been postulated as a two electron irreversible step on the basis of detailed analysis of the cyclic voltammograms. The formal reduction potential for the $B_{10}H_{14}/[B_{10}H_{14}]^{2-}$ couple in acetonitrile being -0.78 ± 0.02V (vs. S.C.E.).

$$B_{10}H_{14} + 2e^- \longrightarrow [B_{10}H_{14}]^{2-} \qquad (1\text{-}48)$$

$$B_{10}H_{14} + [B_{10}H_{14}]^{2-} \underset{k_{-1}}{\overset{k_1}{\rightleftharpoons}} [B_{10}H_{13}]^- + \{[B_{10}H_{15}]^-\} \qquad (1\text{-}49)$$

$$\{[B_{10}H_{15}]^-\} \xrightarrow{k_2} [B_{10}H_{15}]^- \qquad (1\text{-}50)$$

The kinetically important step after charge transfer in both the reduction of $B_{10}H_{14}$ and the oxidation of $[B_{10}H_{14}]^{2-}$ was a proton transfer between $B_{10}H_{14}$ and $[B_{10}H_{14}]^{2-}$. The rate constant for this reaction in acetonitrile was ca. $5\times10^4 M^{-1}s^{-1}$ at 24°C. Therefore, on the short time scale of the polarographic experiment there is a considerable mechanistic difference in the redox characteristics of $B_{10}H_{14}$ in glyme[100] vs. acetonitrile[102] and dichloromethane.[102] However, on a constant potential electrolysis time scale the final reaction products are the same.

1.5.8 $B_{10}H_{12}[CH_3CN]_2$

The cyclic voltammograms of $B_{10}H_{12}[SMe_2]_2$ and $B_{10}H_{12}[CH_3C(NEt_2)_2NH_2]_2$ were very similar to that of $B_{10}H_{12}[CH_3CN]_2$ implying similar electrochemical behaviour. The cyclic voltammogram of $B_{10}H_{12}[CH_3CN]_2$ in acetonitrile at platinum consisted of two irreversible oxidation waves at Ep + 0.75V and Ep + 1.2V ($Ag/AgNO_3$) with no well defined corresponding reduction waves.[105] A broad reduction wave at Ep - 0.8V which appeared after scanning to anodic potentials was interpreted as H^+ reduction. Exhaustive controlled potential electrolysis of $B_{10}H_{12}[CH_3CN]_2$ at +0.9V indicated that the first oxidation involved two electrons. Two minor components of the reaction mixture were identified as $B_9H_{13}[CH_3CN]$ and nido - $B_{10}H_{10}[CH_3CN]_2$. Part of the overall electrochemical oxidation was thought to be:

$$B_{10}H_{12}[CH_3CN]_2 \longrightarrow B_{10}H_{10}[CH_3CN]_2 + 2H^+ + 2e^- \quad (1\text{-}51)$$

1.5.9 $[B_nH_n]^{2-}$ Anions

Polarographic data for several $[B_nH_n]^{2-}$ polyhedral anions[106-109] and halogenated derivatives of the B_{10} and B_{12} cages,[110] have been reported as a criterion of their comparative oxidative stabilities. The order of oxidative stability was $B_7 < B_6 < B_9 < B_8 < B_{11} < B_{10} < B_{12}$, the oxidation potentials being listed in Table 1.1. All of these anions were studied in aqueous solution. The halogenation of the B_n cage increased the oxidative stability, although the nature of the various oxidation products was not studied. Substitution with $[OH]^-$ decreased the oxidative stability of the anions.[111]

TABLE 1.1

Electrochemical Data on Boranes and Borane Anions.

Compound	$E1/_2$ (V)	Comments	Ref.
$[B_3H_8]^-$	+0.40	chronopentiometric ; Ag/AgCl/LiCl	95
$[B_6H_6]^{2-}$	-0.33	0.5M aq. K_2SO_4 ; Pt ; SCE	106
$[B_7H_7]^{2-}$	-		106
$[B_8H_8]^{2-}$	-0.04	"	106
$[B_9H_9]^{2-}$	-0.15	"	106
$[B_9H_{14}]^-$	-	-	98
$[B_{10}H_{10}]^{2-}$	+0.40	$Ep/_2$; CH_3CN ; Pt ; SCE	178,112
$[2\text{-}B_{10}H_9I]^{2-}$	+0.53	"	178
$[1\text{-}B_{10}H_9I]^{2-}$	+0.53	"	178
$[2\text{-}B_{10}H_9NH_3]^-$	+0.78	"	178
$[1\text{-}B_{10}H_9NH_3]^-$	+0.75	"	178
$[2\text{-}B_{10}H_9NMe_3]^-$	+0.90	"	178
$[1\text{-}B_{10}H_9NMe_3]^-$	+0.88	"	178
$[2\text{-}B_{10}H_9SMe_2]^-$	+0.92	"	178
$[1\text{-}B_{10}H_9SMe_2]^-$	+0.92	"	178
$B_{10}H_{14}$	-1.54	glyme ; $Ag/AgNO_3$	100,101
	-2.75	CH_3CN ; SCE	102
$B_{10}H_{12}(NCMe)_2$	+0.75	irreversible, CH_3CN, Pt,	105
	+1.20	$Ag/AgNO_3$	
$[B_{11}H_{11}]^{2-}$	+0.05	$Ep/_2$ at stationary Pt ; SCE, CH_3CN	179
$[B_{11}H_{14}]^-$	+1.60	$Ep/_2$ at stationary Pt ; SCE, CH_3CN	179

TABLE 1.1 (Cont.)

$[B_{11}H_{13}]^{2-}$	-0.45	$Ep/_2$ at stationary Pt ; SCE, CH_3CN	179
$[B_{11}H_{13}]^{2-}$	-0.45	"	179
$[B_{12}H_{12}]^{2-}$	+1.43	$Ep/_2$; Pt ; SCE	118, 119
	+1.50	RPE ; CH_3CN ; SCE	119
$[B_{12}H_{11}I]^{2-}$	+1.88	$Ep/_2$; Pt ; SCE	119
$[B_{12}H_6Br_6]^{2-}$	+2.00	"	119
$[B_{12}Br_{12}]^{2-}$	+2.20	"	119
$[B_{12}Cl_{10}H_2]^{2-}$	+2.20	"	119
$[B_{20}H_{19}]^{3-}$	+0.70	Ep anodic ; Pt ; SCE	112
	-0.10	Ep cathodic ; $H^+ \rightarrow \frac{1}{2}H_2$	
$[B_{20}H_{18}]^{2-}$	-1.48	DME ; SCE	112
$[B_{24}H_{23}]^{3-}$	+1.74	Pt ; CH_3CN ; SCE	119
$[B_{24}H_{21}I_2]^{3-}$	+1.19	"	119
$[B_{24}Br_7H_{16}]^{3-}$	+0.78	"	119
$[B_{24}Br_{10}H_{13}]^{3-}$	+0.98	"	119
$[B_{24}Br_{11}H_{12}]^{3-}$	+1.14	"	119
$[B_{24}Br_{14}H_8]^{4-}$	+1.30	"	119
$[B_{24}Br_{18}H_4]^{4-}$	+1.30	"	119
$[B_{24}Cl_{18}H_4]^{4-}$	+1.76	"	119

1.5.10 $[B_{10}H_{10}]^{2-}$

Various electrochemical techniques have been used to elucidate the mechanism and reaction products of $[B_{10}H_{10}]^{2-}$ at a platinum electrode in acetonitrile.[112] This work represented the first application of non-aqueous polarography utilising operational amplifier circuitry with a three electrode system along with the methods of cyclic voltammetry and chronopotentiometry to boron hydrides. The chemical oxidation of $[B_{10}H_{10}]^{2-}$ (by Fe^{3+} and Ce^{4+}) gave $[B_{20}H_{18}]^{2-}$ [113-117] and under milder conditions the one electron oxidation product, $[B_{20}H_{19}]^{3-}$, was isolated.[115-117] Voltammetry of $[B_{10}H_{10}]^{2-}$ at a rotating platinum electrode (R.P.E) produced two anodic waves. Several electrochemical techniques have been used to establish that the oxidation proceeds via an initial reversible one electron transfer to form a free radical that undergoes a second order chemical reaction to form $[B_{20}H_{19}]^{3-}$ which was further oxidised to $[B_{20}H_{18}]^{2-}$ at a slightly greater potential than that at which $[B_{10}H_{10}]^{2-}$ was oxidised.[112] The second order rate constant for the chemical coupling reaction, as determined by chronopotentiometry with current reversal, was $k=2.8\times10^{3} mol^{-1}s^{-1}$. The overall reaction scheme was:

$$[B_{10}H_{10}]^{2-} \longrightarrow [B_{10}H_{10}]^{-} + e^{-} \qquad (1\text{-}52)$$

$$2[B_{10}H_{10}]^{-} \longrightarrow [B_{20}H_{19}]^{3-} + H^{+} \qquad (1\text{-}53)$$

$$[B_{20}H_{19}]^{3-} \longrightarrow [B_{20}H_{18}]^{2-} + 2e^{-} + H^{+} \qquad (1\text{-}54)$$

The products $[B_{20}H_{19}]^{3-}$ and $[B_{20}H_{18}]^{2-}$ have been isolated by constant potential electrolysis at a rotating platinum gauze electrode with 0.1M $LiClO_4$ as supporting electrolyte. The initial one electron oxidation product was consumed too quickly by the bimolecular reaction,

(1-53), to be isolated, but fast scan cyclic voltammetry has established the reversible nature of the oxidation. Cyclic voltammetry of a solution of $[N(CH_3)_4]_3[B_{20}H_{19}]\cdot 1/2H_2O$ showed an anodic wave at ca. +0.7V (vs. S.C.E.) and a cathodic wave at ca. -0.1V that increased on each cycle and was assumed to be due to the protons liberated by the oxidation of $[B_{20}H_{19}]^{3-}$ to $[B_{20}H_{18}]^{2-}$. The former wave corresponded to the second anodic wave of $[B_{10}H_{10}]^{2-}$. There was no evidence that the oxidation of $[B_{20}H_{19}]^{3-}$ was reversible within the scan rates and potential limits available. At a dropping mercury electrode (D.M.E.) a solution of $[N(CH_3)_4]_2[B_{20}H_{18}]$ displayed a cathodic wave at 1.48V (vs. S.C.E.)

1.5.11 $[B_{12}H_{12}]^{2-}$

Voltammetry of $[N(C_2H_5)_4]_2[B_{12}H_{12}]$ at a rotating platinum electrode (R.P.E.) in acetonitrile with 0.1M$[N(C_2H_5)_4]$ $[ClO_4]$ as supporting electrolyte gave a one electron anodic wave at $E_{1/2}$ = +1.5V (vs. S.C.E.).[117,118] Constant potential electrolysis at +1.45V with a graphite cloth anode, in the presence of supporting electrolyte, and precipitation of the oxidation product with CsF yielded $Cs_3[B_{24}H_{23}]\cdot 3H_2O$. The structure of the dimeric oxidation product has been postulated as consisting of two B_{12} polyhedra joined by a bridge hydrogen, analogous to $[B_{20}H_{19}]^{3-}$.

Although $[B_{24}H_{23}]^{3-}$ has been reported to be resistant to further oxidation without degradation, its partially halogenated derivative $[B_{24}H_{21}(I)_2]^{3-}$[119] can undergo a two electron oxidation in acetonitrile at +1.3V

(vs.S.C.E.) to yield $[B_{24}H_{20}(I)_2]^{2-}$,[120] which is a derivative of the hypothetical parent oxidation production $[B_{24}H_{22}]^{2-}$. Spectroscopic evidence[120] has supported a structure for $[B_{24}H_{20}(I)_2]^{2-}$ analogous to that of the photo-isomer of $[B_{20}H_{18}]^{2-}$.

1.6 2-Dimensional N.M.R. Spectroscopy

1.6.1 Introduction

The power of n.m.r. as a tool for the study of molecular structure has grown steadily with the introduction of stronger magnetic fields, heteronuclear and multiple-frequency experiments, spin decoupling[121] and recently two-dimensional (2.D.) n.m.r.[122] In boron cluster chemistry n.m.r. utilising the ^{11}B nucleus has been important in the characterisation of polyhedral cage structures.[123] However, using ^{11}B n.m.r. as a structural probe for polyhedral structures has serious limitations that become increasingly conspicuous as more complex borane and heteroborane species are synthesised. The primary difficulties encountered in ^{11}B n.m.r. are broad signals (50-150H_z), partly due to unresolved $^{11}B-^{11}B$ coupling,[124] and the absence of a generally applicable theory of ^{11}B chemical shifts. The first of these problems is partly overcome by high-field (>4T) instruments; coupling information is normally restricted to first-order boron-terminal hydrogen interactions as $^{11}B-^{11}B$ coupling is seldom observable even using line-narrowing techniques.[125] The presence of the ^{10}B isotope (I=3, 20% abundance) introduces a further complication via coupling with the ^{11}B nucleus.

The second problem is intrinsic to boron cages. Unlike the chemical shifts exhibited by ^{13}C and ^{1}H nuclei, $^{11}B(I=^{3}/2$, 80% abundance) exhibits few general, reliable correlations with molecular structure. The ^{11}B chemical shifts are largely determined by the paramagnetic term σ_p in Ramsey's equation[126] and can vary considerably with minor variations in structure.

Frequently it is the case that the ^{11}B n.m.r. spectrum of a boron cluster of unknown geometry conveys little more than symmetry information and unambiguous assignment of ^{11}B n.m.r. spectra may require laborious studies involving isotopic labelling or single frequency decoupling experiments.[123(a)]

The first 2-Dimensional n.m.r. experiments involving the ^{11}B nucleus utilised the heteronuclear ^{1}H—^{11}B interaction and revealed correlations between boron resonances and directly bound protons.[128] Recently however, the Jeener 2-D procedure has been successfully applied to homonuclear ^{11}B-^{11}B quadrupolar systems.[127] This technique, based on J-correlated 2-Dimensional spectroscopy, has been developed for the direct determination of boron-boron atom connectivities in all types of boron clusters.

1.6.2 Description of the Technique

(a) Fourier Transform N.M.R.

Recalling the basic principles of the Fourier transform n.m.r.experiment[129] the resonance signals of different Larmor frequency, of the nucleus of interest in the chosen spectral window form the macroscopic

magnetisation,M of magnitude M_o, parallel to the applied external field B_o (Figure 1.10(a)).

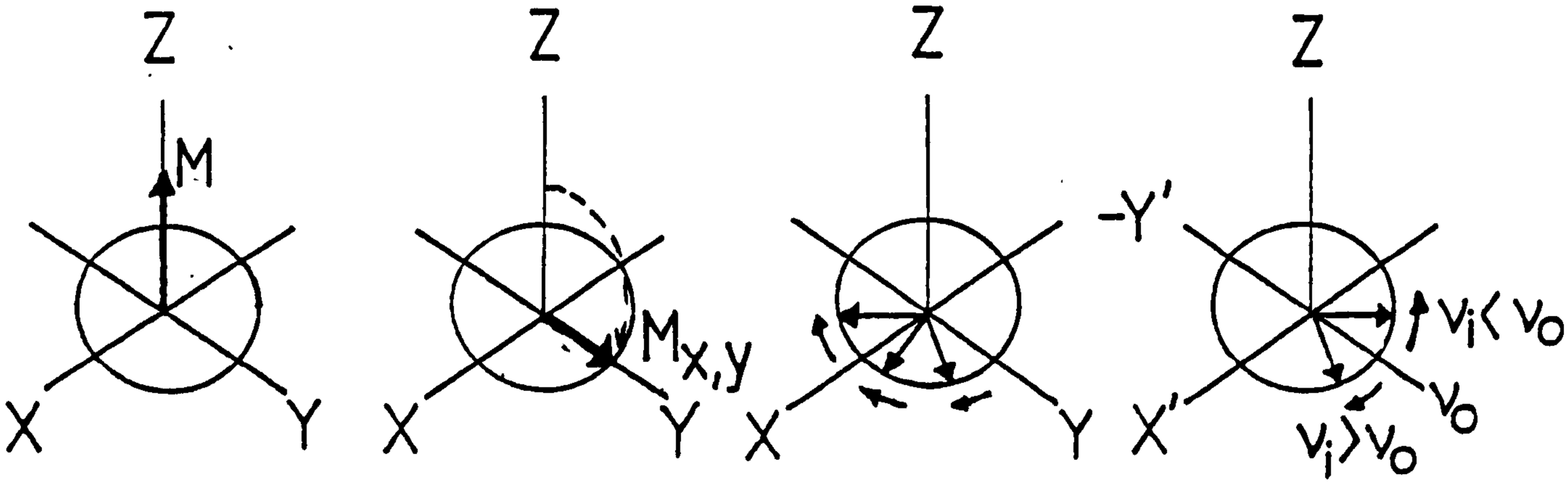

Figure 1.10 The F.T. NMR experiment.

A strong radio frequency (R.F.) field B_1 (i.e. a radio frequency pulse) produced by a radio frequency coil on the x-axis carries M away from the z-axis. The duration and power of the R.F. pulse determines the direction of M after the pulse. If a 90°_x, or $\Pi/2$, pulse is applied, M points along the positive y-axis (Figure 1.10(b)). The longitudinal or z-magnetisation is thus transformed into a transverse magnetisation. This process requires 5-20μs with the power of the R.F. sources used in modern spectrometers.

The Larmor Frequencies of the various nuclear magnetic moments vary and, as a consequence, the vector M now splits into its components (Figure 1.10 (c)). The magnetic vectors rotating in the x,y-

plane produce a voltage in the receiver coil that is detected as the n.m.r. signal. Plotting, for an individual vector, the time dependence of the intensity of its y-component (i.e. the voltage, U,) induced in the receiver coil, and if transverse relaxation is taken into account, i.e. the loss of transverse magnetisation as a consequence of relaxation processes, a damped oscillation of frequency ν_1 results that is known as the free induction decay (F.I.D.) (Figure 1.11).

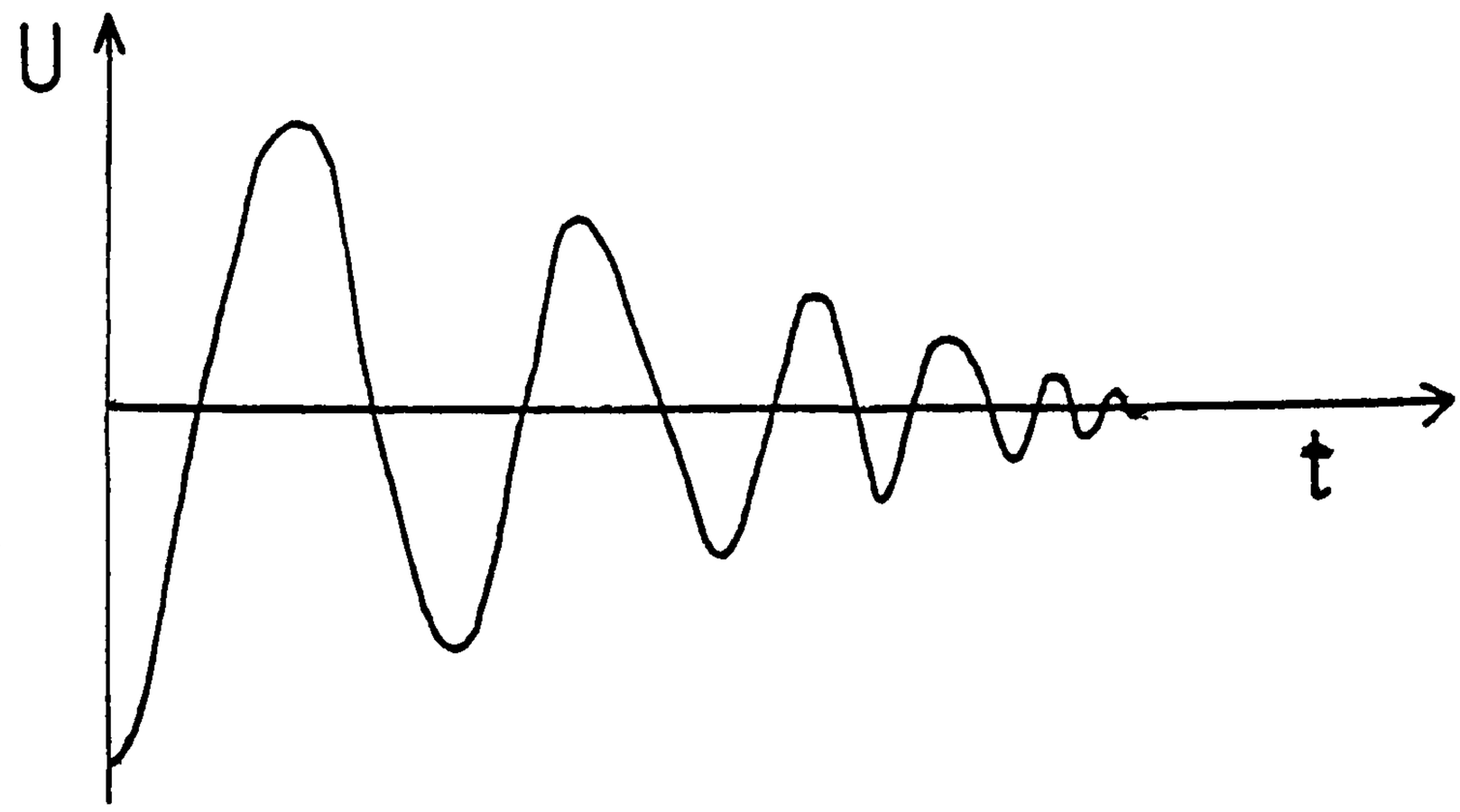

Figure 1.11 Free induction decay of an NMR line.

Fourier transformation of this time signal yields the n.m.r. signal or spectrum. The frequency measured is the difference between the transmitter or carrier frequency, ν_o, and the Larmor frequency, ν_1, of the particular spin.

For the description of n.m.r. experiments the concept of the rotating frame of reference is convenient.[130] It uses a co-ordinate system

K' that rotates in the same sense and with the same frequency, ν_o, as the rotating field vector of the R.F. field. Within the rotating frame, vectors that correspond to signals with frequencies $\nu_1 > \nu_o$ rotate clockwise, whereas those corresponding to signals with a $\nu_1 < \nu_o$ rotate anti-clockwise, a signal with $\nu_1 = \nu_o$ is static in the rotating frame of reference (Figure 1.10(d)).

(b) 2D N.M.R.

In the 2D experiment the data are collected as a t_1, t_2 matrix. The matrix is then double Fourier transformed to yield a frequency spectrum that reveals the presence of connectivity patterns between various nuclei.[122,131] The 2D spectra contain two types of peak, those lying along the diagonal (Figure 1.12), and the off-diagonal or cross peaks. The plots are symmetrical about the diagonal so that the cross peaks are found at δ_1, δ_2 and at δ_2, δ_1 The off-diagonal cross peaks arise from spin-spin ^{11}B-^{11}B coupling, which for boron containing clusters is only significant for adjacent nuclei. Therefore, the atom connectivities in the polyhedral framework are disclosed. These coupling patterns are normally observable even when, as is usually the case, no ^{11}B-^{11}B coupling is observed in the 1-D spectrum.

The COSY (correlated spectroscopy) pulse sequence involves 16 cycles and may be written as:

$$T_w \rightarrow (\Pi/2)\Phi_1 \rightarrow t_1 \rightarrow (\Pi/2)\Phi_2 \rightarrow t_2 \text{ (acquisition)}_\psi$$

Where T_w is a time sufficient for the system to reach thermal

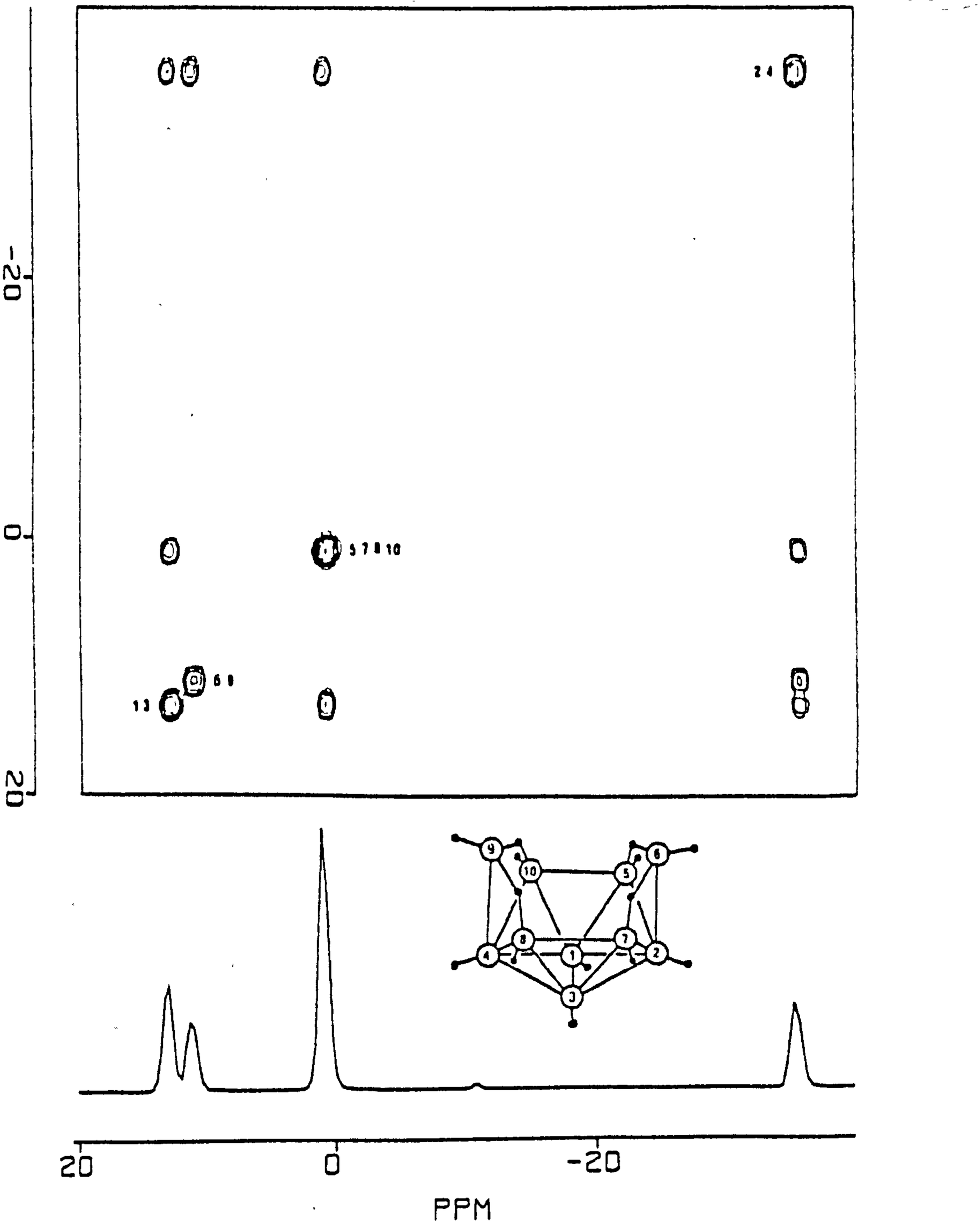

Figure 1.12 The 2-D ^{11}B COSY spectrum (contour plot) of $B_{10}H_{14}$ in C_6D_6. The $^{11}B\{^1H\}$ n.m.r. spectrum is plotted along one axis.

equilibrium. The first 90°, or $\pi/2$, pulse creates transverse magnetisation as in the routine 1-Dimensional experiment, the spins are allowed to process for a time t_1 so that they become frequency labelled. A t_1,t_2 data array is built up by incrementing t_1 by the inverse of the sweep width for the first frequency domain F_1. At the end of t_1 a second 90° pulse is applied that transfers the magnetisation between coupled spins so that the observed spin reflects a modulation based in the chemical shift difference $(\delta_A - \delta_B)$ of the two scalar coupled spins. After the second pulse the transverse magnetisation is acquired for t_2 as in any 1-D spectrum.

The phase shifts Φ_2 and ψ suppress axial peaks and allow quadrature detection in both dimensions.[132] The time domain data matrix $S(t_1,t_2)$ collected is double Fourier transformed to give a frequency domain spectrum $S(F_1,F_2)$. The resulting spectra are presented either as a "stacked" plot, from which relative intensities of cross peaks and diagonal peaks can be determined, or as absolute value contour plots on which the x and y axes represent ^{11}B chemical shifts and resonance intensities are represented in the z direction as contours.

It has been reported that for boron containing clusters a general observation is that coupling between hydrogen bridged boron nuclei is usually absent,[127(a)] which is in agreement with earlier theoretical predictions which stated that the electron density in B-H-B bridge bonds is negligible on the B-B vector. For $B_{10}H_{14}$ Figure 1.12 shows no cross peak between B(5,7,8,10), identified by the unique signal of area 4,, and the resonance at δ 9.0p.p.m. indicating that these sets

of resonances are hydrogen bridged. Therefore, the resonance at δ 9.0p.p.m. represents the apical B(6,9) positions. The resonance at δ -36.0p.p.m. shows a correlation with all other resonances and can therefore be assigned to B(2,4). The final resonance at low field (high frequency) must therefore be due to the remaining B(1,3) nuclei.

Only two cases have been reported[127(a)] in which a correlation is observed between hydrogen bridge boron nuclei. One is for nido - {1,2,3-$[C_6(CH_3)_6]Fe(C_2H_5)_2C_2B_3H_5$}.[134] The correlation observed here may be explained by assuming that the delocalisation of electron density about the basal C_2B_3 ring is greater in the iron complex (resembling the isoelectronic $[C_5H_5]^-$), than in $[(C_2H_5)_2C_2B_4H_6]$ and other B-X-B bridge compounds. In the ferracarbaborane the B-H-B bridge bonds are assumed to approach "protonated double bond" character. The only other reported[127(a)] example where a correlation is observed between hydrogen bridged boron nuclei is in the cobaltaborane $[2\text{-}(C_5H_5)CoB_4H_8]$[135] which is an analogue of B_5H_9. An explanation of the observed correlation in this cluster is not readily apparent, however one theoretical description[136] suggests that replacing BH in B_5H_9 by $[Co(C_5H_5)]$ leads to enhanced boron-boron bonding in the cluster, however aspects of this theoretical study have recently been questioned.[137]

CHAPTER TWO

PREPARATION AND CHARACTERISATION OF SUBSTITUTED OCTAHYDROTRIBORATE ANIONS

2.1 Introduction

It has been shown that the octahydrotriborate (1-) anion can be substituted to form a series of halogenated octahydrotriborate anions, $[B_3H_7(X)]^-$ (.X=F,Cl,Br) by stoichiometric reaction with the respective mercurous halide.[36] It has further been shown that the chloride substituent of $[B_3H_7(Cl)]^-$ was labile and could be replaced by more nucleophilic anions to give $[B_3H_7(X)]^-$(X=NCS,[36] $NCBH_3$,[36] NC[37] and NCO[37]). In addition it was found that by treating the monosubstituted octahydrotriborate (1-) ion with gaseous HCl, in a non-coordinating solvent, the disubstituted derivatives,[37] $[B_3H_6(X)(X')]^-$ (X=Cl and X' = Cl,NCS,$NCBH_3$ and $NCBH_2Cl$) could be produced. In this chapter the preparation and reactions of some novel mono- and disubstituted derivatives of the octahydrotriborate (1-) ion are discussed.

2.2 Results and Discussion

2.2.1 Preparations and Reactions

It has previously been shown that treatment of tetrahydrofuran (T.H.F) solutions of $[B_3H_8]^-$ with mercurous or mercuric chloride gave the adduct B_3H_7[THF] as the major product.[138] Similarly the reaction between $[B_3H_8]^-$ and HCl in dimethylformamide (DMF) gave B_3H_7[DMF].[95]

In contrast to these reactions, the reaction of the $[NBu^n_4]^+$ or $[N(PPh_3)_2]^+$ salts of $[B_3H_8]^-$ with Hg_2X_2 (X=F,Cl,Br)[36] resulted in oxidation and halogenation of the borane anion to give the product $[B_3H_7(X)]^-$. In the chlorination reaction small amounts of the dichlorinated anion $[B_3H_6(Cl)_2]^-$ were formed. This dichlorinated species

was formed exclusively by the reaction of $[B_3H_8]^-$ with two equivalents of Hg_2Cl_2 (reactions (1-18) and (1-19) in Chapter I).

The reaction between HCl and $[NBu^n_4][B_3H_8]$ in CH_2Cl_2 was reported[33] to yield the anion $[B_3H_7(Cl)]^-$ exclusively, but it was found that appreciable amounts (10-30%) of $[B_3H_6(Cl)_2]^-$ were also formed.[99] This testified to the greater reactivity and hence diminished selectivity of HCl over Hg_2Cl_2 with respect to chlorination.

In addition it was reported[36] that the chloride substituent of $[B_3H_7(Cl)]^-$ was labile and was readily substituted by ions such as $[NCS]^-$ and $[NCBH_3]^-$ offering a preparative route to potentially more interesting species(reaction (1.20)).It was initially thought that the reaction between AgCN and $[B_3H_7(Cl)]^-$ in CH_2Cl_2 resulted in $[CN]^-$ displacing the chloride substituent to give the product $[B_3H_7(NC)]^-$[36] However, it was shown by x-ray diffraction[37] that the anion obtained was $[Ag\{B_3H_7(NC)\}_2]^-$ in which two triborane cages are connected via a linear NC-Ag-CN bridge.

In this work several new substituted octahydrotriborate anions are reported and discussed. The reaction of the $[N(PPh_3)_2]^+$ salts of $[NCSe]^-$,$[NCBPh_3]^-$ and $[NCBH_2NCBH_3]^-$ with $[N(PPh_3)_2][B_3H_7(Cl)]$ in dichloromethane resulted in displacement of the labile chloride substituent by the more negatively charged donors to yield the products $[B_3H_7(X)]^-$ (X=NCSe,$NCBPh_3$,$NCBH_2NCBH_3$). In addition, using the novel ion, $[BH_2(CN)_2]^-$ it was possible to substitute one cage to form

$[B_3H_7(NCBH_2CN)]^-$, or two cages to give $[B_3H_7(NCBH_2CN)B_3H_7]^-$, in which the ligand is effectively bridging the cages.

Furthermore, it was found that by treating $[N(PPh_3)_2][B_3H_8]$ with the pseudo-halogens, cyanogen bromide (CNBr) or cyanogen iodide (CNI), in dichloromethane the anion $[B_3H_7NCB_3H_7]^-$ was obtained thus:

$$[N(PPh_3)_2][B_3H_8] + CNBr \rightarrow [N(PPh_3)_2][B_3H_7NCB_3H_7] + HBr + 1/2H_2 \qquad (2\text{-}1)$$

The actual mechanism of this reaction is not known but is thought to proceed via the generation of radicals. The $[B_3H_7NCB_3H_7]^-$ ion is the first example in which two cages are linked via a cyanide bridge. The only other reported example in which borane cages are centrally linked is for the beryllaborane $[Be(B_3H_8)_2]$,[48] but in this case the metal centre is co-ordinated to each $[B_3H_8]$ ligand via two Be-H-B bridge bonds.

2.2.2 Characterisation

(a) N.m.r. spectra

The ^{11}B n.m.r. spectra of the derivatives $[B_3H_7(X)]^-$(X=NCSe,$NCBPh_3$, $NCBH_2NCBH_3$,$NCBH_2CN$ and $NCBH_2CNB_3H_7$), were similar to the spectrum of $[B_3H_7(Cl)]^-$. At high frequency (low field) a resonance of relative area two was observed that can be attributed to the unsubstituted boron atoms B(2),B(3) in structures I and II.

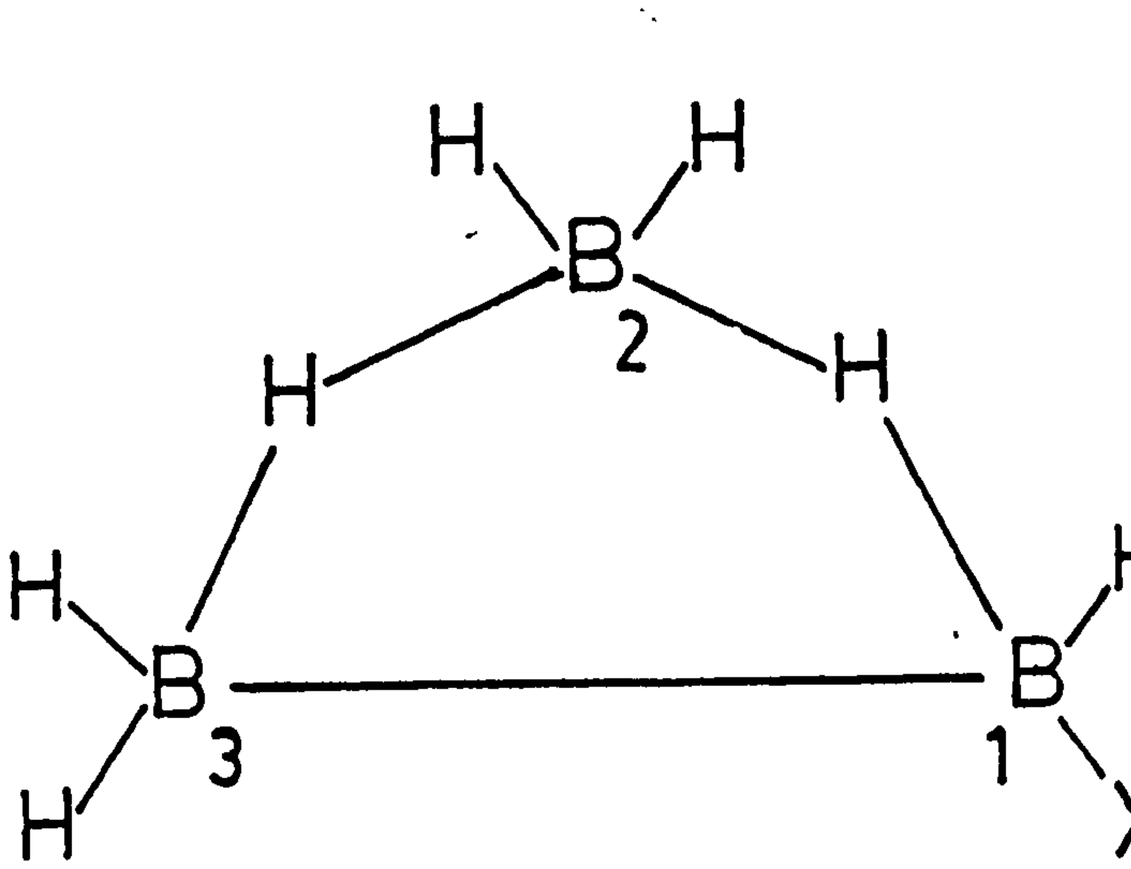

I

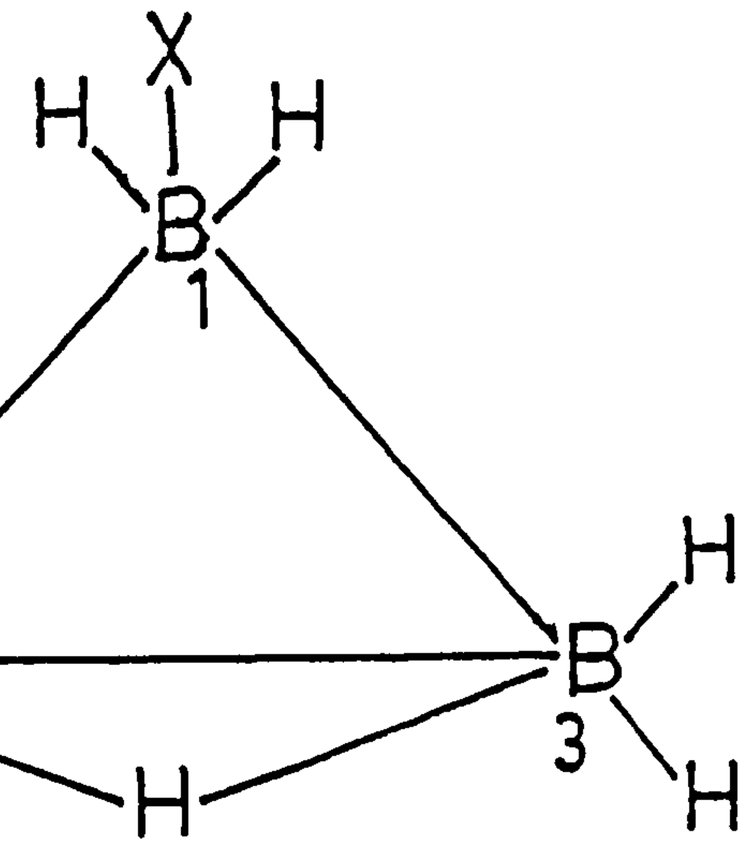

II

A single resonance at lower frequency (higher field) was observed of relative area one and was attributed to the unique substituted boron atom B(1). In addition to the resonances attributed to the triborane fragment in $[B_3H_7(NCBPh_3)]^-$, the resonance due to the boron atom of the substituent appears as a singlet at δ=-10:5p.p.m. The resonance due to the $[BH_3]$ and $[BH_2]$ moieties of the substituent in $[B_3H_7(NCBH_2NCBH_3)]^-$ appear as a well defined quartet (δ = -43.1 p.p.m.,$J_{B-H}=41H_z$) and triplet (δ= -27.7 p.p.m., $J_{B-H}=92H_z$) respectively. In both $[B_3H_7(NCBH_2CN)]^-$ and $[B_3H_7(NCBH_2CN)B_3H_7]^-$ the $[BH_2]$ moiety of the ligand appears as a well defined triplet at δ = -40.8 p.p.m., $J_{B-H}=94H_z$. In the line-narrowed 115.5 MH_z ^{11}B n.m.r. spectra fine structure due to ^{11}B-^{1}H coupling was resolved for the anions. The enhanced resolution of the resonance due to the two equivalent

unsubstituted boron atoms B(2) and B(3) at high frequency showed the six most intense lines of an octet (relative intensities; 1:7:21:35: 35:21:7:1) the two outermost lines being lost in the noise. This indicated that there were seven equivalent hydrogens that are rapidly tautomerising, on the n.m.r. time scale, in solution at room temperature. The relevant ^{11}B n.m.r. data are presented in Table 2.1.

The ^{1}H and $^{1}H\{^{11}B\}$ n.m.r. spectra of $[N(PPh_3)_2][B_3H_7(NCBH_2NCBH_3)]$, at room temperature in $CDCl_3$ at $360MH_z$, as well as showing the resonances due to the cation centred on δ 7.5p.p.m. (relative area;30) showed a resonance at δ +1.58p.p.m. (relative area; 7) corresponding to the seven fluxional hydrogens on the triborane cage. In addition two sharp resonances at δ0.58 p.p.m. (relative area; 3) and δ 1.99 p.p.m. (relative area; 2) were observed, these resonances are attributed to the $[BH_3]$ and $[BH_2]$ moieties of the substituent.

The ^{11}B n.m.r. spectrum of $[N(PPh_3)_2][B_3H_7NCB_3H_7]$ at 115.5 MH_z in $CDCl_3$ clearly shows the asymmetry (Figure 2.1) that arises as a result of one cage being carbon-coordinated and one being nitrogen-coordinated to the bridging cyanide group. Line-narrowing the high frequency resonances (i.e. the unsubstituted boron atoms B(2) and B(3) in each cage) indicated that each cage was fluxional with seven equivalent hydrogens rapidly tautomerising on the n.m.r. time scale. By comparison with the ^{11}B n.m.r. spectra of the simpler known cyanide bridged anions $[B_3H_7(X)]^-$ ($X=NCBPh_3, NCBH_3, NCBH_2NCBH_3, NCBH_2CN$ and $NCBH_2CNB_3H_7$), the resonance at δ -34.9 p.p.m. can be unequivocally attributed to the unique N-coordinated boron atom of

Table 2.1 — 115.5 MH_z ^{11}B N.M.R. Spectral

Data in $CDCl_3$ for Mono-substituted Derivatives of the $[B_3H_8]^-$ Ion

Anion	δ(p.p.m.)B(2),B(3)	δ(p.p.m.)B(1)	Other
$[B_3H_7(Cl)]^-$	-16.3	-22.0	
$[B_3H_7(NCS)]^-$	-13.2	-33.5	
$[B_3H_7(NCSe)]^-$	-10.0	-33.3	
$[B_3H_7(NCBPh_3)]^-$	-9.2	-34.7	-10.5(s)
$[B_3H_7(NCBH_3)]^-$	-9.9	-36.1	-43.8(q)
$[B_3H_7(NCBH_2Cl)]^-$	-9.6	-35.6	-22.5(t)
$[B_3H_7(NCBH_2NCBH_3)]^-$	-8.1	-34.9	-27.7(t) -43.1(q)
$[B_3H_7(NCBH_2CN)]^-$	-8.9	-34.8	-40.8(t)
$[B_3H_7(NCBH_2CN)B_3H_7]^-$	-8.2	-34.7	-40.5(t)
$[B_3H_7NCB_3H_7]^-$	-9.4,* -12.3	-34.9,* -49.5	

s - singlet, q - quartet, t - triplet.

*Nitrogen coordinated cage resonances.

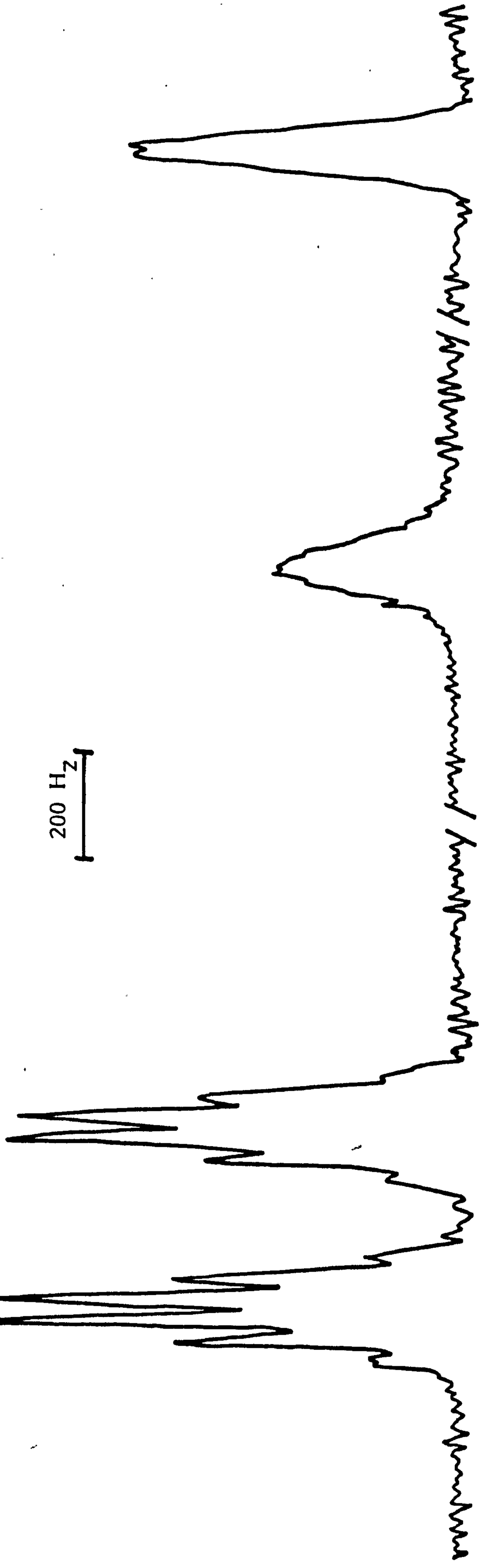

Figure 2.1 The 115.5 MH_z ^{11}B n.m.r. spectrum of $[B_3H_7NCB_3H_7]^-$ in $CDCl_3$ (line-narrowed).

one cage, whilst the other unique boron resonance at δ-49.5 p.p.m. is due to the C-coordinated boron atom of the other cage. From the ^{11}B n.m.r. spectrum alone the two resonances that appear at δ-9.45 p.p.m. and δ-12.36 p.p.m. due to the B(2),B(3) atoms in each cage cannot be assigned. Naively, the resonance at higher frequency (lower field) could be attributed to the B(2),B(3) boron atoms of the N-coordinated cage on electronegativity grounds.

The 360 MH_z ^1H n.m.r. spectrum (Figure 2.2) also reflects the asymmetry of the molecule. The resonances, each of relative area seven, are centred at δ+1.04 p.p.m. and δ+1.51 p.p.m. respectively. These resonances are assigned to the fluxional hydrogens in each cage. Successive single-frequency decoupling experiments at the boron resonance frequencies, corresponding to the chemical shifts of the boron environments, from high frequency (low field) to low frequency (high field) resulted in selective sharpening of the fluxional hydrogens in the cage being irradiated. It was found that irradiating the boron resonance frequencies corresponding to the boron chemical shifts at δ-9.45 p.p.m. and δ-34.9 p.p.m., (N-coordinated boron),caused a selective sharpening of the fluxional hydrogens at δ+1.51 p.p.m. These results show that the resonance at δ+1.51 p.p.m. is due to the fluxional hydrogen atoms of the N-coordinated cage. In addition, the previously unassigned boron resonance at δ -9.45 p.p.m. can now be attributed to the unsubstituted boron atoms, (B(2) and B(3)), of the N-coordinated cage. Similarly the ^{11}B n.m.r. resonance at δ-12.3 p.p.m. in the ^{11}B n.m.r. spectrum was attributed to the unsubstituted boron atoms

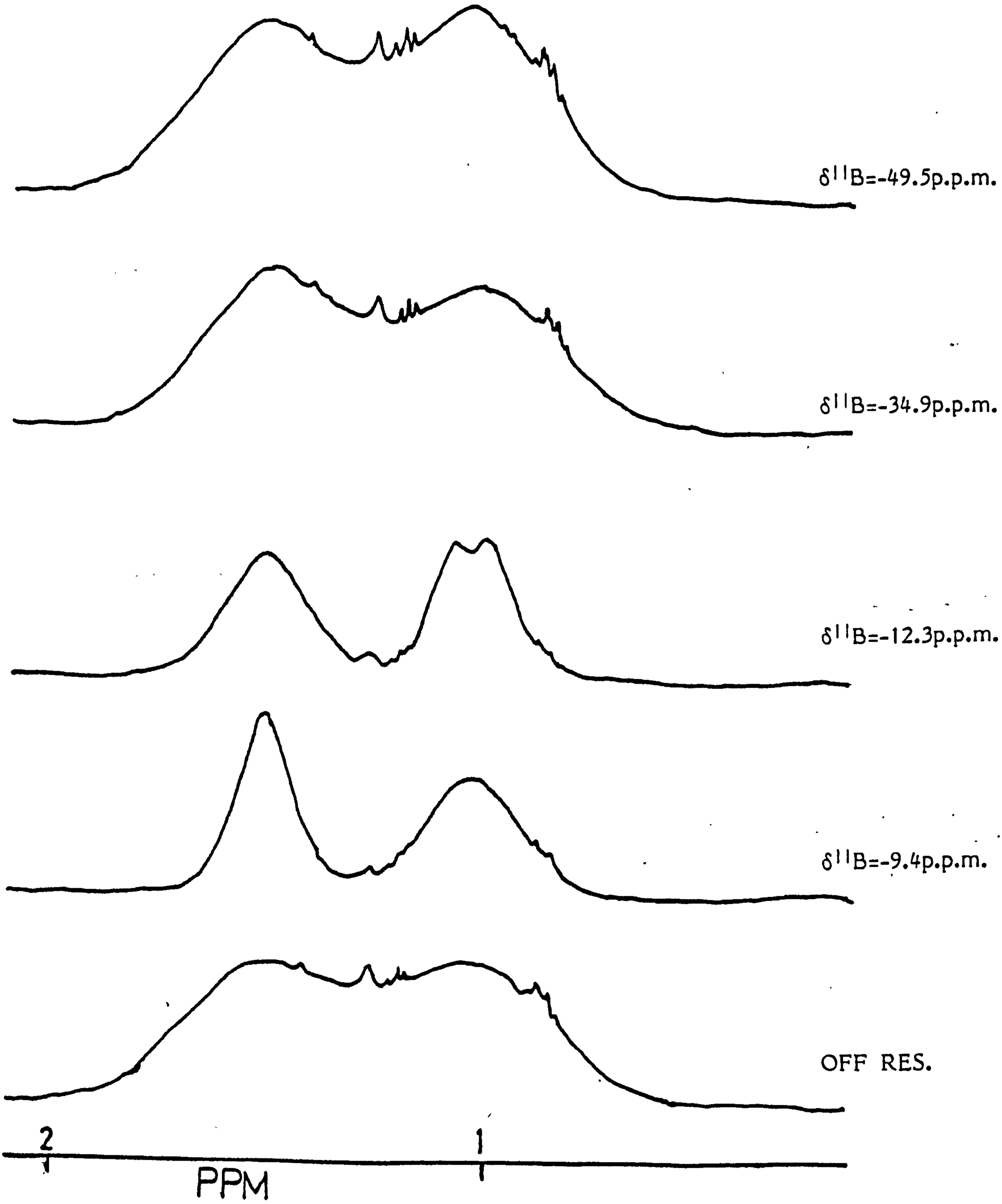

Figure 2.2 The 360 MH_z ^1H-{^{11}B}n.m.r. spectra of $[B_3H_7NCB_3H_7]^-$ in $CDCl_3$

of the carbon-coordinated cage. The ^{1}H n.m.r. resonance at δ-1.04 p.p.m. was attributed to the fluxional hydrogens in the carbon-coordinated cage.

The 2-D $^{11}B-^{11}B$ (COSY) n.m.r. spectrum (Figure 2.3) of $[N(PPh_3)_2][B_3H_7NCB_3H_7]$ confirms the assignments made from the specific frequency decoupling experiments. The cross peaks lying off the diagonal in Figure 2.3 arising from spin-spin $^{11}B-^{11}B$ coupling, which is only significant for adjacent atoms in boron clusters, clearly shows coupling between the resonance at δ-9.45 p.p.m. and the N-coordinated boron atom at δ-34.9 p.p.m. The correlation between the unsubstituted B(2), B(3) boron atoms in the carbon-coordinated cage at δ-12.36 p.p.m. and the resonance due to the carbon substituted boron atom at δ-49.5 p.p.m. is also shown as a clearly defined cross peak.

Previously it was reported that no correlation was observable between hydrogen bridged boron atoms,[127(a)] which is in agreement with earlier theoretical predictions that show that the electron density in B-H-B bridge bonds is negligible on the B-B vector.[133] The only reported[127(a)] cases in which a correlation is observed between hydrogen bridged boron bonds are for two metallaboranes, (discussed in Chapter 1), in which the metal centre plays an important part. In $[N(PPh_3)_2][B_3H_7NCB_3H_7]$ all hydrogen atoms are rapidly tautomerising at room temperature in solution on the n.m.r. time scale. Therefore, at any instant on the n.m.r. time scale, all three boron atoms will be hydrogen bridged, and hence an observable correlation on the 2-D

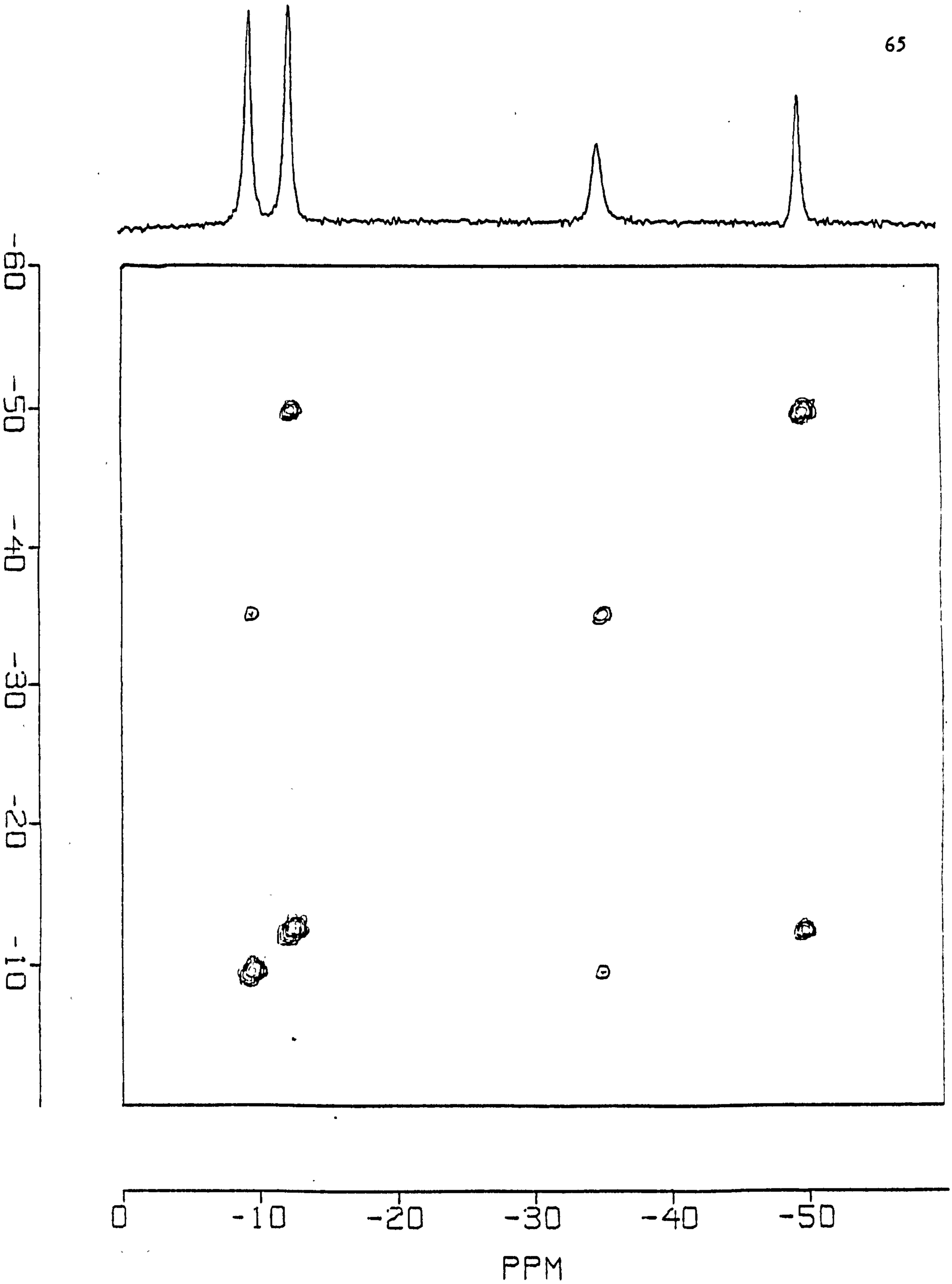

Figure 2.3 The 115.5 MH_z ^{11}B 2-D COSY spectrum of $[B_3H_7NCB_3H_7]^-$ in $CDCl_3$.

$^{11}B-^{11}B$ (COSY) spectrum was not expected. Since there are clearly defined correlations between the boron atoms in both N and C co-ordinated cages, there must be some electron density overlap between the boron atoms in each cage. From these observations it may be possible to predict the nature of the bonding employed in the solution structure of $[B_3H_7NCB_3H_7]^-$ as being three-centred. If the type of bonding employed is three-centred there is electron density overlap between all the boron nuclei and hence a correlation in the $^{11}B-^{11}B$ (COSY) spectrum would be expected. The x-ray crystal structure determination of $[N(PPh_3)_2][B_3H_7NCB_3H_7]$ shows that each triborane cage is three centre bonded (Figure 2.4).

(b) Infra-red Spectra

The i.r. spectra of the substituted octahydrotriborate (1-) ions described in this chapter had many similar features (Table 2.2. lists the relevant i.r. absorption frequencies). The main similarities were in the B-H str. region, all the substituted octahydrotriborate (1-) ions exhibited B-H str. modes in the region $2495cm^{-1}$ and $2430cm^{-1}$.

The i.r. spectrum of $[B_3H_7(NCSe)]^-$ showed, along with the B-H str. modes, a strong band at $2160cm^{-1}$ which has been assigned to the NCSe asymmetric stretch and is indicative of a nitrogen-coordinated isoselenocyanate. Although i.r. spectroscopy is not an infallible guide it has been shown by crystallographic studies that $B_{10}H_{13}(NCS)$[139] and $NH_3BH_2(NCS)$[140] are both isothiocyanates, therefore it is probable

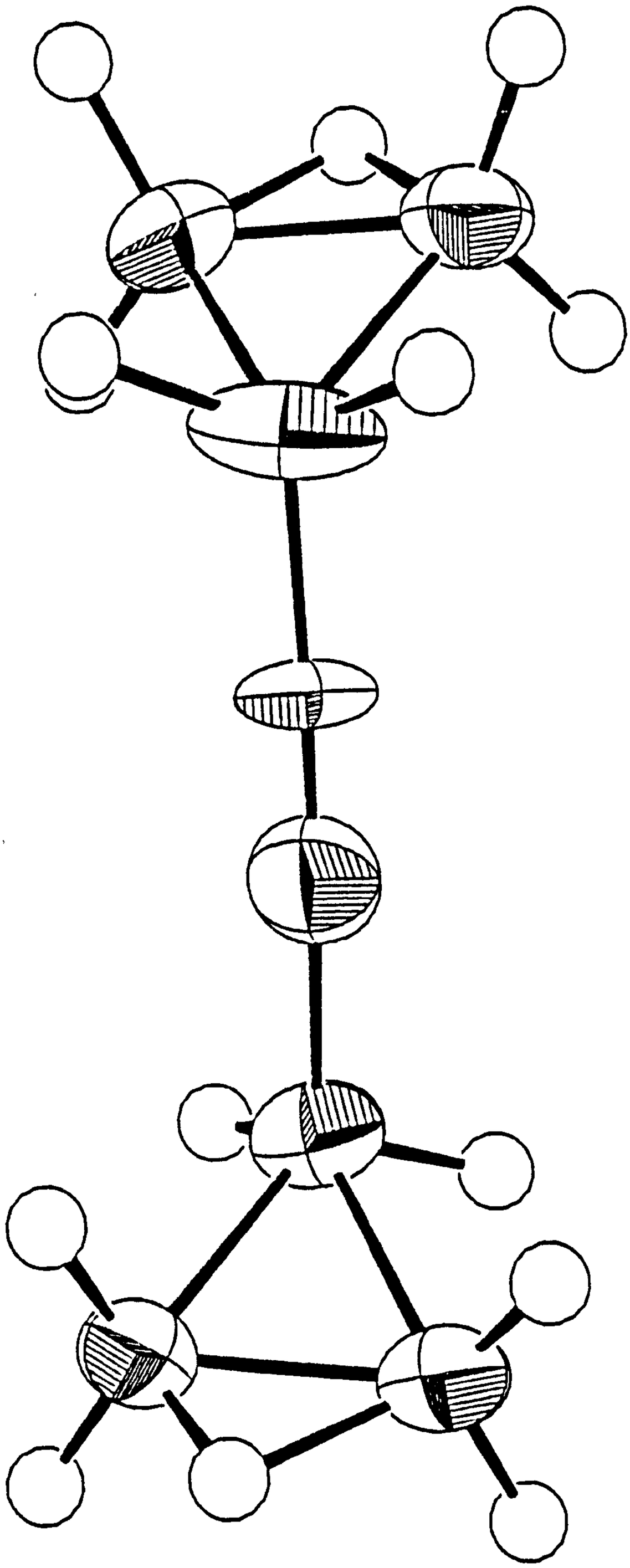

Figure 2.4 The crystal structure of the $[B_3H_7NCB_3H_7]^-$ ion.

Table 2.2

Infra-red Absorption Frequencies of Octahydrotriborate (1-) Derivatives

Substituent	2600 cm^{-1} - 1900 cm^{-1}				
H^-	2450s, 2080m.	2400s,	2300sh,	2130m	
Cl^-	2480s,	2425s,	2300sh.		
$NCSe^-$	2495s,	2480sh,	2435s,	2160s.	
$NCBPh_3^-$	2505s,	2440s,	2165s.		
$NCBH_2NCBH_3^-$	2505s, 2370m,	2440s, 2290w,	2420sh, 2255s.		
$NCBH_2CN^-$	2500s, 2285s,	2440s, 2200w.	2420sh,	2380m,	2360sh,
$NCBH_2CNB_3H_7^-$	2495s,	2435s,	2400m,	2290s	
$NCB_3H_7^-$	2510s,	2425s,	2280s.		

s - strong, m - medium, w - weak, sh. - shoulder

that the $[NCSe]^-$ group in $[B_3H_7(NCSe)]^-$ is also N-coordinated. The i.r. spectra of the cyanide bridged species $[B_3H_7(X)]^-$(X=$NCBPh_3$, $NCBH_3$, $NCBH_2NCBH_3$, $NCBH_2CN$, $NCBH_2CNB_3H_7$ and NCB_3H_7) showed,in addition to the B-H str. modes of the $[B_3H_7]$,$[BH_2]$ and $[BH_3]$ groups, a strong sharp band in the region of 2260 cm^{-1} which was characteristic of a bridging cyanide and was similar to that reported for $[BH_3(CN)BH_3]^-$.[164]

(c) X-Ray Crystallography

Investigation of several triborane (7) adducts and octahydrotriborate (1-) ions by x-ray crystallography has revealed subtle and interesting structural variations that are shown below:

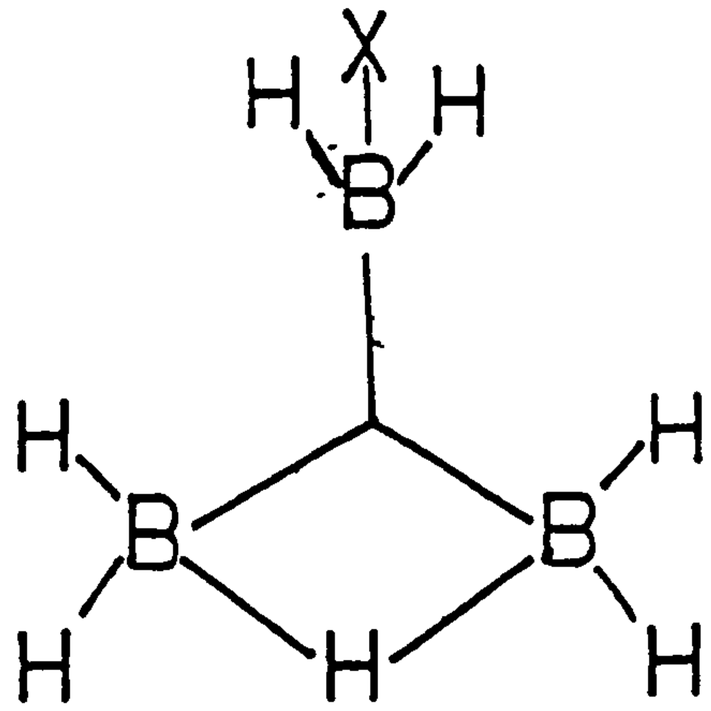

(a)

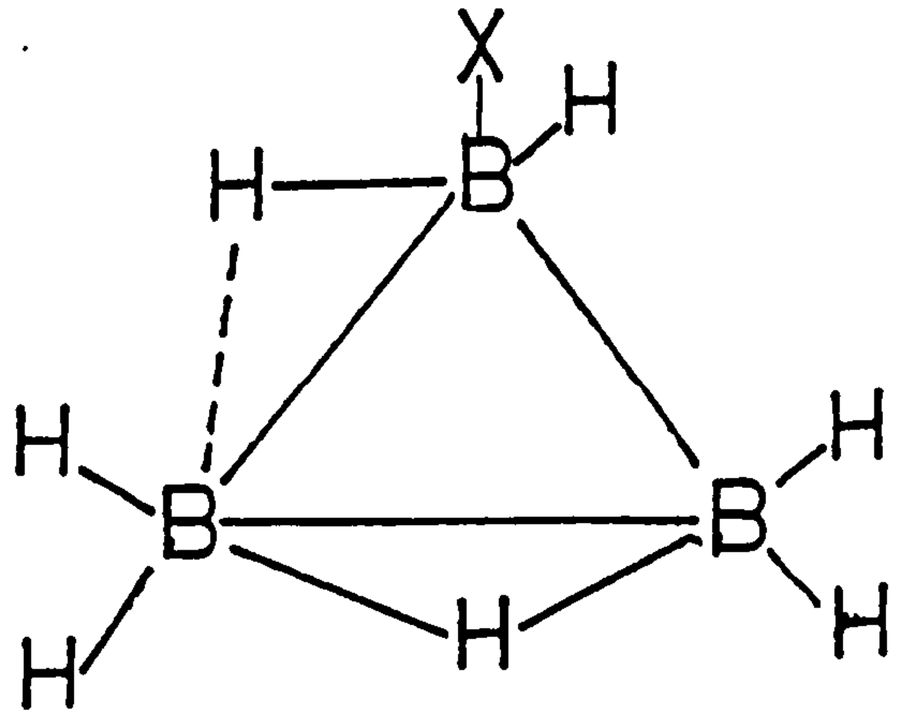

(b)

(c)

(d)

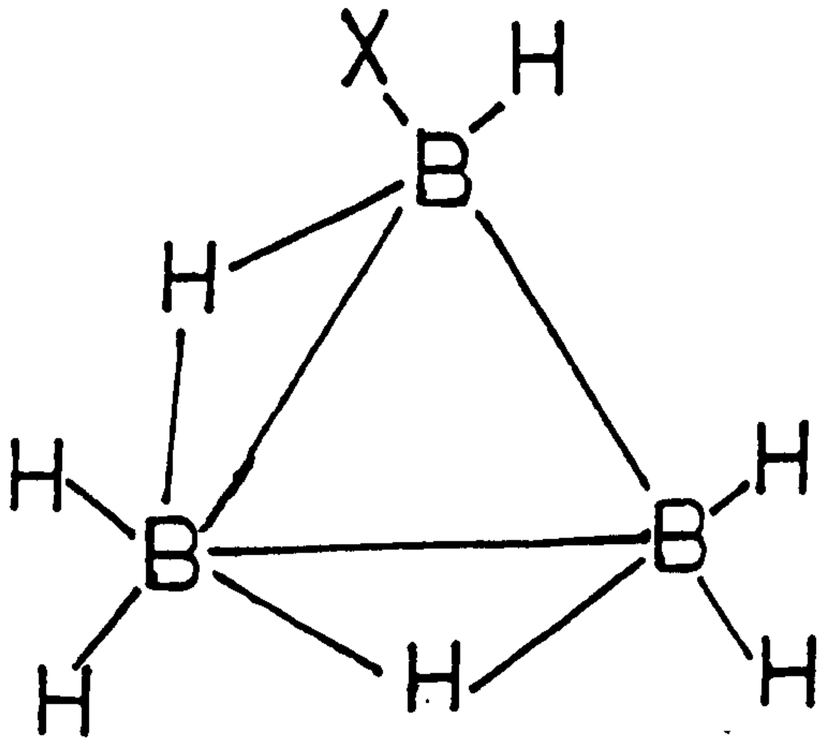

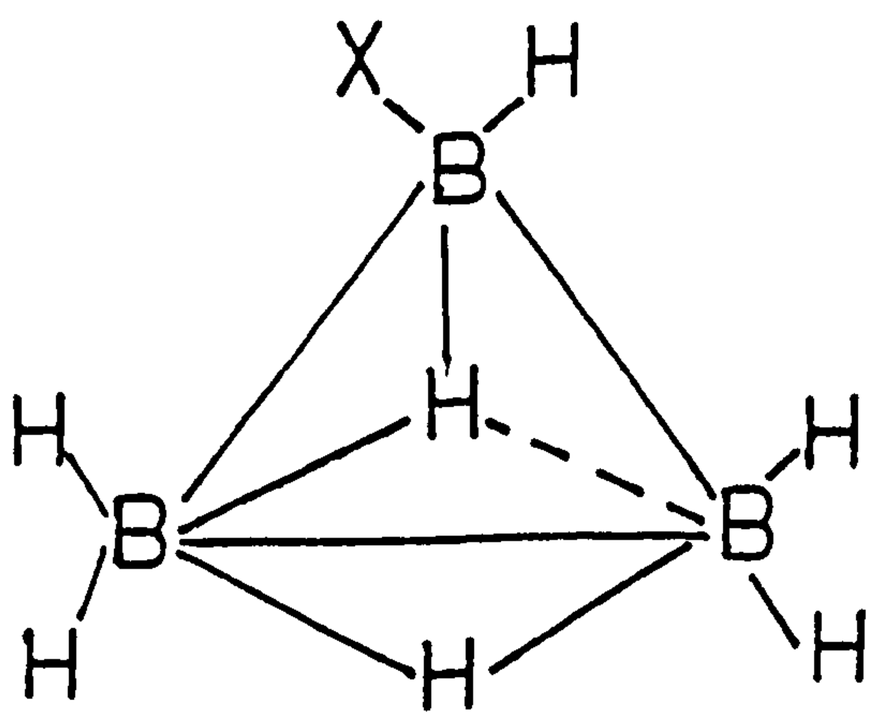

In B_3H_7CO[27(b)] and the low-temperature form of $B_3H_7PR_3$[29] there is effective C_s symmetry (a) and only one bridging hydrogen atom. Such species may be considered as derivatives of diborane (6) in which one μ-H function is replaced by μ-(BH_2L). The molecule $B_3H_7NH_3$[39] is asymmetric (b) with one hydrogen of the [BH_2L] moiety semi-bridging the B(1)-B(3) connectivity. Full two-edge bridging (c) is exemplified by the octahydrotriborate (1-) ion, $[B_3H_8]^-$.[15]

Crystals of $[N(PPh_3)_2][B_3H_7(NCSe)]$ were submitted for structural determination. It was found that $[B_3H_7(NCSe)]^-$ and $[B_3H_7(NCS)]^-$ are isomorphous. At room temperature it appeared as though the $[B_3H_7(NCSe)]^-$ ion was a variant of the dibridged system (c), in which one hydrogen atom is edge bridging and one is located above the triborane cage in an asymmetric face bridging mode (d) as was previously reported for $[N(PPh_3)_2][B_3H_7(NCS)]$.[38] However, at low temperature it was found that both $[B_3H_7(NCSe)]^-$ and $[B_3H_7(NCS)]^-$[142] gave structures consistent with (b). It was proposed that the low temperature crystal structure determination (Figure 2.6) was more realistic than that determined at room temperature (Figure 2.5).

The crystal structure determination of $[N(PPh_3)_2][B_3H_7NCB_3H_7]$ showed that both triborane cages were three-centre bonded with effective C_s symmetry with only one bridging hydrogen atom (Figure 2.7). The crystal structures of $[B_3H_6(Cl)_2]^-$ and $[B_3H_6(Cl)(NCS)]^-$ (Figure 2.8 and Figure 2.9 respectively) relate to that of $[B_3H_8]^-$ with two-edge bridging (c) hydrogens and trans-substituents.

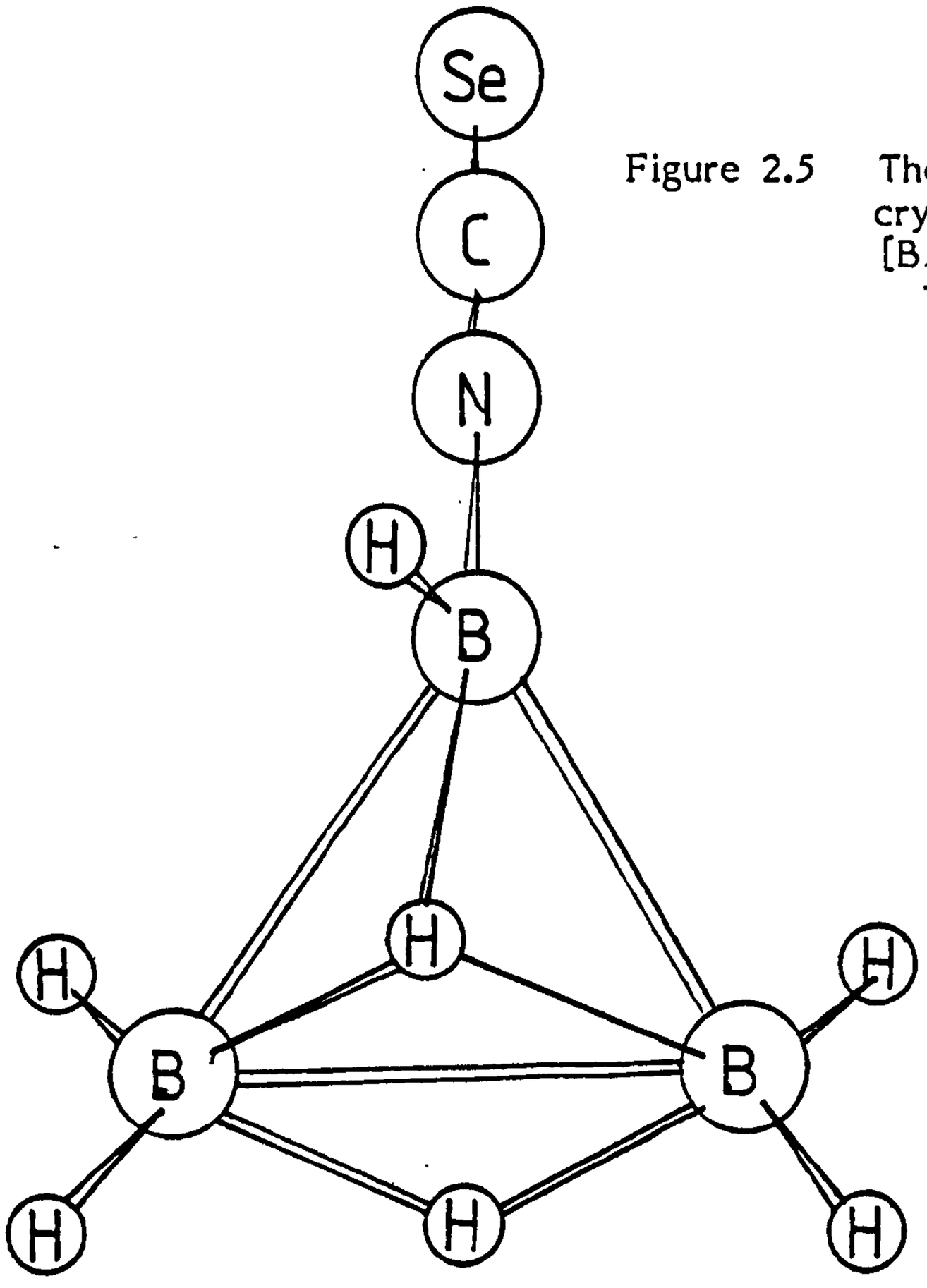

Figure 2.5 The room temperature crystal structure of $[B_3H_7(NCSe)]^-$

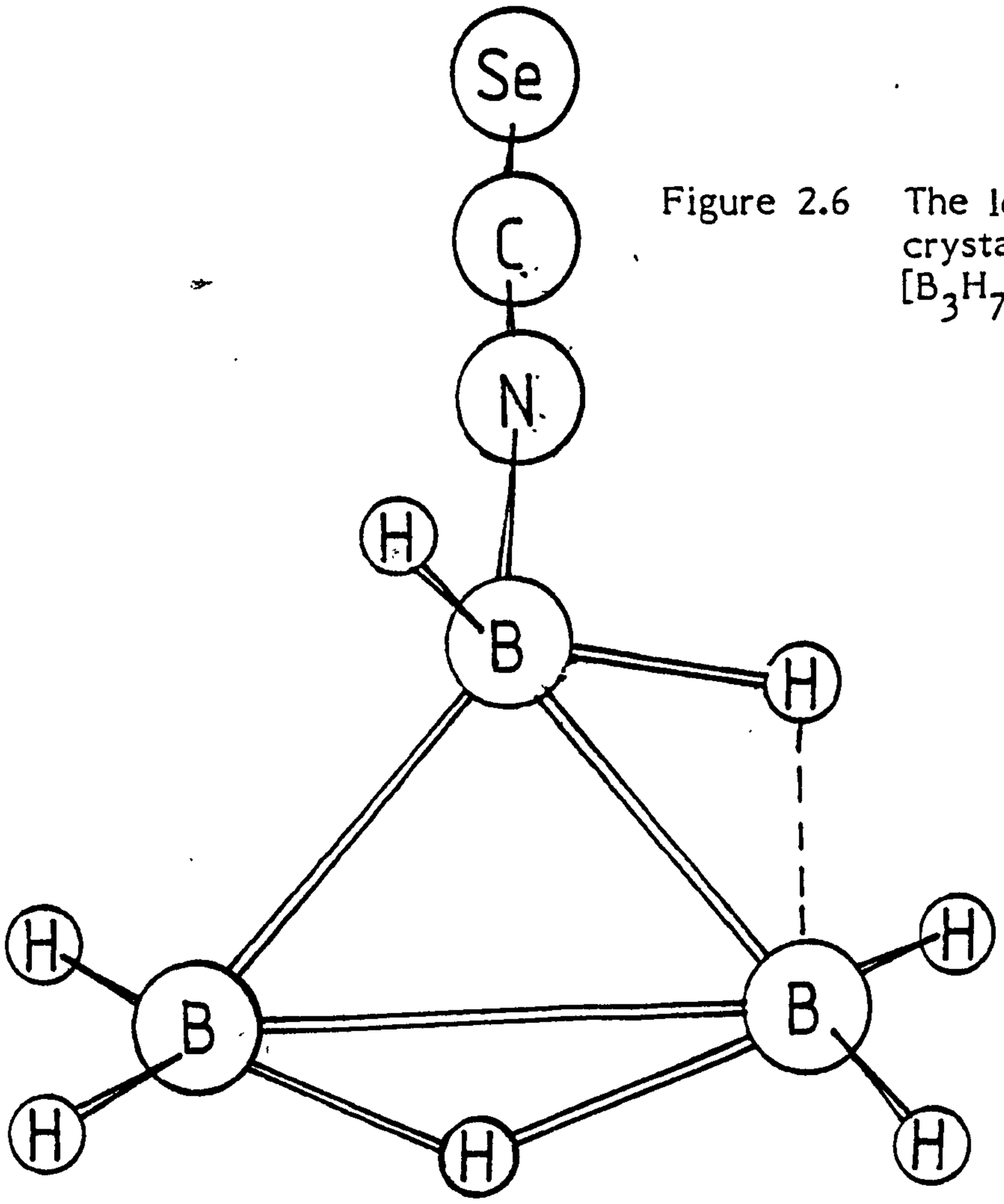

Figure 2.6 The low temperature crystal structure of $[B_3H_7(NCSe)]^-$

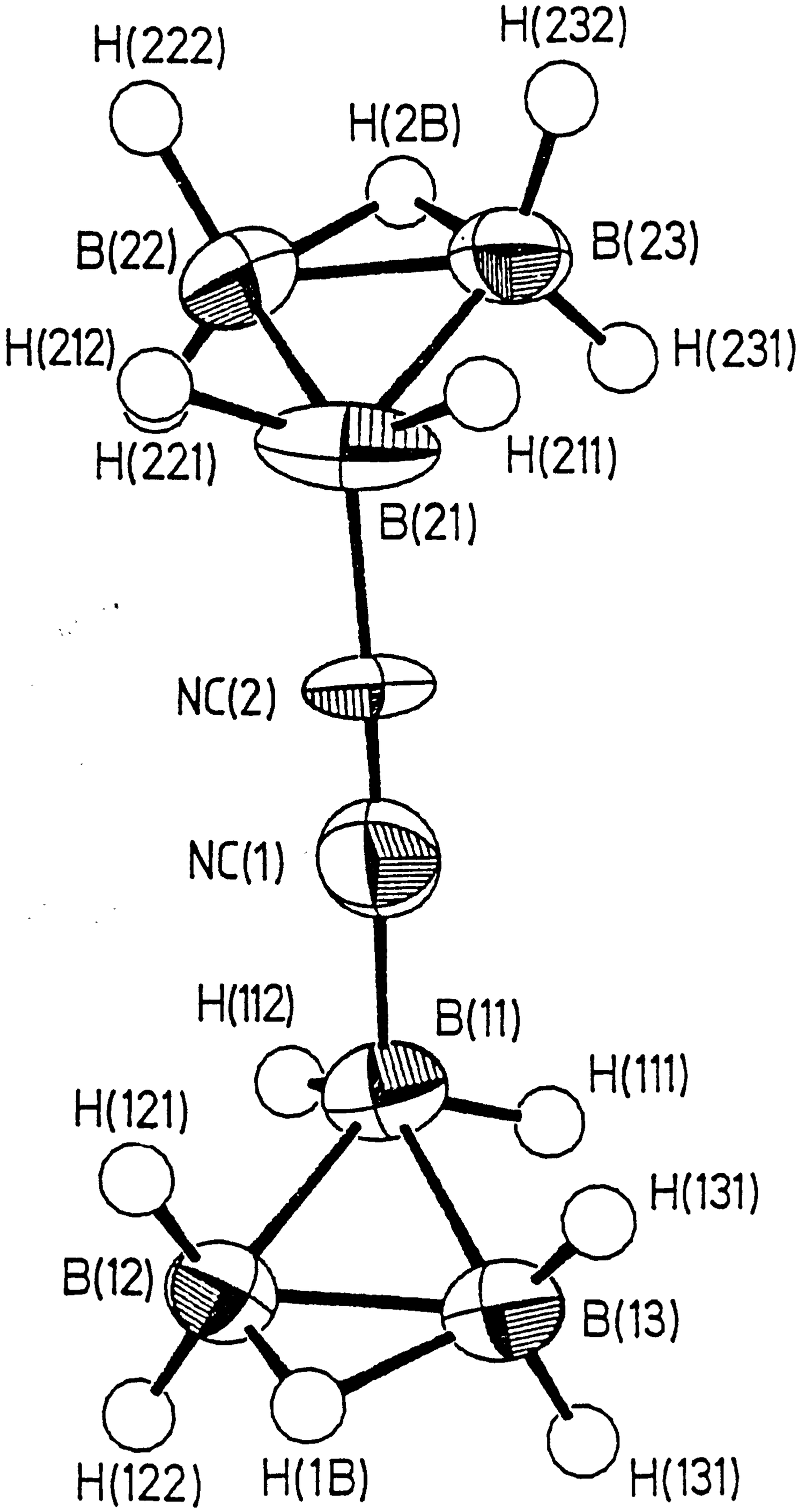

Figure 2.7 The numbered crystal structure of the $[B_3H_7NCB_3H_7]^-$ ion.

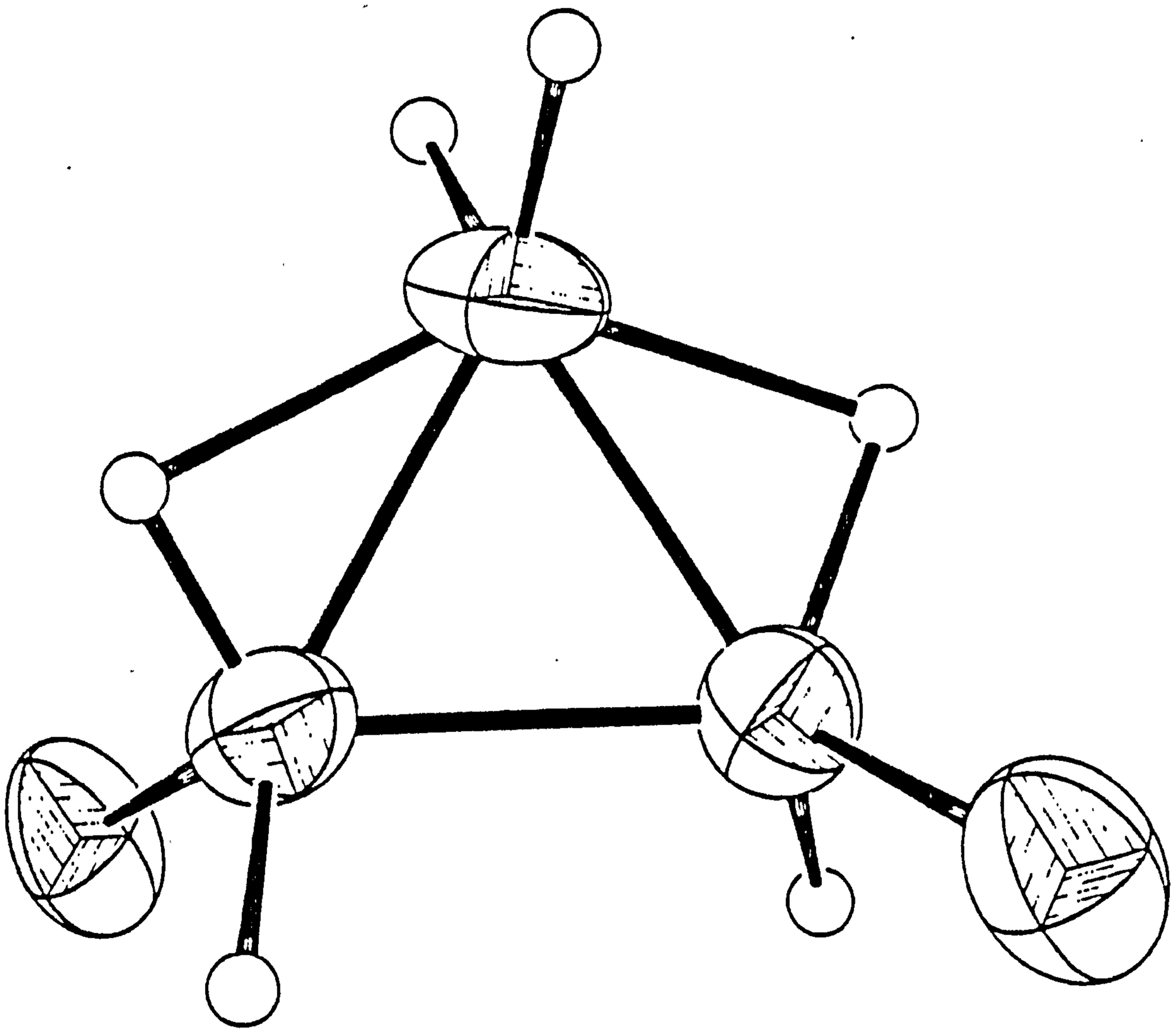

Figure 2.8 The crystal structure of the $[B_3H_6(Cl)_2]^-$ ion.

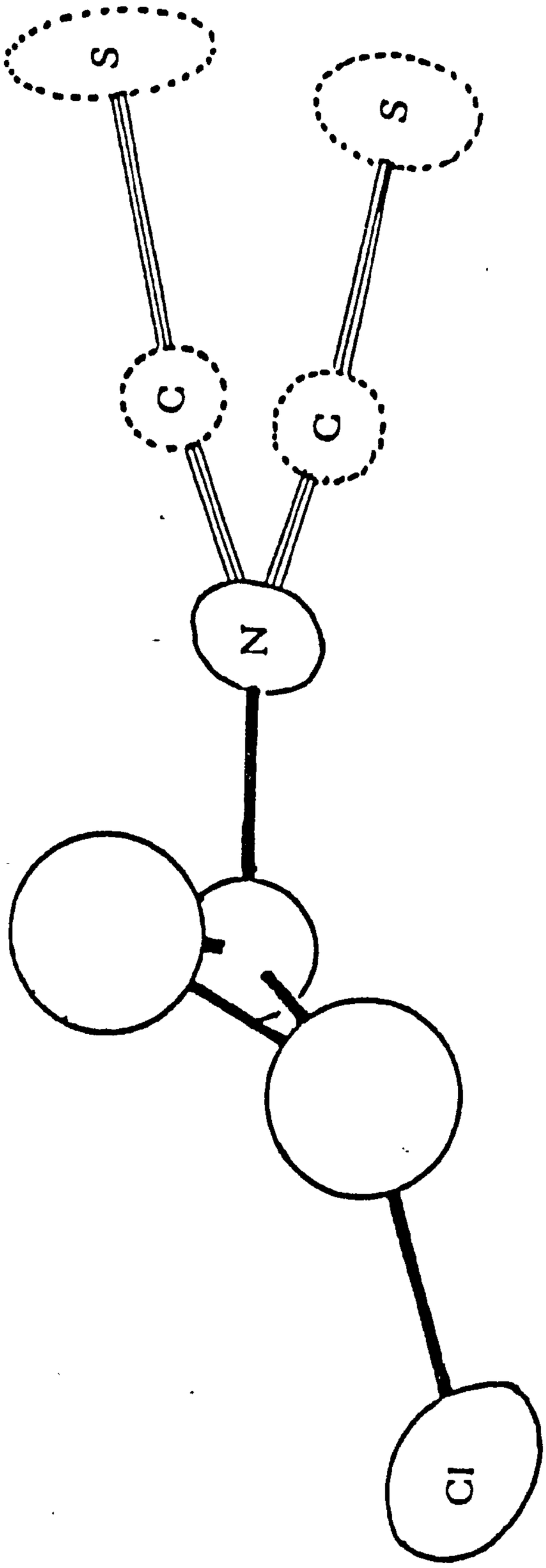

Figure 2.9 The crystal structure of the $[B_3H_6(Cl)(NCS)]^-$ ion.

2.2.3 Reactions of Substituted Derivatives of $[B_3H_8]^-$ ion

It was shown that[37] $[N(PPh_3)_2][B_3H_6(Cl)_2]$ could be prepared by reacting two equivalents of HCl with one of $[N(PPh_3)_2][B_3H_8]$ in dichloromethane. It was further shown that the anions $[B_3H_7(X)]^-$ (X=NCS, $NCBH_3$ and NCO) reacted with HCl in CH_2Cl_2 to produce disubstituted derivatives of the octahydrotriborate (1-) ion, $[B_3H_6(X)(X')]^-$ (X=Cl, X'=NCS,NCO,$NCBH_3$ and $NCBH_2Cl$). In the reaction of HCl with $[B_3H_7(NCBH_3)]^-$, chlorination was shown to be initially at the $[BH_3]$ moiety, with subsequent attack at the triborane fragment when a greater molar ratio of HCl was used.

The chloride substituents on $[B_3H_6(Cl)_2]^-$ were shown to be labile, albeit to a lesser extent than the chloride on the mono-substituted anion $[B_3H_7(Cl)]^-$.[37] When $[B_3H_6(Cl)_2]^-$ was treated with AgNCS the isothiocyanate displaced the labile chloride to produce $[B_3H_6(Cl)(NCS)]^-$ no further substitution was observed. The reaction of $[B_3H_6(Cl)_2]^-$ with $[N(PPh_3)_2][BH_3(CN)]$ gave both $[B_3H_6(Cl)(NCBH_3)]^-$ and $[B_3H_7(NCBH_3)]^-$, exemplifying the dual chemical character of $[BH_3(CN)]^-$, in which the ion can act as a donor ligand or as a hydride transfer reagent.[143] Furthermore, the anion $[Ag\{B_3H_6(Cl)(NC)\}_2]^-$ has been prepared by reaction of $[B_3H_6(Cl)_2]^-$ with AgCN.

In this work the preparation of novel disubstituted derivatives of the octahydrotriborate (1-) ion are described. The reaction of $[B_3H_7(NCSe)]^-$ and gaseous HCl in dichloromethane was carried out in a similar fashion to that described previously for $[B_3H_7(NCS)]^-$.[37] How-

ever the ^{11}B n.m.r. spectrum of the product showed no evidence of disubstitution.

Previously the reaction with $[B_3H_7(NCBH_3)]^-$ and HCl^{37} showed that the chloride reacted initially at the $[BH_3]$ moiety of the substituent. The ^{11}B n.m.r. spectrum of the crude product obtained from the reaction of $[B_3H_7(NCBH_2NCBH_3)]^-$ with excess HCl indicated that a mixture of the disubstituted anion $[B_3H_6(Cl)(NCBH_2NCBH_3)]^-$ and the starting material was obtained. In addition to the resonances due to the $[B_3H_7(NCBH_2NCBH_3)]^-$ anion (Table 2.1), there are additional resonances at δ+0.54 p.p.m. and at δ-3.97 p.p.m. which, by comparison with known disubsubstituted anions,are attributable to the unsubstituted boron atom (B-H) in the disubstituted anion and the chloride substituted boron atom (B-Cl) respectively. The nitrogen-coordinated boron atom of the disubstituted anion appears at δ-28.5 p.p.m., which is δ 6.4 p.p.m. to higher frequency (lower field) relative to the corresponding resonance in the free anion. The quartet due to the $[BH_3]$ moiety of the substituent at δ-43.1 p.p.m., is unaffected on disubstitution, therefore chloride substitution is preferentially at the triborane fragment in this case. No substitution at the ligand was observed even when large excesses of HCl were used. Similarly the reaction between $[B_3H_7(NCBH_2CN)]^-$ and HCl gave a mixture of $[B_3H_6(Cl)(NCBH_2CN)]^-$ and starting material. In the ^{11}B n.m.r. spectrum of the mixture the resonances due to the disubstituted anion appear at δ+0.77 p.p.m., δ-3.86 p.p.m. and δ-31.55 p.p.m., which are attributed to the B-H, B-Cl and B-N resonances respectively. The relative integrals indicate

two $[BH_2]$ units, one in the monosubstituted and one in the disubstituted anions. Once again the chloride substitutes preferentially on the triborane fragment. Line-narrowing the 115.5MH_z ^{11}B n.m.r. spectrum resolves the resonance attributed to the unsubstituted boron atom (B-H) in the disubstituted,$[B_3H_6(Cl)(NCBH_2CN)]^-$ ion into the five major lines of a septet, (relative intensities 1:6:15:20:15:6:1), the two outer-most lines being lost in the noise. This indicated that there are six rapidly tautomerising hydrogen atoms in the disubstituted derivative.

It was found that reaction of the cyanide bridged triborane anion, $[B_3H_7NCB_3H_7]^-$ with excess HCl produced the disubstituted derivative $[B_3H_6(Cl)NCB_3H_7]^-$ By comparison of the ^{11}B n.m.r. of the free anion (Figure 2.1) with that of the chlorinated anion (Figure 2.10) it was found that the carbon-coordinated cage resonances at δ-11.89 p.p.m. due to B(2), B(3) and at δ-49.76 p.p.m. due to the C-coordinated boron atom were unaffected on chloride substitution. However, the remaining resonances due to the N-coordinated cage have all been shifted to higher frequency (lower field). In addition each boron nucleus in the N-coordinated cage is unique indicating a disubstituted cage having different substituents. The resonance that appears at δ-30.97 p.p.m. is attributed to the N-coordinated boron atom by comparison with the corresponding resonance in other disubstituted cyanide bridged anions $[B_3H_6(Cl)(X)]^-(X=NCBH_3^{37}, NCBH_2Cl^{37}, NCBH_2NCBH_3$ and $NCBH_2CN)$. The remaining resonances at δ -0.18 p.p.m. and δ -3.77 p.p.m. are due to the remaining two boron atoms in the N-coordinated cage. Line-narrowing indicates that there are seven fluxional hydrogen atoms

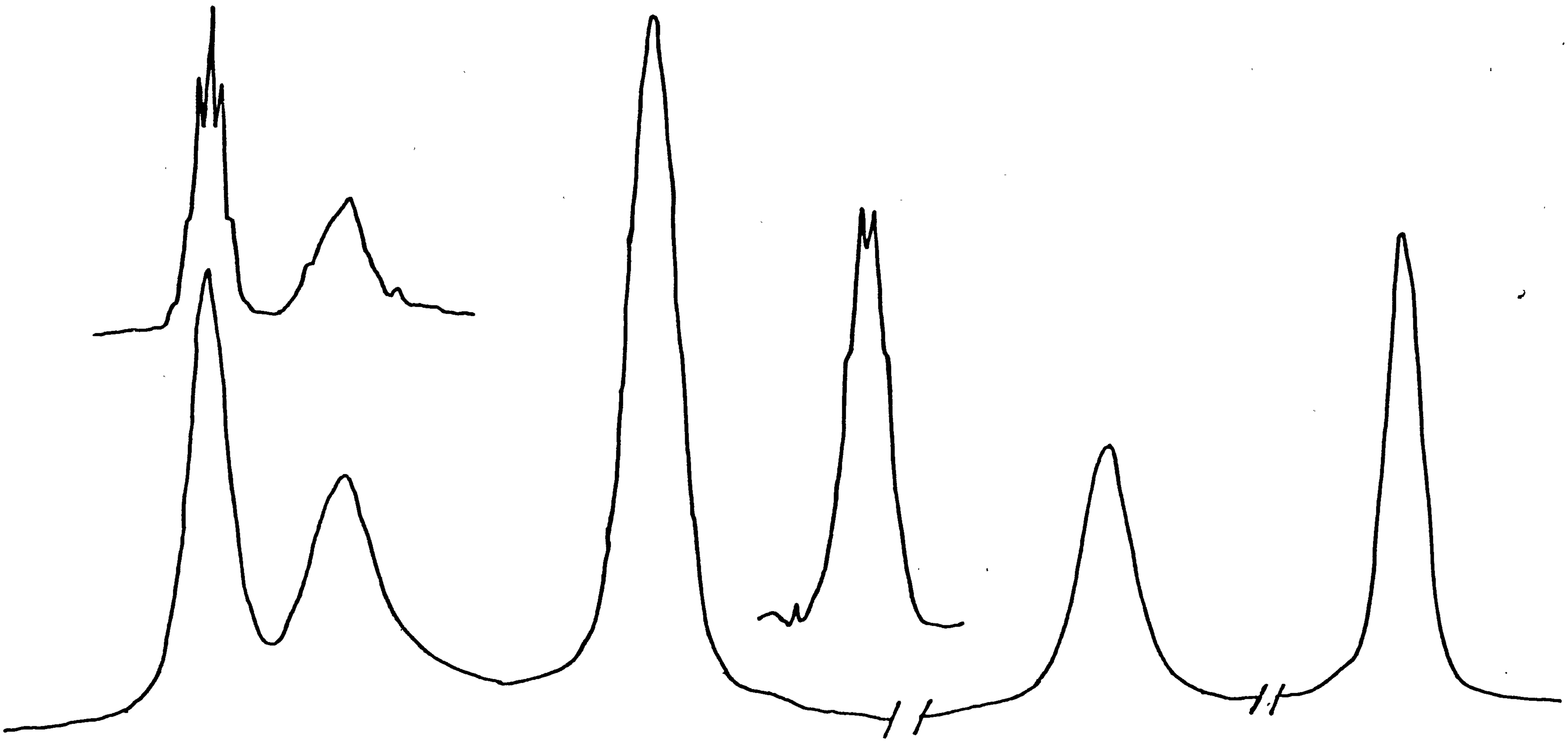

Figure 2.10 The 115.5 MH_z ^{11}B n.m.r. spectrum of $[B_3H_6(Cl)NCB_3H_7]^-$ in $CDCl_3$ (with line-narrowing).

in the C-coordinated cage and six in the N-coordinated cage. The 360MH$_z$ ^{1}H n.m.r. spectrum indicated that there were two types of fluxional hydrogen atoms exemplified by resonances centred on δ 2.19 p.p.m. and δ 1.06 p.p.m. Specific frequency decoupling experiments indicated that the resonance centred on δ 2.19 p.p.m. was due to the six rapidly tautomerising hydrogen atoms of the N-coordinated cage, and the resonance at δ 1.06 p.p.m. was due to the seven fluxional hydrogen atoms of the C-coordinated cage. On chloride substitution there is a proton chemical shift of δ 0.6 p.p.m. to higher frequency.

The 2-D ^{11}B-^{11}B (COSY) spectrum (Figure 2.11) of $[B_3H_6(Cl)NCB_3H_7]^-$ showed two important correlations. The first correlation was between the resonance at δ -11.89 p.p.m. and the resonance at δ -49.76 p.p.m. That is, a correlation between the unsubstituted boron atoms B(2), B(3) and the substituted boron atom B(1) of the carbon-coordinated cage. In the free anion it was proposed that this correlation was due to the electron density overlap between the three boron atoms in a three-centred bond (i.e., type (a), page 69). The second significant correlation is between the resonance at δ-0.18 p.p.m. and δ-30.97 p.p.m. In this case the N-coordinated boron atom of the disubstituted cage is correlated to only one of the remaining two boron atoms. It is proposed that on chloride substitution the type of bonding in the N-coordinated cage is changed from the three-centred type (type (a), page 69) to the full two-edge bridging type (type (c), page 69) as exemplified by $[B_3H_6(Cl)_2]^-$ (Figure 2.8). In $[B_3H_6(Cl)_2]^-$ the two chlorine atoms are trans-substituted and both chlorine substituted

Figure 2.11 The 115.5 MH_z ^{11}B 2-D COSY spectrum of $[B_3H_6(Cl)NCB_3H_7]^-$ in $CDCl_3$.

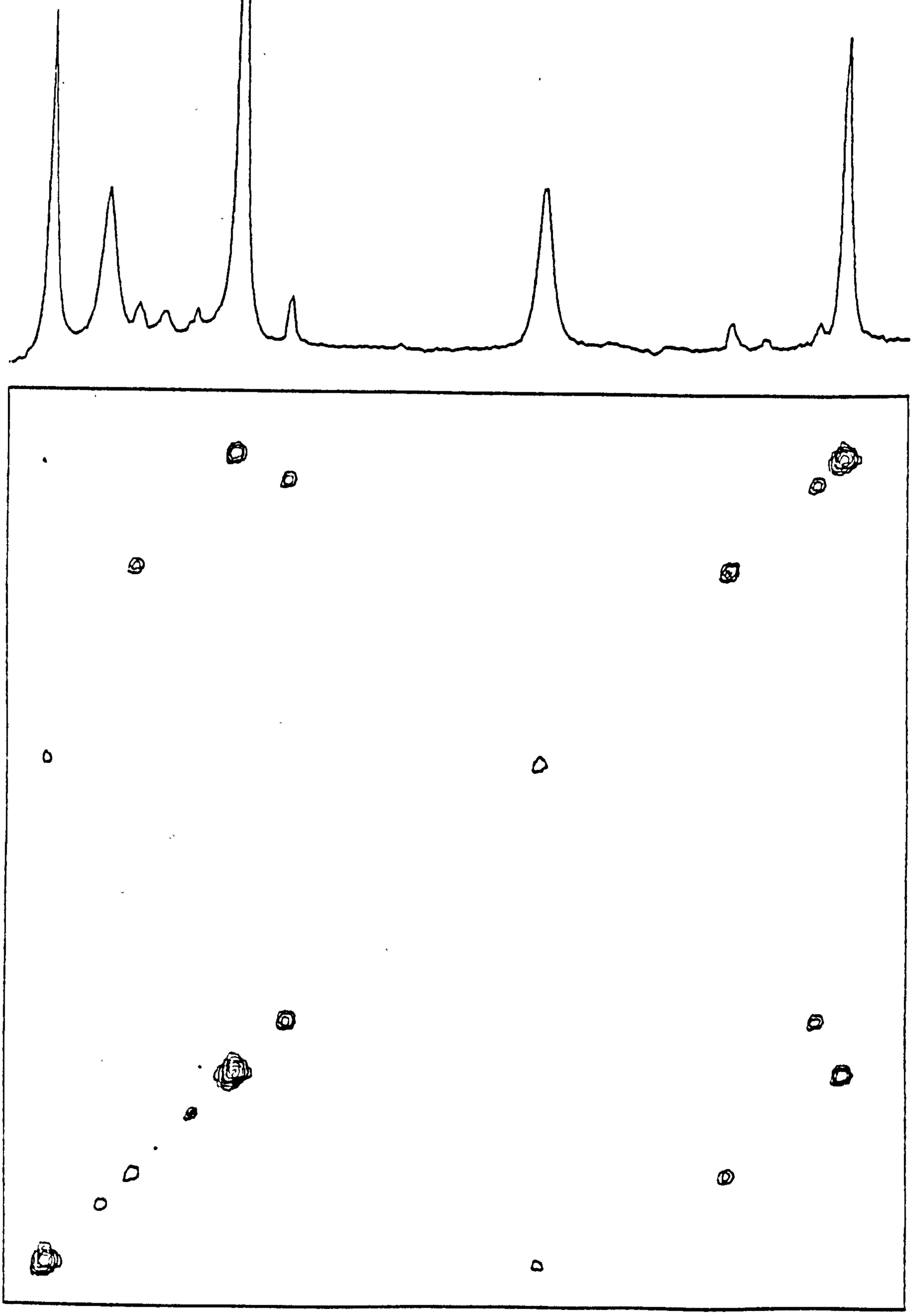

boron atoms are single-bonded to each other and are bridge hydrogen bonded to the remaining unsubstituted boron atom. It is proposed that in $[B_3H_6(Cl)NCB_3H_7]^-$ the chloride and cyanide substituents are trans- to each other and that the chloride substituted boron atom (B-Cl) and the N-coordinated boron atom (B-N) are bonded via a single B-B bond. Hence, there is electron density overlap between these boron atoms resulting in a correlation observed as a cross peak in the 2-D ^{11}B-^{11}B (COSY) n.m.r. spectrum. If the assumption that no observable correlation between hydrogen bridged boron bonds is accurate then no cross peak should be seen between the substituted boron atoms and the unsubstituted atom (B-H). Therefore, in this case the resonance at δ-0.18 p.p.m. was attributed to B-Cl and the resonance at δ -3.77 p.p.m. was attributed to B-H.

The reaction of N-bromo succinimide (N.B.S.) with $[B_3H_7NCB_3H_7]^-$ gave a crystalline solid. The ^{11}B n.m.r. of this solid at 80.2 MH_z showed six resonances all of equal relative intensity. Since all the resonances are unique both N and C coordinated cages are substituted with bromine to give the $[N(PPh_3)_2IB_3H_6(Br)NCB_3H_6(Br)]^-$ anion. (Relevant n.m.r. data are presented in Table 2.3).

The reaction of $[N(PPh_3)_2IB_3H_7(Cl)]$ with CNBr also produced a di-substituted species. The 115.5 MH_z ^{11}B n.m.r. of this species showed two resonances, in the ratio 1:2 at δ-3.70p.p.m. and δ-11.30 p.p.m. respectively. Line-narrowing showed that there were six fluxional hydrogen atoms. However, this disubstituted species has not yet been identified.

Table 2.3 ^{11}B N.M.R. Spectral Data in $CDCl_3$ for $[B_3H_6(X)(X^1)]^-$ Disubstituted Derivatives of the $[B_3H_8]^-$ Ion

Substituents		Boron Chemical Shifts (p.p.m)			
X	X^1	B(H)	B(X)	$B(X^1)$	Other
[a]Cl	Cl	-5.3	-13.4	-13.4	
[a]Cl	NCS	-5.1	-8.8	-25.9	
[a]Cl	$NCBH_3$	-2.5	-4.2	-31.3	-43.6(q)
[a]Cl	$NCBH_2Cl$	-0.53	-0.53	-31.3	-22.5(t)
[b]Cl	$NCBH_2NCBH_3$	-0.5	-3.9	-28.5	-22.9(t) -43.1(q)
[a]Cl	$NCBH_2CN$	-0.77	-3.86	-31.55	-40.8(t)
[a]Cl	NCB_3H_7	-3.77*	-0.18*	-30.97*	-11.8B(2),B(3) -49.6B(1)
[b]Br*	Br	-9.6,*12.6	-15.3,*-20.8	-35.5,*-50.0	

t - triplet, q - quartet.

a - 115.5 MH_z n.m.r. spectra, b - 80.2 MH_z n.m.r. spectra

*Nitrogen coordinated cage resonances.

2.3 Investigation of the Substituted Derivatives of the Octahydrotriborate (1-) Ion by 2-Dimensional N.M.R.

2.3.1 Introduction

In the previous section it was inferred that the nature of the bonding present in the anion, $[B_3H_7NCB_3H_7]^-$, and its derivative $[B_3H_6(Cl)NCB_3H_7]^-$ in solution, could be qualitatively determined from the observed correlations in the 2-D ^{11}B-^{11}B (COSY) spectrum. Using 2-Dimensional n.m.r. as a probe for the qualitative determination of the bonding employed in a structure in solution, would be advantageous because it could be used to augment the solid state information obtained by x-ray crystallography. Furthermore, the 2-D n.m.r. experiment is convenient since it can be done in less than an hour.

To determine the extent to which 2-D n.m.r. could be used as a probe to infer the nature of the bonding in triborane anions, a series of 2-D n.m.r. experiments were carried out on the mono- and disubstituted derivatives of the octahydrotriborate (1-) ion previously described.

2.3.2 Results and Discussion

(a) Monosubstituted Anions

(i) $[B_3H_7(Cl)]^-$

Previously it was reported that[127(a)] in boron clusters no correlation is observed between hydrogen bridged boron nuclei since the electron density in the B-H-B bond is negligible along the B-B vector.[133] However, in $[B_3H_7(Cl)]^-$ a correlation is clearly observed between

the unsubstituted B(2),B(3) atoms at δ-16.3 p.p.m. and the chloride substituted atom at δ-22.0 p.p.m. (Figure 2.12). Previously Brown and Lipscomb[31] calculated that the anion $[B_3H_7(F)]^-$ had a 2013 styx structure (I) similar to that of $[B_3H_8]^-$. The $[B_3H_7(Cl)]^-$ and $[B_3H_7(Br)]^-$ were shown[32] to have similar structures by i.r. spectroscopy.

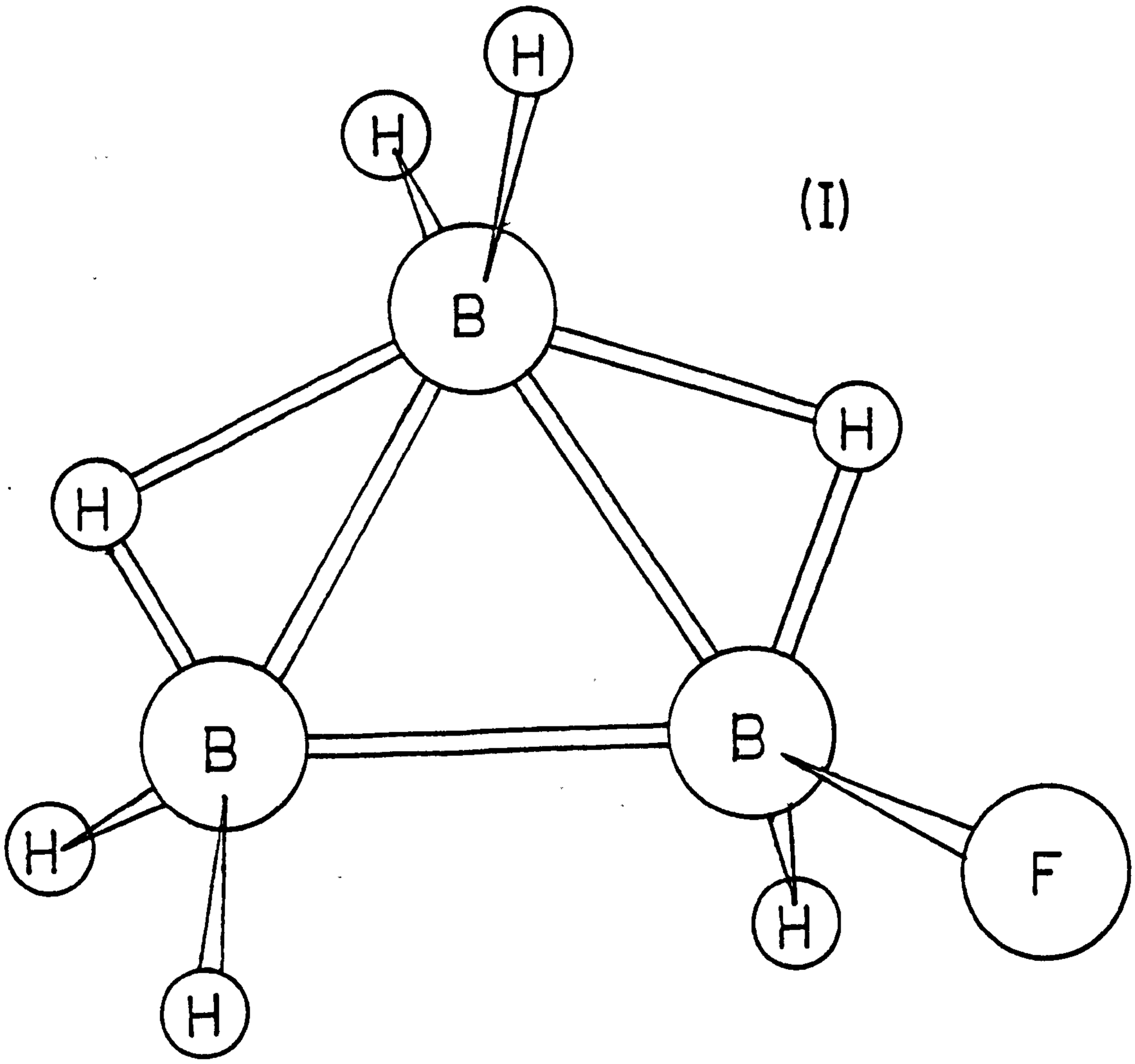

(I)

In the $[B_3H_7(Cl)]^-$ anion all seven hydrogen atoms are rapidly tautomerising on the n.m.r. time scale. Therefore at any instant all three boron atoms will be hydrogen bridged and thus a correlation between the chloride substituted boron atom B(1) and the unsubstituted boron atoms B(2),(B(3) should not be observed. Since a correlation is

Figure 2.12 The 115.5MH$_z$ 2-D COSY n.m.r. spectrum of $[B_3H_7(Cl)]^-$ in $CDCl_3$.

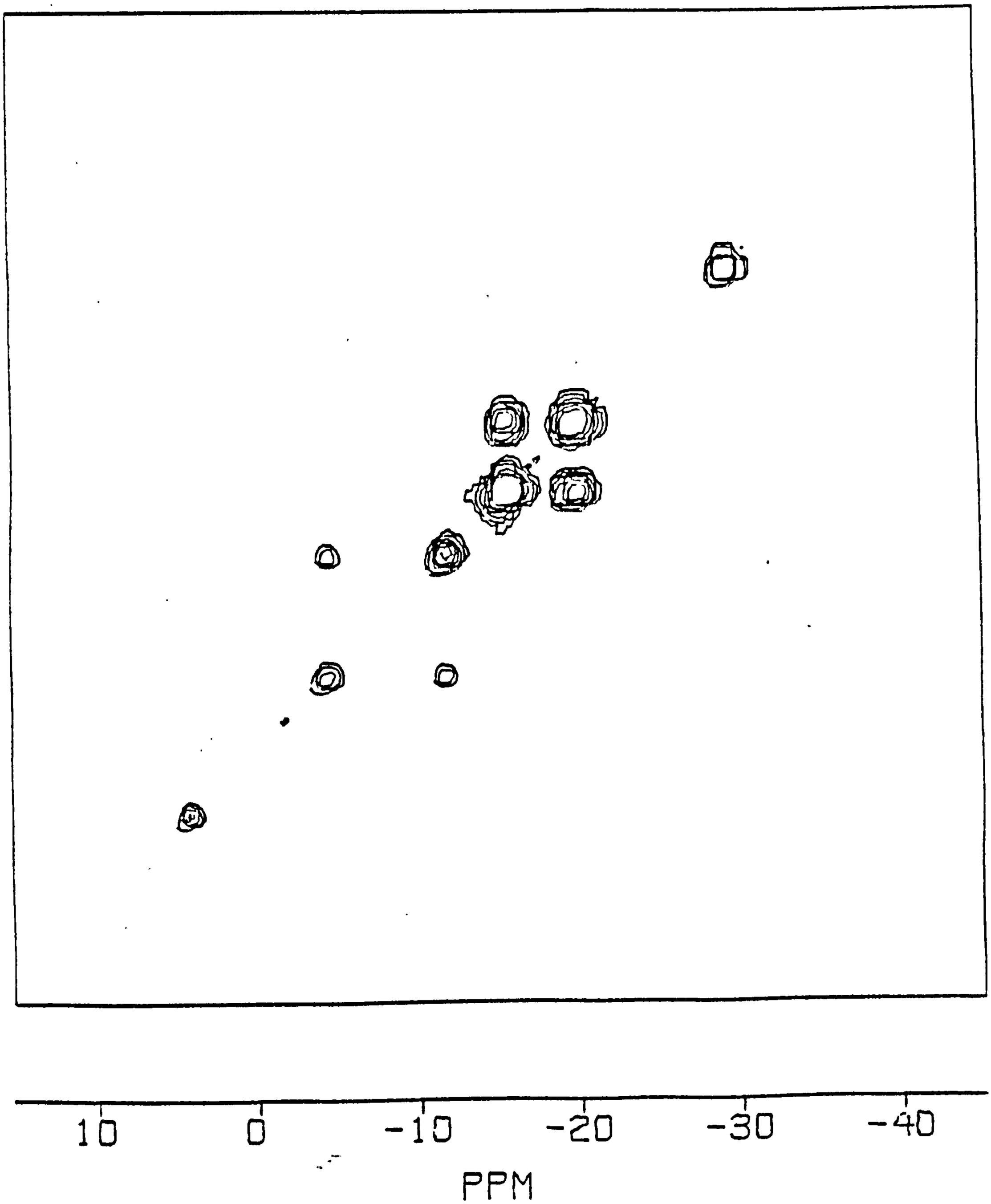

observed there has to be electron density overlap between B(1) and B(2),B(3). If $[B_3H_7(Cl)]^-$ has essentially the same structure as $[B_3H_8]^-$,[15] then the hydrogen bridges are asymmetric; this asymmetry would result in electron density being re-directed into the B-B vector to give the observed correlation. Previously it was reported[99] that the $^{11}B-\{^1H\}$ [proton decoupled] 115.5 MH_z line-narrowed n.m.r.spectrum showed two signals; a 1:1:1:1 quartet of relative area two due to the unsubstituted boron atoms B(2),B(3) at high frequency, and a 1:2:3:4:3:2:1 septet of relative area one due to the substituted boron atom B(1) at low frequency. The observed splitting in this case arose from $^{11}B-^{11}B$ spin-spin coupling (J_{BB} = 21.OH_z), this coupling indicates an overlap of electron density between B(2),B(3) and B(1), and therefore, it is not surprising that a correlation is observed in the 2-D COSY spectrum.

(ii) $\underline{[B_3H_7(NCSe)]^-}$ and $\underline{[B_3H_7(NCS)]^-}$

The 115.5 MH_z 2-D $^{11}B-^{11}B$ (COSY) n.m.r. spectra of both, $[B_3H_7(NCSe)]^-$ (Figure 2.13) and $[B_3H_7(NCS)]^-$(Figure 2.14),showed correlations between the unsubstituted boron atoms B(2),B(3) and the N-coordinated atom B(1). Previous investigation[99] of the $[B_3H_7(NCS)]^-$anion showed that, in $CDCl_3$, no coupling between the unsubstituted equivalent boron atoms B(2),B(3) and the unique substituted boron atom B(1) was observed in the $^{11}B-\{^1H\}$ decoupled n.m.r.spectrum. However, in CD_3CN, $[B_3H_7(NCS)]^-$ exhibited $^{11}B-^{11}B$ spin-spin couplings that were similar to those of $[B_3H_7(Cl)]^-$ in CD_3CN. It appeared from the data that, in any one solvent, as the substituent changed from $[Cl]^-$ to $[NCS]^-$

Figure 2.13 The 115.5 MH_z ^{11}B 2-D COSY n.m.r. spectrum of $[B_3H_7(NCSe)]^-$ in $CDCl_3$.

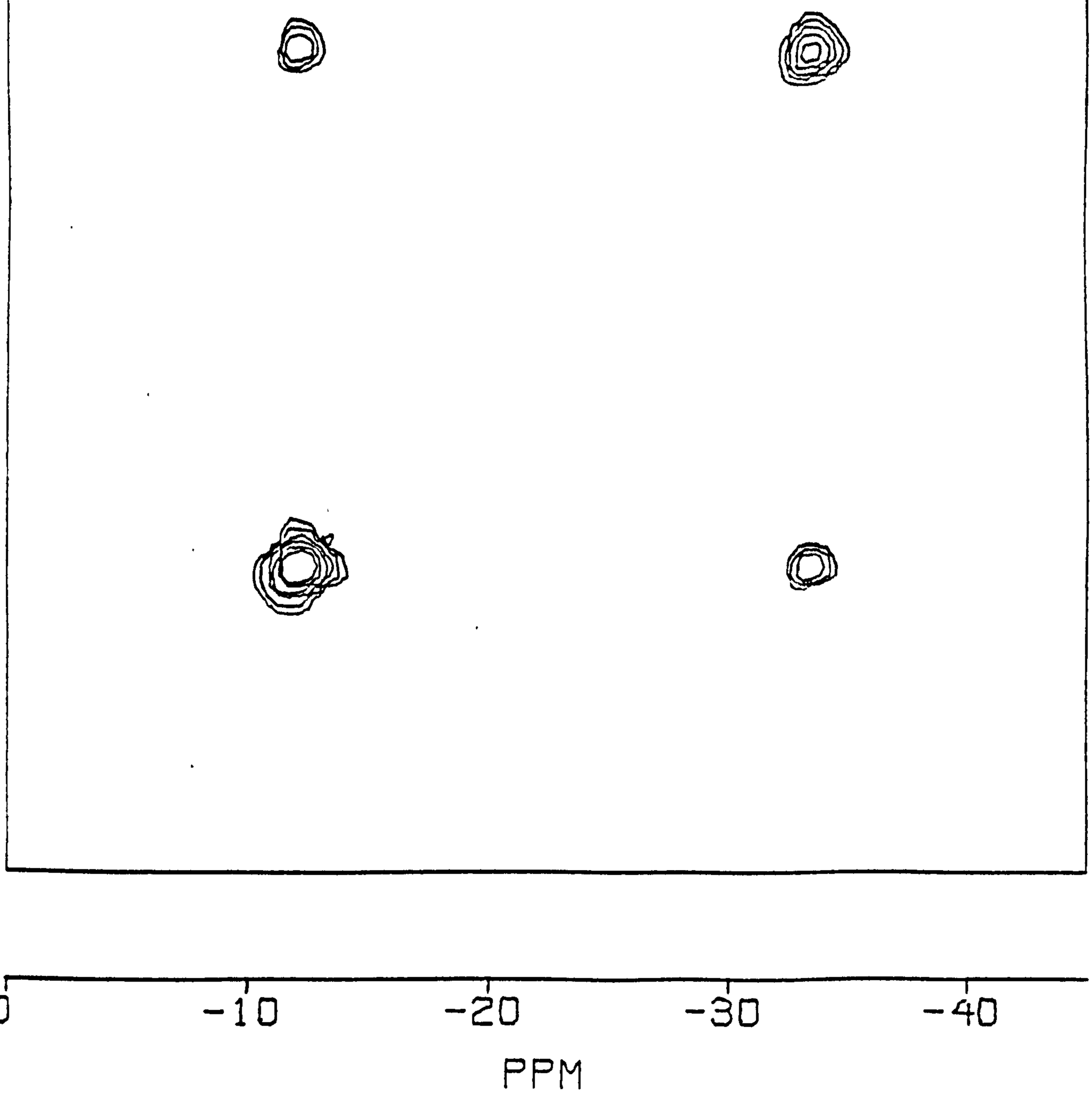

Figure 2.14 The 115.5 MH_z ^{11}B 2-D COSY spectrum of $[B_3H_7(NCS)]^-$ in $CDCl_3$.

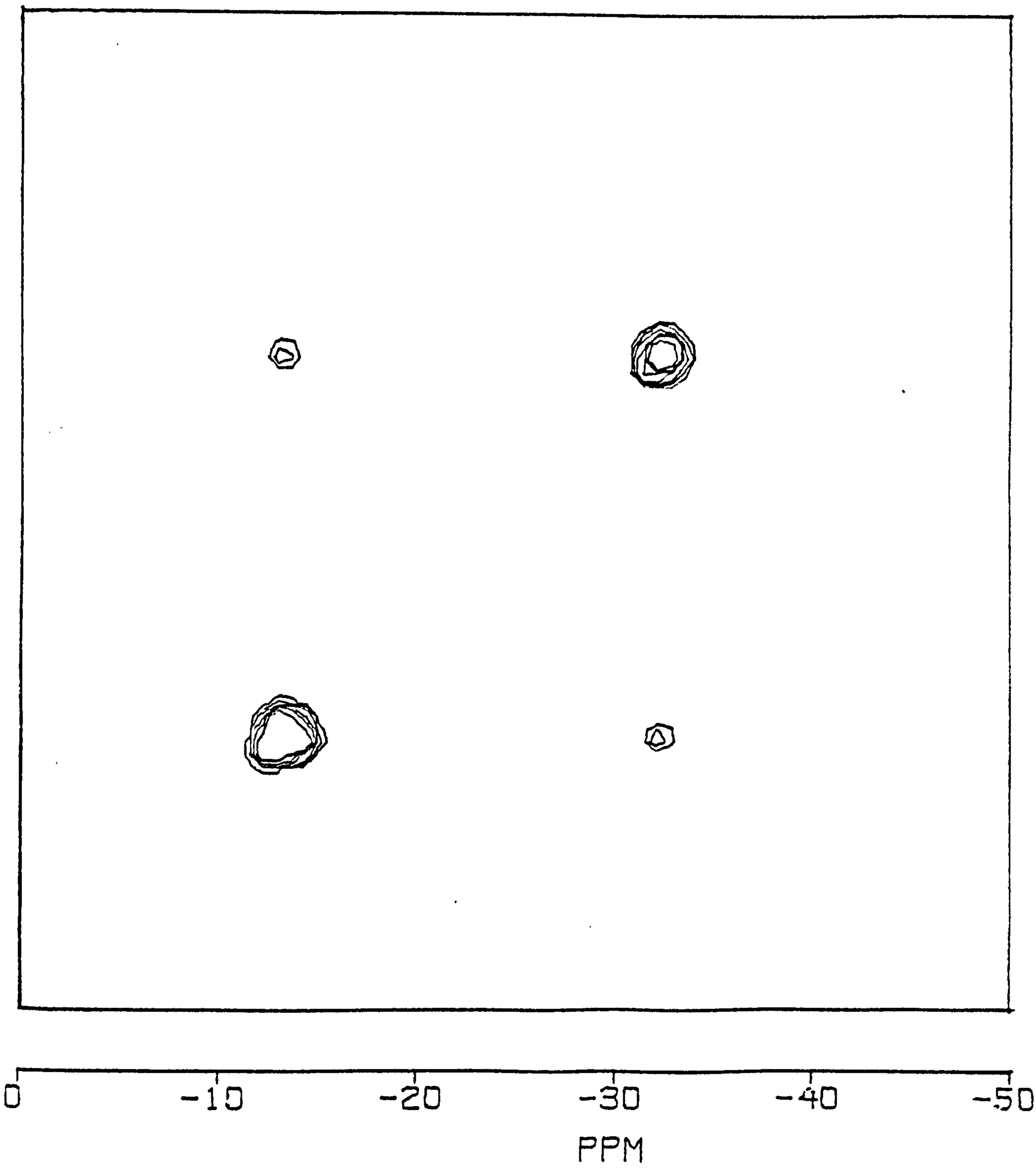

line broadening due to increased quadrupolar relaxation became more important, and hence, as the efficiency of quadrupolar relaxation increased, and the spectral lines became broader, the possibility of observing a ^{11}B-^{11}B coupling was more and more remote. Addition of a substituent affects the electric field gradient at all three boron nuclei, as it also affects the chemical shifts of all three nuclei. It was found that going from the $[Cl]^-$ to the $[NCS]^-$ substituent the efficiency of quadrupolar relaxation was increased, and hence,in $CDCl_3$, no coupling was observed for $[B_3H_7(NCS)]^-$ between boron nuclei, whereas for $[B_3H_7(Cl)]^-$ in $CDCl_3$ a coupling (J_{BB} = 21.OH_z) was observed. In all the substituted derivatives of the octahydrotriborate (1-) anion the resonance due to the substituted boron atom B(1) was more poorly resolved than that due to B(2) and B(3). This observation could be attributed to a combination of spin-spin coupling to the substituent and quadrupolar induced fast relaxation by the substituent resultng in severe line broadening.[144] In addition, it was found that line broadening increased, for any one anion, as the solvent was changed from CD_3CN to $CDCl_3$, this effect was attributed to the formation of ion pairs or ion aggregates in solution.[145] Theoretical calculations by Suzuki and Kubo[146] have shown that the 1:1:1:1 quartet resulting from spin-spin coupling to a nucleus of I = $^3/2$ collapsed as the rate of relaxation of the nucleus increased, by the outer lines moving inward and the inner lines moving outward. This is what was observed[99] for $[B_3H_7(NCS)]^-$ on going from CD_3CN to $CDCl_3$. Since ^{11}B-^{11}B spin-spin coupling is observed in $[B_3H_7(NCS)]^-$ in CD_3CN but not in $CDCl_3$, in the line-narrowed ^{11}B-{^1H} decoupled n.m.r.

spectrum, it might be expected that the same coupling would be observed in the 2-D COSY spectrum that would result in a cross peak representing a correlation between the unsubstituted B(2),B(3) atoms and the unique substituted boron atom B(1), this correlation is observed, (Figure 2.14). It is important to note that the 2-D COSY spectrum was run as a $CDCl_3$ solution, this testifies to the usefulness of the technique in the determination of ^{11}B-^{11}B couplings that are otherwise difficult to see. In the 2-D COSY spectra of $[B_3H_7(NCS)]^-$ and $[B_3H_7(NCSe)]^-$, since a correlation is observed between B(2),B(3) and B(1) in both cases, there has to be overlap of electron density between the substituted and unsubstituted boron nuclei. Since both of the anions are fluxional on the n.m.r. time scale all three boron nuclei will be hydrogen bridged at any instant, and therefore, no correlation should be observed.[127(a)] If however, the solution structure is similar to that of the solid state structure then, as a result of the asymmetric face bridging hydrogen atom, electron density would be re-directed into the B-B vector of the B-H-B bridge bond, giving a significant coupling that appears as cross peaks in the 2-D COSY spectra.

(c) $\underline{[B_3H_7NCBH_3]^-}$

The 115.5 MH_z 2-D ^{11}B-^{11}B (COSY) spectrum (Figure 2.15) shows a correlation between the unsubstituted boron nuclei B(2) and B(3) at δ -9.9 p.p.m. and the unique N-coordinated boron nucleus at δ -36.1 p.p.m. In addition the resonance corresponding to the proton decoupled boron nucleus of the $[BH_3]$ moiety of the substituent appears at δ -43.8 p.p.m. The x-ray crystal structure of this anion has been determined[147]

Figure 2.15 The 115.5 MH_z ^{11}B 2-D COSY spectrum of $[B_3H_7(NCBH_3)]^-$ in $CDCl_3$.

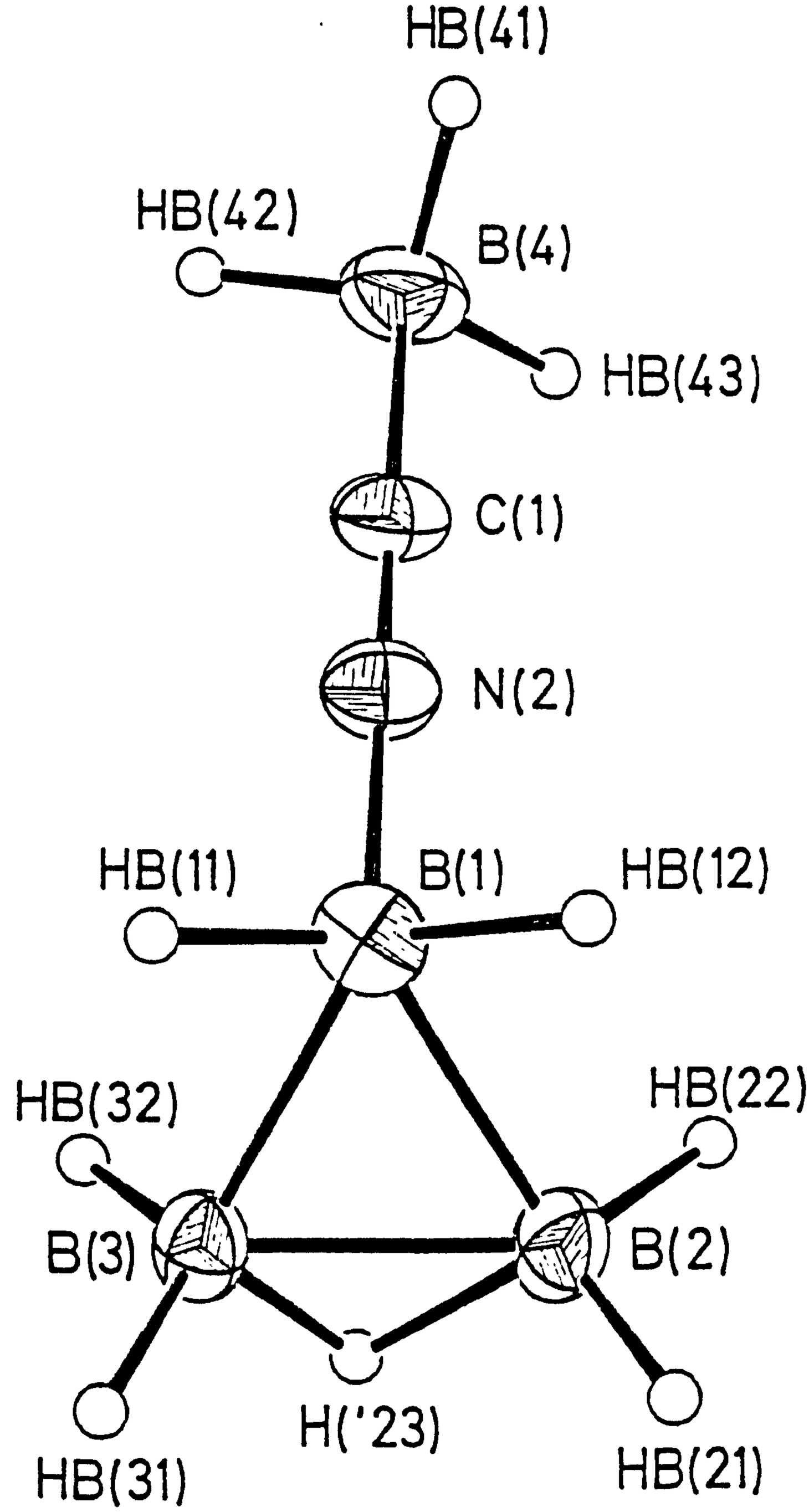

Figure 2.16 The crystal structure of the $[B_3H_7(NCBH_3)]^-$ ion.

and has been shown to have a structure similar to that of $B_3H_7[CO]$, that is a 1104 styx structure (Figure 2.16). The electron density overlap between the three boron nuclei arises as a result of the molecule being three centre bonded, hence there is ^{11}B-^{11}B coupling between the boron nuclei that appears as a cross peak in the 2-D COSY n.m.r. spectrum. Previous investigation of $[B_3H_7(NCBH_3)]^-$ in $CDCl_3$ and CD_3CN[99] showed a single ^{11}B-^{11}B coupling (J_{BB} = 16.5H_z) in CD_3CN and no observable coupling in $CDCl_3$. Going from $[Cl]^-$ to $[NCS]^-$ to $[NCBH_3]^-$ it was found that as the substituents were changed the efficiency of quadrupolar induced relaxation was enhanced.

(d) $\underline{[B_3H_7(NCBH_2CN)]^-}$

Figure 2.17 shows the 115.5 MH_z ^{11}B-^{11}B 2-D (COSY) spectrum obtained for $[B_3H_7(NCBH_2CN)]^-$. In addition to the resonances attributed to the unsubstituted boron nuclei B(2),B(3) at δ -8.9 p.p.m. and the nitrogen-coordinated unique boron nucleus at δ -34.8 p.p.m, there is a triplet of relative intensity 1 at δ -40.8 p.p.m. attributed to the $[BH_2]$ moiety of the substituent. $[B_3H_7(NCBH_3)]^-$, indicated by the presence of a quartet at δ -42.0 p.p.m., was present as a trace impurity. As the cross peak indicates, there is a correlation between the unsubstituted boron nuclei B(2),B(3) and the N-coordinated boron nucleus B(1). There are two possible explanations for this correlation; (i), the correlation arises since the molecule is three centre bonded in solution, and therefore, by definition, has electron density overlap between all three boron nuclei, or (ii), if the molecule has a structure,

Figure 2.17 The 115.5 MH_z ^{11}B 2-D COSY n.m.r. spectrum of $[B_3H_7(NCBH_2CN)]^-$ in $CDCl_3$.

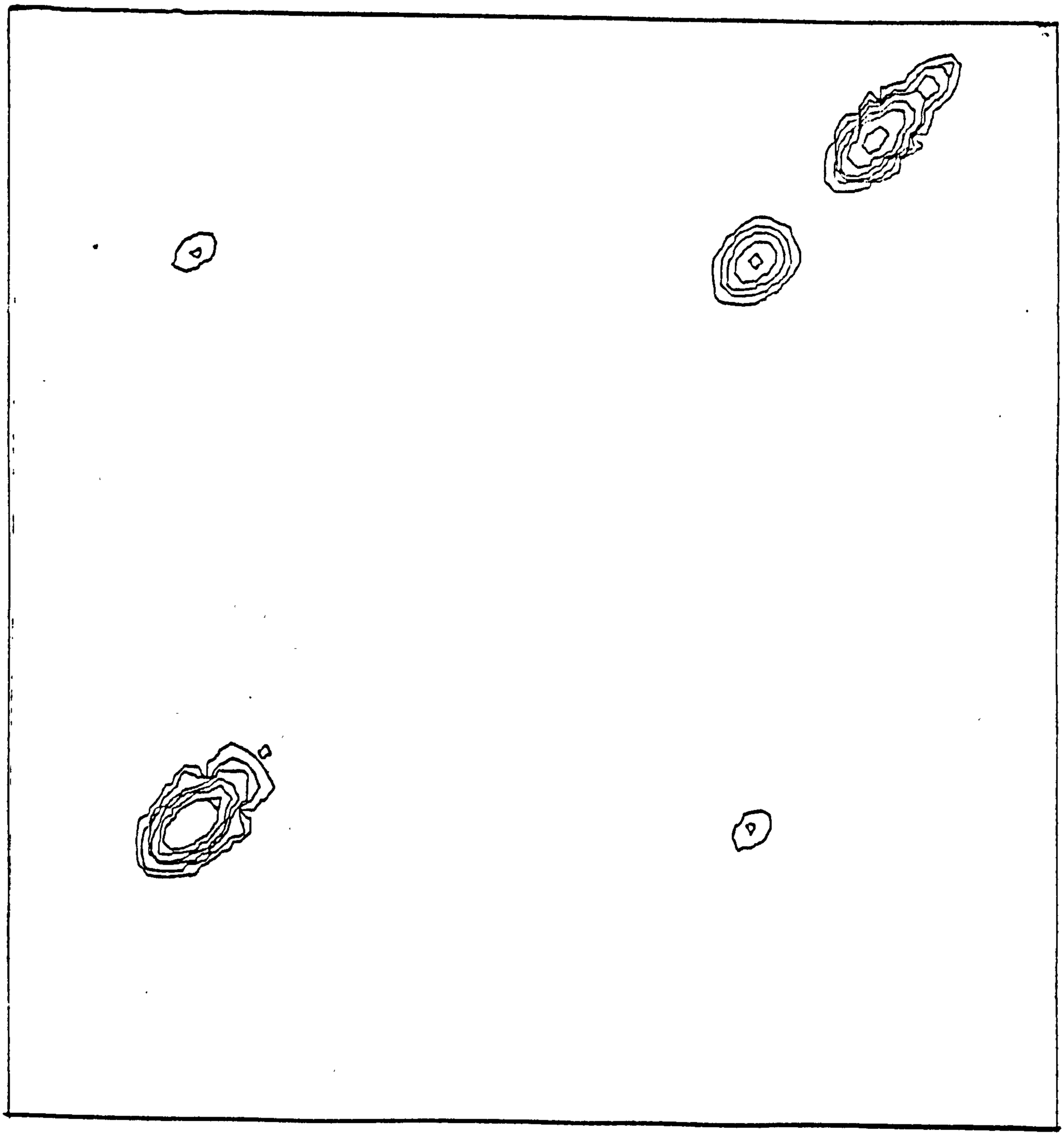

in solution, similar to the structure of $[B_3H_8]^-$, (i.e. a 2013 styx structure), then the hydrogen bridge bonds involved must be asymmetric to re-direct electron density into the B-B vector of the B-H-B bond. Since it is known[147] that both $[B_3H_7(NCBH_3)]^-$ and $[B_3H_7NCB_3H_7]^-$ have three centre bonded structures it is proposed that $[B_3H_7(NCBH_2CN)]^-$ has a similar structure, and that the observed correlation in the 2-D (COSY) spectrum is due to electron density overlap between the three boron centres in a three centred bond.

(e) $\underline{[B_3H_7(NCBPh_3)]^-}$

The $[B_3H_7(NCBPh_3)]^-$ ion was unique in that it was the only mono-substituted derivative of the octahydrotriborate (1-) ion that did not show a correlation in the 2-D COSY n.m.r. spectrum in $CDCl_3$. It is noticeable that in the 115.5 MH_z $^{11}B-\{^1H\}$ decoupled n.m.r. spectrum the line widths of the boron resonances are marginally broader than in the other $[B_3H_7(X)]^-$ (X=Cl,NCS,NCSe,$NCBH_3$,$NCBH_2CN$ and NCB_3H_7) anions studied. This indicated (i) that the electric field gradient at the boron nuclei in $[B_3H_7(NCBPh_3)]^-$ is relatively high *and/or* (ii) that the correlation time of this species is much longer resulting in rapid quadrupolar relaxation and broader lines. This occurs since $[B_3H_7(NCBPh_3)]^-$ is relatively large and hence its rate of molecular reorientation is low, resulting in efficient spin-lattice interactions and relaxation is therefore fast. The relatively large line widths observed in $CDCl_3$ meant that the possibility of "seeing" a $^{11}B-^{11}B$ coupling was reduced. The $^{11}B-\{^1H\}$ n.m.r spectrum of $[B_3H_7(NCBPh_3)]^-$ in CD_3CN at 60°C exhibited much sharper lines testifying to the reduced rate of quadrupolar relaxation due to the formation

of solvated ions.[145] Furthermore at 60°C, the rate of molecular reorientation is relatively high, correlation times are shorter, and spin-lattice relaxation is slower. The 2-D (COSY) n.m.r. experiment was repeated and in CD_3CN at 60°C a correlation was observed between the unsubstituted boron atoms B(2),B(3) at δ-9.2 p.p.m. and the N-coordinated boron resonance at δ -34.7 p.p.m. It is thought that, like $[B_3H_7(NCBH_3)]^-$ and $[B_3H_7NCB_3H_7]^-$, the $[B_3H_7(NCBPh_3)]^-$ anion is three centre bonded and that the observed correlation arises as a result of electron density overlap between the three boron nuclei in the three centred bond.

(b) Disubstituted Anions

(i) $[B_3H_6(Cl)_2]^-$

The 2-Dimensional (COSY) n.m.r. spectrum of $[B_3H_6(Cl)_2]^-$ showed a correlation between the two chloride substituted boron atoms at δ −11.9 p.p.m. and the single unique unsubstituted boron atom at δ −4.3 p.p.m. A study of the structure of $[B_3H_6(Cl)_2]^-$ showed[37] that the two chloride atoms are substituted in trans- fashion (Figure 2.8), furthermore the two hydrogen atoms of the B-H-B bridge bonds asymmetrically bridge between the substituted and unsubstituted boron atoms. It is proposed that the asymmetric nature of the hydrogen bridge bonds causes electron density to be re-directed into the B-B connectivity resulting in a ^{11}B-^{11}B coupling that appears as a cross peak in the 2-D (COSY) n.m.r. spectrum.

(ii) $[B_3H_6(Cl)(NCS)]^-$

In this anion all three boron atoms are unique since one is

N-coordinated, one is Cl substituted and the last is unsubstituted. The 2-D ^{11}B-^{11}B (COSY) spectrum of $[B_3H_6(Cl)(NCS)]^-$ showed only a single correlation between the resonance at δ-25.9 p.p.m., attributed to the N-coordinated boron atom, and the resonance at δ-8.8 p.p.m. No correlation with the resonance that appeared at δ-5.1 p.p.m. was observed. These data indicated that there was electron density overlap between two of the boron nuclei with little, or no, electron density between these boron nuclei and the third. This inferred a structure in which two boron atoms are bonded via a single B-B bond to give a correlation. Since no correlation is observed to the third boron atom, this atom must be bonded via two hydrogen bridge bonds to the other boron nuclei. The x-ray crystal structure determination of $[B_3H_6(Cl)(NCS)]^-$ has shown[37] a heavy atom structure similar to that of $[B_3H_6(Cl)_2]^-$ although no hydrogen atoms were located. The crystal structure of $[B_3H_6(Cl)(NCS)]^-$ indicated a trans-1,2-disubstitution pattern in which the boron atoms that are substituted are singly bonded. Hence, the correlation that appears in the 2-D (COSY) n.m.r. spectrum is due to overlap of electron density between the Cl and NCS substituted boron atoms. Therefore the resonance that appears at δ -8.8 p.p.m. is due to the chloride substituted boron nucleus and not the unsubstituted boron atom as previously thought.[37]

In the disubstituted anions, $[B_3H_6(Cl)(NCS)]^-$ and $[B_3H_6(Cl)NCB_3H_7]^-$, a correlation is observed between the two substituted boron nuclei, it is proposed that on the n.m.r.time scale there is a time-averaged structure similar to the crystallographically determined solid state

structure. In the time-averaged structure the hydrogen atoms of the B-H-B bonds symmetrically bond between the substituted boron atoms (B-Cl) and (B-N) and the unsubstituted boron atom (B-H). Hence, no correlation is observed between the hydrogen bridged boron nuclei in this case. In conclusion, the information obtained from the 2-D ^{11}B-^{11}B (COSY) n.m.r. spectrum supports a solution structure similar to the solid state structure determined crystallographically.[37]

(iii) $\underline{[B_3H_6(Cl)(NCBH_2Cl)]^-}$

The 2-D ^{11}B-^{11}B (COSY) n.m.r. spectrum obtained from the reaction of $[B_3H_7(NCBH_3)]^-$ with excess HCl in dichloromethane indicates the presence of two products identified as $[B_3H_7(NCBH_2Cl)]^-$ and $[B_3H_6(Cl)(NCBH_2Cl)]^-$,(the relevant n.m.r.data are presented in Table 2.3). The 2-D COSY spectrum shows only a single correlation between the N-coordinated boron atom of the disubstituted species at δ-31.3 p.p.m. and the resonance at δ0.53 p.p.m. attributable to the chloride substituted boron atom (B-Cl). The lack of further correlations in this case may be due to the fact that the 2-D (COSY) spectrum was not proton decoupled, hence the spectral lines were relatively broad making the ^{11}B-^{11}B coupling more difficult to see. Alternatively,it is possible,although unlikely, that substitution of a hydrogen atom by chlorine at the $[BH_3]$moiety of the substituent causes a structural change from the expected 1104 styx structure of the parent anion,$[B_3H_7(NCBH_3)]^-$,to a 2013 styx structure as in $[B_3H_6(Cl)_2]^-$,in this case, since no correlation is observed,the solution structure of $[B_3H_7(NCBH_2Cl)]^-$ would have symmetric hydrogen bridged boron bonds withdrawing electron density from the B-B vector. From

the data available, although this model is a possibility, it is thought that the solution structure of $[B_3H_7(NCBH_2Cl)]^-$ is the same as that of $[B_3H_7(NCBH_3)]^-$, i.e. three centre bonded. The absence of correlations to support this hypothesis may be explained in two ways; (i) replacing a hydrogen atom with a chlorine atom at the substituent may cause an increase in the electric field gradient of the boron nuclei of the triborane fragment, resulting in broadened signals and unresolved ^{11}B-^{11}B couplings, or (ii), the sensitivity of the n.m.r. instrument used was not great enough to observe any ^{11}B-^{11}B couplings that may have been present.

In the disubstituted anion, $[B_3H_6(Cl)(NCBH_2Cl)]^-$, it is proposed, by comparison with the other disubstituted anions $[B_3H_6(Cl)(X)]^-$ (X=Cl,NCS and NCB_3H_7), that the structure of this anion is similar to that of $[B_3H_6(Cl)_2]^-$ (Figure 2.8) in solution. That is, the substituents are trans- to each other at either side of a B-B bond, resulting in the observed correlation.

2.3.3 Conclusion

It was evident from these studies that the generally applied rule[127(a)] that a correlation between hydrogen bridged boron nuclei is not observable does not, in general, hold for substituted derivatives of the octahydrotriborate (1-) ion. From the results obtained whether or not a correlation is observed between hydrogen bridged boron nuclei depends on the symmetry of the B-H-B bond. Since this rule is not generally applicable the results obtained from the 2-D (COSY) n.m.r. technique

can be ambiguous. Although it has been shown that the 2-D (COSY) n.m.r. technique can be used as a probe to qualitatively determine the nature of the bonding in substituted derivatives of the octahydrotriborate (1-) ion, more work on other triborane fragments, of known solid state structure, must be done before the technique can be used to elucidate bonding types in higher boranes and metallaboranes.

2.4 Experimental

2.4.1 General

$[NMe_4][B_3H_8]$ was purchased from the Callery Chemical Company and recrystallised from acetonitrile - diethylether before use. $[N(PPh_3)_2][B_3H_8]$ was prepared by addition of an ethanolic solution of $[N(PPh_3)_2][Cl]$ to $[NMe_4][B_3H_8]$ in water and recrystallised from dichloromethane - diethylether. $[N(PPh_3)_2][B_3H_7(Cl)]$ was prepared according to the published procedure.[99] The novel anion, $[BH_2(CN)_2]^-$ was prepared by reaction of $NaBH_4$ with $Hg(CN)_2$ in diglyme.[148] The salts $[N(PPh_3)_2][X]$(X=NCS,NCSe,$NCBH_3$,$NCBH_2NCBH_3$,[93] $NCBH_2CN$ and $NCBPh_3$) were prepared from $[N(PPh_3)_2][Cl]$ and NaX in water and extracting the product by phase transfer to CH_2Cl_2, recrystallisation from CH_2Cl_2/Et_2O yields colourless crystals in all cases. All other reagents were used as received.

2.4.2 Preparation of $[N(PPh_3)_2][B_3H_7(NCSe)]$

$[N(PPh_3)_2][NCSe]$ (1.35g, 2.1 mmol) and $[N(PPh_3)_2][B_3H_7(Cl)]$ (1.22g, 2.0 mmol)were placed in a 250cm³ round-bottomed flask fitted with a stopcock adaptor. Dry CH_2Cl_2 (ca. 30cm³) was condensed onto

the solid reagents and the mixture was allowed to warm to room temperature. The clear solution was stirred for 4 hr. under vacuum, after which time the solvent was removed to yield a white solid. Thin layer chromatographic (t.l.c.) analysis on silica gel using 100% CH_2Cl_2 as eluant indicated a single major component (Rf= 0.45). Purification by chromatography on silica gel using 100% CH_2Cl_2 as eluant gave a white solid. Recrystallisation from CH_2Cl_2/n-pentane yields colourless crystals of $[N(PPh_3)_2IB_3H_7(NCSe)]$.

(Found: C, 64.65; H, 5.49; N, 3.81; P, 9.02%

$C_{37}H_{37}B_3N_2P_2Se$ requires: C, 65.03; H, 5.46; N, 4.10; P, 9.07%).

2.4.3 Preparation of $[N(PPh_3)_2IB_3H_7(NCBPh_3)]$

An identical procedure to that used in 2.4.2 was used to prepare $[N(PPh_3)_2IB_3H_7(NCBPh_3)]$. Dry CH_2Cl_2 (ca. 30cm^3) was condensed onto the solid reagents $[N(PPh_3)_2IB_3H_7(Cl)]$ (0.613g, 1 mmol) and $[N(PPh_3)_2INCBPh_3]$ (0.806g, 1 mmol) under vacuum. After warming to room temperature the clear solution was stirred for 4 hr. after which time the solvent was removed under reduced pressure to yield a white solid. T.l.c. analysis on silica gel using 100% CH_2Cl_2 as eluant indicated a single major product (Rf=0.69). The major fraction was purified by chromatography on silica gel using 100% CH_2Cl_2 as eluant. Recrystallisation from CH_2Cl_2/Et_2O yields $[N(PPh_3)_2][B_3H_7(NCBPh_3)]$ as colourless crystals.

(Found: C, 77.79; H, 6.22; N, 2.99; P, 7.72%

$C_{55}H_{52}B_4N_2P_2$ requires: C, 78.04; H, 6.19; N, 3.31; P, 7.32%).

2.4.4 Preparation of $[N(PPh_3)_2][B_3H_7(NCBH_2NCBH_3)]$

$[N(PPh_3)_2][BH_3CNBH_2CN]$ (0.62g, 1 mmol) and $[N(PPh_3)_2][B_3H_7(Cl)]$ (0.61g, 1 mmol) were placed in a round-bottomed flask fitted with a stopcock : adaptor. Dry CH_2Cl_2 (ca. 30cm^3) was condensed in and the mixture was warmed to room temperature. The clear solution was stirred for 4 hr. after which time the solvent was removed under reduced pressure to yield an oil. T.l.c. analysis on silica gel using 100% CH_2Cl_2 as eluant indicated a single major fraction (Rf=0.80). Purification by chromatography yields the major fraction as an oil. The oil is identified as $[N(PPh_3)_2][B_3H_7(NCBH_2NCBH_3)]$ by ^{11}B, ^1H n.m.r. and by infra-red spectroscopy.

2.4.5 Preparation of $[N(PPh_3)_2][B_3H_7(NCBH_2CN)]$ and $[N(PPh_3)_2][B_3H_7(NCBH_2CN)B_3H_7]$.

$[N(PPh_3)_2][NCBH_2CN]$ (1.80g, 3 mmol) and $[N(PPh_3)_2][B_3H_7(Cl)]$ (1.84g, 3 mmol) were placed in a 250cm^3 round-bottomed flask fitted with a stopcock adaptor. Dry CH_2Cl_2 (ca. 30cm^3) was condensed in under vacuum and the mixture was warmed to room temperature. The clear solution was stirred for 4 hr. after which time the solvent was removed, under reduced pressure, to give a white solid. T.l.c. analysis of the solid on silica gel using 100% CH_2Cl_2 as eluant indicated a minor fraction (Rf=0.75) and a major fraction (Rf=0.52). Separation by chromatography on silica gel using 100% CH_2Cl_2 as eluant yields both minor and major fractions. Characterisation of the minor and major fractions by ^{11}B n.m.r. spectroscopy showed that the products

were $[N(PPh_3)_2][B_3H_7(NCBH_2CN)B_3H_7]$ and $[N(PPh_3)_2][B_3H_7(NCBH_2CN)]$ respectively. The minor fraction, $[N(PPh_3)_2][B_3H_7(NCBH_2CN)B_3H_7]$ can be obtained exclusively by reacting two equivalents of $[B_3H_7(Cl)]^-$ with $[BH_2(CN)_2]^-$.

(Found: C,70.46; H,6.08; N,6.22; P,9.71%

$C_{38}H_{39}B_4N_3P_2$ requires: C,70.96; H,6.11; N,6.54; P,9.64%)

2.4.6 Preparation of $[N(PPh_3)_2][B_3H_7NCB_3H_7]$

Cyanogen bromide (0.61g, 5.8 mmol) was placed in a 250cm³ round-bottomed flask fitted with a stopcock adaptor. Dry CH_2Cl_2 (ca. 30cm³) was condensed into the flask under vacuum and the mixture was warmed to room temperature. When the CNBr had completely dissolved the system was cooled to -196°C and $[N(PPh_3)_2][B_3H_8]$ (6.74g, 11.6 mmol) was introduced. The system was re-evacuated and warmed to room temperature. At room temperature a vigorous reaction took place with gas evolution. When the gas evolution stopped the solvent was removed under reduced pressure to give a white solid. T.l.c. analysis on silica gel using 100% CH_2Cl_2 as eluant indicated a single major fraction (Rf=0.61) and a minor fraction (Rf=0.45). Purification by chromatography on silica gel using 100% CH_2Cl_2 as eluant yields the major and minor products as white solids. The minor product is identified from its ^{11}B n.m.r. spectrum as $[N(PPh_3)_2][B_3H_7(NCBH_3)]$, the major product was recrystallised from CH_2Cl_2/ n-hexane to give colourless crystals and was identified by crystallographic and various spectroscopic techniques as $[N(PPh_3)_2][B_3H_7NCB_3H_7]$.

(Found: C,68.92; H,6.94; N,4.31; P,9.64%

$C_{37}H_{44}B_6N_2P_2$ requires: C,69.02; H,6.89; N,4.35; P,9.63%).

2.4.7 Preparation of $[N(PPh_3)_2IB_3H_6(Cl)(NCBH_2NCBH_3)]$

$[N(PPh_3)_2IB_3H_7(NCBH_2NCBH_3)]$ (0.65g, 1mmol) was placed in a 250 cm^3 round-bottomed flask fitted with a stopcock adaptor. Dry CH_2Cl_2 (ca.30cm^3) was condensed in under vacuum and the system was warmed to room temperature. When all the $[N(PPh_3)_2IB_3H_7(NCBH_2NCBH_3)]$ had dissolved the system was cooled to -196°C and gaseous HCl (0.14g, 4mmol) was condensed in. The system was warmed to room temperature and was stirred for 4 hr.,after which time the solvent was removed from the clear solution under reduced pressure to yield an oil. T.l.c. analysis on silica gel using 100% CH_2Cl_2 as eluant indicated two major products (Rf values are 0.80 and 0.65). The crude product was examined by ^{11}B n.m.r. and shown to be a mixture of $[N(PPh_3)_2IB_3H_6(Cl)(NCBH_2NCBH_3]$ and starting material.

2.4.8 Preparation of $[N(PPh_3)_2IB_3H_6(Cl)(NCBH_2CN)]$

The method employed in 2.4.7 was used to prepare $[N(PPh_3)_2IB_3H_6(Cl)(NCBH_2CN)]$. To a cooled (-196°C) solution of $[N(PPh_3)_2IB_3H_7(NCBH_2CN)]$ (0.64g, 1mmol) in dry CH_2Cl_2 (ca. 30cm^3), gaseous HCl (0.14g, 4mmol) was added. The system was warmed to room temperature and the resulting clear solution was stirred under vacuum for 4hr. The solvent was removed under reduced pressure to give a white solid. T.l.c. analysis on silica gel using 100% CH_2Cl_2 as eluant indicated two major components (Rf values are 0.52 and 0.45). The white solid was analysed by ^{11}B n.m.r. and was shown to be a mixture of the starting material and $[N(PPh_3)_2IB_3H_6(Cl)(NCBH_2CN)]$.

2.4.9 Preparation of $[N(PPh_3)_2IB_3H_6(Cl)NCB_3H_7]$

$[N(PPh_3)_2IB_3H_7NCB_3H_7]$ (1.24g, 1.9 mmol) was placed in a 250cm³ round-bottomed flask fitted with a stopcock adaptor. Dry CH_2Cl_2 (ca.30cm³) was condensed in under vacuum. The system was warmed to room temperature until all the $[N(PPh_3)_2IB_3H_7NCB_3H_7]$ had dissolved, the clear solution was cooled to -196°C and gaseous HCl (0.26g, 7.3 mmol) was condensed in under vacuum. The system was then stirred at room temperature for 4 hr. after which time the solvent was removed under reduced pressure to yield a white solid. T.l.c. analysis on silica gel using 100% CH_2Cl_2 as eluant indicated a single major product (Rf=0.57). Purification by chromatography on silica gel using 100% CH_2Cl_2 as eluant yields the major product as a crystalline white solid. The white solid is recrystallised from CH_2Cl_2/n-hexane to give colourless needle-like crystals in good yield (1.05g, 81.5%).

(Found: C,65.51; H,6.51; Cl,5.76; N,3.95; P,9.00%

$C_{37}H_{43}B_6ClN_2P_2$ requires: C,65.51; H,6.39; Cl,5.23; N,4.13; P,9.14%)

2.4.10 Preparation of $[N(PPh_3)_2IB_3H_6(Br)NCB_3H_6(Br)]$

$[N(PPh_3)_2IB_3H_7NCB_3H_7]$ (0.64g, 1mmol) was placed in a 250cm³ three-necked round-bottomed flask flushed with dry nitrogen. Dry CH_2Cl_2 (ca. 30cm³) was added. To the colourless solution a pale yellow solution of N-bromosuccinimide (0.89g, 5mmol) in CH_2Cl_2 was added dropwise with stirring. On addition the pale yellow solution went clear and a white precipitate (succinimide) was formed. After the N-bromosuccinimide solution was added the system was stirred for

an hour under nitrogen. The solution was filtered to remove the white precipitate and the solvent was removed under reduced pressure to yield a yellow/white solid. T.l.c. analysis on silica gel using 100% CH_2Cl_2 as eluant indicated a single major product (Rf=0.65). Purification by chromatography on silica gel using 100% CH_2Cl_2 as eluant gave the major product as a colourless solid in low yield. The product obtained was analysed by ^{11}B n.m.r. and was shown to be $[N(PPh_3)_2]$ $[B_3H_6(Br)NCB_3H_6(Br)]$.

2.4.11 The Reaction of $[N(PPh_3)_2][B_3H_7(Cl)]$ and CNBr

Cyanogen bromide (0.16g, 1.5 mmol) was placed in a 250cm³ round-bottomed flask fitted with a stopcock adaptor. Dry CH_2Cl_2 (ca.30cm^3) was condensed in and the system was warmed to room temperature until all the CNBr had dissolved. The colourless solution was cooled to -196°C and $[N(PPh_3)_2][B_3H_7(Cl)]$ (0.92g, 1.5 mmol) was added. The system was evacuated and warmed to room temperature where a vigorous reaction took place with severe gas evolution. When gas evolution had stopped the solvent was removed from the system to give a white solid. T.l.c. analysis on silica gel using 100% CH_2Cl_2 as eluant showed a single major component (Rf=0.48) and several minor components. The white solid was examined by ^{11}B n.m.r. and shown to have a disubstituted species as the major constituent.

CHAPTER THREE

ELECTROCHEMICAL STUDIES OF SUBSTITUTED DERIVATIVES OF THE $[B_3H_8]^-$ ION

3.1 Introduction

The electrochemical oxidation of the octahydrotriborate (1-) ion has previously been studied using chronopotentiometry and controlled potential coulometry at platinum or gold anodes in acetonitrile or dimethylformamide.[95] This study showed a one electron oxidation leading ultimately to the adduct B_3H_7L (L=CH_3CN or DMF) although the mechanism of the electrochemical process was not established. The electrochemical oxidation of the $[B_3H_8]^-$ ion has further been studied[97] by cyclic voltammetry, a.c. voltammetry and controlled potential electrolysis. The cyclic voltammogram of $[NMe_4][B_3H_8]$ at a platinum electrode in acetonitrile containing $[NBu^n_4][BF_4]$ (0.1 $mol.dm^{-3}$) as supporting electrolyte showed an irreversible oxidation near +0.75V whose current maximum shifted to +0.53V on repetitive scanning. The a.c. voltammogram of the same solution confirmed the presence of an irreversible oxidation at +0.60V. Controlled potential electrolysis carried out on the acetonitrile solution of $[B_3H_8]^-$ proceeded at potentials of +0.4 → +0.9V and resulted in a one electron oxidation. The presence of $B_3H_7[NCCH_3]$ as the only boron-containing product[95] suggested the following mechanism:

$$[B_3H_8]^- \rightarrow [B_3H_8]^{\bullet} + e^- \qquad (3\text{-}1)$$

$$[B_3H_8]^{\bullet} \rightarrow [B_3H_7] + H^{\bullet} \qquad (3\text{-}2)$$

$$[B_3H_7] + CH_3CN \rightarrow B_3H_7[NCCH_3] \qquad (3\text{-}3)$$

$$2H^{\bullet} \rightarrow H_2 \qquad (3\text{-}4)$$

At potentials greater than +0.90V more than one electron was involved in the electrolysis and exhaustive coulometric oxidation at +1.2V showed

a two electron oxidation. The only boron containing product was again $B_3H_7[NCCH_3]$. These data, together with trace-crossing and pulsed-voltammetric experiments, indicated the overall mechanism:

$$[B_3H_8]^- \longrightarrow [B_3H_7] + H^+ + 2e^- \quad (3\text{-}5)$$

$$[B_3H_7] + CH_3CN \rightarrow B_3H_7[NCCH_3] \quad (3\text{-}6)$$

In addition to the $[B_3H_8]^-$ ion the monosubstituted derivatives $[B_3H_7(X)]^-$(X =Cl,NCS and $NCBH_3$) were studied.[97] The $[B_3H_7(Cl)]^-$ anion underwent an irreversible one electron oxidation at ca. +0.5V in acetonitrile to yield $B_3H_7[NCCH_3]$ and HCl by the mechanism:

$$[B_3H_7(Cl)]^- \rightarrow [B_3H_7(Cl)]^{\bullet} + e^- \quad (3\text{-}7)$$

$$[B_3H_7(Cl)]^{\bullet} \rightarrow [H]^{\bullet} + [B_3H_6(Cl)] \quad (3\text{-}8)$$

$$[B_3H_7(Cl)]^- + [H]^{\bullet} \rightarrow [B_3H_7]^{\bullet -} + HCl \quad (3\text{-}9)$$

$$[B_3H_7]^{\bullet -} \rightarrow [B_3H_7] + e^- \quad (3\text{-}10)$$

$$[B_3H_7] + CH_3CN \rightarrow B_3H_7[NCCH_3] \quad (3\text{-}11)$$

$$[B_3H_6(Cl)] \rightarrow \text{decomposition products} \quad (3\text{-}12)$$

The $[B_3H_7(NCS)]^-$ anion showed an irreversible oxidation wave near +1.3V. At this potential, coulometry indicated a four electron oxidation resulting in complex decomposition of the anion. The $[B_3H_7(NCBH_3)]^-$ anion was stable to oxidation until the irreversible oxidation near +1.1V. Coulometry at this potential indicated that more than four electrons were involved.

In this work, the electrochemical oxidation of the anions $[B_3H_7(X)]^-$ (X=NCSe, $NCBPh_3$, $NCBH_2NCBH_3$, $NCBH_2CNB_3H_7$ and NCB_3H_7) were

investigated by cyclic voltammetry, cyclic a.c. voltammetry and controlled potential electrolysis, to determine the effect of substitution on the electrochemical properties.

3.2 Results and Discussion

3.2.1. Oxidation Studies

(a) $[B_3H_7(NCSe)]^-$

The cyclic voltammogram of $[N(PPh_3)_2][B_3H_7(NCSe)]$ was similar to the cyclic voltammogram of $[B_3H_7(NCS)]^-$ previously described.[97] The cyclic voltammogram of $[B_3H_7(NCSe)]^-$ in acetonitrile with $[NBu^n_4][BF_4]$(0.1 mol dm^{-3}) supporting electrolyte at platinum electrodes consisted of an irreversible oxidation wave near +1.4V and a reduction wave near -0.85V (probably due to H^+), (Figure 3.1). Since the $[B_3H_8]^-$ ion undergoes oxidation at +0.64V in acetonitrile substitution has increased the oxidative stability of the octahydrotriborate(1-) derivative since the potential for oxidation is now +1.4V. Exhaustive controlled potential electrolysis of $[N(PPh_3)_2][B_3H_7(NCSe)]$ at platinum in acetonitrile, at a potential of 1.0V, indicated that the anion underwent a one electron oxidation. The product obtained from the anolyte solution was investigated by ^{11}B n.m.r. spectroscopy, and was shown to be unreacted $[B_3H_7(NCSe)]^-$.

The cyclic voltammogram of $[N(PPh_3)_2][B_3H_7(NCSe)]$ in dichloromethane with $[NBu^n_4][BF_4]$(0.39 mol dm^{-3}) supporting electrolyte, (Figure 3.2), was similar to that obtained in acetonitrile. However, in dichloromethane the peaks were poorly resolved. The cyclic a.c. voltammogram

Figure 3.1(a) Cyclic voltammogram (scan rate = $0.5Vs^{-1}$) and (b) a.c. voltammogram (scan rate = $0.05Vs^{-1}$) of $[B_3H_7(NCSe)]^-$ in CH_3CN.

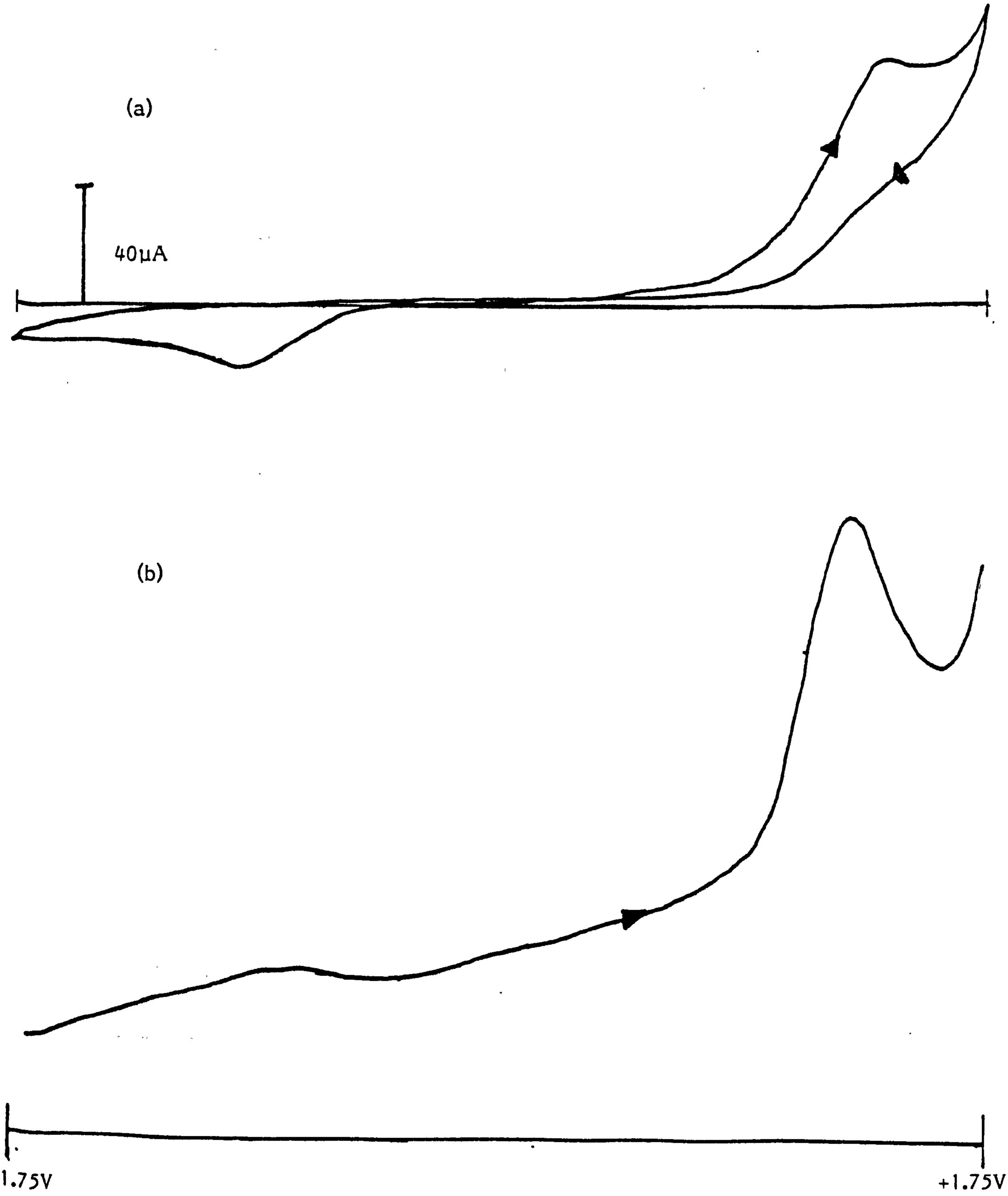

Figure 3.2(a) Cyclic voltammogram (scan rate = 0.5 Vs^{-1}) and (b) cyclic a.c. voltammogram (scan rate = 0.05 Vs^{-1}) of $[B_3H_7(NCSe)]^-$ in CH_2Cl_2.

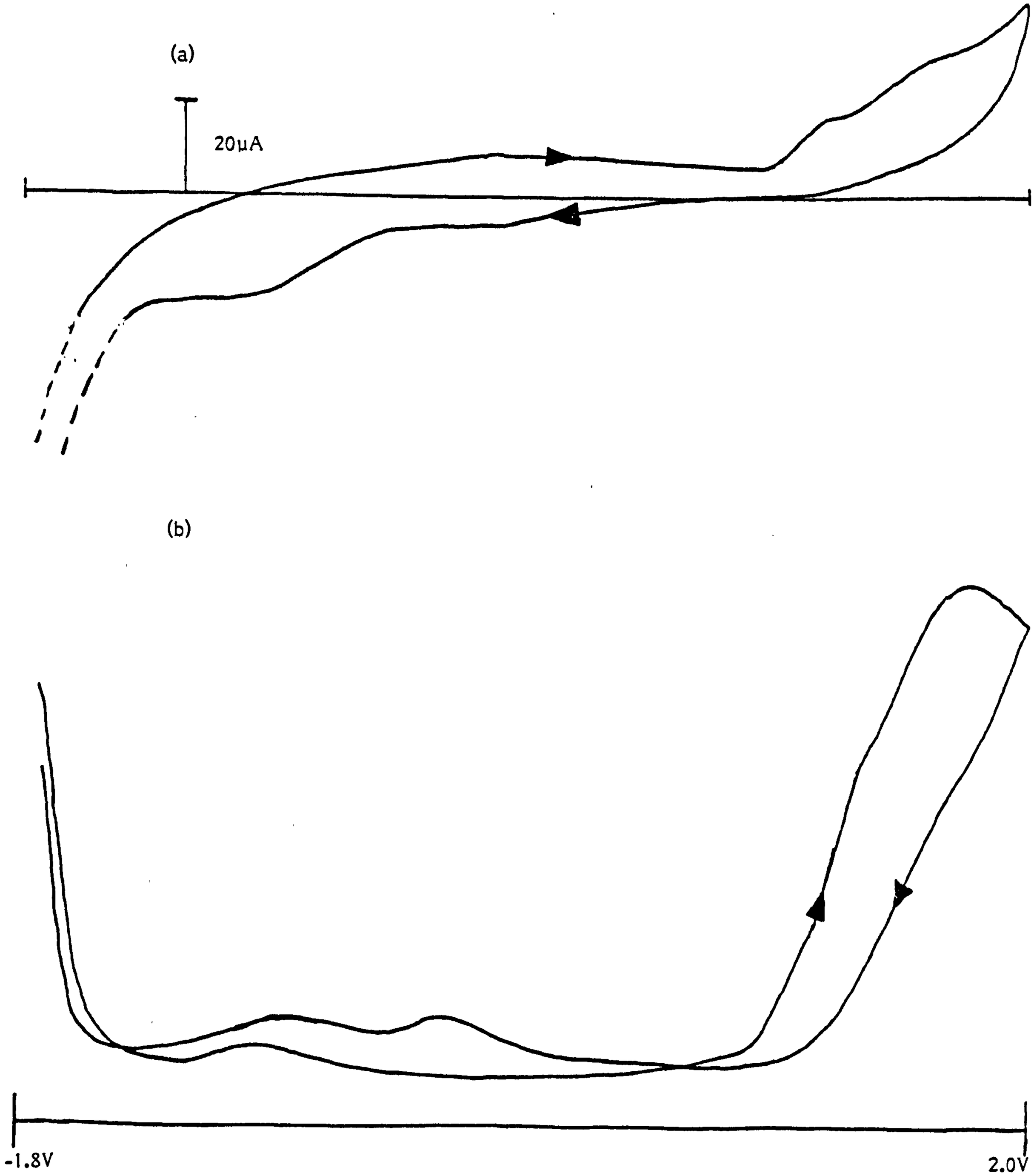

(Figure 3.2) showed a well defined irreversible oxidation near +1.75V that was attributed to solvent oxidation. In addition, a shoulder is observed at +1.4V corresponding to the irreversible oxidation potential of the $[B_3H_7(NCSe)]^-$ anion in dichloromethane. Controlled potential electrolysis of $[N(PPh_3)_2][B_3H_7(NCSe)]$ at platinum in CH_2Cl_2 with $[NBu^n_4][BF_4]$(0.39 mol dm^{-3}) supporting electrolyte proceeded at potentials of 1.2 → 1.6V. After the current corresponding to a one electron oxidation had passed, the anolyte solution was examined by ^{11}B n.m.r. spectroscopy. The only boron containing product was unreacted $[B_3H_7(NCSe)]^-$.

From the cyclic voltammetry and cyclic a.c. voltammetry it was known that the solvent, CH_2Cl_2, oxidised at ca. +1.75V to presumably produce chlorine radicals. Since $[B_3H_7(NCSe)]^-$ was oxidatively stable it was proposed that the disubstituted derivative, $[B_3H_6(Cl)(NCSe)]^-$, could be produced by the reaction of electrochemically generated chlorine radicals with $[B_3H_7(NCSe)]^-$. Exhaustive controlled potential electrolysis at platinum proceeded at a potential of +1.7V and involved more than one electron. Investigation of the crude anolyte solution by ^{11}B n.m.r. spectroscopy showed that no disubstitution had taken place and that the only product obtained was the starting material, $[B_3H_7(NCSe)]^-$. Hence, since disubstitution is not effected, either electrochemically or by reaction with gaseous HCl (Chapter II), then either $[N(PPh_3)_2][B_3H_7(NCSe)]$ is very stable or the disubstituted derivative, $[B_3H_6(Cl)(NCSe)]^-$, is very unstable.

(b) $\underline{[N(PPh_3)_2][B_3H_7(NCBPh_3)]}$

The cyclic voltammogram of $[N(PPh_3)_2][B_3H_7(NCBPh_3)]$ at platinum in acetonitrile with $[NBu^n_4][BF_4]$ (0.1 mol dm^{-3}) supporting electrolyte was similar to the cyclic voltammogram obtained for $[B_3H_7(NCSe)]^-$. An irreversible oxidation wave was observed at ca. +1.7V and an irreversible reduction (probably due to H^+) near -0.8V. The cyclic a.c. voltammogram of $[B_3H_7(NCBPh_3)]^-$ at platinum in acetonitrile (Figure 3.3) showed a well-defined irreversible oxidation at +1.54V that was attributed to the oxidation potential of the anion. A further irreversible oxidation was observed in the cyclic a.c. voltammogram at +1.32V that may have been due to decomposition products. From these data the $[B_3H_7(NCBPh_3)]^-$ anion is oxidatively more stable than the anion, $[B_3H_7(NCSe)]^-$. That is, the $[Ph_3B(CN)]^-$ substituent has stabilised the triborane fragment to a greater extent than the $[NCSe]^-$ substituent. The only identifiable product obtained from the oxidation of $[B_3H_7(NCBPh_3)]^-$ was unreacted starting material, although controlled potential electrolysis indicated a process in which more than one electron was involved.

The cyclic voltammogram (Figure 3.4) of $[B_3H_7(NCBPh_3)]^-$ at platinum in dichloromethane with added $[NBu^n_4][BF_4]$ (0.1 mol dm^{-3}) was identical to that obtained in acetonitrile. It was proposed that controlled potential electrolysis of $[B_3H_7(NCBPh_3)]^-$ in CH_2Cl_2 at 1.6V would produce the disubstituted species $[B_3H_6(Cl)(NCBPh_3)]^-$ via chlorine radical generation by solvent oxidation. However, the only product obtained from this reaction was the starting material, $[B_3H_7(NCBPh_3)]^-$.

Figure 3.4 The cyclic voltammogram (scan rate = 0.5 Vs^{-1}) of $[B_3H_7(NCBPh_3)]^-$ in CH_2Cl_2

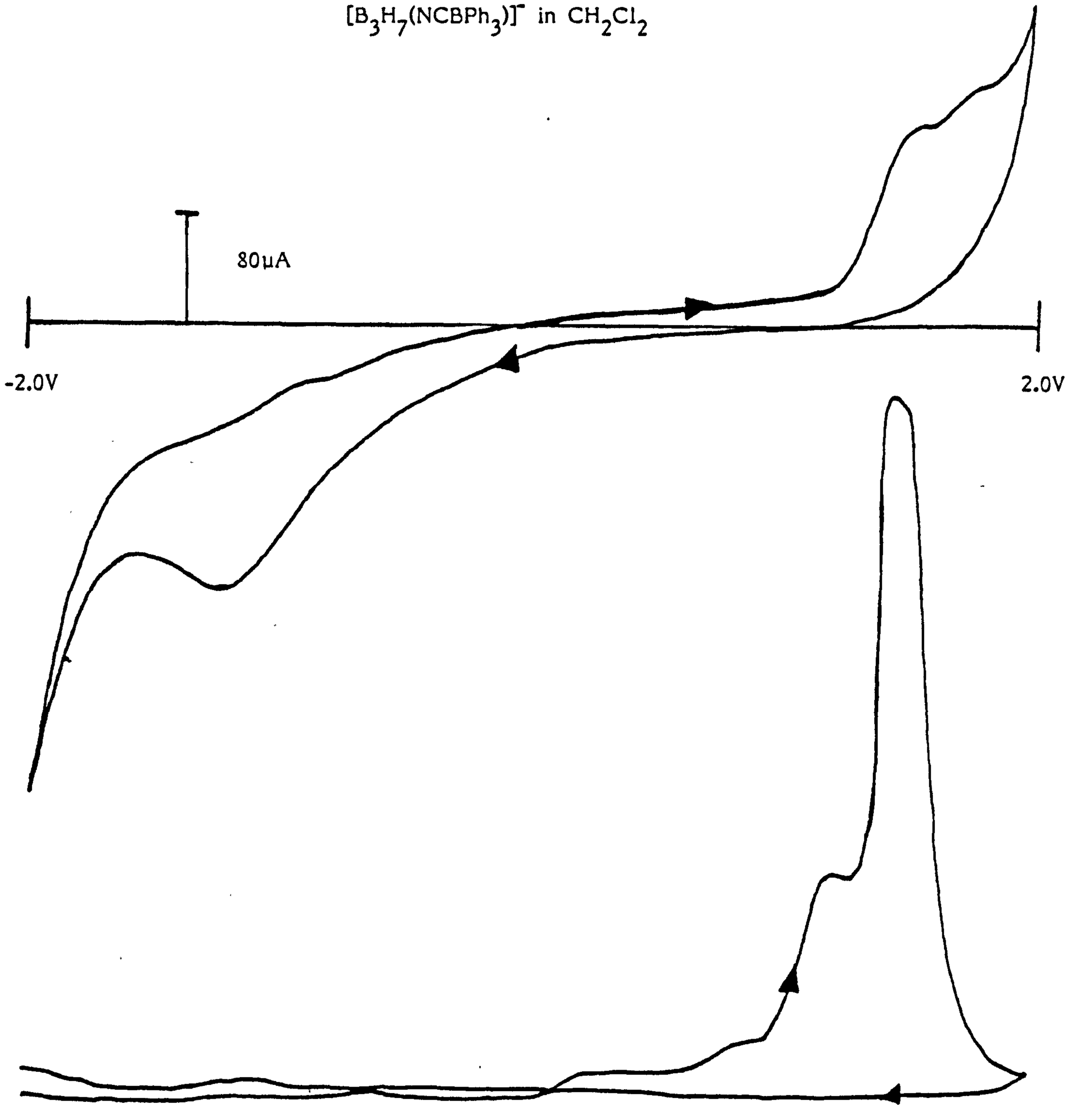

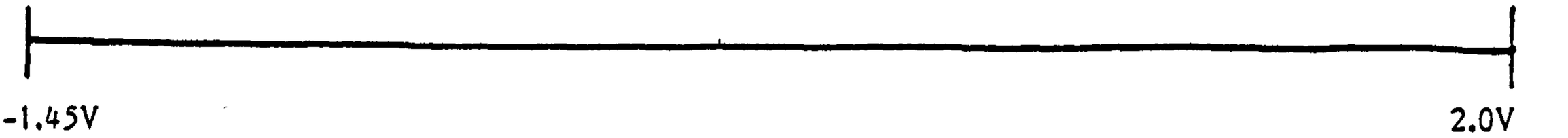

Figure 3.3 The cyclic a.c. voltammogram of $[B_3H_7(NCBPh_3)]^-$ in CH_3CN (scan rate = 0.05Vs^{-1}).

(c) $\underline{[N(PPh_3)_2][B_3H_7(NCBH_2NCBH_3)]}$

The cyclic voltammogram of $[N(PPh_3)_2][B_3H_7(NCBH_2NCBH_3)]$ at platinum in acetonitrile with $[NBu^n_4][BF_4]$ (0.1 mol dm^{-3}) supporting electrolyte added showed an irreversible oxidation at +1.25V and an irreversible reduction wave at -0.8V due to the reduction of $[H]^+$, (Figure 3.5). The oxidation products were not characterised but controlled potential electrolysis indicated that the process was probably complex since it involved more than four electrons.

(d) $\underline{[N(PPh_3)_2][B_3H_7(NCBH_3)]}$

The cyclic voltammogram of $[B_3H_7(NCBH_3)]^-$ at platinum in CH_2Cl_2 with $[NBu^n_4][BF_4]$ (0.1 mol dm^{-3}) supporting electrolyte added was similar to that previously obtained in acetonitrile.[97] An irreversible oxidation wave was observed at +1.2V and a wave due to the reduction of $[H]^+$ was observed at -0.75V.

Controlled potential electrolysis of $[B_3H_7(NCBH_3)]^-$ at platinum in CH_2Cl_2 at +1.6V resulted in the formation of chlorine radicals and subsequent attack at the anion. The 115.5 MH_z ^{11}B n.m.r. spectrum of the crude anolyte solution in $CDCl_3$ showed the presence of (at least) three products that were identified as $[B_3H_7(NCBH_3)]^-$,$[B_3H_6(Cl)(NCBH_3)]^-$ and $[B_3H_7(NCBH_2Cl)]^-$ by comparison of the chemical shifts obtained with those of the known anions.[37] (Relevant n.m.r. data are presented in Table 3.1).

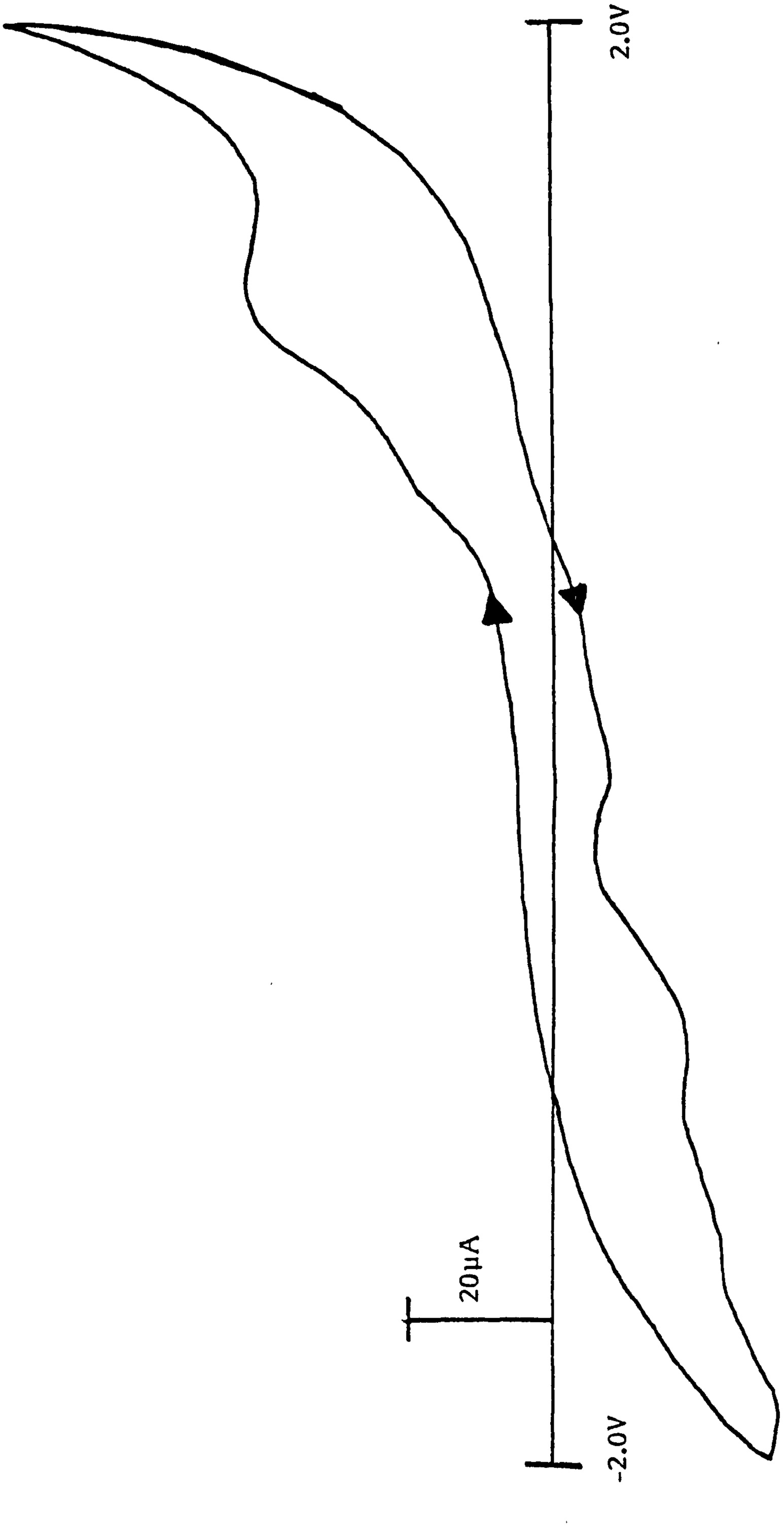

Figure 3.5 The cyclic voltammogram of $[B_3H_7(NCBH_2NCBH_3)]^-$ in CH_3CN (scan rate = $0.5Vs^{-1}$).

Table 3.1 115.5 MH_z ^{11}B N.M.R. Spectral Data for the Disubstituted Derivatives $[B_3H_6(X)(X^1)]^-$ Obtained from the Oxidation of $[B_3H_7(NCBH_3)]^-$ and $[B_3H_7NCB_3H_7]^-$ in Dichloromethane

Substituents		Boron Chemical Shifts in $CDCl_3$ (p.p.m.)			Other
X	X^1	B(H)	B(X)	$B(X^1)$	
H	$NCBH_3$	-10.50	-10.50	-35.40	-43.60(q)
Cl	$NCBH_3$	-2.54	-4.30	-31.30	-43.60(q)
Cl	$NCBH_2Cl$	-0.53	-0.53	-31.11	-27.61(t)
H	NCB_3H_7	-9.45*	-9.45*	-34.90	
		-12.36	-12.36	-49.50	
Cl	NCB_3H_7	-3.77*	-0.18*	-30.97*	
		-11.89	-49.90		
Cl	$NCB_3H_6(Cl)$	16.12*	-13.32*	-31.21*	
		14.61	-16.04	-44.97	

t - triplet, q - quartet

*N-coordinated cage resonances.

(e) $\underline{[N(PPh_3)_2][B_3H_7(NCBH_2CN)B_3H_7]}$

The cyclic voltammogram of $[B_3H_7(NCBH_2CN)B_3H_7]^-$ at platinum in acetonitrile, with added $[NBu^n_4][BF_4]$ (0.1 mol dm^{-3}) supporting electrolyte, showed an irreversible oxidation at +1.26V. The oxidation products obtained by controlled potential electrolysis were not characterised but the process was thought to be complex and may have involved more than two electrons.

(f) $\underline{[N(PPh_3)_2][B_3H_7NCB_3H_7]}$

The $[B_3H_7NCB_3H_7]^-$ was insoluble in acetonitrile and was therefore examined in dichloromethane. The cyclic voltammogram of $[B_3H_7NCB_3H_7]^-$ at platinum in CH_2Cl_2 with supporting electrolyte showed an irreversible oxidation at +1.6V.

Controlled potential electrolysis of $[B_3H_7NCB_3H_7]^-$ at platinum in dichloromethane proceeded at a potential of 1.6V. The supporting electrolyte used was $[N(PPh_3)_2]Cl$ (0.1 mol dm^{-3}) to ensure that no source of radicals other than chlorine radicals was present (i.e. to ensure that no $F^\bullet$ was produced from the tetrafluoroborate (1-) ion). The initial current of ca. 120mA was very high and remained high throughout, this indicated that the solvent was being oxidised. The electrolysis was exhaustive and was continued until sufficient current corresponding to a two electron oxidation had passed. Two products were obtained on purification of the anolyte. The ^{11}B n.m.r. spectrum of the first fraction obtained showed five resonances (Table 3.1) of relative intensities 1:1:2:1:1 reading to low frequency. This fraction

was identified as $[N(PPh_3)_2][B_3H_6(Cl)NCB_3H_7]$ by comparison of its ^{11}B n.m.r. spectrum with that of a genuine sample, (Chapter 2).

The 115.5MH_z ^{11}B n.m.r. spectrum, (Figure 3.6), of the second fraction (Table 3.1) showed six resonances at δ 16.12p.p.m., δ 14.61p.p.m., δ -13.32 p.p.m., δ -16.04p.p.m., δ -31.21p.p.m. and δ-44.97p.p.m., all of equal relative intensity. In addition a trace of impurity identified as $[B_3H_7(NCBH_3)]^-$ was also observed. It was found previously (Chapter 2) that when the $[B_3H_7NCB_3H_7]^-$ anion was reacted with gaseous HCl to produce the disubstituted species $[B_3H_6(Cl)NCB_3H_7]^-$ the resonance due to the N-coordinated boron atom shifted 4p.p.m. to higher frequency on disubstitution. By comparison of the spectrum obtained for fraction two with that of $[B_3H_6(Cl)NCB_3H_7]^-$ it is apparent that the resonance at δ -31.2p.p.m. is due to the N-coordinated boron atom in a disubstituted triborane fragment. Similarly the resonance at δ -44.9p.p.m. due to the C-coordinated boron atom has shifted ca. 4p.p.m. to higher frequency, with respect to the same resonance in $[B_3H_7NCB_3H_7]^-$, indicating that the carbon-coordinated cage may also be further substituted. Line-narrowing the remaining four resonances resolves each of these resonances into the five major lines of a septet, the two outermost lines being lost in noise. This indicated that there were six fluxional hydrogen atoms in each triborane fragment of the species. Thus, the product was identified as $[N(PPh_3)_2][B_3H_6(Cl)NCB_3H_6(Cl)]$ by ^{11}B n.m.r. spectroscopy. Without the ^{11}B-^{11}B 2-D (COSY) or the specific frequency decoupled n.m.r. spectra it is not possible to unambiguously assign the remaining four resonances. However, on electronegativity grounds it would be expected that the two

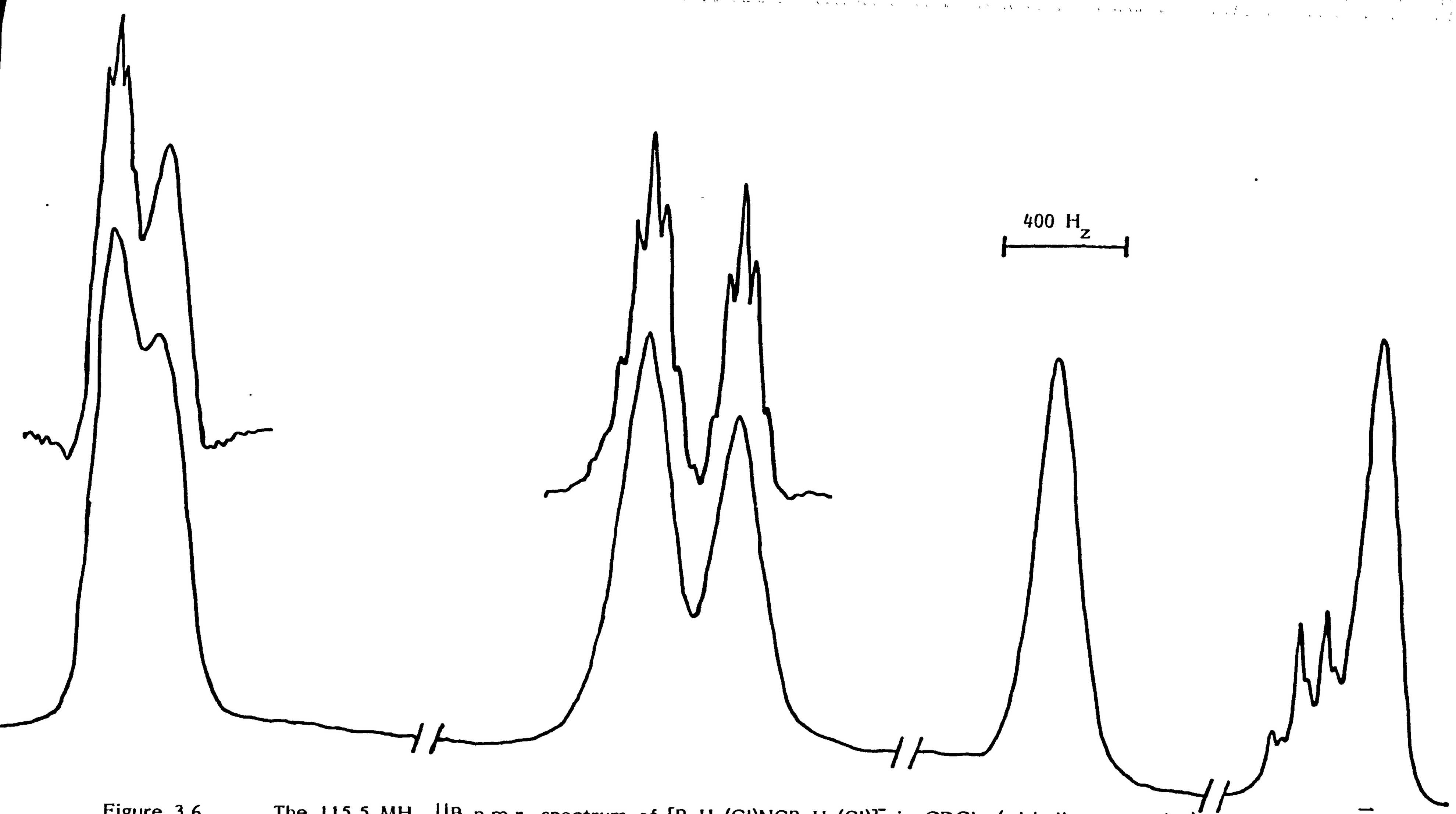

Figure 3.6 The 115.5 MH_z ^{11}B n.m.r. spectrum of $[B_3H_6(Cl)NCB_3H_6(Cl)]^-$ in $CDCl_3$ (with line-narrowing).

high frequency resonances are due to the chlorine substituted boron atoms, and that the higher frequency resonance of these two would be the one in the N-coordinated cage. Therefore the resonance at δ -16.1p.p.m. is due to the chlorine substituted boron atom in the N-coordinated cage. By a similar argument the resonance at δ -13.3 p.p.m. is due to the unsubstituted boron atom of the N-coordinated cage, and the resonance at δ -16.0p.p.m. is due to the unsubstituted boron atom of the C-coordinated cage.

3.2.2 (a) Anodic Behaviour of Transition Metals

Cyclic voltammetry has been shown[90] to be useful for assessing the behaviour and preparative potential of given combinations of anodes and boron-containing electrolytes. In this section the anodic behaviour of a series of transition metals in solutions of the anions; $[B_3H_7(NCSe)]^-$,$[B_3H_7(NCBPh_3)]^-$ and $[B_3H_7NCB_3H_7]^-$, have been investigated.

Initially the cyclic voltammograms of the anions in solution were recorded at an inert electrode such as platinum in the absence of supporting electrolyte. This determined the highest potential available for preparative work that would not cause appreciable oxidation of the anion. It was found that for the anions $[B_3H_7(NCSe)]^-$,$[B_3H_7(NCBPh_3)]^-$ and $[B_3H_7NCB_3H_7]^-$ the potentials above which they underwent oxidation were 0.5V, 1.2V and 1.58V respectively. The potentials were obtained by extrapolation to zero current of the approximately linear slopes of the increase (or decrease) in current in the early part of the anodic or cathodic scans. (This is illustrated in Figure 3.7 for $[B_3H_7(NCSe)]^-$).

The behaviour of a range of transition metals in solutions of the anions without supporting electrolyte were studied by cyclic voltammetry to determine which metals would anodically dissolve. The metals examined were Ag,Al,Au,Cd,Co,Cu,Fe,Mo,Nb,Ni,Pb,Pd,Pt,Sn,Ta,Ti,V,W,Zn and Zr, (Table 3.2). In general three types of behaviour were found. (Figures 3.7 - 3.9 show the cyclic voltammograms of $[B_3H_7(NCSe)]^-$ at Pt,Ta and Cu electrodes illustrating each type of behaviour).

Type (a). A number of metals behaved as inert electrodes, that is similar to platinum, and allowed anodic oxidation of the anions to occur.

Type (b). Other electrodes were essentially inert in the potential range investigated, and showed very low anodic currents even at high positive potentials.

Type (c). The remaining electrodes underwent anodic dissolution and could be used in the synthesis of metallaboranes. The potential at which dissolution commenced was a function of both anion and metal and may be compared with results previously reported[90] for $[BH_3(CN)]^-$ It was found in all cases that Cu,Ag,Zn,Al,Co and Cd undergo anodic dissolution. It was further found that for $[B_3H_7(NCBPh_3)]^-$ and $[B_3H_7(NCSe)]^-$ the metals Ni,Pb,Sn and Fe also underwent anodic dissolution.

(b) Preparative Dissolution

From the results obtained in section 3.2.2(a) attempts were made to

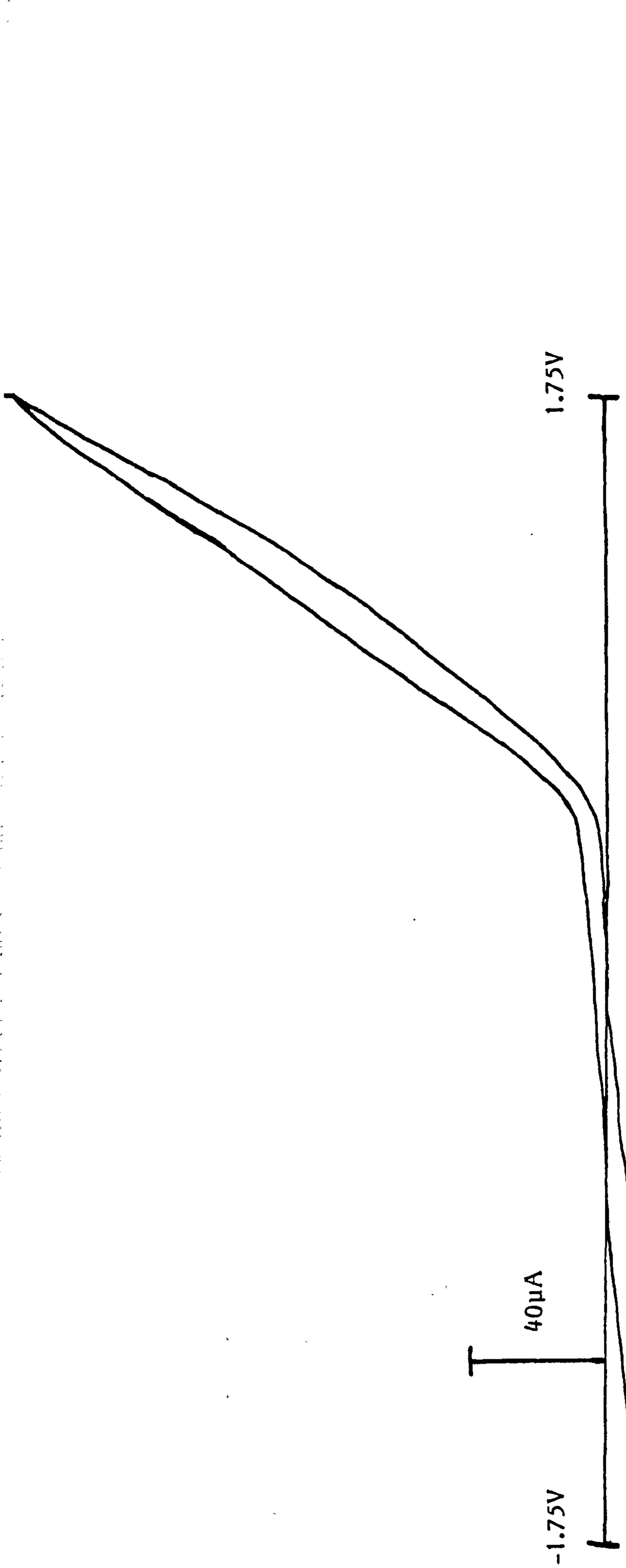

Figure 3.7 The cyclic voltammogram of $[B_3H_7(NCSe)]^-$ (scan rate = 0.5 Vs^{-1}) at a platinum electrode in CH_3CN (no supporting electrolyte). Illustrates type (a) behaviour.

Figure 3.8 Cyclic voltammogram (scan rate = 0.5 Vs^{-1}) of $[B_3H_7(NCSe)]^-$ at a tantalum electrode. Illustrates type (b) behaviour.

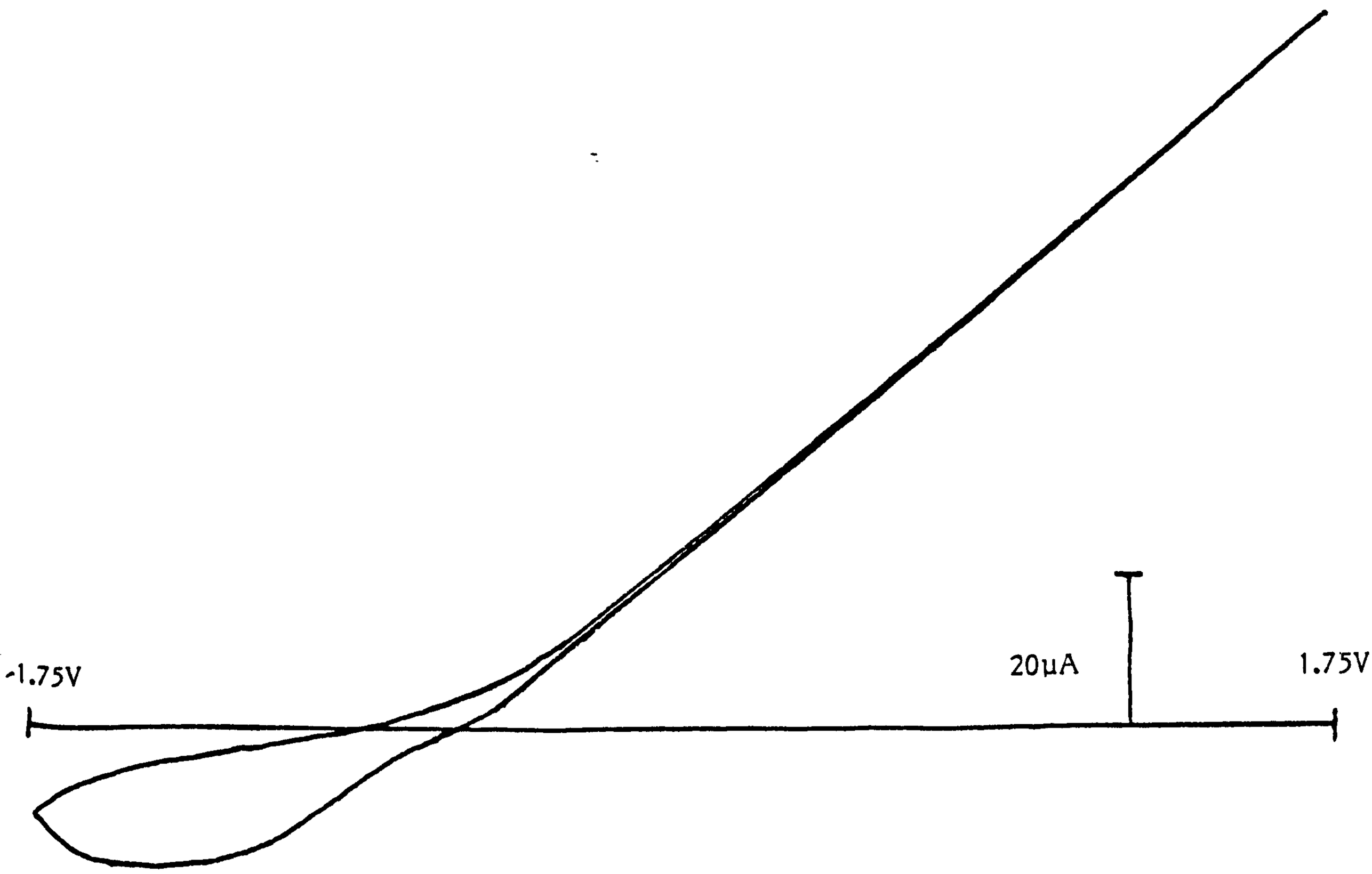

Figure 3.9 Cyclic voltammogram of $[B_3H_7(NCSe)]^-$ at a copper electrode (scan rate = 0.5 Vs^{-1}). Illustrates type (c) behaviour.

Table 3.2 Anodic Properties of Transition Metals in Solutions of Substituted Octahydrotriborate (1-) Derivatives

Metals	$[B_3H_7(NCSe)]^-$		$[B_3H_7(NCBPh_3)]^-$		$[B_3H_7NCB_3H_7]^-$	
	(1)	(2)	(1)	(2)	(1)	(2)
Pt	a	0.50	a	1.20	a	1.58
Ag	c	0.30(3)	a	0.30(3)	c	1.00(3)
Al	c	0.20	c	0.92	c	1.46
Au	a	0.32	a	0.60	a	1.10
Cd	c	-0.60(3)	c	-1.4	c	0.50(3)
Co	c	0.06(3)	c	0.38	c	1.00
Cu	c	-0.60(3)	c	-0.60(3)	c	0.50(3)
Fe	c	-0.30	c	-0.28	a	0.80
Mo	a	0.36	a	0.86	a	1.35
Nb	b	0.70	b	1.20	b	1.30
Ni	c	0.26(3)	c	1.10	a	1.06
Pb	c	-0.30(3)	c	-0.20	a	1.00
Pd	a	0.40	a	0.80	a	1.06
Sn	c	0.00	c	-0.35		
Ta	b	0.80	b	1.30	a	0.48
Ti	b	0.60	b	1.20	b	1.15
V	a	0.40	a	0.30	a	1.38
W	b	0.52	b	1.20	b	1.74
Zn	c	0.46	c	-0.56	c	0.80
Zr	b	0.92	b	1.00	b	0.80

cont'd

(1) Type of behaviour (see discussion)

(2) Potential at which oxidation commenced (Type (a)); potential at which oxidation apparently commenced Type (b));

dissolution potential (Type (c)).

(3) Reduction peak on cathodic scan.

$[B_3H_7(NCSe)]^-$ and $[B_3H_7(NCBPh_3)]^-$ were done as acetonitrile solutions and were referenced to $Ag/AgNO_3$(0.1 mol dm^{-3}). $[B_3H_7NCB_3H_7]^-$ was done in dichloromethane and was referenced to $Ag/[N(PPh_3)_2]Cl$ (0.1 mol dm^{-3}).

prepare metallaboranes by anodic dissolution from the anions $[B_3H_7(NCSe)]^-$, $[B_3H_7(NCBPh_3)]^-$ and $[B_3H_7NCB_3H_7]^-$.

(i) $\underline{[B_3H_7(NCSe)]^-}$

Previously[97] the anodic dissolution of copper in an acetonitrile solution of $[B_3H_7(NCS)]^-$ containing two equivalents of triphenylphosphine resulted in anodic removal of the substituent with isolation of complexes of the type L_3CuCl or L_3CuNCS and $B_3H_7[CH_3CN]$.

The anodic dissolution of copper in an acetonitrile solution of $[N(PPh_3)_2][B_3H_7(NCSe)]$ containing two equivalents of added triphenylphosphine ligand proceeded at a potential of 0.0V. Copper entered the solution as copper (I), and the solution went brown. The $115.5MH_z$ ^{11}B n.m.r. spectrum of the anolyte in $CDCl_3$ was identical to the spectrum obtained from the reaction of $Cu(PPh_3)_2(BH_4)$ and $[B_3H_7(NCSe)]^-$ described in Chapter 7. The major products obtained from the anolyte solution were identified as $Cu(PPh_3)_2(B_3H_7NCSe)$ and $Ph_3P.BH_3$. The $115.5MH_z$ ^{11}B n.m.r. spectrum of the anolyte as an acetonitrile, (CD_3CN), solution indicated that in the more polar solvent dissociation occurred to give the ion pair, $[(CH_3CN)_2Cu(PPh_3)_2][B_3H_7(NCSe)]$. It was proposed that in the original acetonitrile anolyte solution the complex exists as the ion pair, and that when the solvent was removed under vacuum the complex, $Cu(PPh_3)_2(B_3H_7NCSe)$, was formed. There was no evidence for anodic removal of substituent when the anion was $[B_3H_7(NCSe)]^-$.

(ii) $\underline{[B_3H_7(NCBPh_3)]^-}$

The anodic dissolution of copper in an acetonitrile solution of [(NPPh$_3$)$_2$][B$_3$H$_7$(NCBPh$_3$)] containing two equivalents of triphenylphosphine ligand proceeded at a potential of 0.0V. Copper entered the solution as copper (I). The ^{11}B n.m.r. of the crude anolyte in $CDCl_3$ indicated the presence of $Cu(PPh_3)_2(B_3H_7NCBPh_3)$ and $Ph_3P.BH_3$ by comparison with the spectrum obtained from the reaction of $[B_3H_7(NCBPh_3)]^-$ with $Cu(PPh_3)_2(BH_4)$, (Chapter 7).

(iii) $\underline{[B_3H_7NCB_3H_7]^-}$

The anodic dissolution of silver in a dichloromethane solution of [N(PPh$_3$)$_2$][B$_3$H$_7$NCB$_3$H$_7$] with two equivalents of added triphenylphosphine and $[N(PPh_3)_2]Cl$ (0.1 mol dm^{-3}) supporting electrolyte proceeded at a potential of 1.0V. The silver entered the solution as silver (I). The 80.2 MH_z ^{11}B n.m.r. spectrum of the anolyte in $CDCl_3$ showed two resonances at δ-49.5p.p.m. and δ-35.0p.p.m. each of relative area one due to the unique C-coordinated boron atom and N-coordinated boron atom respectively. The final resonance, due to the unsubstituted boron atoms in each cage, had broadened until they had coalesced into one resonance at δ-11.0p.p.m. of relative area four. The ^{11}B-{^{1}H} decoupled n.m.r. spectrum resolved this resonance into its two components. By close examination of the substituted boron resonances it was apparent that the resonances due to the boron atoms in the N-coordinated cage were broadened to a greater extent than those of the C-coordinated cage. This indicated that silver complexation was probably through the N-coordinated cage. The white solid obtained

from the anolyte solution was found to be light sensitive and deposited a silver mirror and a black precipitate when redissolved in CH_2Cl_2 and allowed to stand for 2 hr. It is proposed that the product obtained from the anolyte is $Ag(PPh_3)_2(B_3H_7NCB_3H_7)$although, like $Ag[(p\text{-}CH_3C_6H_4)_3P]_2(B_3H_8)$,[45] the n.m.r. data are structurally inconclusive, that is, no statement can be made concerning the extent or strength of anion binding. The relevant n.m.r. data are presented in Table 3.3.

3.3 Experimental

The details of all electrochemical equipment, cell designs and general reagents and solvents for electrochemistry are presented in Chapter 8.

$[N(PPh_3)_2][B_3H_7(NCSe)]$,$[N(PPh_3)_2][B_3H_7(NCBPh_3)]$ and $[N(PPh_3)_2][B_3H_7NCB_3H_7]$ were prepared as described in Chapter 2.

All other reagents were used as received.

3.3.1 Electrochemical Oxidation of $[B_3H_7(NCSe)]^-$

(i) Acetonitrile Solution

Freshly prepared $[N(PPh_3)_2][B_3H_7(NCSe)]$ (0.68g, 1 mmol) was dissolved in a solution of $[NBu^n_4][BF_4]$ (0.1 mol dm^{-3}) in acetonitrile (20 cm^3) and introduced into the anode compartment of the cell. The cathode compartment contained a solution of $[NBu^n_4][BF_4]$ (0.1 mol dm^{-3}) in acetonitrile (20 cm^3). Both working and secondary electrodes were constructed of platinum foil. A potential of 1.0V was applied to the working electrode and the initially high current (42mA) fell exponentially to 1mA after 84C had passed, (c.f. 87% of theoretical value

Table 3.3 ^{11}B N.M.R. Spectral Data for the Complexes Obtained By Anodic Dissolution

Complex	Boron Chemical Shift in $CDCl_3$ (p.p.m.)		
	δB(1)	δB(2),B(3)	Other
$Cu(PPh_3)_2(B_3H_7NCSe)$	-31.61	-15.85	-37.12($Ph_3P.BH_3$)
$Cu(PPh_3)_2(B_3H_7NCBPh_3)$	-17.35	-30.40	-37.00(Ph_3PBH_3)
			-11.65(BPh_3)
$Ag(PPh_3)_2(B_3H_7NCB_3H_7)$	-34.85*	-12.42*	
	-49.69	-12.42	

* N-coordinated cage resonances.

for a one electron oxidation). Gas evolution was observed at the anode. When the reaction was complete the colourless anolyte solution was reduced to dryness to give an oil. T.l.c. analysis of the oil on silica gel using 100% CH_2Cl_2 as eluant showed a single major fraction (Rf=0.48) and some minor components at lower Rf values. Purification by chromatography on silica gel using 100% CH_2Cl_2 as eluant gave the major product as a white solid. The white solid was recrystallised from CH_2Cl_2/Et_20 and identified as $[N(PPh_3)_2][B_3H_7(NCSe)]$ from its ^{11}B n.m.r. spectrum, (Chapter 2).

(ii) Dichloromethane Solution

$[N(PPh_3)_2][B_3H_7(NCSe)]$ (0.68g, 1 mmol) was dissolved in a solution of $[NBu^n_4][BF_4]$ (0.1 mol dm^{-3}) in dichloromethane (20 cm^3) and introduced into the anode compartment of the cell. Since dichloromethane is a poor conductor 40% aqueous HBF_4 (20cm^3) was used in the cathode compartment to minimise cell resistance. This technique was effective since the two phases were immiscible. Both working and secondary electrodes were made of platinum foil. A potential of 1.2 → 1.6V was applied and the current rose to a constant 130mA. Severe gas evolution was observed in the anodic and cathodic compartments. Localised heating at the interface (i.e. at the Nafion ion-exchange membrane) caused the dichloromethane in the anodic compartment to boil. To prevent boiling the reaction was done in an ice-bath. When 96.5C had passed (i.e. the theoretical for a one electron oxidation) the reaction was stopped and the solvent was removed under reduced pressure to yield a white crystalline solid. The ^{11}B n.m.r.

spectrum of the white solid indicated the presence of the starting material $[B_3H_7(NCSe)]^-$ and $[BF_4]^-$.

In an attempt to prepare the disubstituted species, $[B_3H_6(Cl)(NCSe)]^-$ the reaction was repeated using a potential of 1.7V which was sufficient to generate chlorine radicals by solvent oxidation. The current rose to a constant 140mA and was maintained until 165C had passed (i.e. 85% of the theoretical value for a two electron oxidation). Investigation of the anolyte by ^{11}B n.m.r. spectroscopy indicated that the only boron containing species present was the unreacted starting material, $[B_3H_7(NCSe)]^-$.

3.3.2 Electrochemical Oxidation of $[B_3H_7(NCBPh_3)]^-$

(i) Acetonitrile Solution

The reaction procedure was identical to that described in section 3.3.1(i) for the oxidation of $[B_3H_7(NCSe)]^-$ except that $[N(PPh_3)_2]$ $[B_3H_7(NCBPh_3)]$ (1.0g, 1.2 mmol) was used. A potential of 1.65V was applied to the working electrode and the high initial current (65mA) decayed exponentially to 1mA after 124C, (i.e. 8.2C more than the theoretical value for a one electron oxidation) had passed. The solvent was removed from the anolyte solution under reduced pressure to give a white crystalline solid. T.l.c. analysis of the solid on silica gel using 100% CH_2Cl_2 as eluant indicated a single major product (Rf=0.6) and other minor products at lower Rf values. Purification by chromatography on silica gel using 100% CH_2Cl_2 as eluant gave the major fraction as a white crystalline solid. The solid was re-

crystallised from CH_2Cl_2/Et_2O and identified as $[N(PPh_3)_2][B_3H_7(NCBPh_3)]$ from its ^{11}B n.m.r. spectrum.

(ii) Dichloromethane Solution

The preparation of the disubstituted species, $[B_3H_6(Cl)(NCBPh_3)]^-$, was attempted in the same way as that described in section 3.3.1(ii). A potential of 1.6V was applied to the working electrode and the initial current of 135mA remained constant throughout, indicating solvent oxidation. After 162C had passed, (i.e. 83.99% of the theoretical value for a two electron oxidation of $[N(PPh_3)_2][B_3H_7(NCBPh_3)]$ (0.84g, 1 mmol) in CH_2Cl_2), the reaction was stopped and the anolyte solution was examined by ^{11}B n.m.r. spectroscopy in $CDCl_3$. The only boron containing product was the starting material, $[B_3H_7(NCBPh_3)]^-$.

3.3.3 Electrochemical Oxidation of $[B_3H_7(NCBH_2NCBH_3)]^-$ in Acetonitrile

The reaction was carried out in the same way as that described in section 3.3.1(i) except that $[N(PPh_3)_2][B_3H_7(NCBH_2NCBH_3)]$(0.2g, 0.3 mmol) was used. A potential of 1.3V was applied to the working electrode. The initially high current (38mA) decayed exponentially to 2mA after 121C had passed (i.e. the theoretical value for a 4.2 electron oxidation). T.l.c. analysis of the anolyte solution on silica gel using 100% CH_2Cl_2 as eluant indicated several minor components (Rf=0.2 $\longrightarrow$ 0.65). The inability to obtain the products sufficiently pure precluded characterisation of the products by n.m.r. spectroscopy.

However, it was evident that the oxidation was complex.

3.3.4 Electrochemical Oxidation of $[B_3H_7(NCBH_3)]^-$ in Dichloromethane

$[N(PPh_3)_2]B_3H_7(NCBH_3)]$ (0.61g, 1 mmol) was dissolved in a solution of $[N(PPh_3)_2]Cl$ (0.1 mol dm^{-3}) in dichloromethane (20cm^3) and introduced into the anodic compartment of the cell. The cathodic compartment contained a solution of $[N(PPh_3)_2]Cl$ (0.1 mol dm^{-3}) in dichloromethane (20 cm^3).

The working and secondary electrodes were both made of platinum foil. The entire cell was immersed in an ice-bath to maintain a constant cell temperature. A potential of 1.6V was applied to the working electrode. The current rose to a maximum of 120mA and was constant throughout the experiment. The reaction was stopped after 220C had passed (i.e. 27C more than the theoretical value for a two electron oxidation). The solvent was removed from the colourless solution under reduced pressure to yield a crystalline white solid. T.l.c. analysis of the white solid on silica gel using 100% CH_2Cl_2 as eluant indicated three major products, (Rf=0.68, 0.62, 0.50). The 115.5 MH_z ^{11}B n.m.r. spectrum of the crude anolyte indicated that the products were a mixture of $[B_3H_7(NCBH_3)]^-$,$[B_3H_7(NCBH_2Cl)]^-$ and $[B_3H_6(Cl)(NCBH_3)]^-$.

3.3.5 Electrochemical Oxidation of $[B_3H_7(NCBH_2CN)B_3H_7]^-$ in Acetonitrile

The procedure followed in this reaction was the same as that described

in section 3.3.1(i) except that $[N(PPh_3)_2][B_3H_7(NCBH_2CN)B_3H_7]$ (0.23g, 0.33 mmol) was used. A potential of 1.3V was applied to the working electrode. The high initial current (64mA) decayed exponentially to 2mA after 66.8C had passed (i.e. 3.1C more than the theoretical value for a two electron oxidation). T.l.c. analysis of the anolyte on silica gel using 100% CH_2Cl_2 as eluant indicated the presence of several minor components (Rf=0.23-0.65). The products obtained from this reaction have not yet been characterised but it is evident that the oxidation is complex.

3.3.6 Electrochemical Oxidation of $[B_3H_7NCB_3H_7]^-$ in Dichloromethane

The procedure followed in this reaction was identical to that described in section 3.3.4 except that $[N(PPh_3)_2][B_3H_7NCB_3H_7]$(0.6g, 0.93 mmol) was used. A potential of 1.6V was applied to the working electrode and the initial high current (120mA) remained constant throughout the reaction. The reaction was stopped when 179.5C had passed (i.e. the theoretical value for a two electron oxidation). T.l.c. analysis of the anolyte on silica gel using 100% CH_2Cl_2 as eluant indicated the presence of a major component (Rf=0.6) and a minor component (Rf=0.35). Purification by chromatography gave the major fraction as a white crystalline solid in good yield (0.29g,46%). The minor fraction was also obtained as a white crystalline solid in relatively low yield (0.15g, 22.6%). The 115.5MH_z ^{11}B n.m.r. spectra of the major and minor fractions in $CDCl_3$ identified them as $[B_3H_6(Cl)NCB_3H_7]^-$ and $[B_3H_6(Cl)NCB_3H_6(Cl)]^-$ respectively.

3.3.7 Anodic Dissolution of Copper in an Acetonitrile Solution of $[B_3H_7(NCSe)]^-$

$[N(PPh_3)_2][B_3H_7(NCSe)]$ (0.682g, 1 mmol) and Ph_3P (0.526g, 2mmol) were dissolved in acetonitrile (20 cm^3) and introduced into the anode compartment of the electrochemical cell. The cathode compartment contained a solution of $[NBu^n_4][BF_4]$ (0.1 mol dm^{-3}) in acetonitrile (20 cm^3). Both working and secondary electrodes were constructed of copper foil. A potential of 0.0V was applied to the working electrode and the high initial current (57mA) fell exponentially to 2mA after the passage of 98C. The initially colourless anolyte solution went red then brown as the electrolysis progressed. The net weight loss of the copper anode was 0.0620g [c.f. the theoretical value of 0.0635g for Cu → Cu(I)]. The anolyte solution was filtered to remove any insolubles and the acetonitrile was removed under reduced pressure to yield a brown solid. T.l.c. analysis on silica gel using 100% CH_2Cl_2 as eluant showed a single major product (Rf=0.65) and several minor products. Purification by chromatography on silica gel using 100% CH_2Cl_2 as eluant gave the major product as a brown solid. The ^{11}B n.m.r. spectrum of the brown solid indicated the presence of $Cu(PPh_3)_2(B_3H_7NCSe)$ and $Ph_3P.BH_3$.

3.3.8 Anodic Dissolution of Copper in an Acetonitrile Solution of $[B_3H_7(NCBPh_3)]^-$

This experiment was carried out in the same way as that described in section 3.3.7 except that $[N(PPh_3)_2][B_3H_7(NCBPh_3)]$ (0.845g, 1 mmol) was used. A potential of 0.0V was applied to the working electrode

and the initially high current (32mA) fell exponentially to 2mA after 121C had passed. In this case the anolyte did not change colour as the electrolysis progressed. The net weight loss of the copper anode is 0.0602g [c.f. the theoretical value of 0.0635g for Cu → Cu(I)]. The solvent was removed under reduced pressure to give a white solid. T.l.c. analysis of the white solid on silica gel indicated the presence of a single major product (Rf=0.62) and several minor products. Purification by chromatography on silica gel yields the major component as a white solid. The ^{11}B n.m.r. spectrum of the purified product indicates the presence of $Cu(PPh_3)_2(B_3H_7NCBPh_3)$ and Ph_3PBH_3.

3.3.9 Anodic Dissolution of Silver in a Dichloromethane Solution of $[B_3H_7NCB_3H_7]^-$

$[N(PPh_3)_2][B_3H_7NCB_3H_7]$ (0.643g, 1mmol) and Ph_3P (0.526g, 2 mmol) were dissolved in a solution of $[N(PPh_3)_2]Cl$ (0.1 mol dm^{-3}) in dichloromethane (20 cm^3) and introduced into the anode compartment of the electrochemical cell. The cathode compartment contained a solution of $[N(PPh_3)_2]Cl$ (0.1 mol dm^{-3}) in CH_2Cl_2 (20 cm^3). The working electrode was a silver wire and the secondary electrode was platinum foil. A potential of 1.0V was applied to the working electrode and the initially high current (64mA) fell exponentially to 2mA after 103C had passed. A crystalline white precipitate was formed during electrolysis that redissolved on heating. The white precipitate was thought to be $[N(PPh_3)_2]Cl$. The net weight loss of the silver anode was 0.1066g [c.f. the theoretical value of 0.1078g for Ag → Ag(I)]. The

solvent was removed from the anolyte under reduced pressure to give a white crystalline solid. T.l.c. analysis on silica gel using 100% CH_2Cl_2 as eluant showed a single major fraction (Rf=0.52). The 80.2 MH_z ^{11}B n.m.r. spectrum of the crude product indicated the presence of the metallaborane, $Ag(PPh_3)_2(B_3H_7NCB_3H_7)$.

CHAPTER FOUR

PREPARATION AND CHARACTERISATION OF SUBSTITUTED DERIVATIVES OF THE $[B_9H_{14}]^-$ ION

4.1 Introduction

In this chapter, the preparation of substituted anionic derivatives of the tetradecahydrononaborate (1-) ion, $[B_9H_{14}]^-$, are described. The structures and dynamics of these anions have been studied by high field ^{11}B and ^1H n.m.r. spectroscopy and the results indicated important differences to those of the parent anion, the neutral nonaborane(13) adducts and between the anions themselves.

4.2 Results and Discussion

4.2.1 Preparative Routes

Previously the anion $[B_9H_{13}(NCS)]^-$ has been prepared by the degradative reaction between nido-$B_{10}H_{14}$ and $[NCS]^-$ in aqueous dioxane.[68] However, it was found[143] that this type of reaction could not be extended to include other potential substituents. For example, NaCN was shown[173] to react with $B_{10}H_{14}$ in aqueous solution to yield the substituted dianion $[B_{10}H_{13}(CN)]^{2-}$. It was found[143] that the anionic ligands $[NCS]^-$ and $[BH_3(CN)]^-$ produced the substituted anions $[B_9H_{13}(X)]^-$. (X=NCS,$NCBH_3$) by a ligand displacement reaction with $B_9H_{13}[SMe_2]$. In addition to $[B_9H_{13}(NCS)]^-$, the reaction of $B_9H_{13}[SMe_2]$ and $[NCS]^-$ produced the novel anion $[B_8H_{12}(NCS)]^-$. The dual chemical character of $[BH_3(CN)]^-$ was exemplified by the formation of $[B_9H_{14}]^-$, $[B_9H_{13}(NCBH_3)]^-$ and $[BH_3(CN)BH_2(CN)]^-$ from the reaction of $B_9H_{13}[SMe_2]$ with $[BH_3(CN)]^-$. Here the $[BH_3(CN)]^-$ anion acts as a two-electron σ-donor ligand in the formation of $[B_9H_{13}(NCBH_3)]^-$ and as a hydride-transfer reagent in the formation of $[B_9H_{14}]^-$ and $[BH_3(CN)BH_2(CN)]^-$.

In this work it was found that the anions $[NCSe]^-$,$[NCBPh_3]^-$ and $[NCBH_2NCBH_3]^-$ also react with $B_9H_{13}[SMe_2]$ to produce the anions $[B_9H_{13}(X)]^-$ (X = NCSe, $NCBPh_3$, $NCBH_2NCBH_3$) by a ligand displacement reaction. Furthermore, the anions $[B_9H_{13}(NCBH_2CN)]^-$ and $[B_9H_{13}(NCBH_2CN)B_9H_{13}]^-$ were prepared by reaction of $[BH_2(CN)_2]^-$ with one or two equivalents of $B_9H_{13}[SMe_2]$ respectively.

The tetradecahydrononaborate (1-) ion, $[B_9H_{14}]^-$, has been shown to have the solid-state crystal structure of C_s symmetry,[61,62] (Figure 4.1), in which the arachno-$[B_9H_{14}]^-$ is formally derived from the closo-eleven atom polyhedron, with two bridge hydrogen atoms between B(4) and B(5) and B(4) and B(9), and BH_2 groups with exo- and endo-hydrogen atoms at positions B(6), B(7) and B(8). The neutral derivatives, $B_9H_{13}L$, (Chapter 1) have been shown to have the same heavy atom structure as $[B_9H_{14}]^-$. However, the crystal structure[65] of $B_9H_{13}[NCCH_3]$ differs from that of $[B_9H_{14}]^-$ in position of bridge hydrogen atoms, (Figure 4.2). In $B_9H_{13}[NCCH_3]$ there are two hydrogen bridge bonds between B(5) and B(6) and B(8) and B(9), with exo- and endo-hydrogen atoms at atoms B(6) and B(8), and endo-hydrogen and exo-ligand at B(4).

In solution, ^{11}B[62,63] and ^{1}H[62] n.m.r. studies of $[B_9H_{14}]^-$ were consistent with a structure of higher symmetry (C_{3V}) than that in the solid state. In the ^{11}B n.m.r. three boron resonances were observed indicating a three-fold axis of symmetry. The ^{1}H n.m.r. spectrum showed five bridging hydrogen atoms, arising from dynamic equilibration of

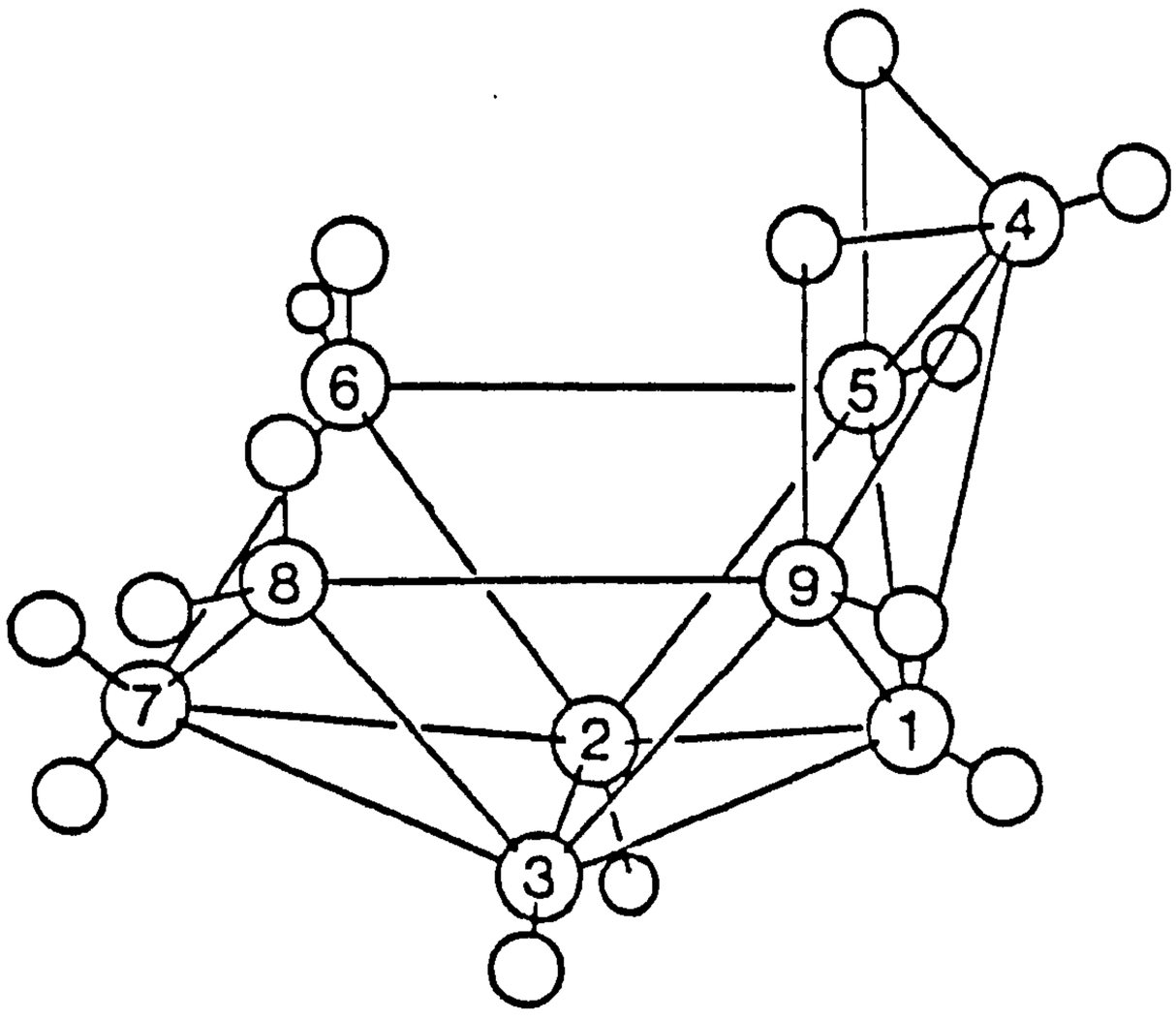

Figure 4.1 The structure of $[B_9H_{14}]^-$

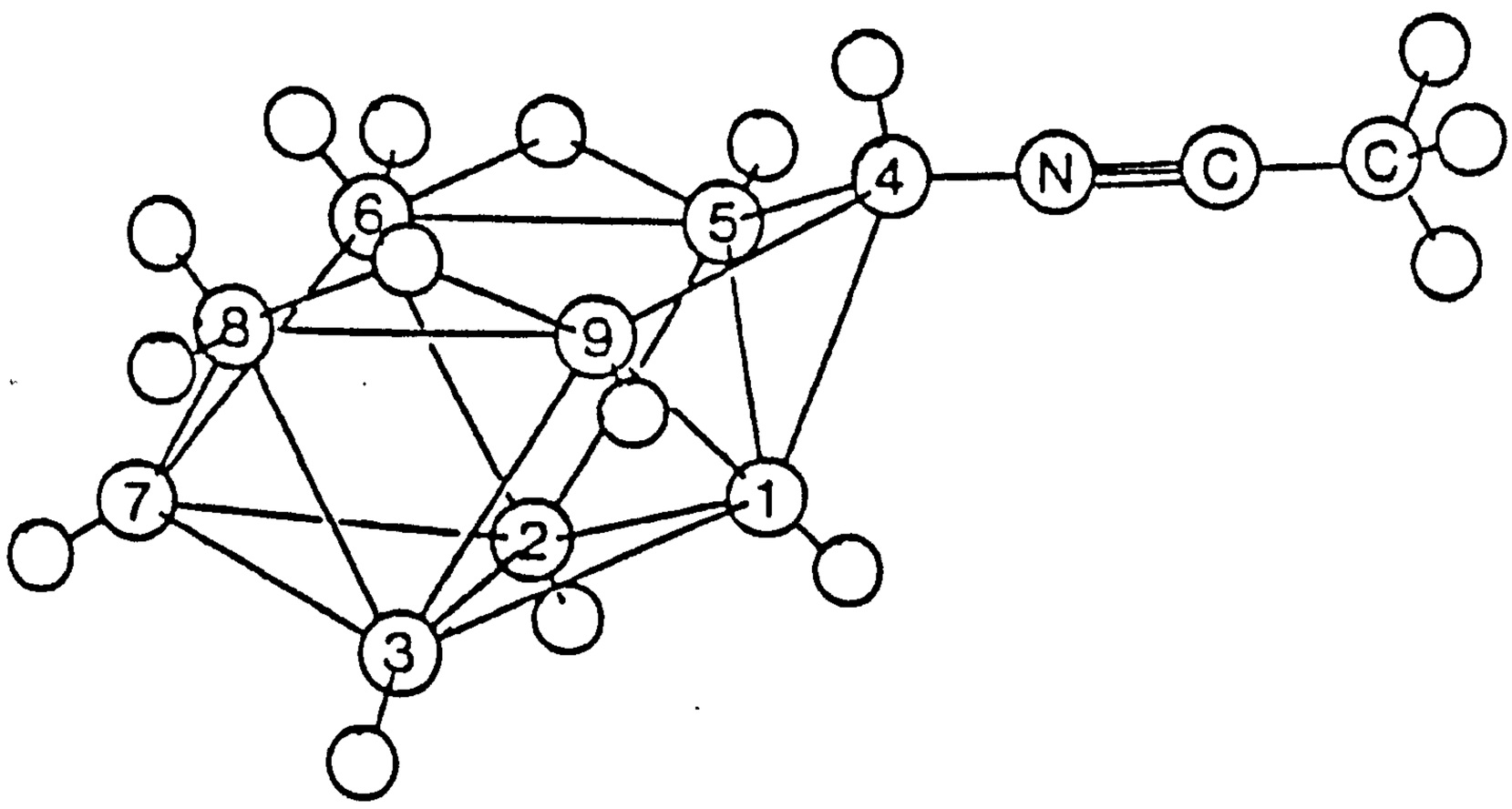

Figure 4.2 The structure of $B_9H_{13}[NCCH_3]$

the crystallographically determined bridging hydrogen atoms and one of the terminal hydrogen atoms from each of the BH_2 groups. These observations indicated that $[B_9H_{14}]^-$ is fluxional in solution on the n.m.r. time scale. Contrary to this, the high-field ^{11}B n.m.r. spectra of $B_9H_{13}[X](X = SMe_2, SEt_2, NCCH_3)$ indicated[71,143] the presence of six non-equivalent boron environments, consistent with the crystallographically observed C_s symmetry of $B_9H_{13}[NCCH_3]$. Furthermore, it was evident that at room temperature, on the n.m.r. time scale, the neutral $B_9H_{13}L$ adducts were static. This was evident since the resonance due to the substituted boron atom B(4) appeared as a doublet ($J_{B-H} = 134H_z$), indicating coupling between B(4) and the attached endo-hydrogen atom.

For the anions $[B_9H_{13}(X)]^-(X = NCS, NCBH_3)$ it was reported[143] that these molecules were fluxional. The high field ^{11}B n.m.r. spectra of these anions were virtually the same as those of the $B_9H_{13}L$ neutral adducts, indicating that the anions retained the C_s symmetry observed for $B_9H_{13}[NCCH_3]$ in solution. In contrast to the neutral derivatives, the resonance due to the substituted boron atom B(4) in the anionic derivatives appeared as a singlet. This indicated that the endo hydrogen atom on B(4) was involved in intramolecular hydrogen exchange which was fast on the n.m.r. time scale, effectively decoupling the terminal hydrogen atom from B(4) resulting in a singlet being observed. The 360 MH_z ^1H n.m.r. spectrum of $[N(PPh_3)_2]B_9H_{13}(NCS)]$ confirmed the fluxional nature of these anions by indicating the presence of five bridge hydrogen atoms at δ -1.4 p.p.m. at room temperature.

4.2.2 N.M.R. Studies of Derivatives of the $[B_9H_{14}]^-$ Ion

Investigation of the n.m.r. spectra of the substituted anions revealed some interesting and subtle differences. The 115.5 MH_z ^{11}B n.m.r. spectra (Table 4.1) of the anions, $[B_9H_{13}(X)]^-$ (X=NCSe,$NCBPh_3$, $NCBH_2$ $NCBH_3$,$NCBH_2CN$ and $NCBH_2CNB_9H_{13}$), showed six resonances of relative intensities 1:1:2:2:1:2, reading from high frequency, due to the $[B_9H_{13}]$ fragment. The ^{11}B n.m.r. spectra of the anions all resembled the spectrum of $B_9H_{13}[NCCH_3]$, (Figure 4.2), indicating that, in solution, the C_s symmetry of the neutral adduct is retained in the anion. The ^{11}B n.m.r. spectra of the anions differed from the neutral adduct in that the resonance due to B(4) appeared as a singlet, this indicated that all of the anions were fluxional in solution at room temperature. However, 360 MH_z ^1H specific frequency decoupling experiments showed that only $[B_9H_{13}(NCSe)]^-$ and $[B_9H_{13}(NCBPh_3)]^-$ were fluxional. In addition to the six resonances observed for the $[B_9H_{13}]$ fragment the $[B_9H_{13}(NCBPh_3)]^-$ anion exhibited a resonance at δ -10.7 p.p.m. due to the $[BPh_3]$ moiety of the substituent. For the anion, $[B_9H_{13}(NCBH_2NCBH_3)]^-$, the resonance due to the $[BH_3]$ moiety of the substituent appeared as a quartet at δ -43.3 p.p.m. (J_{B-H} = 92 H_z). The resonance due to the $[BH_2]$ moiety of the substituent is observed at δ -27.3 p.p.m., this resonance appeared as a singlet, rather than a triplet, due to coincidental overlap with the B(4) resonance of the cage. In $[B_9H_{13}(NCBH_2CN)]^-$ and $[B_9H_{13}(NCBH_2$ $CN)B_9H_{13}]^-$ the resonance due to the $[BH_2]$ moiety of the substituent appeared as a triplet at δ -40.9 p.p.m. (J_{B-H} = 90H_z).

Table 4.1 115.5 MH_z ^{11}B N.M.R. and 360 MH_z ^{1}H N.M.R. Spectral Data for the Substituted Derivatives of $[B_9H_{14}]^-$

Substituents	$\delta(^{11}B)$p.p.m.	$\delta(^{1}H)$ p.p.m.	J_{B-H}/H_z	Assignment
NCSe[(a)]	15.84 (1)	3.73 (1)	142	7
	5.19 (1)	2.86 (1)	136	1
	-15.68 (2)	1.58 (2)	143	5,9
	-17.79 (2)	1.87 (2)	141	6,8
	-22.73 (1)	-	-	4
	-37.83 (2)	0.22 (2)	145	2,3
		-1.42 (5)		bridge
		7.53 (30)		$[N(PPh_3)_2]^+$
$NCBPh_3$[(b)]	16.58 (1)	-	-	7
	5.19 (1)	-	136	1
	-10.77 (1)	-	-	$[BPh_3]$
	-14.96 (2)	1.83 (2)	140	5,9
	-19.56 (2)	1.91 (2)	-	6,8
	-25.75 (1)	-	-	4
	-38.44 (2)	-	144	2,3
$NCBH_2$ — $NCBH_3$[(b)]	17.11 (1)	3.90 (1)	-	7
	5.07 (1)	3.03 (1)	139	1
	-14.70 (2)	1.79 (2)	139	5,9
	-20.22 (2)	1.88 (2),exo -0.27 (2),endo		6,8
	-27.27 (2)	0.43 (1) 2.09 (2)	-	4,$[BH_2]$
	-38.64 (2)	0.37 (2)	146	2,3
	-43.28 (1)	0.57 (3)	92	$[BH_3]$

Table 4.1 Ctd/...

Substituents	$\delta(^{11}B)$p.p.m.	$\delta(^{1}H)$ p.p.m.	J_{B-H}/H_z	Assignment
		3.53 (2)		bridge
		7.50 (30)		$[N(PPh_3)_2]^+$
$NCBH_2CN$[b]	16.90 (1)	-	-	7
	5.03 (1)	-	138	1
	-14.87 (2)	-	138	5,9
	-19.98 (2)	1.87(2),exo -0.31(2),endo	-	6,8
	-26.44 (1)	0.41 (1)	-	4
	-38.61 (2)	-	144	2,3
	-40.71 (1)	1.87 (2)	90	$[BH_2]$
$NCBH_2CN$-B_9H_{13}[b]	17.26 (2)		-	7
	5.15 (2)		138	1
	-14.58 (4)		138	5.9
	-20.24 (4)		-	6,8
	-26.98 (2)		-	4
	-38.64 (4)		144	2,3
	-40.35 (1)		90	$[BH_2]$
$(CN)_2$[b][c]	13.20 (2)	3.13 (2)	138	2,3
	4.36 (1)	2.82 (1)	140	4
	-7.77 (2)	-	-	6,8
	-9.77 (2)	2.18 (2)	138	5,9
	-29.86 (1)	1.01 (1)	138	7
	-48.04 (1)	-0.35 (1)	142	1
		-0.43 (5)		bridge
		7.50 (30)		$[N(PPh_3)_2]^+$

Table 4.1 Ctd/...

Substituents	$\delta(^{11}B)$p.p.m.	$\delta(^{1}H)$p.p.m.	J_{B-H}/H_z	Assignment
NCAgCN-B_9H_{13}[b]	18.48 (1)			7
	5.08 (1)			1
	-15.59 (2)			5,9
	-20.72 (2)			6,8
	-26.32 (1)			4
	-38.52 (2)			2,3
CN[b]	17.12 (1)	-	138	7
	4.93 (1)	-	138	1
	-14.76 (2)	1.73 (2)	138	5,9
	-19.84 (2)	1.83 (2)	138	6,8
	-37.10 (1)	-	-	4
	-37.73 (2)	0.36 (2)	144	2,3
		-1.57 (5)		bridge
		7.50 (30)		$[N(PPh_3)_2]^+$

(a) CD_3CN solution

(b) $CDCl_3$ solution

(c) the numbering system used throughout is retained in this example.

Figures in parenthesis represent relative integrals.

The ^{11}B n.m.r. spectrum of $[B_9H_{13}(NCSe)]^-$ was identical to the spectrum obtained for $[B_9H_{13}(NCS)]^-$, and it was therefore proposed that the selenocyanate substituted derivative had the same crystalline structure as the thiocyanate substituted derivative,[143,174] (Figure 4.3). The 360 MH_z ^1H and ^1H-{^{11}B} n.m.r. spectra of these anions confirmed that both anions were fluxional. Specific frequency irradiation at the boron resonance corresponding to B(6) and B(8) results in only the exo-terminal hydrogen atoms being observed at ca. δ 1.68 p.p.m. in each case, Irradiation at the B(4) (i.e. the substituted) position shows that no hydrogen atom resides on B(4) on the n.m.r. time scale. The 360 MH_z ^1H n.m.r. spectra indicated that there are five bridging or fluxional hydrogen atoms in both anions by comparison of the relative integrals of the $[N(PPh_3)_2]^+$ resonance with the resonance due to the fluxional hydrogen atoms, (Table 4.1). These data indicated that the endo-terminal hydrogen atoms on B(4), B(6) and B(8), with the bridge hydrogen atoms between B(5) and B(6) and B(9) and B(8), were involved in rapid intramolecular hydrogen exchange in solution on the n.m.r. time scale. It was found that[143] on cooling $[B_9H_{13}(NCS)]^-$ below 233K the molecule became static with the endo-polyhedral hydrogen atoms at δ-0.41 p.p.m. attached to B(6) and B(8) and the endo-terminal hydrogen at δ 0.6 p.p.m. attached to B(4) being resolved.

It is evident that the energy barrier to intramolecular hydrogen exchange on boron is lowered on going to the anion from the neutral adduct. It is proposed that the electron density that is donated into

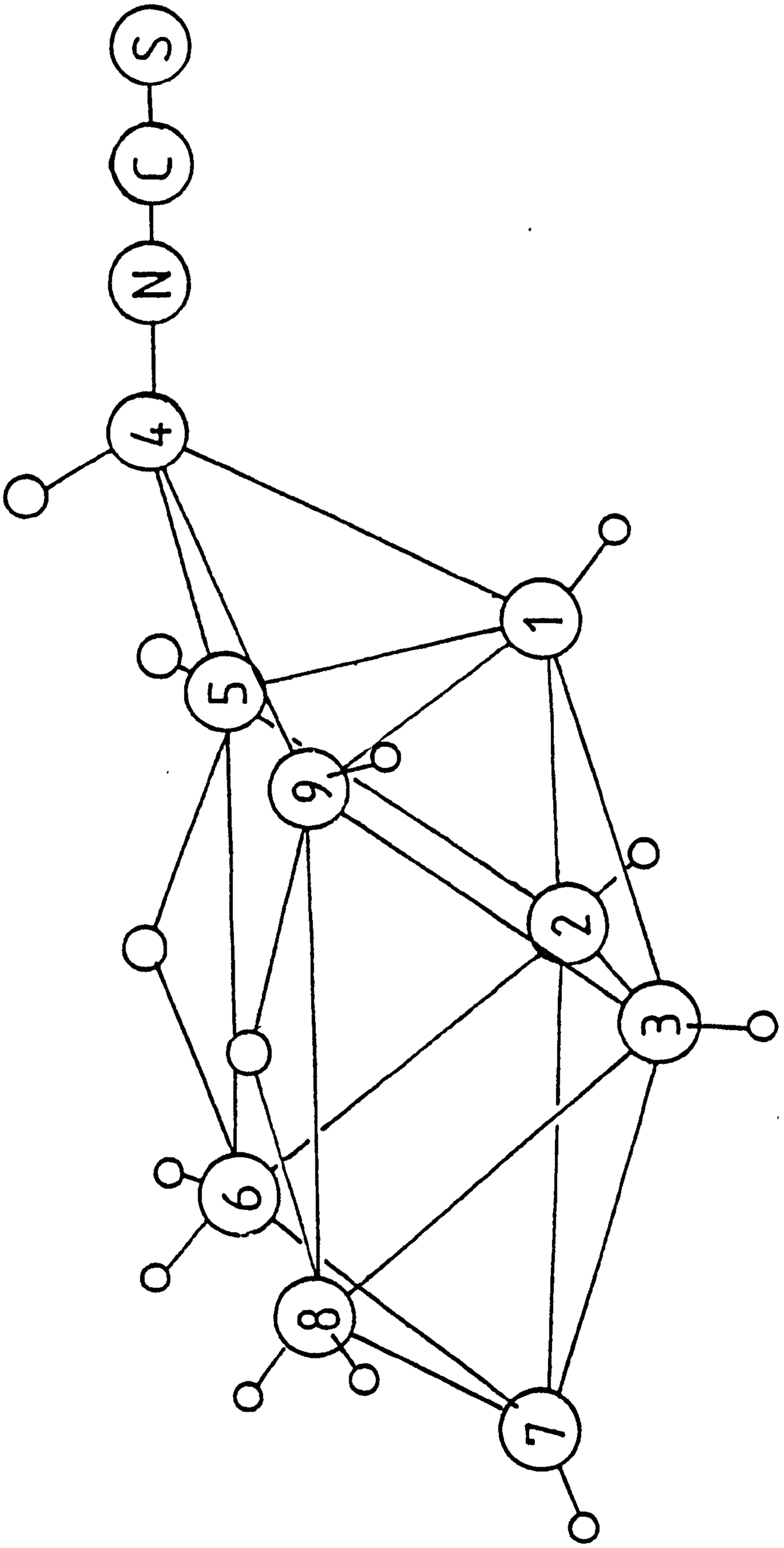

Figure 4.3 The crystal structure of the $[B_9H_{13}(NCS)]^-$ ion.

the cage by the cyano substituent, on anion formation, is the major contributor to this phenomenon.

The anion, $[B_9H_{13}(NCBPh_3)]^-$, like $[B_9H_{13}(NCS)]^-$ and $[B_9H_{13}(NCSe)]^-$ was shown to be fluxional by ^{11}B, ^1H and $^1H-\{^{11}B\}$ n.m.r. spectroscopy. The ^{11}B n.m.r. spectrum of $[B_9H_{13}(NCBPh_3)]^-$ indicated that the C_s symmetry of the neutral adduct, $B_9H_{13}[NCCH_3]$, was retained in the anion. This data was consistent with a structure similar to that of the $[B_9H_{13}(NCS)]^-$ ion in which the $[NCS]^-$ substituent is replaced by $[NCBPh_3]^-$.

Preliminary studies of the anions $[B_9H_{13}(X)]^-$ (X = $NCBH_2NCBH_3$, $NCBH_2CN$, $NCBH_2CNB_9H_{13}$ and $NCBH_3$[143]) by ^{11}B n.m.r. spectroscopy indicated that these anions retained the C_s symmetry of the neutral analogue, $B_9H_{13}[NCCH_3]$, and were fluxional in solution, (Figure 4.4). In these anions the resonance attributed to B(4) is an apparent singlet, indicating that the endo-terminal hydrogen atom on B(4) is effectively decoupled due to rapid intramolecular hydrogen exchange on boron. The 360 MH_z ^1H and $^1H-\{^{11}B\}$ specific frequency decoupling experiments indicated that these anions were not fluxional but, like the neutral $B_9H_{13}L$ adducts, were static. Figure 4.5 shows the results obtained from 360 MH_z $^1H-\{^{11}B\}$ specific frequency decoupling experiments for $[B_9H_{13}(NCBH_2NCBH_3)]^-$. It can be seen that irradiation at the B(6),B(8) resonance frequency results in both exo- and endo-terminal hydrogen atoms being decoupled. Similarly, irradiation at the boron resonance frequency corresponding to the B(4) position results

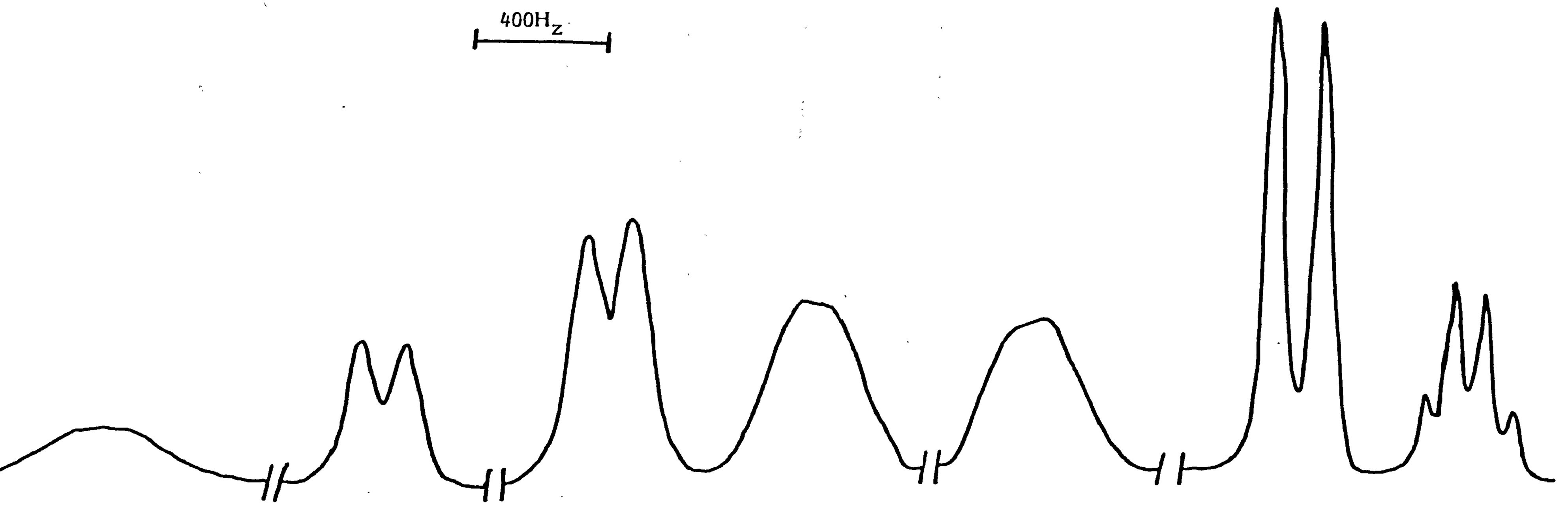

Figure 4.4 The 115.5MHz ^{11}B n.m.r. spectrum of the $[B_9H_{13}(NCBH_2NCBH_3)]^-$ ion in $CDCl_3$.

Figure 4.5 The ^{1}H-{^{11}B} specific frequency decoupled spectra for the $[B_9H_{13}(NCBH_2NCBH_3)]^-$ ion in $CDCl_3$ at 360 MH_z

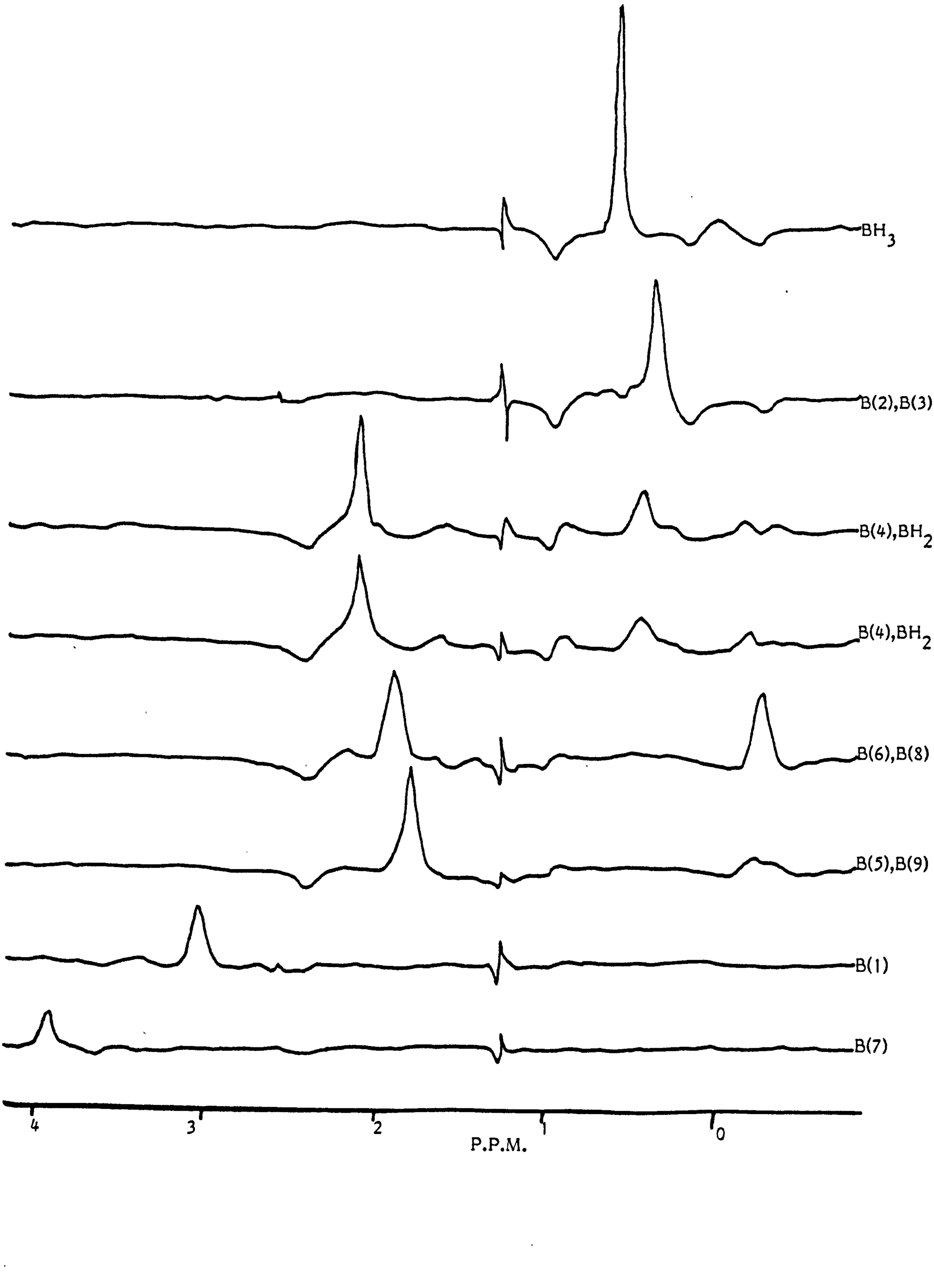

in the endo-terminal hydrogen atom associated with B(4) being decoupled. These data are consistent with a static structure in solution, at room temperature, on the n.m.r. time scale, that is similar to $B_9H_{13}[NCCH_3]$.

Specific frequency $^1H-\{^{11}B\}$ decoupling experiments on $[B_9H_{13}(X)]^-$ (X = $NCBH_2CN$, $NCBH_2CNB_9H_{13}$ and $NCBH_3$) indicated that these anions were also static at room temperature in solution.

It is interesting to note that when the substituent has electron withdrawing species attached, such as the hydrogen atoms in $NCBH_2NCBH_3$, $NCBH_2CN$, $NCBH_2CNB_9H_{13}$ and $NCBH_3$, the resulting anions are static. It is proposed that in the anions, $[B_9H_{13}(X)]^-$ (X = $NCBH_2$ $NCBH_3$, $NCBH_2CN$, $NCBH_2CNB_9H_{13}$ and $NCBH_3$), the electron density from the [CN] moiety of the substituent, that is normally donated into the nonaborane cage, is reduced by the electron withdrawing effect of the hydrogen atoms of the substituent. In effect, the electron density that is donated into the cage is not enough to overcome the energy barrier to intramolecular hydrogen exchange.

It is known that,[143] for $[B_9H_{13}(NCS)]^-$ lowering the temperature causes the anion to become static. Conversely, by raising the temperature it should be possible to force the static anions to become fluxional. A variable temperature n.m.r. study of the $[B_9H_{13}(X)]^-$ (X = NCS, NCSe, $NCBPh_3$, $NCBH_2NCBH_3$, $NCBH_2CN$, $NCBH_2CNB_9H_{13}$ and $NCBH_3$) could be used to indicate the relative stabilities of the anions

and may also give some insight into the fluxional process.

It was previously reported[143] that, in the neutral $B_9H_{13}[NCCH_3]$ adduct, the resonance attributed to B(6) and B(8) was broadened due to poorly resolved couplings of ca. 60 and 30 H_z. It is proposed that in the static anions discussed the B(4) resonance appears as a singlet due to unresolved couplings.

4.2.3 The Reaction of AgCN with $[B_9H_{13}(Cl)]^-$

The preparation of the arachno-$[B_9H_{13}(Cl)]^-$ ion is described in Chapter 6. The 115.5 MH_z ^{11}B n.m.r. spectrum of $[B_9H_{13}(Cl)]^-$ exhibited five resonances of relative intensities 1:1:1:4:2 reading from high frequency, (Table 6.2). In this anion the resonance due to the substituted boron atom B(4) appears at the relatively high frequency δ-12.9 p.p.m., which is ca. 10p.p.m. to higher frequency than the corresponding resonance in other anionic and neutral nonaborane derivatives. The ^1H, ^{11}B and $^1H-\{^{11}B\}$ n.m.r. spectra are consistent with a structure that is fluxional in solution at room temperature. It was shown previously, (Chapter 2), that in the anion, $[B_3H_7(Cl)]^-$, the chloride substituent was labile and was readily replaced by stronger electron pair donors. By comparison with $[B_3H_7(Cl)]^-$ it was expected that the chloride substituent in $[B_9H_{13}(Cl)]^-$ would also be labile and would be easily replaced by stronger electron pair donors, thus offering a preparative route to potentially more interesting species.

(a) Reaction with AgCN

It was previously reported[37] that the reaction of $[B_3H_7(Cl)]^-$ with two equivalents of AgCN resulted in the $[CN]^-$ displacing $[Cl]^-$ to produce $[Ag\{B_3H_7(NC)\}_2]^-$ in which two triborane fragments are linked via a linear NC-Ag-CN bridge. A similar reaction using two equivalents of AgCN to one of $[B_9H_{13}(Cl)]^-$ was carried out in an attempt to prepare the bridged nonaborane analogue $[Ag\{B_9H_{13}(CN)\}_2]^-$. However, the product obtained from this reaction was a disubstituted nonaborane species.

The 115.5 MH_z ^{11}B n.m.r. spectrum of the product obtained from this reaction exhibited six resonances of relative intensities 2:1:2:2:1:1 reading from high frequency. The chemical shifts of the respective resonances reading from high frequency were; δ 13.20, δ-4.36, δ-7.77, δ -9.77, δ-29.86, and δ-48.04 p.p.m. In addition, minor resonances due to the starting material $[B_9H_{13}(Cl)]^-$ were also observed, (Figure 4.6). All of the major resonances in the spectrum of the product appeared as doublets, ($J_{B-H} \approx 138H_z$), except the resonance at δ-7.77 p.p.m. of relative area two which appeared as a singlet. This data indicated that the product was a fluxional disubstituted species. The appearance of the ^{11}B n.m.r. spectrum indicated that the product has C_s symmetry in solution. The symmetry of the species can only be retained if (i) the substituents are the same, and (ii) if they are both substituted on or symmetrically above and below, a plane of symmetry. Hence, the product must either be $[B_9H_{12}(CN)_2]^-$ or $[B_9H_{12}(Cl)_2]^-$. Since during the reaction a silver mirror is deposited onto the walls of the reaction vessel, it is proposed that the product is the di-cyano derivative, $[B_9H_{12}(CN)_2]^-$. This assignment is confirmed

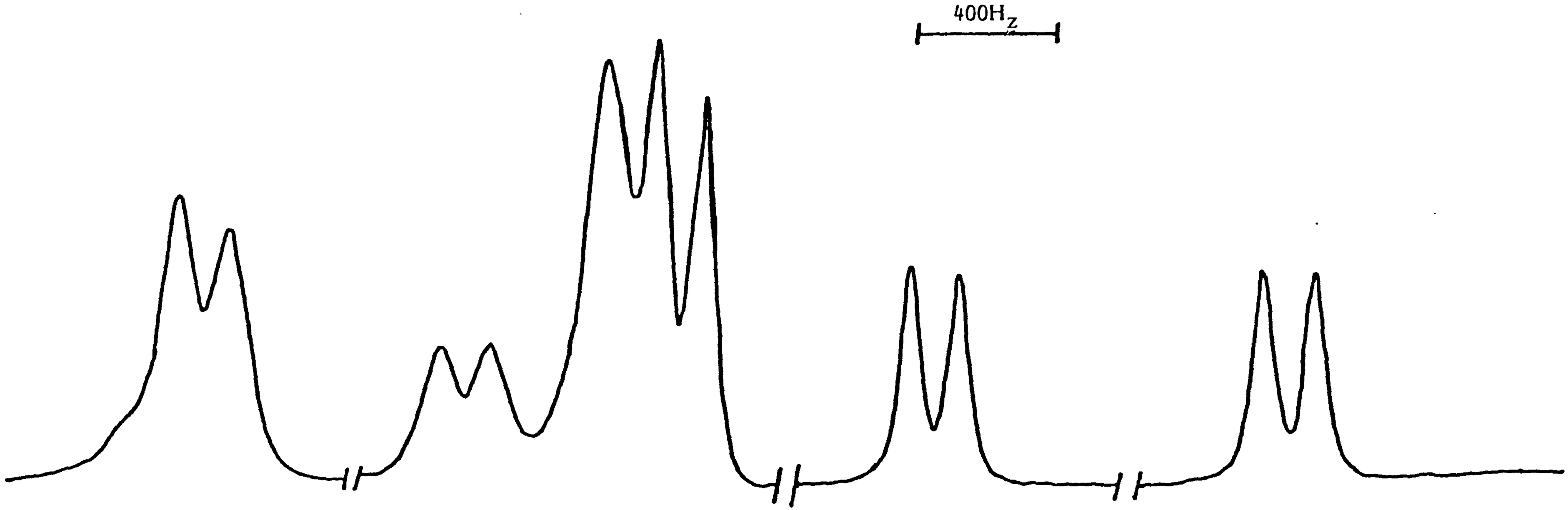

Figure 4.6 The 115.5MHz ^{11}B n.m.r. spectrum of the $[B_9H_{12}(CN)_2]^-$ ion in $CDCl_3$.

by the presence of a strong, sharp band at 2175 cm^{-1} attributed to CN str. in the infra-red. The only other feasible disubstituted species which could be present is $[B_9H_{12}(CN)(Cl)]^-$, but in this case the resonances due to the substituted boron atoms would have to coincidentally overlap. This product is not favoured because the different substituents would disrupt the symmetry of the rest of the molecule. The 360 MH_z $^1H-\{^{11}B\}$ specific frequency decoupling experiments showed that there were five bridge hydrogen atoms present at δ-0.43 p.p.m., indicating that the molecule was fluxional in solution at room temperature on the n.m.r. time scale., Irradiation of the boron resonance frequency corresponding to the substituted boron atoms showed that the terminal hydrogen atoms (presumably endo-) were effectively decoupled due to rapid intramolecular hydrogen exchange. Figure 4.7 shows a topological representation of the structure of $[B_9H_{12}(CN)_2]^-$, (cf. Fig. 4.3), retaining the same numbering system. The remaining resonances in the ^{11}B n.m.r. spectrum can be assigned by examining the effect of specific frequency decoupling experiments on the bridge hydrogen atoms. It was found that irradiating the boron resonance frequency at δ -4.36 p.p.m. resulted in a terminal hydrogen atom being observed at δ 2.82 p.p.m. However, in addition there was considerable enhancement of the resonance at δ -0.43 p.p.m. due to the fluxional bridge hydrogen atoms. This indicated that the hydrogen atoms attached to the boron resonance at δ-4.36 p.p.m. were involved in the fluxional process. If the structure of $[B_9H_{12}(CN)_2]^-$ is basically the same as that of $[B_9H_{13}(NCS)]^-$ (Figure 4.3), with the cyano substituents on B(6) and B(8), then the resonance at δ -4.36 p.p.m. in the

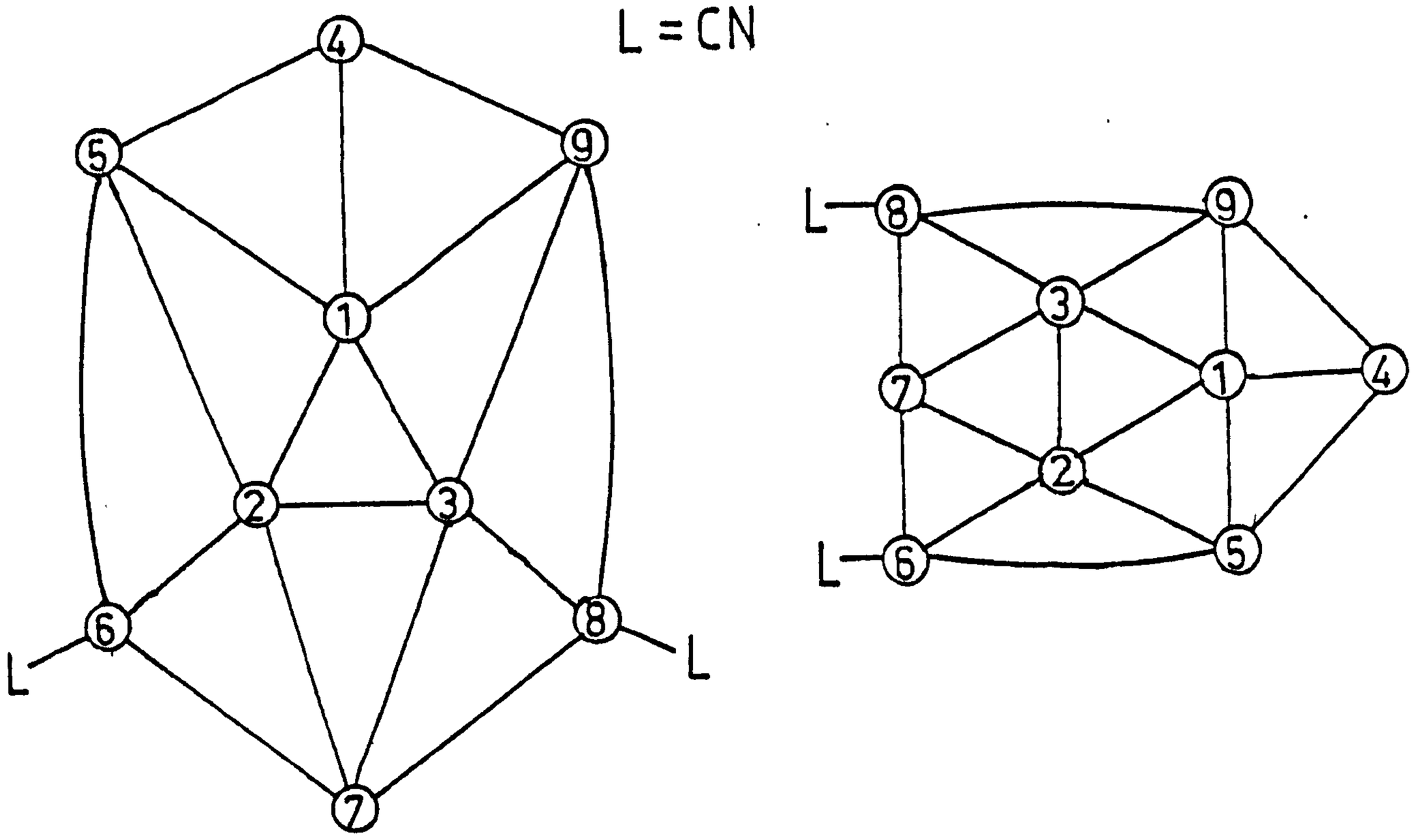

Figure 4.7 Topological representations of the $[B_9H_{12}(CN)_2]^-$ ion

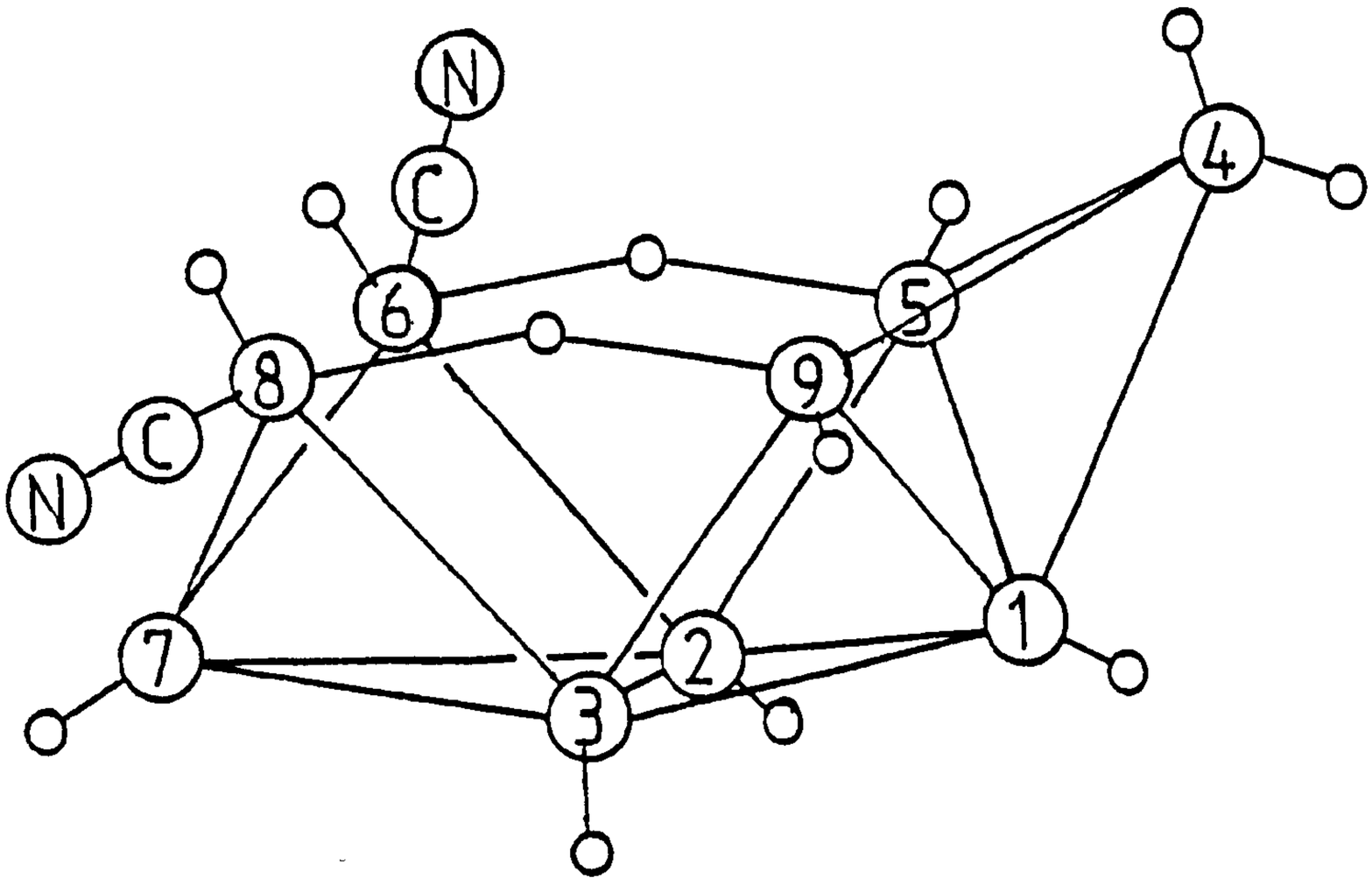

Figure 4.8 The proposed structure of the $[B_9H_{12}(CN)_2]^-$ ion

^{11}B n.m.r. spectrum must be due to the unique unsubstituted boron atom B(4), which has an endo-hydrogen atom involved in intramolecular hydrogen atom exchange. Irradiation at δ -9.77 p.p.m. in the ^{11}B n.m.r. spectrum resulted in the resonance due to the bridge hydrogen atoms at δ-0.43 p.p.m. being resolved. This data indicated that the resonance at δ-9.77 p.p.m. was due to B(5) and B(9). Therefore, by elimination, the resonance of relative intensity two at δ13.20 p.p.m. is due to B(2) and B(3). It is known that, in general, an apical boron atom appears at low frequency. If this trend is followed then the resonance at δ-48.06 p.p.m. is due to the apical B(1) atom. Finally, the resonance at δ-29.86 p.p.m. is due to B(7).

Table 4.2 Infra-red Absorption Frequencies for Substituted Derivatives of $[B_9H_{14}]^-$

Derivative	2700 - 1900 cm^{-1}
$NCSe^{(a)}$	2540s, 2490sh, 2150s
$NCBPh^{(a)}$	2540s, 2250s
$NCBH_2NCBH_3^{(b)}$	2550s, 2420sh, 2370s 2280sh, 2260s, 2210sh
$NCBH_2CN^{(b)}$	2540s, 2400m, 2370sh 2280s, 2110w
$NCBH_2CNB_9H_{13}^{(b)}$	2540s, 2420m, 2285m
$CN^{(a)}$	2530s, 2500sh, 2485m 2180s.

Abbreviations: s, strong; w, weak; sh, shoulder; m, medium.

(a) Nujol or HCBD mull

(b) Thin film

Previously it was reported[99] that the reaction of $B_9H_{13}[SMe_2]$ with $[PPh_4][CN]$ produced an equilibrium mixture of $[B_9H_{13}(CN)]^-$ and $[B_9H_{13}(CN)B_9H_{13}]^-$ via a ligand displacement reaction. It is proposed that a similar reaction occurred with AgCN and $[B_9H_{13}(Cl)]^-$ to produce AgCl and $[B_9H_{13}(CN)]^-$, in which the $[CN]^-$ substitutes at the B(4) position. In the presence of excess AgCN the disubstituted species, $[B_9H_{12}(CN)_2]^-$, was formed with Ag^I being reduced to Ag^o and hydrogen being evolved.

4.2.4 The Reaction of $[Ag(CN)_2]^-$ with $B_9H_{13}[SMe_2]$

Since the reaction of $[B_9H_{13}(Cl)]^-$ and AgCN did not produce the bridged species, $[Ag\{B_9H_{13}(NC)\}_2]^-$ a different route to this product was sought. The reaction of $B_9H_{13}[SMe_2]$ and $[N(PPh_3)_2][Ag(CN)_2]$ gave three chromatographically separated products, indicating that the mechanism of reaction was complex. The second of the three products obtained from this reaction was identified as $[B_9H_{14}]^-$ by comparison of its ^{11}B n.m.r. spectrum with that of an authentic sample.

The 115.5 MH_z ^{11}B n.m.r. spectrum of the first product obtained from this reaction retained the C_s symmetry of the starting material, $B_9H_{13}[SMe_2]$ in solution. However, the resonances at δ -23.6 p.p.m. and δ -31.8 p.p.m. due to B(6),B(8) and B(4) respectively are considerably broadened. In the anion,$[Ag\{B_3H_7(NC)\}_2]^-$ all the boron resonances are also broadened. It is proposed that this product is the anion, $[Ag\{B_9H_{13}(NC)\}_2]^-$ in which the relative bulk of the anion reduces the rate of molecular reorientation, which increases the correlation time,

causing the aforementioned resonances to be broadened. The ^{11}B n.m.r. spectrum of $[Ag\{B_9H_{13}(NC)\}_2]^-$ also showed traces of the final product that was obtained from the reaction. It was noticeable that, like $[Ag\{B_3H_7(NC)\}_2]^-$[37] solutions of $[Ag\{B_9H_{13}(NC)\}_2]^-$ decomposed on standing at room temperature depositing silver.

The 115.5 MH_z ^{11}B n.m.r. spectrum (Table 4.1) of the final product obtained from the reaction of $B_9H_{13}[SMe_2]$ and $[Ag(CN)_2]^-$ is shown in Figure 4.9. It can be seen that in solution the C_s symmetry of the $B_9H_{13}[SMe_2]$ adduct is retained. The presence of the singlet due to the substituted B(4) at δ-37.10 p.p.m. indicated that this species was fluxional. This was confirmed by specific frequency decoupling experiments. Irradiation at the boron resonance frequency corresponding to the substituted B(4) position showed that the endo-terminal hydrogen atom associated with B(4) was undergoing rapid intramolecular hydrogen exchange. In this product the resonance attributed to the substituted B(4) position is at relatively low frequency, that is, more than 10 p.p.m. to lower frequency than the corresponding resonance in any of the other substituted derivatives of $[B_9H_{14}]^-$ discussed. The relatively low frequency position of the substituted B(4) resonance indicated that the cyano substituent was carbon-coordinated, (cf. $[B_3H_7NCB_3H_7]^-$, Chapter 2). Of the two possible products, $[B_9H_{13}(CN)]^-$ or $[B_9H_{13}(NCAgCN)]^-$, the first is thought to be the product obtained since the infra-red spectrum (Table 4.2) showed only one cyanide resonance at 2185 cm^{-1} which was attributed to terminal CN stretching. There was no evidence indicating the presence of a bridging cyanide moiety

Figure 4.9 The 115.5MH$_z$ ^{11}B and ^{11}B-{^{1}H} n.m.r. spectra of $[B_9H_{13}(CN)]^-$ in $CDCl_3$

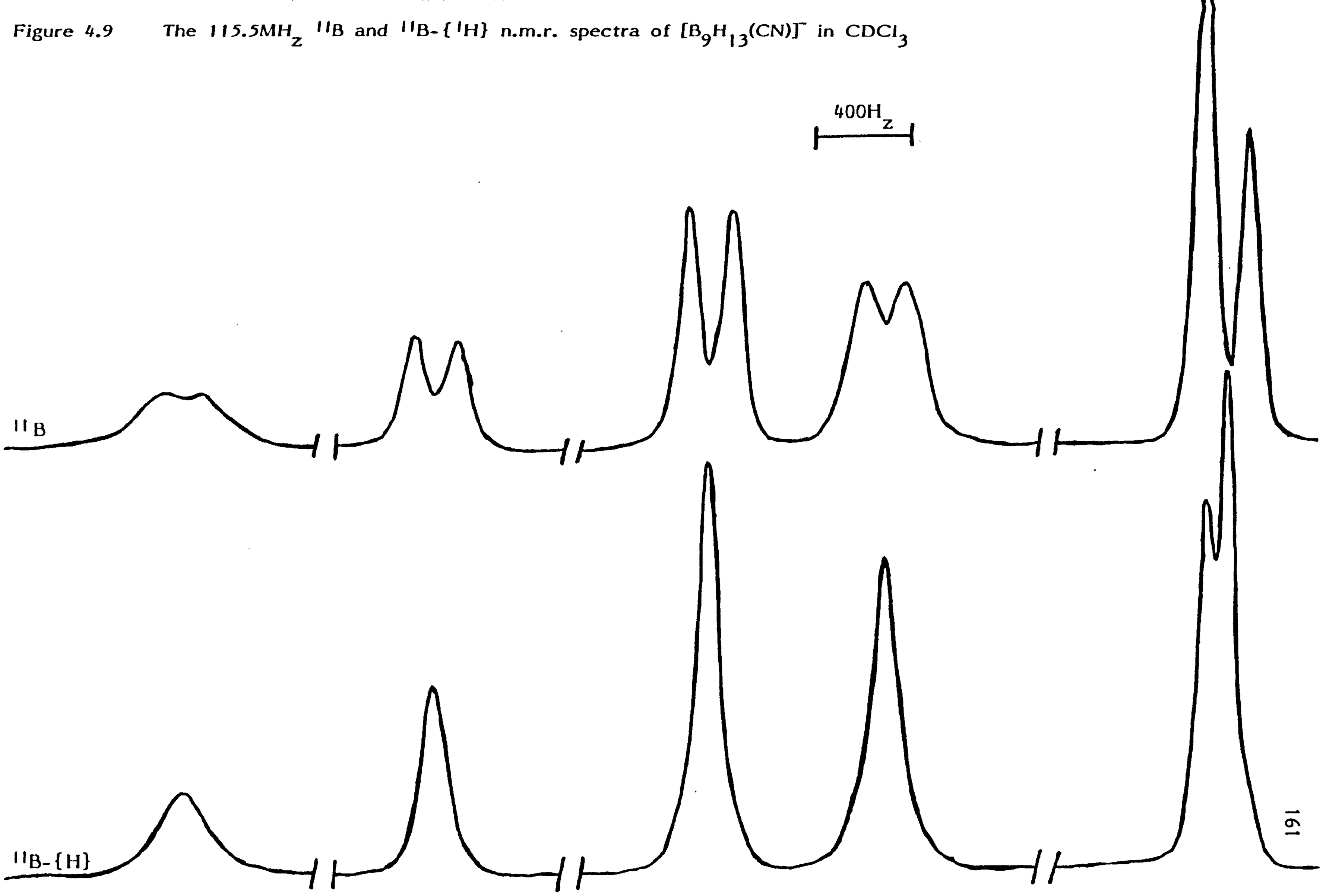

from the infra-red spectrum. In addition, the product decomposed in solution at room temperature to give a black solid, but no silver mirror was deposited. The data are consistent with the final product being $[N(PPh_3)_2][B_9H_{13}(CN)]$.

Since three products are obtained from this reaction the mechanism of reaction is complex. It is possible that initially the anion, $[Ag\{B_9H_{13}(NC)\}_2]^-$, is formed by base displacement of dimethylsulphide from $B_9H_{13}[SMe_2]$ by $[Ag(CN)_2]^-$ to produce $[B_9H_{13}(NCAgCN)]^-$ which undergoes a second base displacement reaction to form $[Ag\{B_9H_{13}(NC)\}_2]^-$. This product is light and heat sensitive and is readily decomposed in solution. It is proposed that the decomposition products are Ag^o, $[CN]^-$ and the reactive $[B_9H_{13}]$ moiety. Subsequent attack on the $[B_9H_{13}]$ fragment by $[CN]^-$ gives $[B_9H_{13}(CN)]^-$. The mechanism for the formation of $[B_9H_{14}]^-$ is not readily apparent but must involve some kind of hydride transfer.

4.3 Experimental

4.3.1 General

Nido-decaborane was purchased from the Callery Chemical Company and was purified by sublimation before use. $[N(PPh_3)_2][Ag(CN)_2]$ was prepared by addition of $[N(PPh_3)_2]Cl$ in ethanol to an aqueous solution of $AgNO_3$ and excess NaCN. The salts $[N(PPh_3)_2][X]$(X = NCS, NCSe, $NCBH_3$, $NCBH_2NCBH_3$, $NCBPh_3$ and $NCBH_2CN$) were prepared as described in Chapter 2. The preparation of $[N(PPh_3)_2][B_9H_{13}(Cl)]$ is described in Chapter 6. All other reagents were used as received.

4.3.2 Preparation of $B_{10}H_{12}[SMe_2]_2$

$B_{10}H_{12}[SMe_2]_2$ was prepared by a slight modification of the method of Greenwood et al.[175] $B_{10}H_{14}$ (5.00g, 41 mmol) was dissolved in an excess of dimethylsulphide (ca. $30cm^3$) and set aside for 5 days at room temperature in a flask equipped with a reflux condenser and a drying tube. The white crystals that were formed were washed with diethyl ether and dried under vacuum (9.02g, 90%). The product was identified as $B_{10}H_{12}[SMe_2]_2$ by comparison of its ^{11}B n.m.r.spectrum with that in the literature.[176]

4.3.3 Preparation of $B_9H_{13}[SMe_2]$

$B_9H_{13}[SMe_2]$ was prepared by a slight modification of the method described by Hawthorne et al.[13] $B_{10}H_{12}[SMe_2]_2$ (9.02g, 37 mmol) was refluxed in methanol (ca. $30cm^3$) for 0.5 hr. The reaction mixture was cooled to room temperature and the solvent was removed under reduced pressure. The residue was extracted into diethyl ether (ca. $150cm^3$) . and the ether was removed under reduced pressure to yield a white solid. The solid was identified as $B_9H_{13}[SMe_2]$ (4.53g, 71%) by comparison of its ^{11}B n.m.r. spectrum with that in the literature.[71]

4.3.4 Preparation of $[B_9H_{13}(NCSe)]^-$

$B_9H_{13}[SMe_2]$ (0.34g, 2 mmol) and $[N(PPh_3)_2]NCSe]$ (1.35g, 2.1 mmol) were placed in a $250cm^3$ round-bottomed flask fitted with a reflux condenser and flushed with dry nitrogen. Dry 1,2-dichloroethane (ca. $30cm^3$) was introduced and the colourless solution was refluxed at

82°C for 2hr. During the reaction a black precipitate was formed, after cooling to room temperature the solution was filtered and the black precipitate was identified as mainly $B(OH)_3$. The solvent was removed under reduced pressure from the colourless solution to give a white solid. T.l.c. analysis of the white solid on silica gel using 100% CH_2Cl_2 as eluant showed a major fraction (Rf = 0.65) and a minor fraction (Rf = 0.38). Purification by chromatography on silica gel using 100% CH_2Cl_2 as eluant gave the first fraction as a white solid. The solid was recrystallised from CH_2Cl_2/n-hexane (0.69g, 46%) and was identified as $[B_9H_{13}(NCSe)]^-$ from its ^{11}B and ^1H n.m.r. spectra.

Preliminary investigations of the minor fraction indicated a species similar to $[B_8H_{12}(NCS)]^-$,[143] however, further work is required before the minor species can be completely characterised.

4.3.5 Preparation of $[B_9H_{13}(NCBPh_3)]^-$

The procedure for the preparation of $[B_9H_{13}(NCBPh_3)]^-$ was identical to that described in Section 4.3.4. $B_9H_{13}[SMe_2]$ (0.34g, 2 mmol) and $[N(PPh_3)_2][NCBPh_3]$ (1.61g, 2 mmol) were placed in a 250cm^3 round-bottomed flask fitted with a reflux condenser and flushed with dry nitrogen. Dry 1,2-dichloroethane (ca. 30cm^3) was introduced and the colourless solution was refluxed for 2hr after which time a white precipitate was formed. The solution was cooled to room temperature and filtered. The white solid was identified as $B(OH)_3$ from its infra-red spectrum. The solvent was removed from the system under reduced

pressure to yield a white solid. T.l.c. analysis of the solid on silica gel using 100% CH_2Cl_2 as eluant indicated a single major component (Rf = 0.67). Purification by liquid chromatography on silica gel gave the major component as a white solid. The solid was recrystallised from CH_2Cl_2/n-hexane to give colourless crystals identified as $[N(PPh_3)_2][B_9H_{13}(NCBPh_3)]$ by ^{11}B and ^{1}H n.m.r. spectroscopy. (Yield; 1.12g, 61%).

4.3.6 Preparation of $[B_9H_{13}(NCBH_2NCBH_3)]^-$

$B_9H_{13}[SMe_2]$(0.17g, 1 mmol) and $[N(PPh_3)_2][BH_3(CN)BH_2(CN)]$ (0.67g, 1.1 mmol) were placed in a 250cm^3 three-necked round-bottomed flask fitted with a reflux condenser and flushed with dry nitrogen. Dry 1,2-dichloroethane (ca. 30cm^3) was added and the colourless solution was refluxed for 2hr. after which time the solvent was removed under vacuum to give a colourless oil. T.l.c. analysis of the oil on silica gel using 100% CH_2Cl_2 as eluant indicated a single major fraction (Rf = 0.7). Purification by liquid chromatography on silica gel using 100% CH_2Cl_2 as eluant gave the single major fraction as a colourless oil. The oil was identified as $[N(PPh_3)_2][B_9H_{13}(NCBH_2NCBH_3)]$ from its ^{1}H, ^{11}B and infra-red spectra.

4.3.7 Preparation of $[B_9H_{13}(NCBH_2CN)B_9H_{13}]^-$ and $[B_9H_{13}(NCBH_2CN)]^-$

$B_9H_{13}[SMe_2]$(0.86g, 5 mmol) and $[N(PPh_3)_2][BH_2(CN)_2]$ (3.70g, 6.1 mmol) were placed in a 250cm^3 three-necked round-bottomed flask fitted

with a reflux condenser and flushed with dry nitrogen. Dry 1,2-dichloroethane was added and the resulting colourless solution was refluxed for 1.5hr., after which time the solvent was removed under reduced pressure to give a white solid. T.l.c. analysis of the white solid on silica gel using 100% CH_2Cl_2 as eluant showed a major fraction (Rf = 0.42) and a minor fraction (Rf = 0.67). Purification by liquid chromatography on silica gel using 100% CH_2Cl_2 as eluant gave both fractions as white solids when the solvent was removed under reduced pressure. The minor fraction was identified as $[N(PPh_3)_2][B_9H_{13}(NCBH_2CN)B_9H_{13}]$ (0.48g, 23%), by ^{1}H and ^{11}B n.m.r. spectroscopy. The major fraction was identified, in the same way, as $[N(PPh_3)_2][B_9H_{13}(NCBH_2CN)]$, (2.2g, 62%).

It was found that if the reaction was repeated using two equivalents of $B_9H_{13}[SMe_2]$ to one equivalent of $[N(PPh_3)_2][BH_2(CN)_2]$ the major product was the $[N(PPh_3)_2][B_9H_{13}(NCBH_2CN)B_9H_{13}]$ species. (Yield ≈54%).

4.3.8 Preparation of $[B_9H_{12}(CN)_2]^-$

$[N(PPh_3)_2][B_9H_{13}(Cl)]$ (0.68g, 1 mmol) and a large excess of AgCN were placed in a $100cm^3$ round-bottomed flask fitted with a stopcock adaptor. Dry dichloromethane (ca. $30cm^3$) was condensed in under vacuum. The system was allowed to warm to room temperature (ca. 20°C) and was stirred under vacuum. Initially there was severe gas evolution and the AgCN discoloured and a silver mirror was deposited onto the walls of the flask. The dark solution was filtered and the

solvent was removed under reduced pressure to yield a black solid. T.l.c. analysis of the black solid on silica gel using 100% CH_2Cl_2 as eluant indicated a single major product (Rf = 0.65). The black product was not very stable and decomposed rapidly in solution. The ^{11}B and ^{1}H n.m.r. spectra of the crude product indicated that the major component was the disubstituted species $[N(PPh_3)_2][B_9H_{12}(CN)_2]$.

4.3.9 Preparation of $[Ag\{B_9H_{13}(CN)\}_2]^-$ and $[B_9H_{13}(CN)]^-$

$B_9H_{13}[SMe_2]$ (0.93g, 5.4 mmol) and $[N(PPh_3)_2][Ag(CN)_2]$ (3.85g, 5.5 mmol) were placed in a $250cm^3$ three-necked round-bottomed flask fitted with a reflux condenser and flushed with dry nitrogen. Dry 1,2-dichloroethane (ca. $30cm^3$) was introduced and the resulting colourless solution was refluxed for 1.5hr. On refluxing the solution went yellow then dark, a grey precipitate was formed and a silver mirror was deposited on the wall of the flask. After filtration the solvent was removed under reduced pressure from the dark solution to give a black solid. T.l.c. analysis of the black solid on silica gel using 100% CH_2Cl_2 as eluant showed three components (Rf = 0.67, 0.52 and 0.38). Purification by liquid chromatography on silica gel using 100% CH_2Cl_2 as eluant gave the individual fractions that were subsequently examined by ^{11}B, ^{1}H and infra-red spectroscopy. The second fraction eluted was identified from its ^{11}B n.m.r. spectrum as $[B_9H_{14}]^-$ by comparison with the spectrum of a genuine sample. The first fraction eluted gave a black solid which was unstable and decomposed in solution to give a silver mirror and a black precipitate. It was

found that this species was heat and light sensitive. Due to the instability of this species characterisation was not complete, however the ^{11}B n.m.r. spectrum of the product indicated that it was $[N(PPh_3)_2][Ag\{B_9H_{13}(NC)\}_2]$. The final fraction eluted also gave a black solid that decomposed in solution. However, in this case no silver mirror was formed. This product was identified as $[N(PPh_3)_2][B_9H_{13}(CN)]$ by ^{11}B and ^{1}H n.m.r. spectroscopy.

CHAPTER FIVE

ELECTROCHEMICAL STUDIES OF SUBSTITUTED DERIVATIVES OF $[B_9H_{14}]^-$

5.1 Introduction

Previously it was found that oxidation of CsB_9H_{14} in acetonitrile at a platinum electrode at low current density gave crystals of $B_9H_{13}[NCCH_3]$ identified by X-ray analysis.[98] Studies of $[NMe_4]B_9H_{14}$ by cyclic and a.c. voltammetry in acetonitrile at a platinum electrode showed two irreversible oxidations at 0.68V and 1.35V (Ag/0.1 M $AgNO_3$; + 0.34V vs. SCE). Controlled potential electrolysis at the first oxidation potential, in acetonitrile, at platinum, proceeded via a one electron oxidation to produce $B_9H_{13}[NCCH_3]$.[99]

$$[B_9H_{14}]^- \longrightarrow [B_9H_{14}]^\bullet + e^- \qquad (5\text{-}1)$$

$$[B_9H_{14}]^\bullet \longrightarrow [B_9H_{13}] + H^\bullet \qquad (5\text{-}2)$$

$$[B_9H_{13}] + CH_3CN \longrightarrow B_9H_{13}[NCCH_3] \qquad (5\text{-}3)$$

$$H^\bullet \longrightarrow \tfrac{1}{2}.H_2 \qquad (5.4)$$

Cyclic and a.c. voltammetry of $[B_9H_{13}(NCS)]^-$ and $B_9H_{13}[SMe_2]$ in acetonitrile at platinum both showed irreversible oxidation waves at 0.88V and 1.42V respectively (Ag/0.1M $AgNO_3$; + 0.34V vs SCE). Controlled potential electrolysis indicated a two-electron oxidation in each case. Although the oxidation products were not characterised it was proposed that the major products were the <u>nido</u>-derivatives, $[B_9H_{11}(NCS)]^-$ and $B_9H_{11}[SMe_2]$.[99]

$$[B_9H_{13}(NCS)]^- \xrightarrow[-2H^+]{-2e} [B_9H_{11}(NCS)]^- \qquad (5\text{-}5)$$

Electrochemical oxidation of <u>arachno</u>-derivatives to <u>nido</u>-derivatives has previously been reported for the oxidation of $B_{10}H_{12}[NCCH_3]_2$

in acetonitrile at a platinum electrode.[105]

In this chapter the electrochemical properties of substituted derivatives of $[B_9H_{14}]^-$ are examined in acetonitrile and dichloromethane using cyclic voltammetry, cyclic a.c. voltammetry and controlled potential electrolysis. The results obtained were used to determine the effect of the various substituents on the oxidative stabilities of the anions.

In addition, some attempts to prepare metallaboranes from the substituted derivatives of $[B_9H_{14}]^-$ by anodic dissolution of reactive metals in solutions of the anions are described.

5.2 Results and Discussion

5.2.1 Oxidation Studies

(a) $[B_9H_{13}(NCSe)]^-$

(i) Acetonitrile Solution

The cyclic voltammogram of $[N(PPh_3)_2][B_9H_{13}(NCSe)]$, at a platinum electrode in acetonitrile containing $[NBu^n_4][BF_4]$ (0.1 mol dm^{-3}) as supporting electrolyte, was recorded and is shown in Figure 5.1. The voltammogram showed a highly irreversible oxidation wave at Ep = 0.98V. On the reduction scan an irreversible wave was observed near -1.2V. The cyclic a.c. voltammogram of $[B_9H_{13}(NCSe)]^-$ in acetonitrile at platinum showed an irreversible oxidation wave at Ep = 0.86V, this oxidation potential was the same as that observed for $[B_9H_{13}(NCS)]^-$ within experimental error. Thus replacing the sulphur atom of the substituent with selenium does not affect the oxidative stability

Figure 5.1(a) The cyclic voltammogram (scan rate = $0.5Vs^{-1}$) and (b) the cyclic a.c. voltammogram (scan rate = $0.05Vs^{-1}$) of $[B_9H_{13}(NCSe)]^-$ in CH_3CN.

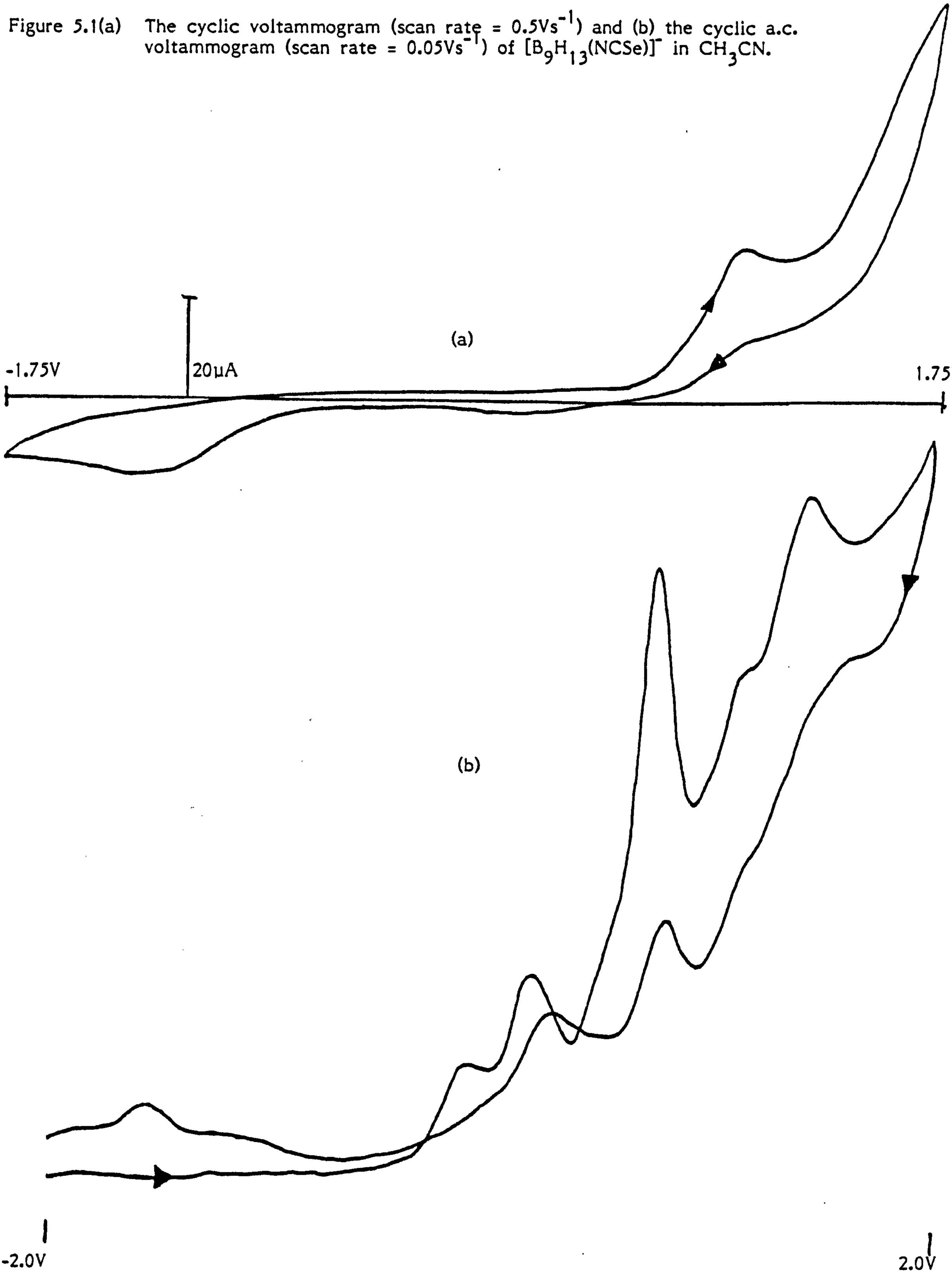

of the anion. Substitution of $[B_9H_{14}]^-$ with $[NCSe]^-$ increased the oxidative stability of the anion by ca. 0.20V with respect to $[B_9H_{14}]^-$. In addition to the irreversible oxidation wave at Ep = 0.86V in $[B_9H_{13}(NCSe)]^-$, two further irreversible oxidation waves were observed in the cyclic a.c. voltammogram at Ep = 1.24V and 1.48V. The presence of these waves indicated that further oxidations occurred subsequent to the initial oxidation at Ep = 0.86V. Therefore, it was probable that the electrochemical processes involved in anion oxidation would be complex.

Controlled potential electrolysis, at a platinum electrode, of $[B_9H_{13}(NCSe)]^-$ in acetonitrile containing $[NBu^n_4]BF_4$ (0.1 mol dm^{-3}) supporting electrolyte (ca. $10cm^3$) proceeded at a potential of 1.0V. The overall process corresponded to a two electron oxidation of the $[B_9H_{13}(NCSe)]^-$ anion. During the electrolysis a brick red precipitate was formed in the anodic compartment indicating decomposition of the products. Although the products of this reaction have not been fully characterised the ^{11}B n.m.r. data (Table 5.1) of the anolyte solution are consistent with the presence of the nido-$[B_9H_{11}(NCSe)]^-$ species, that is similar to the nido-$[B_9H_{11}(NCS)]^-$ anion[99] previously obtained from the oxidation of $[B_9H_{13}(NCS)]^-$.

(ii) Dichloromethane Solution

In dichloromethane the cyclic voltammograms of $[B_9H_{13}(NCS)]^-$ and $[B_9H_{13}(NCSe)]^-$ at a platinum electrode with $[NBu^n_4]BF_4$ (0.5 mol dm^{-3}) supporting electrolyte added, were poorly resolved. The cyclic

Table 5.1 ^{11}B, ^{1}H N.M.R. Spectral Data for $[B_9H_{11}(X)]^-$ Oxidation Products

X	$\delta^{11}B$/p.p.m.	J_{B-H}/Hz	$\delta^{1}H$/p.p.m.	Integral
NCSe	17.50	142		1
	3.90	-		1
	-4.58	-		1
	-7.29	-		1
	-13.96	130		1
	-20.00	-		1
	-26.66	-		1
	-38.54	142		1
	-48.95	-		1
NCS	15.21	-	4.19	1
	2.17	-	2.74	1
	-0.35	120	2.71	1
	-3.97	120	2.83	1
	-10.55	143	2.15	1
	-15.92(s)	-	-	1
	-24.14	134	-	1
	-31.45	138	0.91	1
	-48.07	143	-0.42	1
$NCBPh_3$	18.19	-		1
	2.15	-		1
	-4.59	130		1
	-10.83	-		1
	-14.95	130		1
	-20.01	-		1
	-24.25	138		1
	-29.03	130		1
	-38.47	138		1
	-47.82	138		1

s - singlet

^{11}B n.m.r. spectra obtained at 115.5MH_z in $CDCl_3$

^{1}H n.m.r. spectra obtained at 360MH_z in $CDCl_3$

voltammogram of $[B_9H_{13}(NCS)]^-$ (Figure 5.2) showed irreversible oxidations at Ep > 1.4V.

The cyclic a.c. voltammogram (Figure 5.2) clearly showed an irreversible oxidation at Ep = 1.67V attributed to solvent oxidation. In addition two minor irreversible oxidation waves were observed at Ep = 0.96V and 1.22V. These waves were attributed to the oxidation potentials of $[B_9H_{13}(NCS)]^-$ in dichloromethane. From these results $[B_9H_{13}(NCS)]^-$ is oxidatively more stable in dichloromethane by ca. 0.2V, than it is in acetonitrile.

Controlled potential electrolysis, at a platinum electrode, of a dichloromethane solution of $[B_9H_{13}(NCS)]^-$ containing $[NBu^n_4]BF_4$ (0.1 mol dm^{-3}) supporting electrolyte proceeded at a potential of 1.5V. The overall process corresponded to a two electron oxidation. The 115.5 MH_z ^{11}B n.m.r. spectra of the purified products obtained from the anolyte solution showed the presence of a nonaborane species in which all nine boron resonances were unique (Table 5.1). Since all nine boron atoms were unique, the C_s symmetry that was present in the original anion, $[B_9H_{13}(NCS)]^-$ in solution, has been destroyed during the electrolysis. All the resonances appear as doublets ($J_{B-H} \approx 138H_z$), except the resonance at δ-15.92 p.p.m. that appears as a singlet, indicating that the species is mono-substituted and fluxional. The infra-red spectrum had a strong sharp band at $2160cm^{-1}$ attributed to cyanide stretching, showing that the $[NCS]^-$ substituent had been retained and had not been replaced by $[Cl]^-$ which is generated by

Figure 5.2(a) The cyclic voltammogram (scan rate$_1$ = 0.5Vs^{-1}) and (b) the cyclic a.c. voltammogram (scan rate = 0.05 Vs^{-1}) of $[B_9H_{13}(NCS)]^-$ in CH_2Cl_2

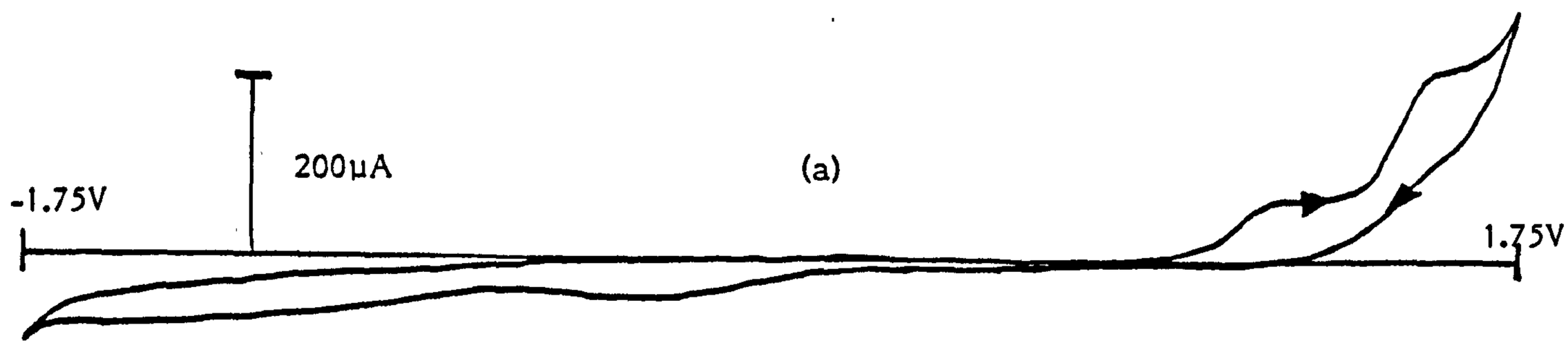

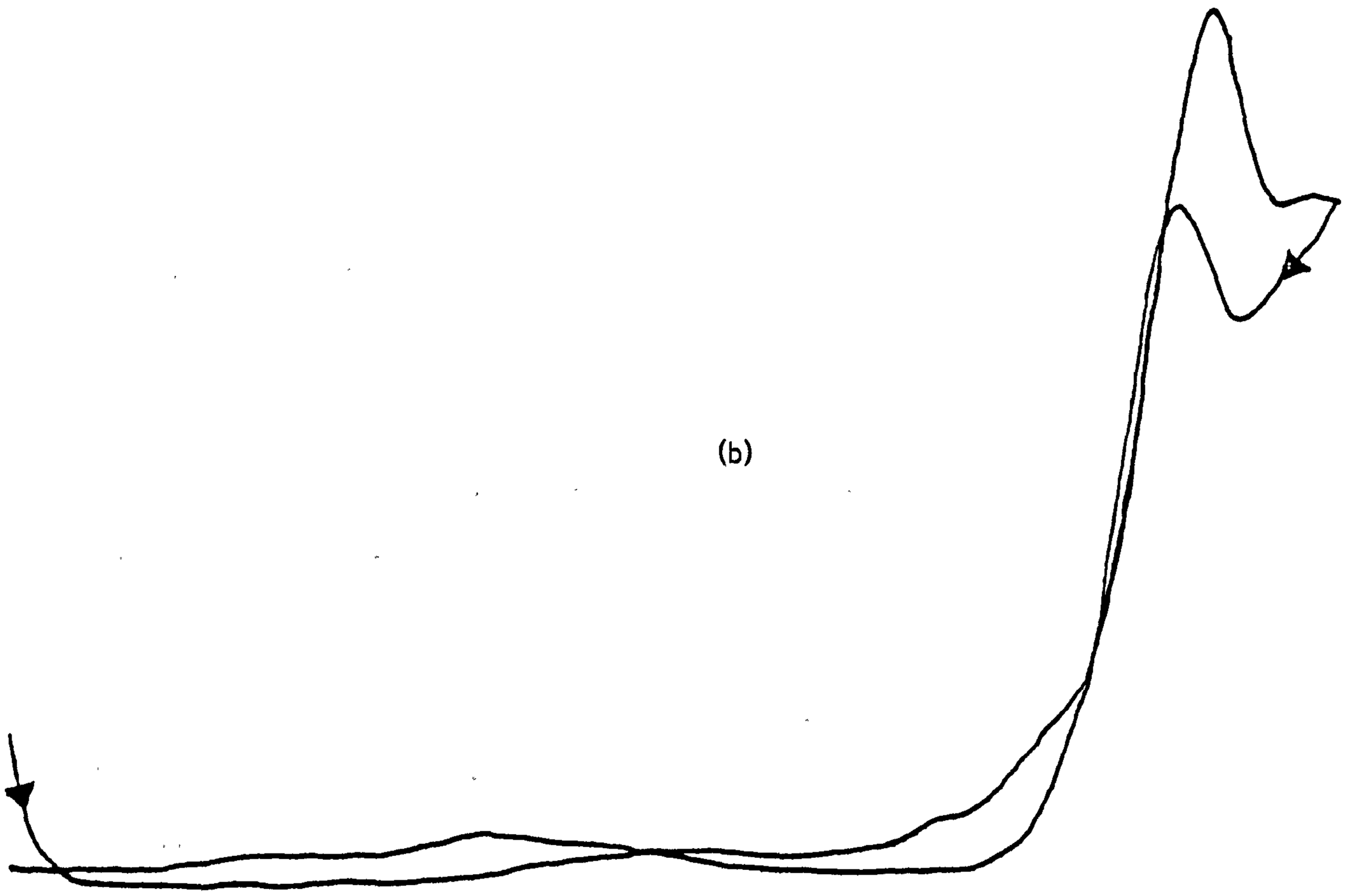

solvent oxidation. It is proposed that oxidation of $[B_9H_{13}(NCS)]^-$ in dichloromethane at platinum, results in the formation of nido-$[B_9H_{11}(NCS)]^-$, which is a substituted derivative of $[B_9H_{12}]^-$. For a nido-cluster to be prepared from arachno-$[B_9H_{13}(NCS)]^-$ a new boron-boron bond must be formed across the open faces made by B(4), B(5) and B(6). The structure of the nido-anion would be that of $[B_9H_{12}]^-$ in which the terminal hydrogen atom on B(5) or B(2), (Figure 6.1), is replaced by the [NCS] substituent. Examination of the 115.5 MH_z ^{11}B n.m.r. spectra of the nido-anions obtained by electrolysis in acetonitrile[99] and dichloromethane showed that the compounds were different (Table 5.1). Therefore, it is proposed that in the different solvents, different structural isomers are formed. The 360 MH_z specific frequency decoupled ^1H n.m.r. spectra are consistent with a structure similar to that shown in Figure 5.3. Irradiation at the boron frequency corresponding to the substituted boron atom indicated that the terminal hydrogen atom associated with this boron atom is undergoing intramolecular hydrogen exchange.

The cyclic voltammogram of $[N(PPh_3)_2][B_9H_{13}(NCSe)]$ at a platinum electrode in dichloromethane with added $[NBu^n_4][BF_4]$ (0.5 mol dm^{-3}) supporting electrolyte was similar to that of $[B_9H_{13}(NCS)]^-$, (Figure 5.4). The cyclic voltammogram of $[B_9H_{13}(NCSe)]^-$ showed irreversible oxidation waves at Ep > 1.4V. In addition, an irreversible reduction appeared at Ep = -1.8V on scans subsequent to the initial scan, that is, the reduction only occurred after oxidation, indicating that one of the oxidation products is reduced on the reverse scan. The cyclic

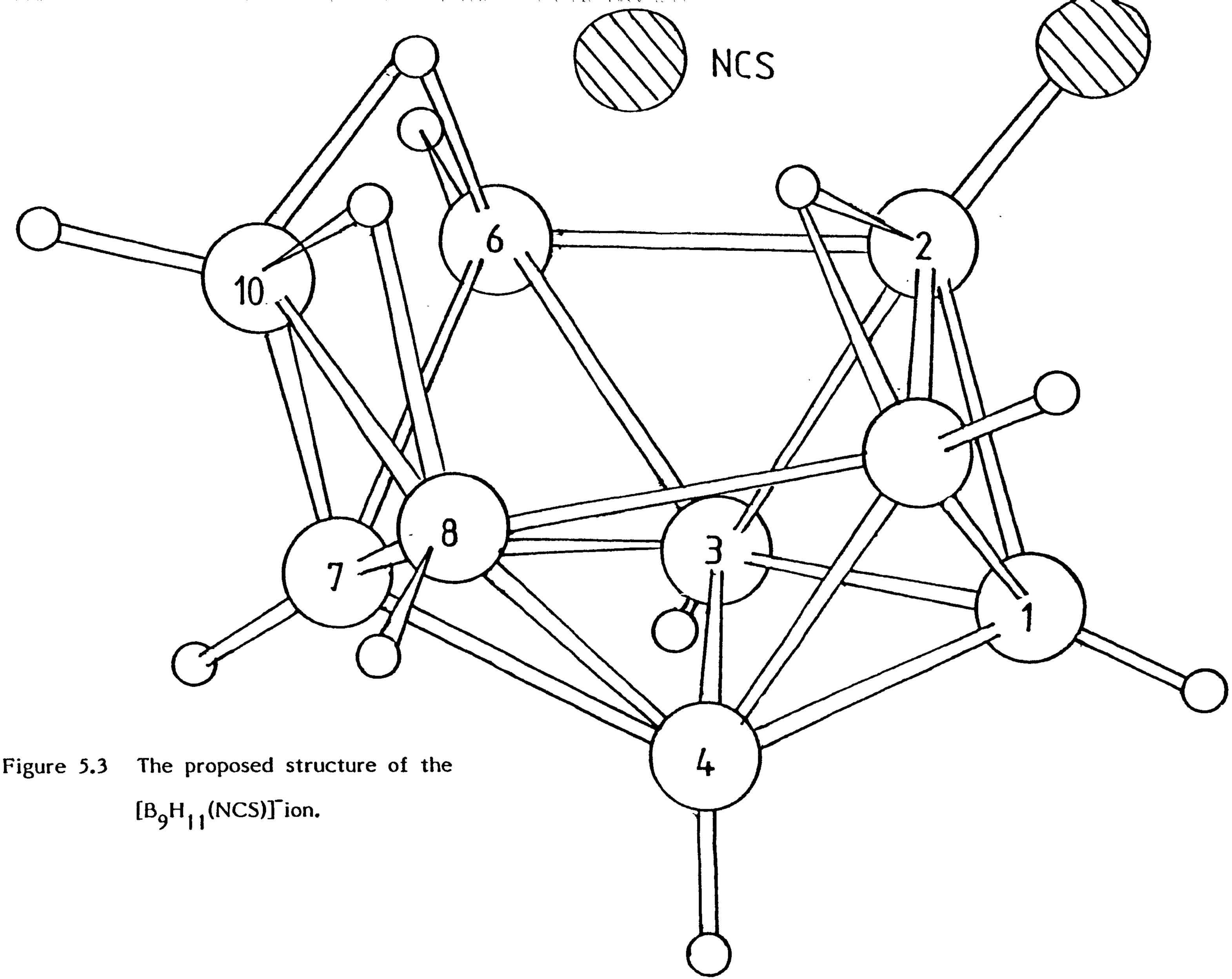

Figure 5.3 The proposed structure of the $[B_9H_{11}(NCS)]^-$ ion.

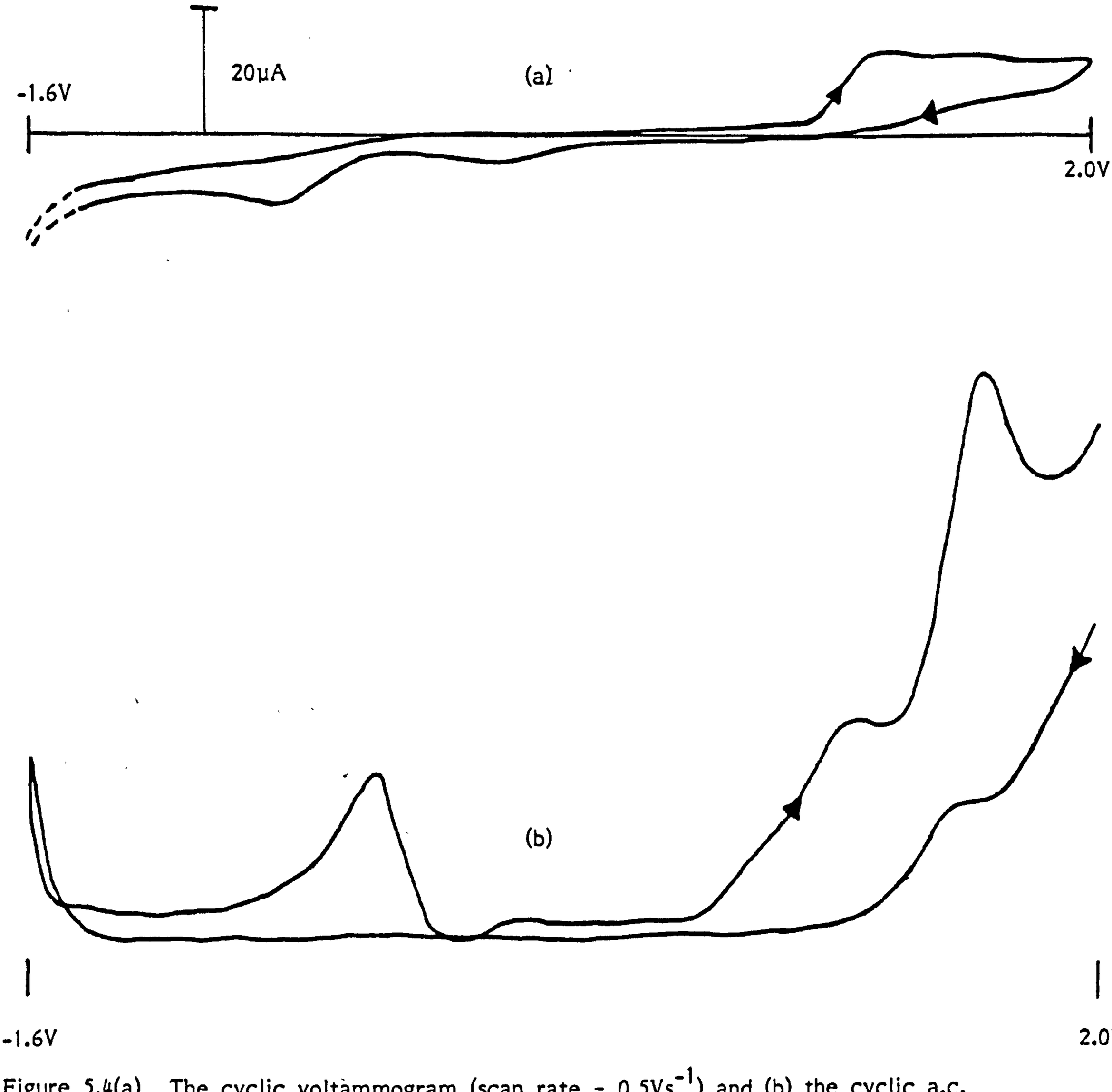

Figure 5.4(a) The cyclic voltammogram (scan rate = $0.5Vs^{-1}$) and (b) the cyclic a.c. voltammogram (scan rate = $0.05Vs^{-1}$) of $[B_9H_{13}(NCSe)]^-$ in CH_2Cl_2.

a.c. voltammogram of $[B_9H_{13}(NCSe)]^-$ in CH_2Cl_2 showed an irreversible oxidation wave at Ep = 1.62V that was attributed to solvent oxidation. A further irreversible oxidation was observed at Ep = 1.17V. This wave was attributed to anion oxidation. Comparison of this oxidation potential with that of the first oxidation potential (Ep = 0.86V) of $[B_9H_{13}(NCSe)]^-$ in acetonitrile indicated that in dichloromethane the anion was oxidatively more stable by ca. 0.3V. The irreversible reduction previously observed in the cyclic voltammogram appeared at Ep= 0.42V. By varying the limiting oxidation potential in the cyclic a.c. voltammograms of the $[B_9H_{13}(NCSe)]^-$ anion in solution, it was found that the reduction only occurred once the oxidation at Ep = 1.17V was traversed. This data showed that the reduction process was related to anion oxidation and was independent of solvent oxidation.

Controlled potential electrolysis, at a platinum electrode, of $[B_9H_{13}(NCSe)]^-$ in dichloromethane containing $[NBu^n_4][BF_4]$ (0.4 mol dm^{-3}) proceeded at a potential of 1.5V. The overall process corresponded to a 1.5 electron oxidation. The 115.5 MH_z ^{11}B n.m.r. of the purified product indicated the presence of $[B_9H_{13}(NCSe)]^-$ and a minor product that has not yet been identified.

(b) $[B_9H_{13}(NCBPh_3)]^-$

(i) Acetonitrile Solution

The cyclic voltammogram of $[N(PPh_3)_2][B_9H_{13}(NCBPh_3)]$, at a platinum electrode, in acetonitrile with $[NBu^n_4][BF_4]$ (0.1 mol dm^{-3}) supporting electrolyte added was recorded and is shown in Figure 5.5. The cyclic

Figure 5.5(a) The cyclic voltammogram (scan rate = $0.5Vs^{-1}$) and (b) the cyclic a.c. voltammogram (scan rate = $0.05Vs^{-1}$) of $[B_9H_{13}(NCBPh_3)]^-$ in CH_3CN

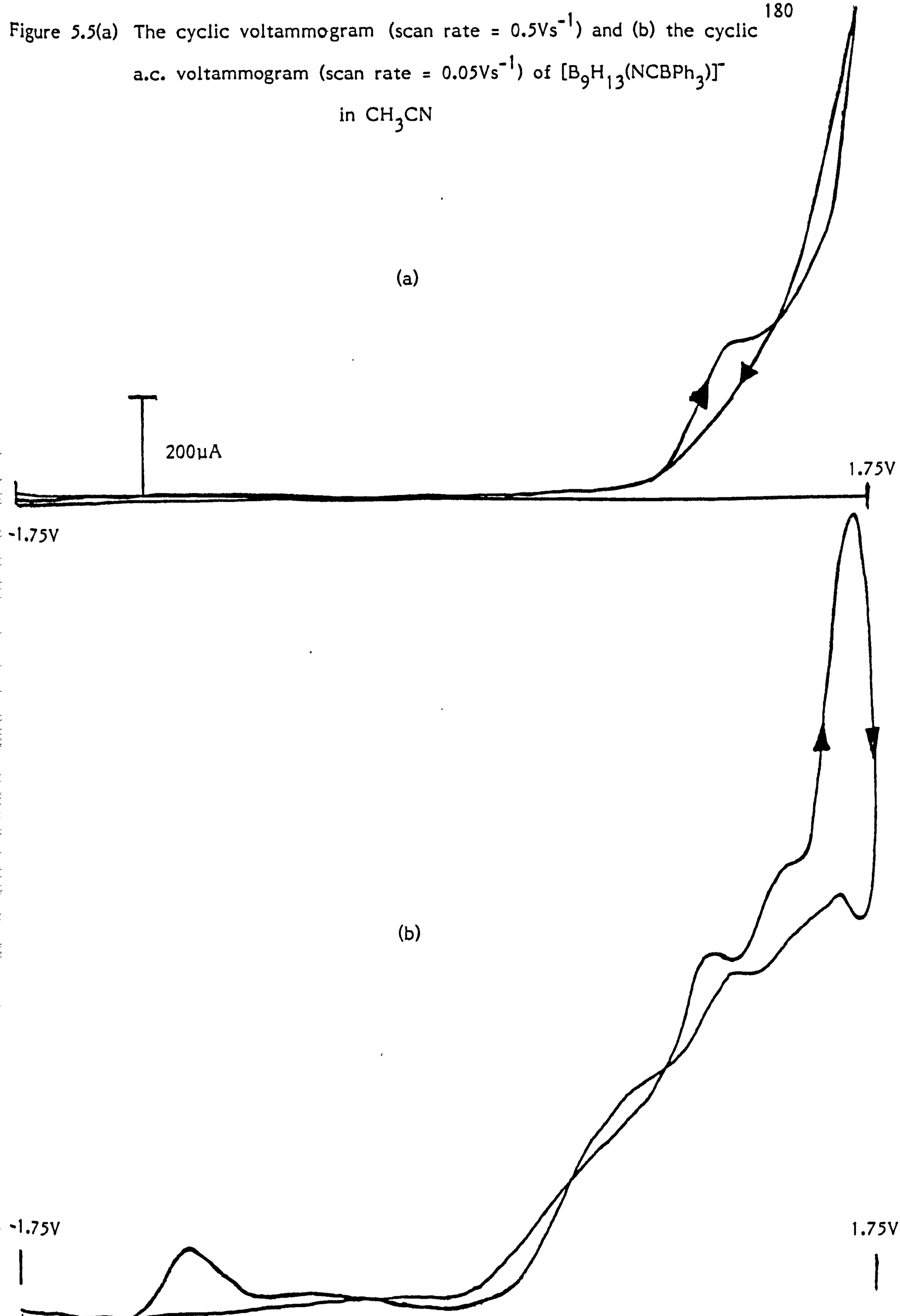

voltammogram of $[B_9H_{13}(NCBPh_3)]^-$ exhibited an irreversible oxidation wave at Ep = 1.35V. The oxidation potentials of $[B_9H_{13}(NCS)]^-$ and $[B_9H_{13}(NCSe)]^-$ were 0.88V and 0.86V respectively. Therefore, when the substituent was $[Ph_3B(CN)]^-$ rather than $[NCS]^-$ or $[NCSe]^-$ the nonaborane anion was more stable to oxidation.

Controlled potential electrolysis of $[N(PPh_3)_2]B_9H_{13}(NCBPh_3)]$, at a platinum electrode, in acetonitrile, with added $[NBu^n_4]BF_4]$ (0.1 mol dm^{-3}) supporting electrolyte proceeded at a potential of 1.5V. The overall process corresponded to a 1.6 electron oxidation. The 115.5 MH_z ^{11}B n.m.r. spectrum of the crude anolyte solution indicated the presence of several components that are, as yet, uncharacterised.

(ii) Dichloromethane Solution

The cyclic voltammogram of $[N(PPh_3)_2]B_9H_{13}(NCBPh_3)]$ at a platinum electrode in dichloromethane with $[NBu^n_4]BF_4]$ (0.4 mol dm^{-3}) supporting electrolyte added was poorly resolved. An irreversible oxidation wave, attributed to solvent oxidation was observed at Ep = 1.68V. In addition, a small irreversible oxidation wave was observed at Ep = 1.52V.

Controlled potential electrolysis of a dichloromethane solution of $[N(PPh_3)_2]B_9H_{13}(NCBPh_3)]$ at a platinum electrode proceeded at a potential of 1.6V. The overall oxidative process involved two electrons. Two products were obtained from the anolyte solution. The 115.5 MH_z ^{11}B n.m.r. spectrum of the first product obtained from the electrolysis has not yet been characterised. The 115.5 MH_z ^{11}B n.m.r.

spectrum of the second electrolysis product exhibited nine boron resonances. Since all the boron resonances are unique the C_s symmetry that existed in the anion, $[B_9H_{13}(NCBPh_3)]^-$, has been destroyed on oxidation. The resonance attributed to the substituted boron atom at δ-20.01 p.p.m. appeared as a singlet indicating that the product is fluxional. The resonance due to the $[BPh_3]$ moiety of the substituent appeared at δ-10.83 p.p.m. It is proposed that on oxidation the nido-derivative $[B_9H_{11}(NCBPh_3)]^-$ is formed, in which the substituent is located off the plane of symmetry.

(c) $[B_9H_{13}(NCBH_2NCBH_3)]^-$

(i) Acetonitrile Solution

The cyclic voltammogram (Figure 5.6) of $[N(PPh_3)_2][B_9H_{13}(NCBH_2NCBH_3)]$ in acetonitrile at a platinum electrode, with $[NBu^n_4][BF_4]$ (0.1 mol dm^{-3}) supporting electrolyte added, showed two irreversible oxidation waves and an irreversible reduction wave. The first irreversible oxidation wave appeared at Ep = 1.25V and the second at Ep = 1.56V, the irreversible reduction wave appeared at ca. Ep = -0.98V. In addition two waves attributed to solvent impurities appeared at Ep = 0.36V and Ep = -0.18V. Comparison of the initial oxidation potential at Ep = 1.25V with the oxidation potentials previously determined it was found that $[B_9H_{13}(NCBH_2NCBH_3)]^-$ was oxidatively more stable than $[B_9H_{13}(NCS)]^-$ and $[B_9H_{13}(NCSe)]^-$, but was less stable than $[B_9H_{13}(NCBPh_3)]^-$. Thus, the oxidative stability of the substituted derivatives of $[B_9H_{14}]^-$ increases sequentially in the order $[NCBPh_3]^-$ > $[NCBH_2NCBH_3]^-$ > $[NCS]^-$ ≈ $[NCSe]^-$.

Figure 5.6 The cyclic voltammogram (scan rate = $0.5Vs^{-1}$) of $[B_9H_{13}(NCBH_2NCBH_3)]^-$ in CH_3CN

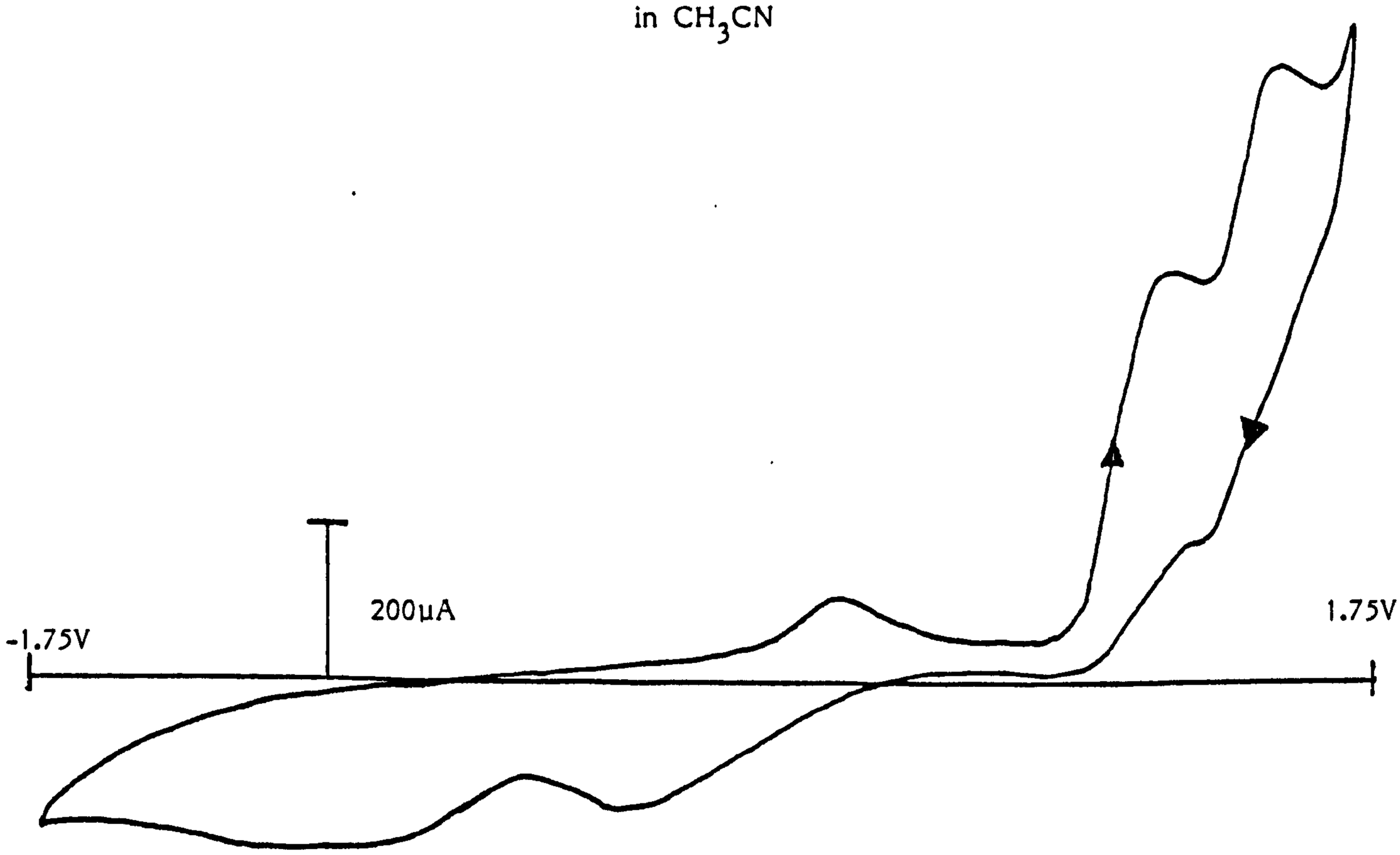

Figure 5.7 The cyclic a.c. voltammogram (scan rate = $0.05Vs^{-1}$) of $[B_9H_{13}(NCBH_2NCBH_3)]^-$ in CH_2Cl_2

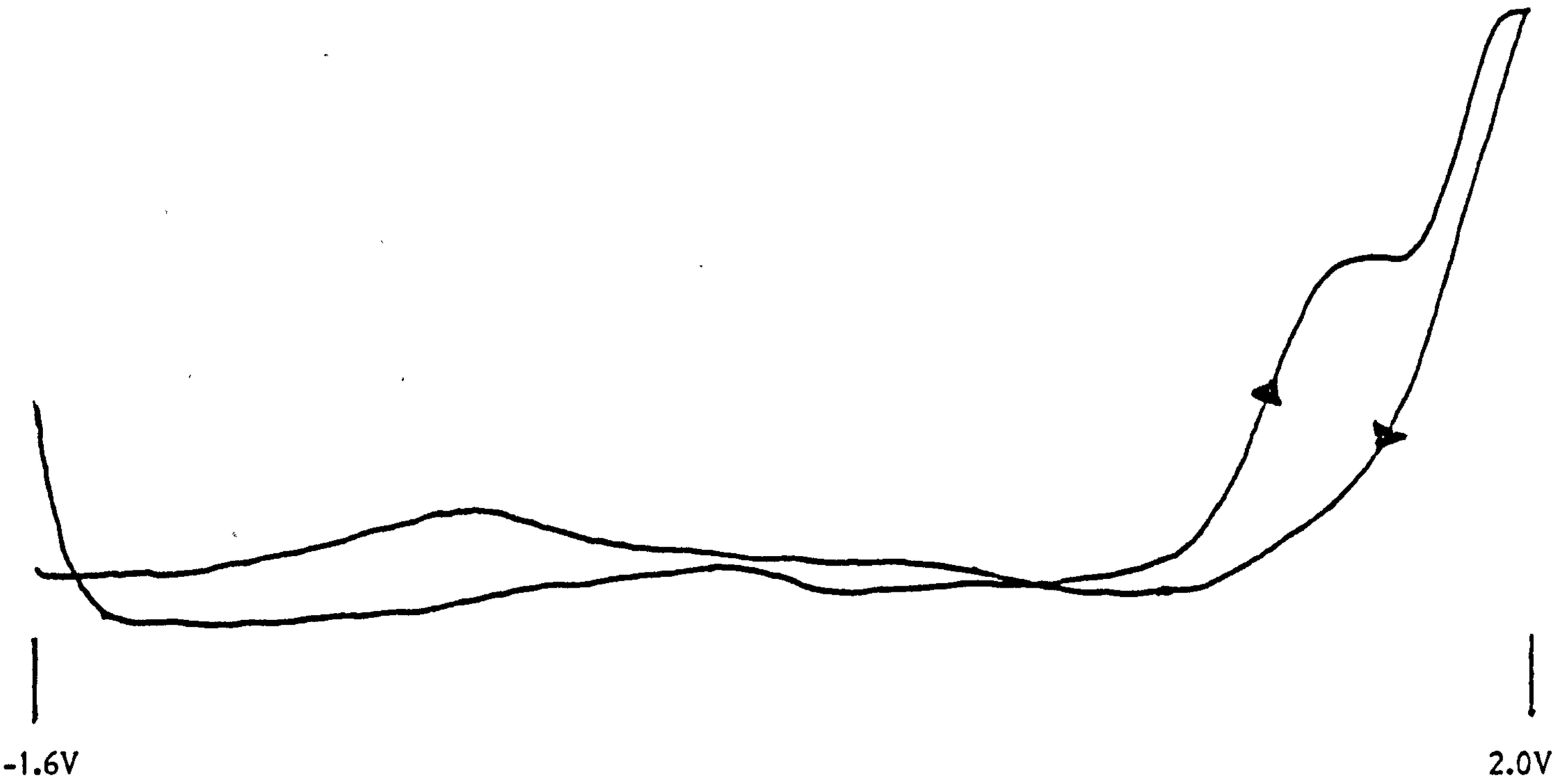

Controlled potential electrolysis of $[B_9H_{13}(NCBH_2NCBH_3)]^-$ in acetonitrile at platinum with supporting electrolyte added proceeded at a potential of 1.6V. The oxidative process involved three electrons and was complex. No products have yet been isolated from this oxidation.

(ii) Dichloromethane Solution

The cyclic voltammogram of $[(PPh_3)_2N][B_9H_{13}(NCBH_2NCBH_3)]$ in dichloromethane at a platinum electrode with $[NBu^n_4][BF_4]$ (0.1 mol dm^{-3}) supporting electrolyte added was poorly resolved, therefore no clearly defined oxidation or reduction waves were observed. However, using the more sensitive cyclic a.c.voltammetry(Figure 5.7) an irreversible oxidation wave was observed at Ep = 1.64V that was attributed to dichloromethane oxidation. Exhaustive controlled potential electrolysis on a dichloromethane solution of $[B_9H_{13}(NCBH_2NCBH_3)]^-$ at a platinum electrode with added $[NBu^n_4][BF_4]$ (0.1 mol dm^{-3}) supporting electrolyte proceeded at a potential of 1.5V. The overall oxidation involved 3.4 electrons, which indicated that the oxidation was complex. Purification of the anolyte solution gave a single major product that was examined by ^{11}B n.m.r. spectroscopy. The 115.5 MH_z ^{11}B n.m.r. spectrum (Table 5.2) of the oxidation product indicated the presence of a species that retained the C_s symmetry of the starting material. However in the oxidation product the quartet due to the $[BH_3]$ moiety of the substituent is no longer present. In addition to the singlet that appears at δ -27.13 p.p.m., due to coincidental overlap of the substituted boron atom B(4) and the $[BH_2]$ moiety of the substituent,

Table 5.2 ^{11}B N.M.R. Spectral Data for $[B_9H_{13}(NCBH_2NCBCl_3)]^-$

$\delta^{11}B$/p.p.m.	J_{B-H}/H_z	Assignment
17.11	-	7
4.78	130	1
-15.11	138	5,9
-20.21	138	6,8
-22.20 (s)	-	BCl_3
-27.13 (s)	-	4, BH_2
-38.81	138	2,3

s - singlet

Spectrum obtained at 115.5 MH_z in $CDCl_3$

there is a further singlet that appears at δ-22.20 p.p.m. of relative intensity one. It is proposed that in this case the solvent has undergone oxidation to produce chlorine radicals which subsequently replace the hydrogen atoms of the $[BH_3]$ moiety to produce $[B_9H_{13}(NCBH_2NCBCl_3)]^-$.

(d) $\underline{[B_9H_{13}(NCBH_2CN)B_9H_{13}]^-}$

The cyclic voltammogram of $[N(PPh_3)_2][B_9H_{13}(NCBH_2CN)B_9H_{13}]$ in acetonitrile with added $[NBu^n_4][BF_4]$(0.1 mol dm^{-3}) at a platinum electrode showed an irreversible oxidation wave at Ep = 1.3V. In addition, an irreversible reduction wave was observed at Ep = -1.06V. The cyclic a.c. voltammogram of $[B_9H_{13}(NCBH_2CN)B_9H_{13}]^-$ in acetonitrile at a platinum electrode with added supporting electrolyte (Figure 5.8) clearly showed an irreversible oxidation wave at Ep = 1.19V. When the substituent is $[(NCBH_2CN)B_9H_{13}]^-$, the anion is oxidatively more stable than for the $[NCBH_2NCBH_3]^-$ substituted anion but less stable than the $[NCBPh_3]^-$ substituted anion. Therefore, the series is $[NCBPh_3]^-$ > $[(NCBH_2CN)B_9H_{13}]^-$ > $[NCBH_2NCBH_3]^-$ > $[NCS]^-$ ≈ $[NCSe]^-$ reading from oxidatively most stable to oxidatively least stable.

The cyclic voltammogram of $[B_9H_{13}(NCBH_2CN)B_9H_{13}]^-$ in dichloromethane at a platinum electrode with added $[NBu^n_4][BF_4]$ (0.1 mol dm^{-3}) supporting electrolyte was uninformative. However, the cyclic a.c. voltammogram of $[B_9H_{13}(NCBH_2CN)B_9H_{13}]^-$ in dichloromethane showed an irreversible oxidation wave at Ep = 1.86V due to solvent oxidation.

Figure 5.8(a) The cyclic voltammogram (scan rate = $0.5Vs^{-1}$) and (b) the cyclic a.c. voltammogram (scan rate = $0.05Vs^{-1}$) of $[B_9H_{13}(NCBH_2CN)B_9H_{13}]^-$ in CH_3CN

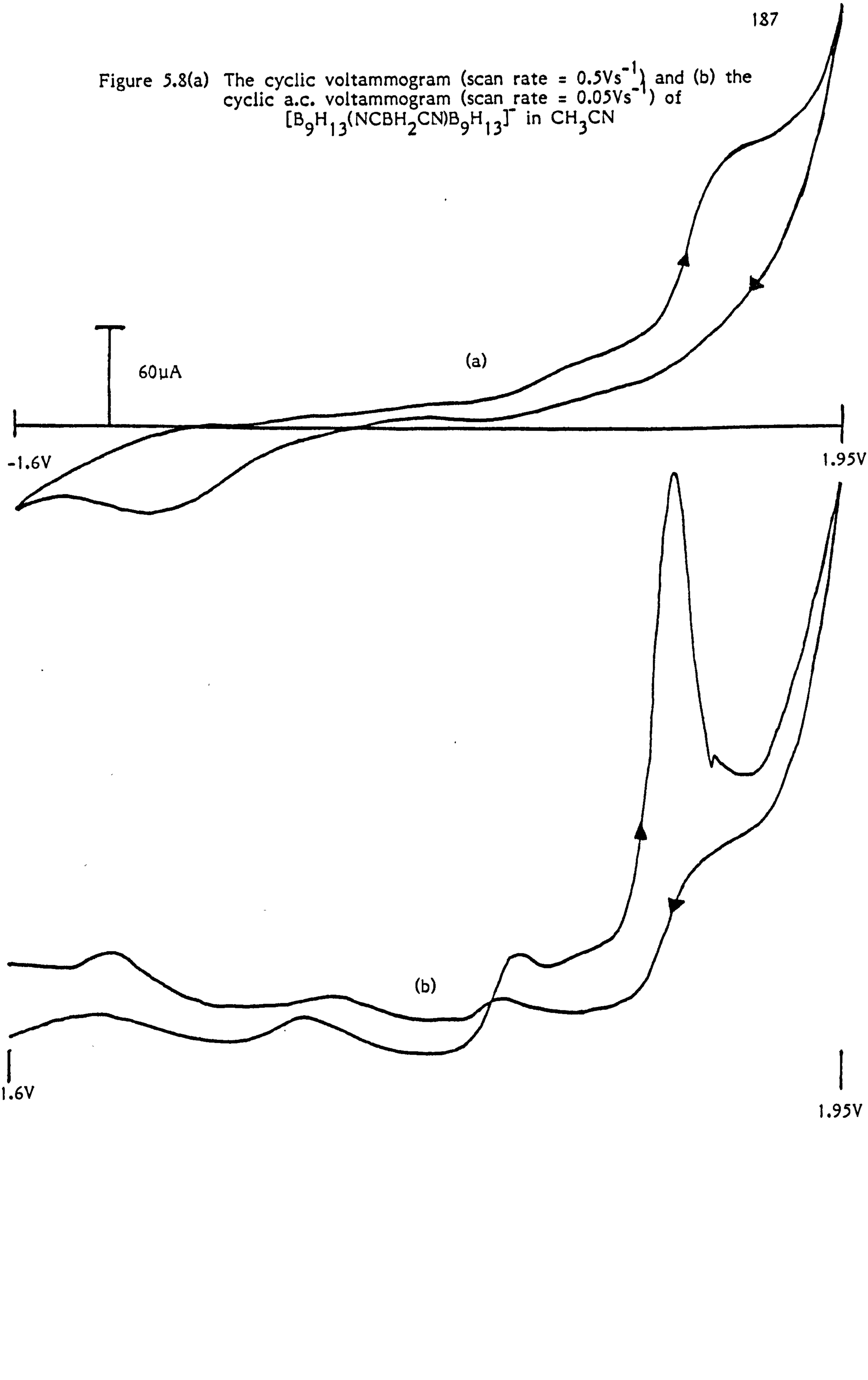

(e) $\underline{[B_9H_{13}(NCBH_2CN)]^-}$

(i) Acetonitrile Solution

The cyclic voltammogram of $[N(PPh_3)_2][B_9H_{13}(NCBH_2CN)]$ in acetonitrile at a platinum electrode with added $[NBu^n_4][BF_4]$(0.1 mol dm^{-3}) showed two irreversible oxidation waves at Ep = 1.40V and Ep = 1.64V. The cyclic a.c. voltammogram of $[B_9H_{13}(NCBH_2CN)]^-$ in acetonitrile also showed two irreversible oxidation waves at Ep = 1.25V and Ep = 1.43V. This data indicates that the $[B_9H_{13}(NCBH_2CN)]^-$ anion is the most stable to oxidation of those anions investigated. It has been found that in acetonitrile, using the $[N(PPh_3)_2]^+$ salt of the anion, that the oxidative stability of the anion is affected by the substituent. In all cases substitution resulted in enhanced oxidative stability compared to the parent ion, $[B_9H_{14}]^-$ The order of decreasing stability was found to be $[NCBH_2CN]^-$ > $[NCBPh_3]^-$ > $[(NCBH_2CN)B_9H_{13}]^-$ > $[NCBH_2NCBH_3]^-$ > $[NCS]^- \approx [NCSe]^-$. It is evident that addition of the electron rich cyano substituents increases the stability of the cluster.

Controlled potential electrolysis of $[B_9H_{13}(NCBH_2CN)]^-$ in acetonitrile at a platinum electrode with added $[NBu^n_4][BF_4]$(0.1 mol dm^{-3}) supporting electrolyte proceeded at a potential of 1.4V. The overall oxidative process involved two electrons. The 115.5 MH_z ^{11}B n.m.r. spectrum of the anolyte solution indicated that the major product was the $[B_9H_{13}(NCBH_2CN)]^-$ starting material.

(ii) Dichloromethane Solution

The cyclic voltammogram of $[N(PPh_3)_2][B_9H_{13}(NCBH_2CN)]$ in dichloromethane at a platinum electrode with added $[NBu^n_4][BF_4]$ (0.1 mol dm^{-3}) supporting electrolyte was poorly resolved and was uninformative. The cyclic a.c. voltammogram of $[B_9H_{13}(NCBH_2CN)]^-$ in dichloromethane showed an irreversible oxidation wave at Ep = 1.60V attributed to solvent oxidation.

Controlled potential electrolysis of $[B_9H_{13}(NCBH_2CN)]^-$ in dichloromethane at a platinum electrode with added supporting electrolyte proceeded at a potential of 1.6V. The electrolysis was exhaustive and involved 2.5 electrons. The 115.5 MH_z ^{11}B n.m.r. spectrum of the crude anolyte solution showed only the unreacted starting material.

5.2.2 Anodic Behaviour of Transition Metals in Solutions of $[B_9H_{13}(X)]^-$ (X=NCS,NCSe,$NCBPh_3$).

(a) Preliminary Cyclic Voltammetric Investigation

The approach used in Chapter 3 for the substituted octahydrotriborate (1-) derivatives was used to determine which transition metals would be suitable for preparative work. The first stage of the study involved recording the cyclic voltammograms of the various anions at an inert electrode, such as platinum, to determine the highest potential available for preparative work in the relevant solvent. For $[B_9H_{13}(NCS)]^-$ in acetonitrile this was found to be 0.76V by extrapolation to zero current of the approximately linear slopes of the increase (or decrease) in current in the early part of the anodic (or cathodic) scans. (Chapter 3). In dichloromethane the limiting potential for preparative work

that did not allow significant oxidation of $[B_9H_{13}(NCS)]^-$ was 1.22V. The limiting potentials for the anions $[B_9H_{13}(NCSe)]^-$ and $[B_9H_{13}(NCBPh_3)]^-$ in acetonitrile were 0.59V and 0.72V respectively.

After determining the highest potential available for preparative work, the behaviour of a range of transition metals in solutions of the various anions was determined by cyclic voltammetry in the absence of supporting electrolyte. Three basic types of behaviour were found. Type (a); a number of metals acted in the same way as platinum and allowed anodic oxidation of the anions, a significant current passed at potentials more anodic than that at which oxidation commenced. Type (b); some metals were essentially inert over the potential range studied, and exhibited very low anodic currents even at high positive potentials. These metals were unsuitable for both anodic oxidation and anodic dissolution experiments. Type (c); the remaining transition metals appeared to undergo anodic dissolution. The metals examined by cyclic voltammetry and the results obtained are summarised in Table 5.3.

(b) Preparative Dissolutions

(i) Dissolution of Copper in an Acetonitrile Solution of $[B_9H_{13}(NCS)]^-$

The anodic dissolution of copper in an acetonitrile solution of $[N(PPh_3)_2][B_9H_{13}(NCS)]$ with added Ph_3P ligand proceeded at a potential of 0.00V. Copper entered the solution as copper (I). The 115.5 MH_z ^{11}B n.m.r. spectrum of the crude anolyte solution in acetonitrile showed

Table 5.3 Anodic Properties of Metals in Solutions of $[B_9H_{13}(NCS)]^-$, $[B_9H_{13}(NCSe)]^-$ and $[B_9H_{13}(NCBPh_3)]^-$

	$[B_9H_{13}(NCS)]^{-*}$		$[B_9H_{13}(NCS)]^{-\ddagger}$		$[B_9H_{13}(NCSe)]^{-*}$		$[B_9H_{13}(NCBPh_3)]^{-*}$	
Metals	(1)	(2)	(1)	(2)	(1)	(2)	(1)	(2)
Ag	-	-	c	0.44(3)	c	0.52(3)	-	-
Al	-	-	a	0.48	a	0.54	c	0.00
Au	a	0.64	a	1.08	a	0.57	a	0.20
Cd	c	-0.64	a	0.68	c	-0.33	c	-0.20
Co	c	-0.04	b	0.84	c	0.49	c	0.50
Cu	c	-0.45	c	-0.38(3)	c	-0.54(3)	c	-0.62(3)
Fe	c	-0.34	c	0.00	-	-	c	-0.24
In	c	-0.46	-	-	-	-	c	-1.20
Mo	a	0.67	a	1.18	a	0.73	a	0.72
Nb	b	1.23	b	0.94	b	0.84	b	0.96
Ni	c	-0.01	a	0.84	c	0.49(3)	c	0.00
Pb	c	-0.31	c	1.18(3)	c	0.36	c	0.25
Pd	a	0.74	a	1.14	a	0.63	a	0.87
Pt	a	0.76	a	1.22	a	0.59	a	0.72
Sn	c	-0.34	-	-	c	0.78(3)	c	-1.60(3)
Ta	b	1.06	b	1.20	-	-	b	1.00
Ti	b	1.29	b	1.10	b	0.70	b	0.96
V	a	0.36	a	1.20	a	0.57	a	0.54
W	b	1.03	b	1.16	b	0.70	b	1.02
Zn	c	-0.92	c	0.48(3)	c	-0.44	c	-0.66
Zr	b	1.02	b	0.75	b	1.03	b	0.95

*Acetonitrile Solution

‡Dichloromethane Solution

(1) Type of Behaviour (see discussion).

(2) Potential at which oxidation commenced [Type (a)]; potential at which oxidation apparently commenced [Type (b)]; dissolution potential [Type (c)].

(3) Reduction peak on cathodic scan.

Acetonitrile solutions are referenced to $Ag/AgNO_3$(0.1 mol dm^{-3}). Dichloromethane solutions are referenced to $Ag/[N(PPh_3)_2]Cl$ (0.1 mol dm^{-3}).

only starting material $[B_9H_{13}(NCS)]^-$. However, removing the acetonitrile and then examining the 115.5 MH_z ^{11}B n.m.r. spectrum of the anolyte in $CDCl_3$ indicated the presence of the complex $Cu(PPh_3)_2(B_9H_{13}NCS)$. It is apparent that in acetonitrile dissociation occurred to produce the ion pair $[(CH_3CN)_2Cu(PPh_3)_2][B_9H_{13}(NCS)]$. When the less polar solvent, $CDCl_3$, is used dissociation does not occur.

(ii) Silver Dissolution in a Dichloromethane Solution of $[B_9H_{13}(NCS)]^-$

The anodic dissolution of silver in a dichloromethane solution of $[N(PPh_3)_2][B_9H_{13}(NCS)]$, with added Ph_3P ligand, proceeded at a potential of 0.75V. The silver entered the solution as silver (I). The product that was formed rapidly decomposed to give a black precipitate. The 115.5 MH_z ^{11}B n.m.r. spectrum of the anolyte in $CDCl_3$ was similar to that of $[B_9H_{13}(NCS)]^-$ the only difference being that the resonance due to B(6), B(8) at δ-18.0 p.p.m. and the resonance at δ-22.0 p.p.m. due to the substituted boron atom were broadened. The ^{11}B n.m.r. spectrum of the product showed a marked similarity to the spectrum of $Cu(PPh_3)_2(B_9H_{13}NCS)$, (Chapter 7). It is proposed that the product obtained from the dissolution is $Ag(PPh_3)_2(B_9H_{13}NCS)$.

5.3 Experimental

The details of all electrochemical equipment, cell design and reagents and solvents for electrochemistry are described in Chapter 8.$[N(PPh_3)_2][B_9H_{13}(NCS)]$ was prepared as previously described.[143] The preparation of $[N(PPh_3)_2][B_9H_{13}(NCSe)]$ and $[N(PPh_3)_2][B_9H_{13}(NCBPh_3)]$ has been described previously in Chapter 4.

Table 5.4 ^{11}B N.M.R. Spectral Data for $Cu(PPh_3)_2(B_9H_{13}NCS)$ and $Ag(PPh_3)_2(B_9H_{13}NCS)$

	$\delta^{11}B$/p.p.m.	J_{B-H}/Hz	Assignment
Copper complex	15.46	-	7
	4.52	127	1
	-15.64	134	5,9
	-19.12	-	6,8
	-24.05	-	4
	-38.45	142	2,3
Silver complex	15.00	-	7
	3.98	143	1
	-16.98	143	5,9
	-20.00	-	6,8
	-24.28	-	4
	-39.64	143	2,3

Spectra obtained at 115.5MHz in $CDCl_3$

5.3.1 Electrochemical Oxidation of $[B_9H_{13}(NCSe)]^-$ in Acetonitrile

$[N(PPh_3)_2][B_9H_{13}(NCSe)]$ (0.753g, 1 mmol) was dissolved in a solution of $[NBu^n_4][BF_4]$ (0.1 mol dm^{-3}) in acetonitrile (ca. 10 cm^3). The solution was introduced into the anodic compartment of the electrochemical cell. The cathodic compartment contained a solution of $[NBu^n_4][BF_4]$ (0.1 mol dm^{-3}) in acetonitrile (ca. 10cm^3). Both working and secondary electrodes were constructed of platinum foil. A potential of 1.0V was applied to the working electrode and 192C were passed (99.5% of the theoretical value for a $2e^-$ oxidation). Gas evolution was observed in the anode compartment and a brick red precipitate was formed. T.l.c. analysis on silica gel using 100% CH_2Cl_2 as eluant indicated the presence of a single major component (Rf = 0.65) and several minor components at lower Rf values. The anolyte was filtered and the solvent was removed under reduced pressure from the pale yellow solution to yield a yellow/white solid. Purification by liquid chromatography on silica gel using 100% CH_2Cl_2 as eluant gave the major product as a pale yellow solid. The solid was examined by ^{11}B n.m.r. spectroscopy at 115.5 MH_z.

5.3.2 Electrochemical Oxidation of $[B_9H_{13}(NCS)]^-$ in Dichloromethane

$[N(PPh_3)_2][B_9H_{13}(NCS)]$ (0.654g, 0.92 mmol) was dissolved in a solution of $[NBu^n_4][BF_4]$ (0.1 mol dm^{-3}) in dichloromethane (10 cm^3) and introduced into the anode compartment of the electrochemical cell. The cathode compartment contained $[NBu^n_4][BF_4]$ (0.1 mol dm^{-3}) in dichloromethane (or 40% aqueous HBF_4). Aqueous HBF_4 can only be used

in the cathodic compartment since it is immiscible with dichloromethane (Chapter 3). Both working and secondary electrodes were constructed from platinum foil or gauze. A potential of 1.5V was applied to the working electrode and the initially high current of 64mA decayed exponentially to 5.4mA after 179C had passed (i.e., the theoretical value for a $2e^-$ oxidation). The anolyte turned faint yellow during electrolysis and gas was evolved in the anodic and cathodic compartments. T.l.c. analysis of the anolyte solution on silica gel using 100% CH_2Cl_2 as eluant indicated the presence of a single major constituent (Rf = 0.52) and several minor constituents. Purification by liquid chromatography on silica gel using 100% CH_2Cl_2 as eluant gave the major product as a pale yellow solid. The product was investigated by ^{11}B n.m.r. spectroscopy.

5.3.3. Electrochemical Oxidation of $[B_9H_{13}(NCSe)]^-$ in Dichloromethane

The procedure followed in this electrolysis was identical to that followed in sect. 5.3.2. $[N(PPh_3)_2][B_9H_{13}(NCSe)]$ (0.72g, 0.95 mmol) underwent controlled potential electrolysis in dichloromethane at platinum with added $[NBu^n_4][BF_4]$ (0.5 mol dm^{-3}). A potential of 1.5V was applied to the working electrode and the initially high current (ca 120mA) decayed exponentially to 5mA after 137.5C had passed (i.e. the theoretical value for a $1.5e^-$ oxidation). T.l.c. analysis on silica gel using 100% CH_2Cl_2 as eluant indicated a major product (Rf = 0.65) and a minor product (Rf = 0.52). Purification by liquid chromatography on silica gel using 100% CH_2Cl_2 as eluant gave both

products as white solids. The major product was identified as $[B_9H_{13}(NCSe)]^-$ by comparison of its ^{11}B n.m.r. spectrum with that of an authentic sample. The minor product was not identified from its ^{11}B n.m.r. spectrum.

5.3.4 Electrochemical Oxidation of $[B_9H_{13}(NCBPh_3)]^-$ in Acetonitrile

$[N(PPh_3)_2][B_9H_{13}(NCBPh_3)]$ (0.56g, 0.61 mmol) was dissolved in a solution of $[NBu^n_4][BF_4]$ (0.1 mol dm^{-3}) in acetonitrile (10cm^3), and placed in the anode compartment of the electrochemical cell. The cathode compartment contained a solution of $[NBu^n_4][BF_4]$ (0.1 mol dm^{-3}) in acetonitrile (10 cm^3). Both working and secondary electrodes were made from platinum foil. A potential of 1.6V was applied to the working electrode and the initially high current of 38mA decayed exponentially to 3mA after 95.0C had passed (i.e. the theoretical value for a 1.6 e^- oxidation). T.l.c. analysis of the colourless anolyte solution on silica gel using 100% CH_2Cl_2 as eluant showed the presence of several components. Purification of the anolyte by liquid chromatography on silica gel using 100% CH_2Cl_2 as eluant gave the final product as a mixture. The final product has not been obtained pure enough to allow characterisation.

5.3.5 Electrochemical Oxidation of $[B_9H_{13}(NCBPh_3)]^-$ in Dichloromethane

$[N(PPh_3)_2][B_9H_{13}(NCBPh_3)]$ (2.41g, 2.63 mmol) was dissolved in a solution of $[NBu^n_4][BF_4]$ (0.4 mol dm^{-3}) in dichloromethane (20 cm^3)

and placed in the anode compartment of the electrochemical cell. The cathode compartment contained $[NBu_4][BF_4]$(0.4 mol dm^{-3}) in dichloromethane. Both working and secondary electrodes were constructed from platinum foil. A potential of 1.6V was applied to the working electrode and the initially high current of 120mA gradually decayed to 8mA after 509C had passed (i.e. the theoretical value for a $2e^-$ oxidation). T.l.c. analysis of the colourless anolyte solution on silica gel using 100% CH_2Cl_2 as eluant indicated the presence of two products (Rf = 0.58, 0.41). Purification of the crude anolyte by liquid chromatography on silica gel using 100% CH_2Cl_2 as eluant gave both products as white solids. The first product obtained from the electrolysis has not yet been characterised but the 115.5 MH_z ^{11}B n.m.r. spectrum of the second product indicated the presence of $[B_9H_{11}(NCBPh_3)]^-$.

5.3.6 Electrochemical Oxidation of $[B_9H_{13}(NCBH_2NCBH_3)]^-$ in Acetonitrile

$[N(PPh_3)_2][B_9H_{13}(NCBH_2NCBH_3)]$ (0.95g, 1.31 mmol) was dissolved in a solution of $[NBu^n_4][BF_4]$ (0.1 mol dm^{-3}) in acetonitrile (10 cm^3) and placed in the anode compartment of the electrochemical cell. $[NBu^n_4][BF_4]$ (0.1 mol dm^{-3}) in acetonitrile was placed in the cathode compartment of the electrochemical cell. Both working and secondary electrodes were made from platinum foil. A potential of 1.6V was applied to the working electrode and the initially high current of 129mA fell exponentially to 2.5mA when 381 C had passed (i.e. the theoretical value for a $3e^-$ oxidation. T.l.c. analysis of the anolyte

on silica gel using 100% CH_2Cl_2 as eluant showed the presence of several components. None of the components have yet been isolated for characterisation.

5.3.7 Electrochemical Oxidation of $[B_9H_{13}(NCBH_2NCBH_3)]^-$ in Dichloromethane

$[N(PPh_3)_2][B_9H_{13}(NCBH_2NCBH_3)]$ (0.54g, 0.75 mmol) was dissolved in a solution of $[NBu^n_4][BF_4]$ (0.1 mol dm^{-3}) in CH_2Cl_2 (10 cm^3) and introduced into the anode compartment of the electrochemical cell. The cathode compartment contained $[NBu^n_4][BF_4]$ (0.1 mol dm^{-3}) in CH_2Cl_2($10cm^3$). Both working and secondary electrodes were constructed from platinum foil. A potential of 1.5V was applied to the working electrode and the initial high current of 73mA remained constant throughout the electrolysis, indicating that the solvent was being oxidised. The anolyte remained colourless throughout the electrolysis and gas evolution was observed in both the anode and cathode compartments. The electrolysis was exhaustive and was continued until 246C had passed (i.e., the theoretical value for a $3.4e^-$ oxidation). T.l.c. analysis of the anolyte on silica gel using 100% CH_2Cl_2 as eluant indicated the presence of a single major component (Rf = 0.58) and several minor components at lower Rf values. Purification of the anolyte by liquid chromatography on silica gel using 100% CH_2Cl_2 as eluant gave the major component as a white solid. The 115.5 MH_z ^{11}B n.m.r. spectrum of the product indicated that it was $[B_9H_{13}(NCBH_2NCBCl_3)]^-$.

5.3.8 Electrochemical Oxidation of $[B_9H_{13}(NCBH_2CN)]^-$ in Acetonitrile

$[N(PPh_3)_2][B_9H_{13}(NCBH_2CN)]$ (0.85g, 1.20 mmol) was dissolved in a solution of $[NBu^n_4][BF_4]$ (0.1 mol dm^{-3}) in acetonitrile (10 cm^3) and introduced into the anode compartment of the electrochemical cell. The cathode compartment contained $[NBu^n_4][BF_4]$ (0.1 mol dm^{-3}) in acetonitrile (10 cm^3). Both working and secondary electrodes were constructed from platinum foil. A potential of 1.4V was applied to the working electrode and the initially high current of 109mA decayed exponentially to 3.2mA after 231C had passed (i.e., the theoretical value for a $2e^-$ oxidation). T.l.c. analysis of the anolyte on silica gel using 100% CH_2Cl_2 as eluant showed the presence of a single major component (Rf = 0.48). Purification of the anolyte by liquid chromatography on silica gel using 100% CH_2Cl_2 as eluant gave the major product as a white solid. ^{11}B n.m.r. spectroscopy identified the white solid as the starting material, $[B_9H_{13}(NCBH_2CN)]^-$.

5.3.9 Electrochemical Oxidation of $[B_9H_{13}(NCBH_2CN)]^-$ in Dichloromethane

$[N(PPh_3)_2][B_9H_{13}(NCBH_2CN)]$ (0.73g, 1.02 mmol) was dissolved in a solution of $[N(PPh_3)_2]Cl$ (0.1 mol dm^{-3}) in CH_2Cl_2 (10 cm^3) and placed in the anode compartment of the electrochemical cell. The cathode compartment contained $[N(PPh_3)_2]Cl$ (0.1 mol dm^{-3}) in CH_2Cl_2 (10 cm^3). Both working and secondary electrodes were constructed from platinum foil. A potential of 1.6V was applied to the working electrode and the initial high current of 35mA remained constant

throughout the electrolysis. The electrolysis was exhaustive and was continued until 246C had passed (i.e., the theoretical value for a $2.5e^-$ oxidation). T.l.c. analysis of the anolyte solution on silica gel using 100% CH_2Cl_2 as eluant indicated the presence of a single major component (Rf = 0.44). The ^{11}B n.m.r. spectrum of the crude anolyte in $CDCl_3$ showed that the major product was the starting material $[B_9H_{13}(NCBH_2CN)]^-$.

5.3.10 Anodic Dissolution of Copper in an Acetonitrile Solution of $[B_9H_{13}(NCS)]^-$

$[N(PPh_3)_2][B_9H_{13}(NCS)]$ (0.56g, 0.79 mmol) and Ph_3P (0.42g, 1.59 mmol) were dissolved in acetonitrile (10 cm^3) and introduced into the anode compartment of the electrochemical cell. The cathode compartment contained $[NBu^n_4][BF_4]$ (0.1 mol dm^{-3}) in acetonitrile (10 cm^3). The working and secondary electrodes were constructed from copper foil. A potential of 0.00V was applied to the working electrode and the initially high current of 64.2mA decayed slowly to 3mA after 154C had passed. The weight loss of the copper anode was 0.0496g (theoretical weight loss for Cu → Cu(I) is 0.0501g). T.l.c. analysis of the brown anolyte solution on silica gel using 100% CH_2Cl_2 as eluant indicated a single major component (Rf = 0.65). The acetonitrile was removed under reduced pressure to give a brown solid that was redissolved in dichloromethane and purified by liquid chromatography on silica gel using 100% CH_2Cl_2 as eluant. The major component was obtained as a brown solid. The 115.5 MH_z ^{11}B n.m.r. spectrum of the brown solid showed that it was the copper complex, $Cu(PPh_3)_2$

($B_9H_{13}NCS$), by comparison with the spectrum of a genuine sample, (Chapter 7)..

5.3.11 Anodic Dissolution of Silver in a Dichloromethane Solution of $[B_9H_{13}(NCS)]^-$

$[N(PPh_3)_2][B_9H_{13}(NCS)]$ (0.70g, 1 mmol) and Ph_3P (0.52g, 2 mmol) were dissolved in dichloromethane (ca. $10cm^3$) and placed in the anode compartment of the electrochemical cell. The cathode compartment contained $[NBu^n_4][BF_4]$ (0.1 mol dm^{-3}) in CH_2Cl_2. The working electrode was a silver wire and the secondary electrode was constructed from platinum foil. A potential of 0.75V was applied to the working electrode and the initial current of 38mA decayed slowly to 3mA after 96.4C had passed. As the reaction progressed the anolyte solution went dark and a black precipitate was formed. The weight loss of the silver anode was 0.1129g (the theoretical weight loss for $Ag \rightarrow Ag(I)$ is 0.1078g). T.l.c. analysis of the anolyte on silica gel using 100% CH_2Cl_2 as eluant indicated the presence of a single major constituent (Rf = 0.72). The anolyte was filtered and the solvent removed under reduced pressure to yield a white solid that rapidly decomposed. ^{11}B n.m.r. analysis of the solid in $CDCl_3$ indicated the complex, $Ag(PPh_3)_2(B_9H_{13}NCS)$.

CHAPTER SIX

STUDIES OF THE $[B_9H_{12}]^-$ ANION

6.1 Introduction

In this chapter the synthesis of $[N(PPh_3)_2][B_9H_{12}]$ is reported which has proved suitable for determination of the x-ray crystal and molecular structure. The ^{11}B n.m.r. spectrum of $[B_9H_{12}]^-$ is assigned unambiguously from the 2-D ^{11}B (COSY) n.m.r. spectrum. The ^1H and $^1H\{^{11}B$ C.W.$\}$ n.m.r. spectra together with a correlation for the proton chemical shifts with the boron positions are reported for the first time.* These data are shown to be entirely consistent with the crystallographically determined structure.

In addition it was found that in dichloromethane, $[N(PPh_3)_2][B_9H_{12}]$ underwent an addition reaction with HCl to give the <u>arachno</u> - $[B_9H_{13}(Cl)]^-$ anion, using $[NBu^n_4][B_9H_{12}]$ the product obtained from the reaction with HCl was <u>anti</u>-$B_{18}H_{22}$. The reaction of $[NBu^n_4][B_9H_{12}]$ with CF_3CO_2H in CH_2Cl_2 produces $B_{10}H_{14}$ and <u>anti</u>-$[B_{18}H_{21}]^-$. The electrochemical properties of the anion were also investigated.

6.2 Results and Discussion

It has been shown that the $[B_9H_{12}]^-$ anion can be prepared by degradation of <u>nido</u>-decaborane (14)[13] or by treatment of $B_9H_{13}L$ ($L=SMe_2$, SEt_2) with strong base.[66(b)] Several attempts have been made to establish the structure of the <u>nido</u>- $[B_9H_{12}]^-$ anion. However, x-ray diffraction studies [80] of the $[NMe_4]^+$ and $[NMe_2Et_2]^+$ salts of the

*During the course of this work some ^1H n.m.r. data on the compound was received from Professor N.N. Greenwood.[149]

$[B_9H_{12}]^-$ anion have been frustrated by orientational disorder problems, but did suggest that the ion was monomeric.

From ^{11}B n.m.r. data Todd et al[81,82] have suggested that the gross arrangement of the boron atoms in nido-$[B_9H_{12}]^-$ is similar to that found in arachno-$B_9H_{13}[NCCH_3]$[65] although the data were not sufficiently definitive for the unambiguous determination of the structure. This comparison of nido and arachno clusters with the same number of polyhedral atoms does have some merit in that a 9-debor-(1441) polyhedron is related to a 1,3-didebor-(12422) polyhedron by the formal breaking of only one connectivity. It has thus been assumed[150(a)] that $[B_9H_{12}]^-$ has the boron skeleton of its closo-parent, $[B_{10}H_{10}]^{2-}$[151] from which a high connectivity vertex is removed.

In the presence of $[N(PPh_3)_2][OCN]$, $B_9H_{13}[SMe_2]$ is deprotonated with loss of ligand to produce $[B_9H_{12}]^-$ cleanly as the $[N(PPh_3)_2]^+$ salt, the by-products were volatile or gave volatile hydrolysis products on work-up.

$$B_9H_{13}[SMe_2] + [OCN]^- \rightarrow [B_9H_{12}]^- + SMe_2 + HOCN \quad (6\text{-}1)$$

$$HOCN + H_2O \rightarrow CO_2 + NH_3 \quad (6\text{-}2)$$

The crystals of $[N(PPh_3)_2][B_9H_{12}]$ obtained from this reaction proved suitable for x-ray crystallographic analysis. The crystal structure (Figure 6.1) unambiguously identifies the polyhedral arrangement in the solid state as the expected nido-derivative obtained from the

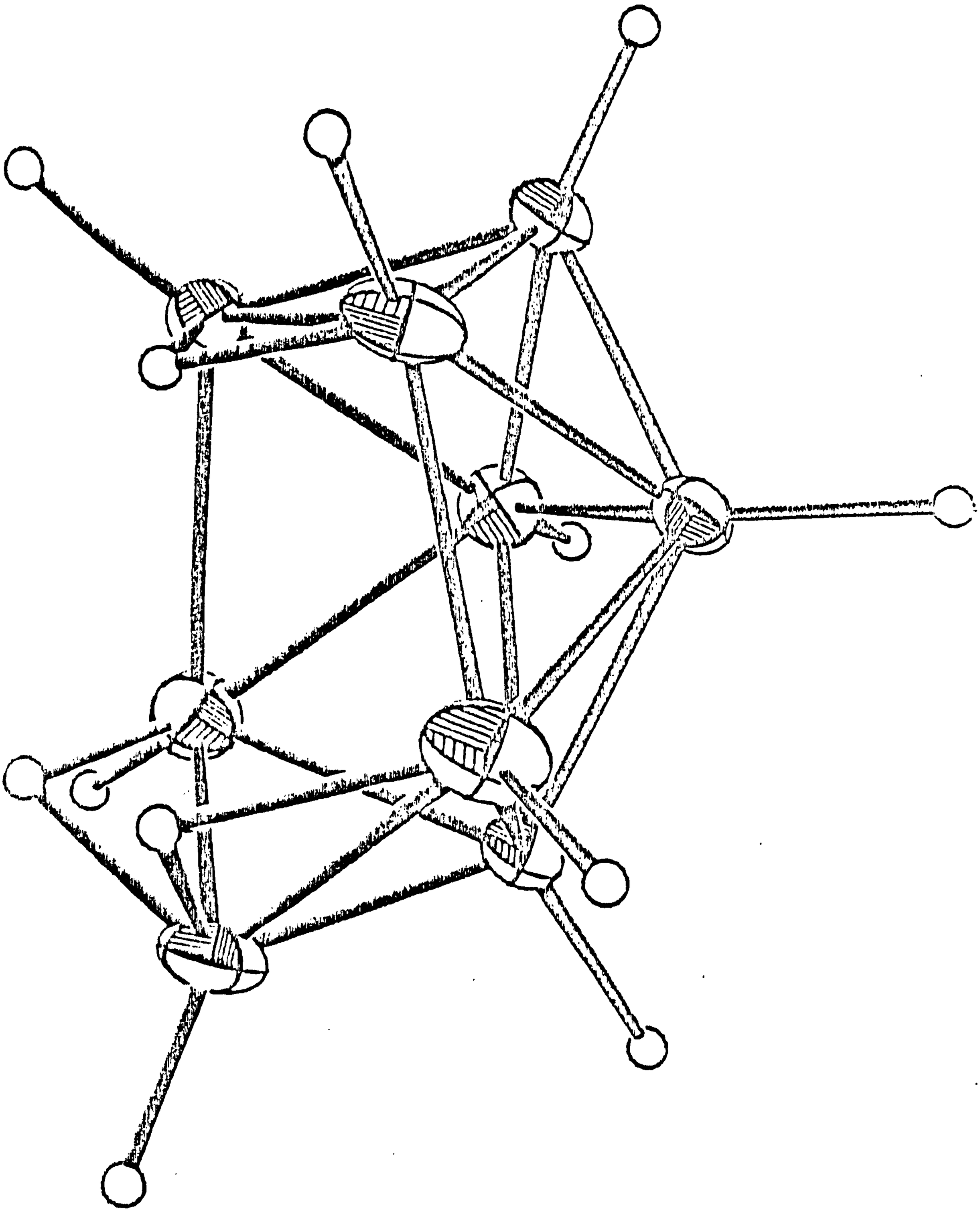

Figure 6.1 The crystal structure of $[B_9H_{12}]^-$

parent closo-$[B_{10}H_{10}]^{2-}$. The structure is that of a nido-9-vertex cage based on the parent bicapped square antiprism with one 5-connected vertex removed. The pentagonal open face is symmetrically bridged by three μ_2H atoms (two involving the lowest connected boron), conferring effective C_s symmetry upon the polyhedron. There are eleven skeletal electron pairs available for cluster bonding and therefore the polyhedral geometry is that predicted by empirical electron-counting rules.[152]

6.2.1 N.m.r. Discussion

The ^{11}Bn.m.r.spectrum(shown in Figure 6.2) of the $[B_9H_{12}]^-$ anion has not been interpreted previously, partly as a result of the unknown structure of the anion and partly as a result of the inadequate understanding of the variations of chemical shift with cage structure. Two-dimensional ^{11}B-^{11}B(COSY) n.m.r. has recently been shown[127,128,153] to be of substantial help in both the assignment of the spectra of boron cages of known structure and also in elucidating the structures of unknown compounds. The existence of ^{11}B-^{11}B couplings in the homonuclear 2-D spectra have been established through the observation of cross peaks (Chapter 1 page 53). The spin-spin ^{11}B-^{11}B coupling has been shown to be significant only between adjacent nuclei in boron clusters. In general, no correlation is observed between hydrogen bridged boron nuclei, which is in agreement with the theoretical prediction that the electron density in hydrogen bridged boron bonds is negligible along the B-B vector.[133] The 2-D ^{11}B-^{11}B (COSY) n.m.r. spectrum of $[B_9H_{12}]^-$ is presented in Figure 6.3. Correlations between

Figure 6.2 The 115.5 MH_z ^{11}B n.m.r. spectrum of $[B_9H_{12}]^-$

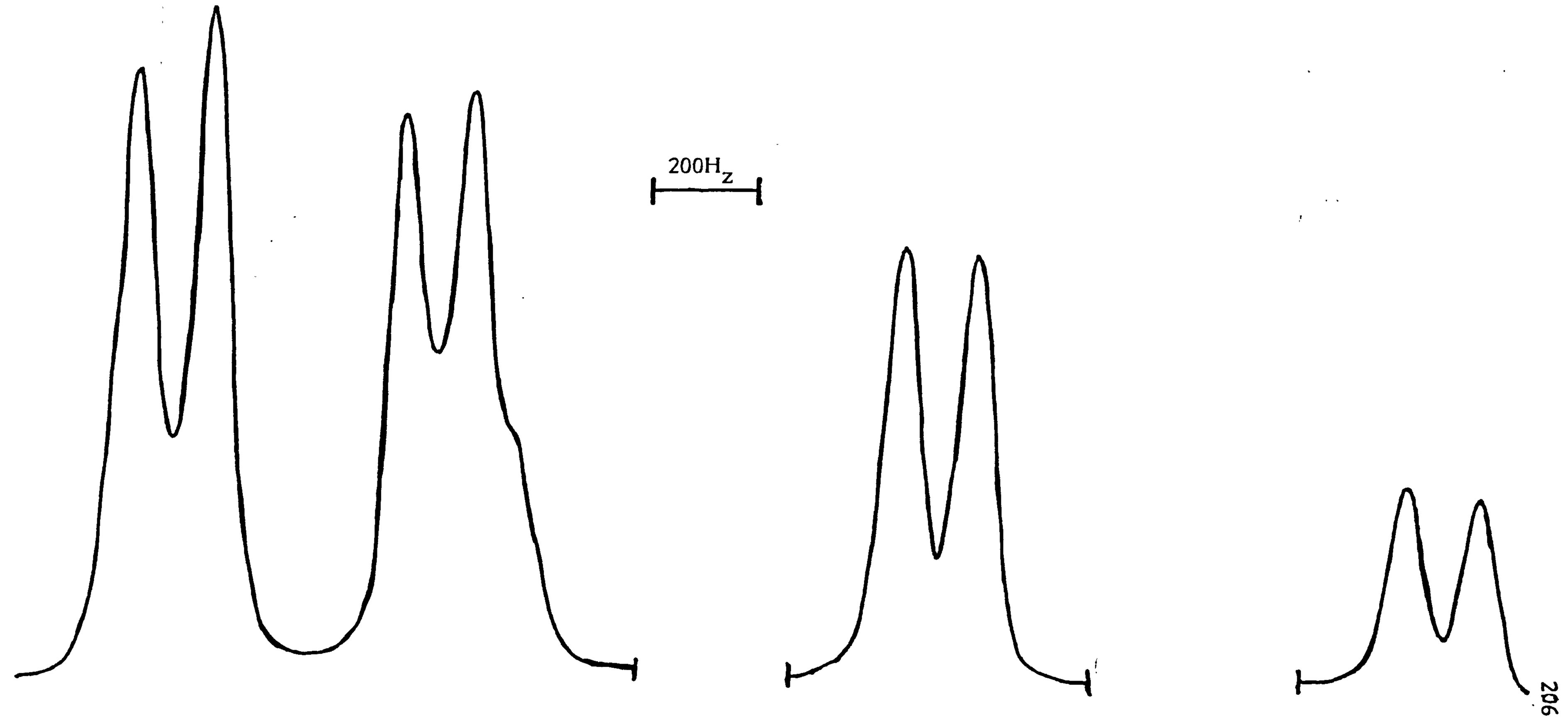

Figure 6.3 The 115.5 MH_z ^{11}B 2-D COSY spectrum of $[B_9H_{12}]^-$ in $CDCl_3$

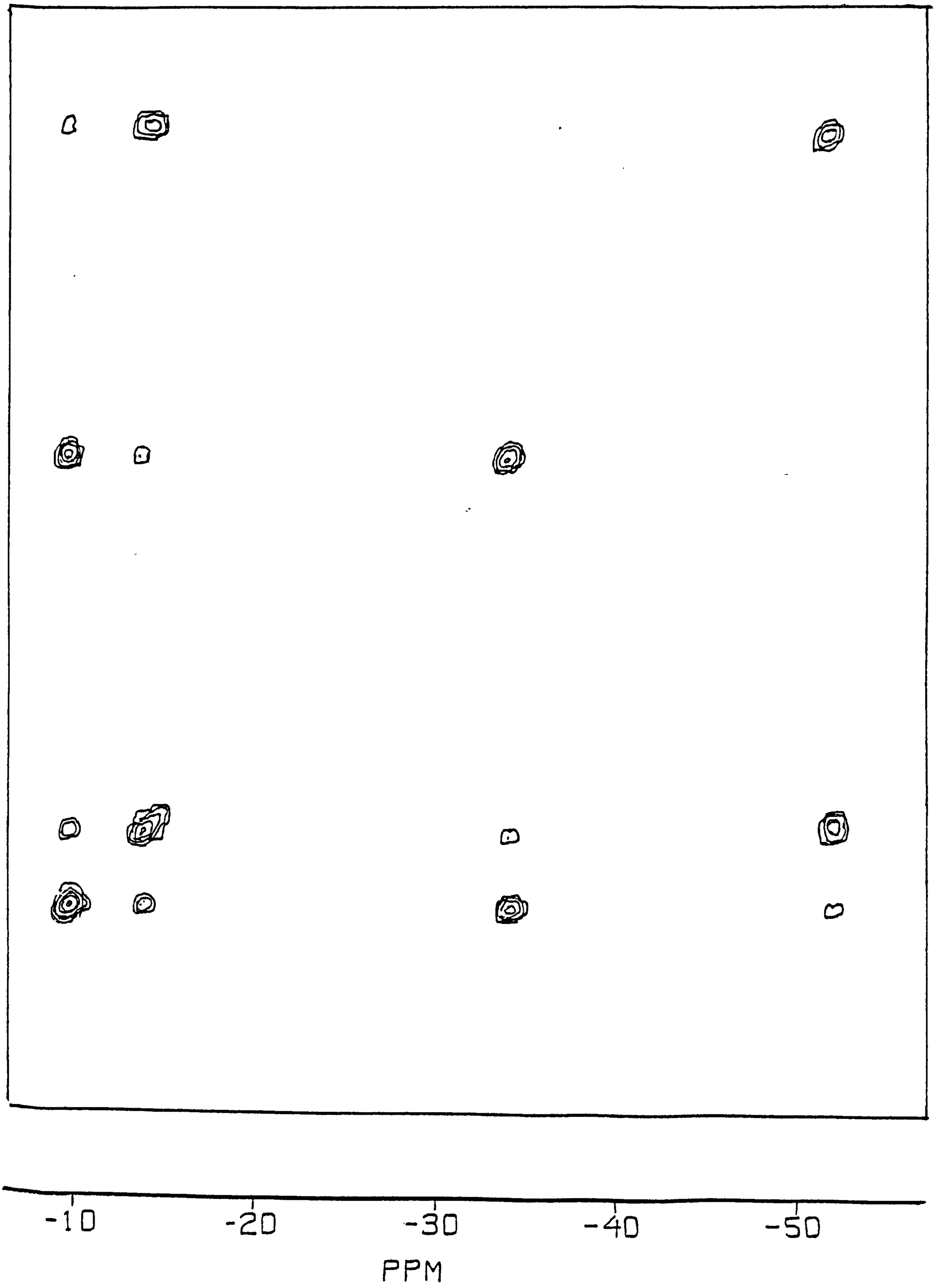

the chemical shifts of the ^{1}H resonances and the ^{11}B environments to which the protons are coupled have been obtained by examining the $^{1}H\{^{11}B$, broad band$\}$ and $^{1}H\{^{11}B$, C.W.$\}$ spectra. At room temperature the terminal hydrogen environments have been observed in the relative intensity ratio of 1:2:2:1:2:1 by successive single-frequency decoupling at the boron resonance frequencies corresponding to the chemical shifts of the boron environments from high frequency to low frequency, as indicated in Table 6.1. Greenwood and co-workers have reported similar shifts for most of the ^{1}H resonances but failed to resolve fully all the environments. *Bould* [149] found that upon lowering the temperature to -78°C the three fluxional bridge hydrogens that occurred as a single resonance at room temperature are resolved into two resonances. Of these two ^{1}H n.m.r. resonances the one of relative area 2 near δ -3.0p.p.m. was associated with the boron resonances near δ -10 p.p.m. and δ-14 p.p.m., the other ^{1}H resonance of relative area 1 at δ -7.2 p.p.m. was associated with the boron resonance near δ-34 p.p.m.

These low temperature decoupling experiments established that the unique bridge hydrogen (δ-7.2. p.p.m.) was coupled to the two boron atoms at δ -34.1 p.p.m.,and therefore identified these boron positions as B(2,5). Since some selective decoupling of the two bridge hydrogens at δ -3.0 p.p.m. occurred by irradiation at the ^{11}B frequency corresponding to δ -9.85 p.p.m. and either (or both) of δ -13.9 p.p.m. and δ -14.5 p.p.m., one of two possiblities was implied. Either (i) the resonance at δ -13.9 p.p.m. corresponded to B(6,8) and one of the

Table 6.1 Correlations Between Boron Atom Positions and ^{11}B and ^{1}H Parameters for $[B_9H_{12}]^-$

Position	1	6,8	3,4	10	2,5	7
$\delta^{11}B$ (ppm)	-9.85		-13.9	-14.5	-34.1	-51.9
Rel. Area	3		2	1	2	1
$\delta^{1}H$ (ppm) terminal	2.75	1.68	1.74	2.58	0.72	-0.92
Rel. Area	1	2	2	1	2	1
$\delta^{1}H$ (ppm) bridge			-2.98		-7.22	
Rel. Area			2		1	
^{11}B-^{11}B Couplings (A with B)	A		B	-	B	B
	B		A	-	B	-
	-		-	A	-	B
	B		B	-	A	-
	B		-	B	-	A

three resonances at δ -9.85 p.p.m. corresponded to B(10); or (ii) two of the resonances at δ -9.85 p.p.m. corresponded to B(6,8) and the resonance at δ -14.5 p.p.m. was due to B(10). In the first case, (i), the remaining two resonances at δ -9.85 p.p.m. must have been associated with B(3,4), in the second case, (ii), the resonances at δ -13.9 p.p.m. must have resulted from B(3,4). The ambiguity has been resolved by the couplings which are observed in the 2-D ^{11}B-^{11}B (COSY) spectrum.

Well pronounced coupling was observed between B(2,5) at δ -34.1 p.p.m., and the resonances at δ -9.85 p.p.m. and δ -13.94 p.p.m. corresponding to the directly bonded coupling of B(2,5) to both B(6,8) and B(3,4). Similarly the resonance at δ -13.94 p.p.m. showed coupling with the resonance at δ -9.85 p.p.m. and with B(2,5) at δ -34.1 p.p.m., confirming that the resonances at δ -13.94 p.p.m. and δ-9.85 p.p.m. arose from boron positions B(6,8) and B(3,4) respectively. Additional support for this assignment resulted from the observed coupling of the B(6,8) and B(1) resonance at δ -9.85 p.p.m. with the resonances due to B(2,5) and B(3,4) at δ -34.1 p.p.m. and δ -13.9 p.p.m. respectively, and with the resonance at δ-51.9 p.p.m., which is due to B(7) by elimination. In addition the resonance at δ -14.5 p.p.m. only exhibits a coupling with the resonance at δ -51.9 p.p.m. whereas the latter also couples with B(6,8) at δ -9.85 p.p.m. The resonances at δ -14.5 p.p.m. and δ-51.9 p.p.m. are therefore unambiguously established as boron atoms B(10) and B(7) respectively. The details of the correlation between the boron atom positions and ^{11}B shifts, ^{1}H shifts and ^{11}B - ^{11}B couplings are summarised in Table 6.1.

The observed 2-D ^{11}B - ^{11}B (COSY) couplings are in full accord with the stereochemical arrangement shown in Figure 6.1.

6.3 Electrochemistry of $[B_9H_{12}]^-$

6.3.1 Voltammetry and Coulometry

The electrochemical properties of $[B_9H_{12}]^-$ were found to be mechanistically complex and dependent on the conditions, notably the solvent, used. The cyclic d.c. voltammogram and the cyclic a.c. voltammogram of $[NBu^n_4IB_9H_{12}]$ in CH_3CN at Pt are presented in Figure 6.4. The oxidation wave in the cyclic voltammogram near 1.4V, whose degree of reversibility was not known, corresponded to a peak in the cyclic a.c. voltammogram near 1.1V whose superimposition of forward and reverse scans suggested an electrochemical process which was close to being reversible.[84] In addition, the weak reduction wave near -0.8V was not observed in scans which did not encompass the oxidation, indicating that the wave arose as a result of the reduction of an oxidation product.

Previous workers* in this laboratory have carried out constant potential coulometry at 0.86V using Pt electrodes. This resulted in the consumption of $1e^-$ per mol of $[B_9H_{12}]^-$. In CH_3CN the only identifiable soluble product was $B_9H_{13}[NCCH_3]$, a small quantity of insoluble material identified as $B_{18}H_{22}$ was also obtained.

*G.B. Jacobsen and C. Thompson

Figure 6.4(a) The cyclic voltammogram (scan rate = $0.5Vs^{-1}$) and (b) the cyclic a.c. voltammogram (scan rate = $0.05Vs^{-1}$) of $[B_9H_{12}]^-$ in CH_3CN.

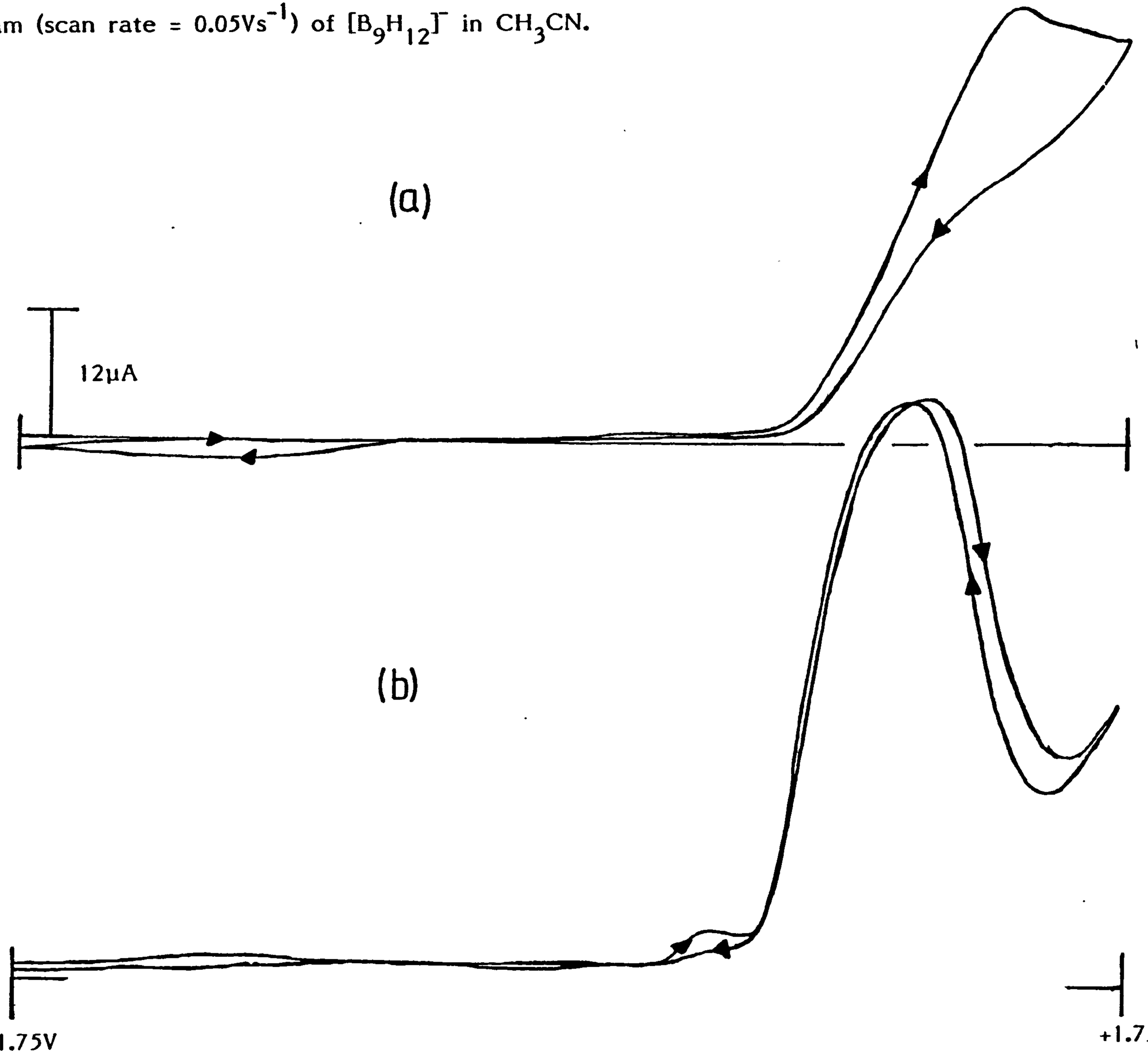

In the low-polarity solvents dichloromethane and 1,2-dichloroethane voltammetry indicated that the first oxidation wave of $[NBu^n_4IB_9H_{12}]$ was observed near 1.55V. In ethereal solvents (T.H.F., 1.2-dioxalane) no clearly defined oxidation wave was observed below 1.6V. Coulometric oxidation of $[NBu^n_4IB_9H_{12}]$ in CH_2Cl_2 at 1.2V corresponded to less than a $1e^-$ oxidation with the formation of anti-$[B_{18}H_{21}]^-$ and traces of $B_{10}H_{14}$. A related isomer-specific oxidation of $[B_9H_{12}]^-$ to anti-$[B_{18}H_{21}]^-$ was recently reported by Greenwood and co-workers[154] through the reaction of $[B_9H_{12}]^-$ with $[Os(CO)_3Cl_2]_2$.

6.3.2 Anodic Dissolution

The behaviour of metals as anodes in acetonitrile solutions of $[B_9H_{12}]^-$ may be characterised into three types, (as previously described in Chapter 3). Metals that underwent anodic dissolution, together with their effective dissolution potentials were: Zn(-0.78V), Cd(-0.64V), Cu(-0.40V), Pb(-0.25V,-0.05V)†, Ag(0.05V), Co(0.05V) and Al(0.30V, 0.76V)†. Those metals that did not dissolve but enabled anion oxidation to occur, together with their effective oxidation potentials were, Au(0.58V), Pd(0.67V), Pt(0.70V), Ni(0.70V), Mo(0.75V) and V(0.80V). Metals with low currents that were essentially inert or passive, with their effective potentials were: W(0.85V), Zr(0.86V), Ti(1.25V), Fe (1.29V), Nb(1.33V) and Ta(1.35V).

†Two potentials are quoted since the anodic and cathodic scans were

different with the dissolution current higher on the cathodic scan.

6.3.3 Preparative Dissolutions Involving $[B_9H_{12}]^-$

Using the results obtained from the cyclic voltammetric investigation described above, preparative experiments using lead and copper anodes were attempted.

(a) Lead Anode

The anodic dissolution of lead in an acetonitrile solution of $[B_9H_{12}]^-$ proceeded at a potential of 0.5V. Lead entered the solution as Pb(II). T.l.c. analysis of the anolyte solution indicated a mixture of four products. ^{11}B n.m.r. of the anolyte solution indicated several components that have not yet been characterised.

(b) Copper Anode

The anodic dissolution of copper in an acetonitrile solution of $[B_9H_{12}]^-$ proceeded at 0.0V. Copper entered the solution as Cu(I) which resulted in the solution turning red. The experiment was repeated with added phosphine ligand (Ph_3P) and the solution again turned red. In both cases (i.e., with and without added phosphine ligand), when the solvent was removed a brown residue was obtained. The brown solid obtained from the reaction which did not have added phosphine ligand was found to be insolu ble in dichloromethane. The only identifiable product from the ^{11}B n.m.r. spectrum of the anolyte was the starting material, $[B_9H_{12}]^-$. It is proposed that the copper enters the acetonitrile solution to form the solvated ion-pair $[(CH_3CN)_4Cu][B_9H_{12}]$. When

the acetonitrile is removed under vacuum a polymeric solid is formed, $[Cu.B_9H_{12}]_n$, that is insoluble in organic solvents. The product obtained from the dissolution in which phosphine ligand was added was soluble in dichloromethane, and has a ^{11}B n.m.r. spectrum identical to that obtained for the $Cu(PPh_3)_2(B_9H_{12})$ complex described in Chapter 7. It is proposed that, in this case, the copper again forms an ion-pair, $[(Ph_3P)_2Cu(CH_3CN)_2][B_9H_{12}]$, when it enters the acetonitrile solution. When the acetonitrile is removed at low pressure the complex $Cu(PPh_3)_2(B_9H_{12})$ is obtained.

6.4 Chemical Reactions of $[B_9H_{12}]^-$

Previously $[B_9H_{12}]^-$ has been shown to react with HCl in ethereal media to give $B_9H_{13}[OR_2]$ and in diethylsulphide to give $B_9H_{13}[SEt_2]$.[64] It has been found that the reaction of protonic acids with $[B_9H_{12}]^-$ depends on both the acid (e.g., HCl or CF_3CO_2H) and the counter cation (e.g., $[NBu^n_4]^+$ or $[N(PPh_3)_2]^+$.

The reaction of HCl in the non-coordinating solvent dichloromethane, (i.e.,in the absence of donor ligands) with $[N(PPh_3)_2][B_9H_{12}]$ resulted in the addition product, $[N(PPh_3)_2][B_9H_{13}(Cl)]$, being formed. The ^{11}B n.m.r. and the $^1H-\{B,C.W\}$ n.m.r. spectra (Table 6.2) indicated that this molecule was fluxional at room temperature and is substituted at the B(4) position, this is consistent with the data found previously for $[B_9H_{13}(NCS)]^-$ and related systems.[143] The reaction of HCl with $[NBu^n_4][B_9H_{12}]$ in CH_2Cl_2 produced anti-$B_{18}H_{22}$, the same reaction

Table 6.2 The ^{11}B and $^{1}H\{^{11}B.C.W.\}$ n.m.r spectra of $[B_9H_{13}(Cl)]^-$ in $CDCl_3$

Assignment	$\delta^{11}B$/p.p.m.	$\delta^{1}H$/p.p.m.	J_{B-H}/H_z
7	13.04	3.72(1)	137
1	4.59	3.20(1)	134
4	-12.91	-	-
5,9,6,8	-16.41	1.99(2),1.68(2)	137
2,3	-37.23	0.38(2)	142
bridge protons		-1.13(5)	
$[N(PPh_3)_2]^+$		7.50(30)	

Figures in parenthesis represent relative intensities.

^{11}B n.m.r. spectrum was obtained at $115.5MH_z$

^{1}H n.m.r. spectra were obtained at $360MH_z$

using CF_3CO_2H produced <u>anti</u>-$[B_{18}H_{21}]^-$ and small quantities of $B_{10}H_{14}$.

As previously reported[64] it is thought that the reaction of $[B_9H_{12}]^-$ with protonic acids proceeds via the reactive intermediate $[B_9H_{13}]$, which is presumably formed by protonation of a B-B bond, [e.g. B(2)-B(6) or B(5)-B(8)]. Attack of the ligand (OR_2,SEt_2 or Cl^-) at B(2) with cleavage of the B(2)-B(5) hydrogen bridged bond results in opening of the structure and conversion from the <u>nido</u> to the <u>arachno</u> species. As a result of the fluxional nature of the bridge and potential <u>endo</u>-hydrogens, the observed products are $B_9H_{13}L$ or $[B_9H_{13}(Cl)]^-$ when a suitable electron pair donor is present. In the absence of electron pair donors the products obtained are, <u>anti</u>-$B_{18}H_{22}$, <u>anti</u>-$[B_{18}H_{21}]^-$ and $B_{10}H_{14}$. The reaction of HCl with $[NBu^n_4]B_9H_{12}]$ in dichloromethane produces <u>anti</u>-$B_{18}H_{22}$ rather than the addition product, $[B_9H_{13}(Cl)]^-$. It is proposed that the reactive $[B_9H_{13}]$ is formed and undergoes dimerisation with loss of hydrogen to produce <u>anti</u>-$B_{18}H_{22}$.

$$2[B_9H_{13}] \rightarrow \underline{\text{anti}}\text{-}B_{18}H_{22} + 2H_2 \qquad (6\text{-}3)$$

In addition, the disproportionation of two $[B_9H_{13}]$ fragments may produce B_8H_{12} and $B_{10}H_{14}$. This may be expressed thus:

$$2[B_9H_{13}] \rightarrow B_8H_{12} + B_{10}H_{14} \qquad (6\text{-}4)$$

However, in the reaction with HCl, neither of these products are observed. The formation of <u>anti</u>-$B_{18}H_{22}$ rather than $[B_9H_{13}(Cl)]^-$ in the HCl reaction when $[NBu^n_4]^+$ is used rather than $[N(PPh_3)_2]^+$ may reflect the ease of formation of $[NBu^n_4]Cl$ in which the $[Cl]^-$

ion is more extensively involved in ion pair or ion aggregate formation than in $[N(PPh_3)_2]Cl$. If $[NBu^n_4]Cl$ is readily formed in the reaction then the only available electron pair donor is being removed, resulting in $[B_9H_{13}]$ dimerisation to form the anti - $B_{18}H_{22}$.

In the reaction with CF_3CO_2H the products obtained are $B_{10}H_{14}$ and anti-$[B_{18}H_{21}]^-$. The formation of $B_{10}H_{14}$ indicated that the disproportionation reaction, occurred although no B_8H_{12} was isolated. It is proposed that anti-$[B_{18}H_{21}]^-$ is formed by the reaction of $[B_9H_{13}]$ with $[B_9H_{12}]^-$ with hydrogen elimination thus:

$$[B_9H_{13}] + [B_9H_{12}]^- \rightarrow \text{anti-}[B_{18}H_{21}]^- + 2H_2 \qquad (6\text{-}5)$$

The $[B_9H_{13}]$ molecule has been predicted by Lipscomb to exist in an environment free of electron pair donors.[155] The ^{11}B n.m.r. and ^1H $\{^{11}B.C.W.\}$ spectra for anti-$[B_{18}H_{21}]^-$ are listed in Table 6.3 and are in agreement with the ^{11}B n.m.r. spectra previously obtained[156] for $[N(CH_3)_4][B_{18}H_{21}]$ at 80.2 MH_z. Attempts to assign the ^{11}B n.m.r. spectrum using the ^{11}B 2-D (COSY) technique were unsuccessful since only a few of the possible correlations were observed (Table 6.3).

6.5 Experimental

6.5.1 Reagents

Decaborane (14) was purchased from the Callery Chemical Company and was sublimed before use. $B_9H_{13}[SMe_2]$ was prepared from $B_{10}H_{14}$ via degradation of $B_{10}H_{12}[SMe_2]_2$ with CH_3OH.[66(b)] $[N(PPh_3)_2][OCN]$ was obtained by treating $[N(PPh_3)_2]Cl$ with an equimolar quantity

Table 6.3 $^{11}B,^{1}H\{^{11}B, C.W.\}$ Correlated [a] and ^{11}B COSY N.M.R Spectra of anti-$[B_{18}H_{21}]^-$

^{11}B δ(ppm)[b]	Rel. int.	COSY coupling[c]	^{1}H δ(ppm)[d]	Rel. int.	Comments
11.50(S)	1		-		
14.06	1	A B D	3.53	1	
10.19	1		3.76	1	
5.72	1	E	3.00	1	
4.04	1		3.56	1	
0.87(S)	1	G	-		
-0.37	1	H	2.97	1	
-3.73	2	D F	2.97	1	
			2.67	1	
-7.12	1	C	2.57	1	
-9.89	2		2.14	1	
			2.48	1	
-12.70	2		2.66	1	
			1.88	1	
-23.33	1	E	-0.40	1	
-28.46	1	B F G	-0.89	1	
-38.44	1	A	0.20	1	
-40.39	1	C H	0.21	1	
			-1.04		Bridges
			-1.60		
			-1.93		
			-3.34		
			-3.94		

[a] ^{11}B and ^{1}H data correlated from specific frequency decoupling experiments

[b] Reference BF_3OEt_2; all resonances are doublets except those labelled (S)

[c] Borons which give rise to off-diagonal maxima are identified by a common letter

[d] Reference TMS

of Na[OCN] in water and extracting the product by phase transfer to CH_2Cl_2. The product was recrystallised from CH_2Cl_2/Et_2O to give white needle-like crystals. The solvents and reagents used were dried by standard procedures.

6.5.2 Synthesis of $[NBu^n_4][B_9H_{12}]$

The $[NBu^n_4]^+$ and $[NMe^n_4]^+$ salts of $[B_9H_{12}]^-$ were obtained by the literature method.[13,66(b)]

6.5.3 Synthesis of $[N(PPh_3)_2][B_9H_{12}]$

$B_9H_{13}[SMe_2]$ (0.43g,2.5 mmol) and $[N(PPh_3)_2][OCN]$ (1.51g, 2.6 mmol) were placed in a 250 cm^3 three-necked round-bottomed flask fitted with a reflux condenser and flushed with dry nitrogen. Dry 1,2-dichloroethane was introduced and the clear solution was refluxed for 1.5hr., after which time a white precipitate, identified as $B(OH)_3$, was formed. Thin-layer chromatography of the filtered solution on silica gel using 100% CH_2Cl_2 as eluant indicated the presence of a single major fraction (Rf = 0.32). The solvent was removed under reduced pressure and the resulting white solid was redissolved in the minimum quantity of CH_2Cl_2 and purified by chromatography on silica gel using 100% CH_2Cl_2 as eluant. The major fraction was collected and the solvent was removed under reduced pressure to give a white crystalline solid. Recrystallisation from CH_2Cl_2/n-pentane yielded colourless, needle-like crystals suitable for x-ray crystallography (yield; 0.486g, 30%) (Found: C, 66.6; H, 6.5; N 2.2. Calculated for $C_{36}H_{42}B_9NP_2$: C,66.7; H,6.5; N 2.2%).

Alternatively $[N(PPh_3)_2I B_9H_{12}]$ can be prepared quickly in high yield by the dropwise addition of an ethanolic solution of $[N(PPh_3)_2IOCN]$, in excess, to a stirred solution of $B_9H_{13}[SMe_2]$ (0.69g, 4.0 mmol) in hot ethanol. A crystalline white precipitate was formed which was filtered and recrystallised from CH_2Cl_2/Et_2O. The colourless crystals were identical to those obtained previously, (yield; 2.07g, 80%).

6.5.4 Synthesis of $[N(PPh_3)_2IB_9H_{13}(Cl)]$

A 100cm³ round-bottomed flask fitted with a stopcock adaptor was charged with $[N(PPh_3)_2IB_9H_{12}]$ (0.53g, 0.82 mmol) and evacuated. Degassed CH_2Cl_2 was condensed in under vacuum and the mixture was warmed to room temperature until all the $[N(PPh_3)_2IB_9H_{12}]$ had dissolved. The solution was cooled to -196°C and gaseous HCl (0.30g, 0.83 mmol) was condensed in and the mixture was again warmed to room temperature. After stirring for 3 hr. under vacuum, the solvent was removed from the clear solution to yield a white solid. T.l.c. analysis on silica gel using 100% CH_2Cl_2 as eluant indicated a single major product (Rf = 0.47). Purification by chromatography on silica gel using CH_2Cl_2 as eluant and recrystallisation from CH_2Cl_2/ /n-hexane yields colourless crystals (0.2g, 34%) which were identified as $[N(PPh_3)_2IB_9H_{13}Cl)]$ by ^{11}B and ^{1}H n.m.r.

6.5.5 Synthesis of $[NBu^n_4IB_{18}H_{21}]$

$[NBu^n_4IB_9H_{12}]$ (1.0g, 3 mmol) was placed in a 100cm³ three-necked round-bottomed flask that was flushed with dry nitrogen. Dried, degassed

CH_2Cl_2 (ca.30cm³) was added. To the stirred clear solution an excess of CF_3CO_2H was added dropwise. On addition there was severe gas evolution and the solution went pale yellow. After stirring for 1 hr. t.l.c. analysis on silica gel using 100% CH_2Cl_2 as eluant indicated one minor product (Rf = 0.77), and one major product, (Rf = 0.48). The solvent was removed under reduced pressure to yield a yellow /white solid. Purification by chromatography on silica gel using 100% CH_2Cl_2 as eluant yields the minor fraction as a white solid and the major fraction as a yellow solid, these fractions are identified by ^{11}B and ^{1}H n.m.r. as $B_{10}H_{14}$ and anti-$[NBu^n_4][B_{18}H_{21}]$ (yield; 0.46g, 33.4%) respectively.

6.5.6 Synthesis of anti-$B_{18}H_{22}$

$[NBu^n_4][B_9H_{12}]$ (2.16g, 6.14 mmol) was placed in a 100cm³ round-bottomed flask fitted with a stopcock adaptor. Degassed CH_2Cl_2 (ca.30cm³) was condensed into the flask under vacuum and the mixture was warmed to room temperature until all the $[NBu^n_4][B_9H_{12}]$ had dissolved. The temperature was lowered to -196°C and gaseous HCl (0.37g, 10.2 mmol) was condensed into the flask. The system was warmed to room temperature and stirred for 3 hr., t.l.c. analysis on silica gel using 100% CH_2Cl_2 as eluant indicated a single major fraction (Rf = 0.8). The solvent was removed under reduced pressure to yield a colourless oil. Purification by chromatography on silica gel using 100% CH_2Cl_2 as eluant yields the major fraction as a yellow solid (yield; 0.75g, 56.5%) identified as anti-$B_{18}H_{22}$ by comparison of its ^{11}B n.m.r. spectrum with that of an authentic sample.

6.5.7 Anodic Dissolution of Lead in an Acetonitrile Solution of $[B_9H_{12}]^-$

$[NBu^n_4IB_9H_{12}]$ (0.13g, 0.2 mmol) was dissolved in acetonitrile (ca. 10cm^3) and introduced into the anode compartment of the electrochemical cell. The cathode compartment contained a solution of $[NBu^n_4IBF_4]$ (0.1 mol dm^{-3}) in acetonitrile (ca.20cm^3). The working electrode was a high area lead anode and the secondary electrode was platinum foil. A potential of 0.5V was applied to the working electrode. The current rose to a value of 23mA and decayed exponentially to 6mA after 19.8C had passed. The weight loss of the lead electrode was 0.0182g (theoretical weight loss for $Pb \rightarrow Pb^{2+}$ is 0.0212g). T.l.c. analysis on silica gel using 100% CH_2Cl_2 as eluant indicated a mixture of four components (Rf = 0.64, 0.53, 0.43, 0.18). The ^{11}B n.m.r. spectrum of the yellow anolyte solution was obtained but was uninformative.

6.5.8 Anodic Dissolution of Copper in an Acetonitrile Solution of $[N(PPh_3)_2IB_9H_{12}]$

$[N(PPh_3)_2IB_9H_{12}]$(0.16g, 0.24 mmol) in acetonitrile (ca. 10cm^3) was introduced into the anode compartment of the electrochemical cell. A solution of $[NBu^n_4IBF_4]$ (0.1 mol dm^{-3}) in acetonitrile (ca. 10cm^3) was used as supporting electrolyte in the cathode compartment. The working and secondary electrodes were both pieces of copper foil. A potential of 0.0V was applied to the working electrode. The initial current of 28mA decayed exponentially to 3mA after 23.7C had passed, (i.e., the theoretical number of Coulombs required for

the oxidation Cu → Cu^+). The weight loss of the copper working electrode was 0.0157g (theoretical weight loss for Cu → Cu^+ is 0.0156g). The secondary electrode did not gain weight therefore the Cu^+ ions that were deposited into the anolyte reacted with the $[B_9H_{12}]^-$ anion. Initially the solution was yellow but turned deep red when 8.0C had passed. T.l.c. analysis of the anolyte on silica gel using 5%CH_3CN/95% CH_2Cl_2 as eluant indicated two major components, (Rf = 0.40, 0.18), and one minor component, (Rf = 0.53). The solvent was removed under reduced pressure to yield a brown solid that was insoluable in CH_2Cl_2 making purification by chromatography on silica gel impractical. The ^{11}B n.m.r. spectrum of the anolyte indicated that the major component was the anion, $[B_9H_{12}]^-$.

6.5.9 Anodic Dissolution of Copper in an Acetonitrile Solution of $[B_9H_{12}]^-$ With Added Ph_3P Ligand

$[N(PPh_3)_2][B_9H_{12}]$ (0.21g, 0.33 mmol) and two equivalents of Ph_3P (0.17g, 0.66 mmol) in acetonitrile (ca. $10cm^3$), were introduced into the anode compartment of the electrochemical cell. The cathode compartment contained a solution of $[NBu^n_4][BF_4]$ (0.1 mol dm^{-3}) in acetonitrile. The working and secondary electrodes were pieces of copper foil. A potential of 0.0V was applied to the working electrode. The initial current of 36mA decayed exponentially to 3mA after 32.1C had passed. The weight loss of the copper working electrode was 0.0212g (theoretical weight loss for Cu → Cu^+ is 0.0211g), the secondary electrode did not gain weight. T.l.c. analysis of the anolyte on silica gel using 100% CH_2Cl_2 as eluant indicated a single major

component (Rf = 0.81). The solvent was removed under reduced pressure to yield a brown solid that was purified by chromatography on silica gel using 100% CH_2Cl_2 as eluant. The ^{11}B n.m.r. spectrum of the product at 115.5MH_z is identical to the ^{11}B n.m.r. spectrum of the $Cu(PPh_3)_2(B_9H_{12})$ complex obtained from the reaction of $[N(PPh_3)_2IB_9H_{12}]$ and $Cu(PPh_3)_2BH_4$ described in Chapter 7.

CHAPTER SEVEN

METALLABORANES DERIVED FROM SUBSTITUTED DERIVATIVES OF $[B_3H_8]^-$ AND $[B_9H_{14}]^-$

7.1 Copper Metallaboranes Derived from Substituted Derivatives of $[B_9H_{14}]^-$

7.1.1 Introduction

Studies of metallaboranes derived from Cu(I) borane anions have shown that in general the metal centre achieves four coordination in covalent complexes. The various types of metal-boron interaction are exemplified by the metalla complexes of the tetrahydroborate (1-) anion, $[BH_4]^-$. The tetrahydroborate (1-) anion in metallaborane complexes may act as an isolated anion (I),[157] or interact with a metal centre through monodentate (II),[158] bidentate (III)[157] or tridentate (IV)[157] hydrogen bridges. The tetrahydroborate (1-) anion may also act as a bridging ligand between two metal centres, (V).[157,

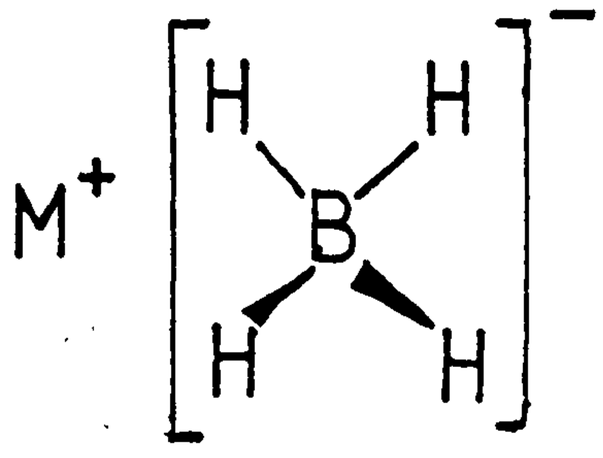

I

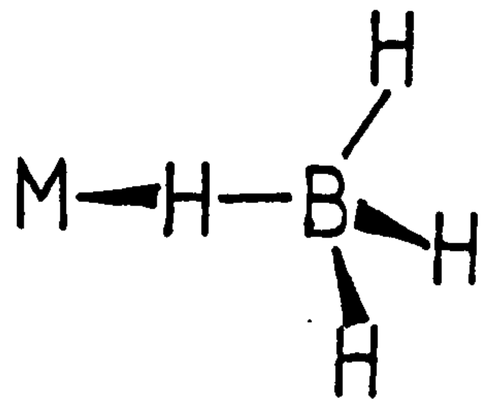

II

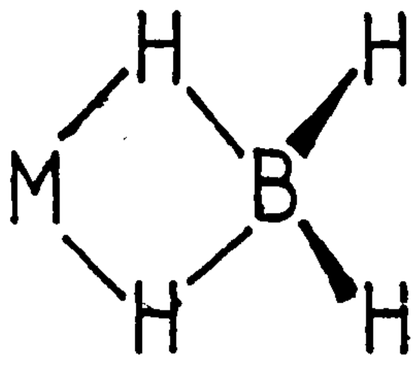

III

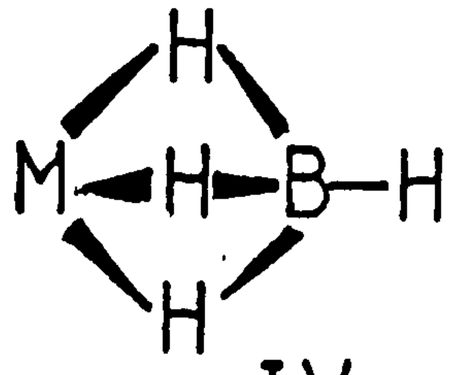

IV

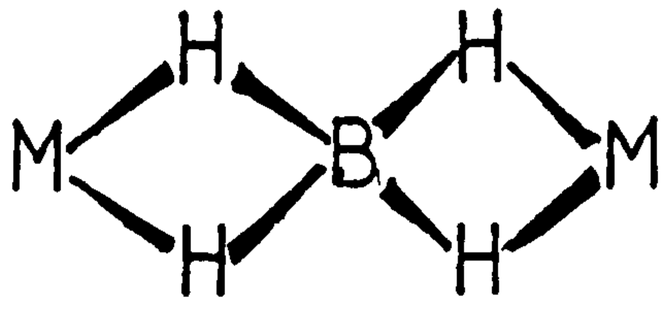

V

It has been shown that in the cupraboranes $Cu(PPh_2Me)_3(BH_4)$,[158(a),(b)] $[Cu(PPh_3)_2(NCBH_3)]_2$[158(c)] and $Cu(PR_3)_3(H_3BCO_2R)$,[158(d),(e)] the copper centre achieves four coordination via a single hydrogen bridge bond (II). Cupraboranes for which the mode of attachment is bidentate (III) through two Cu-H-B bridge bonds are $Cu(PPh_3)_2(BH_4)$,[46,160] $Cu(PPh_3)_2(B_3H_8)$[3,17(e),44,45,161] $Cu(PPh_3)_2(H_3BCO_2R)$,[158(e)] $Cu(PPh_3)_2(H_3BCNB_3H_7)$[99] and $[Cu(PPh_3)_2]_2B_{10}H_{10}$.[113,151,162] Solution studies of $Cu(PPh_3)(BH_4)$, $Cu(PPh_3)(B_3H_8)$ and $Cu_2B_{10}H_{10}$[54] indicated that coordination was via three Cu-H-B bridge bonds (IV). Four coordination, and subsequent ion pair association has been suggested for $[Cu(PR_3)_4]IB_9H_{14}]$ and $[Cu(PR_3)_4]IB_9H_{12}S]$;[163] ion pairing has also been proposed for $[Cu(PR_3)_3]IB_9H_{14}]$,$[Cu(PR_3)_3]IB_9H_{12}S]$ and $[Cu(PPh_3)_3][B_{11}H_{14}]$.[3(b),45] Complexes in which the coordination environment of the copper is not so readily described include $Cu(PPh_3)_2(B_5H_8)$[164] and $Cu(PPh_3)_2B_{10}H_{13}\cdot CH_2Cl_2$[3(b)] in which metal-borane interactions play an important role.

The most frequently used synthetic methods for all of these derivatives have involved metathesis of a group I metal salt of the borane anion with either a preformed phosphine-copper halide complex, e.g., $Cu(PPh_3)_3Cl$, or with a copper(II) salt in the presence of phosphine ligands. It has further been shown that, in many cases, the phosphine ligands are labile and this lability resulted in equilibria between complexes containing 2,3 or 4 phosphine ligands; furthermore, by removal of a phosphine ligand through complexation, compounds with fewer phosphines were obtained.

In this chapter a more versatile and convenient route to metallaborane complexes containing the $Cu(PPh_3)_2$ moiety is reported. Using the $[N(PPh_3)_2]^+$ salts of tetradecahydrononaborate (1-) anion, $[B_9H_{14}]^-$, and its substituted derivatives, $[B_9H_{13}(X)]^-$, in the weakly polar solvent dichloromethane, borane displacement of the $[BH_4]$ moiety from Cu $(PPh_3)_2(BH_4)$ with the larger boranes has been effected to yield a new class of metallaborane, $Cu(PPh_3)_2(B_9H_{13}X)$ (X = H(i), NCS(ii), NCSe(iii) and $NCBPh_3$(iv)). A further class has been obtained where the substituent, X, is $NCBH_3$(v), $NCBH_2NCBH_3$ (vi) and $NCBH_2CNB_9H_{13}$(vii). In addition, with the borane anion $[B_9H_{13}(NCBH_2CN)]^-$, the dimeric copper complex, $[Cu(PPh_3)_2(NCBH_2CNB_9H_{13})]_2$, (viii), has been formed. The complexes (i) - (vi) were shown to be covalent in dichloromethane by conductivity measurements. In acetonitrile the complexes dissociated. The complexes (i) - (iv) have been shown by their ^{11}B, ^1H and ^{31}P n.m.r. spectra to be fluxional down to -50°C. The data are consistent with structures that involve bidentate interaction of the copper with the nonaborane anion via two hydrogen bridged boron bonds resulting in a time-averaged environment in which there is a plane of symmetry. The ^{11}B, ^1H and ^{31}P n.m.r. spectra of complexes (v), (vi) and (vii) are consistent with complexes in which the copper centre is coordinated via two hydrogen bridge Cu-H-B bonds to the substituent. The ^1H n.m.r. spectra of complexes (v) - (viii) indicated that these complexes were static at room temperature, in solution, on the n.m.r. time scale.

7.1.2 Results and Discussion

The reaction of $[N(PPh_3)_2][B_9H_{13}(X)]$(X = H, NCS, NCSe and $NCBPh_3$)

and $Cu(PPh_3)_2(BH_4)$ in dichloromethane resulted in displacement of the $[BH_4]$ moiety of the copper borohydride complex by the larger nonaborane anions to produce copper complexes of the type $Cu(PPh_3)_2(B_9H_{13}X)$. The compounds have been fully characterised by spectroscopic and analytical techniques. Conductivity measurements made on dichloromethane and acetonitrile solutions (Table 7.1) of the complexes (i) - (vi), indicated that in the weakly polar solvent, CH_2Cl_2, the complexes were undissociated. However, in acetonitrile it was found that the equivalent conductivity increased dramatically which showed that dissociation to form the ion pair had occurred.

$$Cu(PPh_3)_2(B_9H_{13}X) \xrightarrow{CH_3CN} [Cu(PPh_3)_2(CH_3CN)_2]^+[B_9H_{13}(X)]^- \quad (7\text{-}1)$$

Dissociation of the cupraboranes $[CuL_3(NCBH_3)]$ and $[CuL_2(NCBH_3)]_2$ has previously been observed in polar solvents.[165]

Table 7.1 Equivalent Conductivities of Complexes (i) - (vi)

Complex	CH_2Cl_2 (Λ/Scm^{2}mol^{-1})	CH_3CN (Λ/Scm^{2}mol^{-1})
(i)	1.34	119.27
(ii)	9.67	96.46
(iii)	2.23	19.92
(iv)	4.21	32.96
(v)	4.55	31.75
(vi)	4.70	27.91

The 115 MH_z ^{11}B n.m.r. spectrum of $Cu(PPh_3)_2(B_9H_{13}NCSe)$ in $CDCl_3$, taken as an example, is shown in Figure 7.1. The ^{11}B n.m.r. spectra

Figure 7.1 The 115.5MH_z ^{11}B and ^{11}B-{^1H} n.m.r. spectra of $Cu(PPh_3)_2(B_9H_{13}NCSe)$ in $CDCl_3$

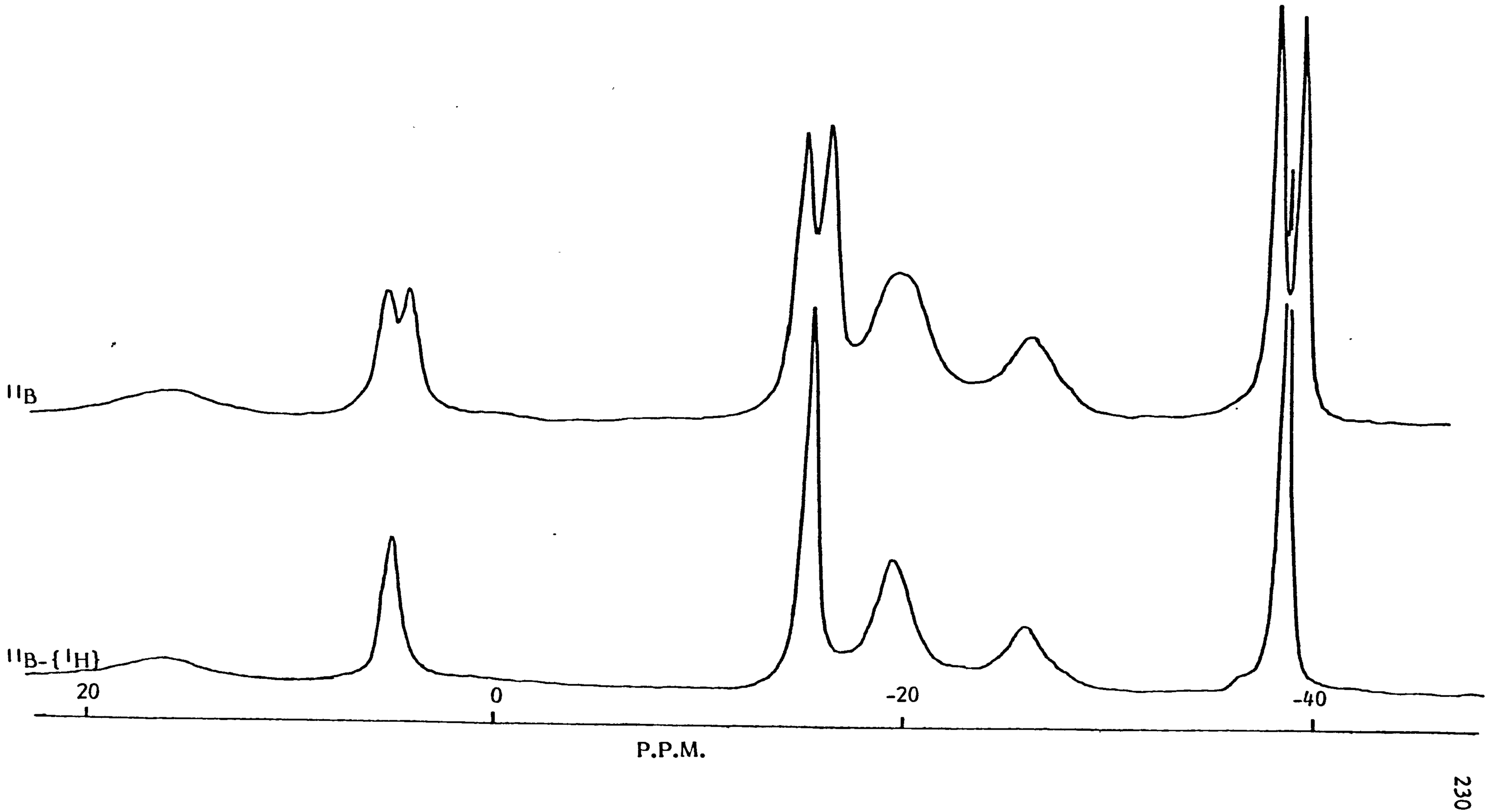

of all the complexes, (Table 7.2), strongly resembled the ^{11}B n.m.r. of the original uncomplexed anions. Besides providing valuable structural information, the ^{11}B chemical shift data contains information on the nature of the bonding environment of the observed boron atom. In particular, the changes in chemical shift of the boron atoms on being bound to a metal fragment constitute a measure of the perturbation of the borane cage on complex formation. In the complexes (i) - (iv), the resonance due to the boron atoms B(7), B(6), B(8) and B(4) are all considerably broadened with respect to the uncomplexed anion, this indicates that the copper centre has a direct effect on these particular boron nuclei on complexation. Further evidence for copper complexation to these boron nuclei is observed when the n.m.r. solvent used is $CD_3C_6D_5$ rather than $CDCl_3$. For the complexes (i) - (iv) in deuterio toluene at room temperature, the resonances due to B(4), B(6), B(8) and B(7) are all broadened to such an extent as to be unobservable. Increasing the temperature to 330K results in the broadened resonances being resolved, this indicates that the broadening that is observed on complex formation is due to the quadrupolar effect of the copper nucleus[166] (^{63}Cu,^{65}Cu, I = $^3/2$, 100% abundance). In the relatively viscous $CD_3C_6D_5$ the efficiency of quadrupolar relaxation of the copper nucleus is enhanced. The quadrupole moment of copper interacts with time-dependent electric field gradients produced by molecular re-orientation, providing a very efficient spin-lattice relaxation mechanism that causes broadening of the ^{11}B resonances associated with the copper nucleus. Increasing the temperature reduces the efficiency of spin-lattice relaxation

resulting in the enhanced resolution of the broadened resonances. Going from $CDCl_3$ to $CD_3C_6D_5$ did not cause any appreciable change in the line-width of the remaining boron resonances.

The 360 MH_z ^1H n.m.r. spectra, (Table 7.2), of complexes (ii) - (iv) indicated that they were fluxional with three bridge hydrogen atoms, unlike the free anions which had five bridge hydrogen atoms. The remaining two bridge hydrogen atoms in the complexes are involved in Cu-H-B hydrogen bridge bonds. These hydrogen bridges are broadened to extinction by the combined quadrupolar effect of the copper and boron nuclei. The ^1H n.m.r. spectrum of the $Cu(PPh_3)_2(B_9H_{14})$ indicates that the copper is tetrahedrally bound in a bidentate manner to the borane fragment in two Cu-H-B bridge hydrogen bonds. Previously the only reported copper nonaborane derivatives were the salts $[Cu(PR_3)_4IB_9H_{14}]$,[163] $[Cu(PR_3)_4IB_9H_{12}S]$,[163] $[Cu(PR_3)_3IB_9H_{14}]$[3(b),45] and $[Cu(PR_3)_3IB_9H_{12}S]$.[3(b),45] In the ^1H n.m.r. spectrum of $Cu(PPh_3)_2(B_9H_{14})$ a resonance of relative intensity 2 was observed at δ0.42p.p.m. that could be attributed to the endo-hydrogen atoms interacting with copper in the Cu-H-B bridge bonds.

The 145.7 MH_z ^{31}P n.m.r. spectra of complexes (ii) and (iv) indicated fluxional or exchange behaviour of the phosphine ligands that could be quenched at low temperatures. The ^{31}P n.m.r. spectrum of (ii) at room temperature in CD_2Cl_2 comprised a singlet at δ0.76 p.p.m. (ref: 85% H_3PO_4), which, on cooling to 206K split into two resonances at δ0.95 p.p.m. and δ0.11 p.p.m. of relative intensity ca. 1:2 respectively. The spectrum of (iv) at room temperature was also a singlet

Table 7.2 ^{11}B and ^{1}H $\{^{11}B$, C.W.$\}$ N.M.R. Spectral Data for $Cu(PPh_3)_2(B_9H_{13}X)$ Complexes in $CDCl_3$

	Substituent(X)	$\delta^{11}B$(p.p.m)	$\delta^{1}H$(p.p.m)	Assignment
(i)	H	-5.3	2.70 (3)	5,7,9
		-22.5	1.26 (3)	4,6,8
		-25.4	1.62 (3)	1,2,3
			-1.61 (3)	bridge
			7.4 (30)	PPh_3
			0.42 (2)	CuHB
(ii)	NCS	15.4	3.91 (1)	7
		3.3	3.0 (1)	1
		-15.6	1.68 (2)	5,9
		-19.1	1.99 (2)	6,8
		-24.0	-	4
		-38.4	0.4 (2)	2,3
			-1.3 (3)	bridge
			7.4 (30)	PPh_3
(iii)	NCSe	16.7	3.90 (1)	7
		5.2	3.05 (1)	1
		-15.1	1.73 (2)	5,9
		-19.4	1.91 (2)	6,8
		-25.7	-	4
		-38.4	0.38 (2)	2,3
			-1.30 (3)	bridge
			7.4 (30)	PPh_3

(iv) $NCBPh_3$	16.93	4.00 (1)	7
	5.20	3.16 (1)	1
	-10.67	-	BPh_3
	-15.11	1.83 (2)	5,9
	-19.40	2.00 (2)	6,8
	-26.03	-	4
	-28.41	0.50 (2)	2,3
(v) $NCBH_3$	17.5	3.97 (1)	7
	4.9	2.97 (1)	1
	14.8	1.70 (2)	5,9
	-20.0	1.94 (2)exo	6,8
		-0.25 (2) endo	6,8
	-26.6	0.24 (1)	4
	-38.6	0.41 (2)	2,3
	-36.5	1.73 (3)	BH_3
		-3.55 (2)	bridge
(vi) $NCBH_2NCBH_3$	17.97	4.08 (1)	7
	5.30	3.21 (1)	1
	-14.40	1.99 (2)	5,9
	-20.20	2.07 (2) exo	6,8
		-0.12 (2) endo	6,8
	-26.90	0.55 (1)	4
	-26.90	2.07 (2)	BH_2
	-38.44	0.59 (2)	2,3
	-37.00	1.83 (3)	BH_3
		7.45 (30)	PPh_3
		3.37 (2)	bridge

(vii) $NCBH_2CNB_9H_{13}$	17.68	-	7
	5.25	-	1
	-14.53	-	5,9
	-20.17	2.01 (2) exo	6,8
		-0.15 (2) endo	6,8
	-27.01	-	4
	-36.72	-	BH_2
	-38.53	-	2,3
		3.36 (2)	bridge
(viii)$NCBH_2CN$	16.96	-	7
	5.15	-	1
	-14.73	-	5,9
	-20.11	1.98 (2) exo	6,8
		-0.17 (2) endo	6,8
	-26.91	-	4
	-38.59	0.62 (2)	2,3
	-40.30	0.49 (1b)	BH_2
		1.44 (1s)	"
		-3.45 (2)	bridge

Figures in parenthesis represent relative intensities.

b - broad, s - sharp.

at δ0.71 p.p.m. which, on cooling, resolved into two resonances at δ 0.65 p.p.m. and δ -1.71 p.p.m. of relative intensity 2:1 respectively. Additional small resonances at ca. δ21.5 p.p.m. and ca δ 2.2 p.p.m. attributed to impurities were also observed at low temperatures in both complexes. Further cooling to 171K of either complex failed to reveal any further structure, although some broadening of the resonances occurred.

The ^{31}P, ^{11}B and ^{1}H n.m.r. data of the complexes (i) - (iv) together indicate a structure that is fluxional at ambient temperature, resulting in a time-averaged environment on the n.m.r. time scale containing a plane of symmetry. This type of behaviour has previously been observed in alkylaluminium and alkylgallium, $B_9C_2H_{12}MR_2$, complexes.[167] The most feasible time-averaged structure is one in which the copper centre formally replaces the B(9) position in $B_{10}H_{14}$. Fluxionality is achieved by having two of the three endo-hydrogen atoms from B(4), B(6) and B(8) involved in Cu-H-B bridge bonding to the $Cu(PPh_3)_2$ moiety (Figure 7.2). This type of pseudorotation has previously been observed in $Cu(PPh_3)_2(B_3H_8)$[17(e),46] as illustrated in Chapter 1.

The complexes (i) - (iv) can be viewed as having a central copper atom around which the top face of the nonaborane fragment B(4), B(6) and B(8) rotates.

Several ^{31}P n.m.r. studies of $Cu(PPh_3)_2(B_3H_8)$ indicated that the phosphine ligands are labile in solution.[3(b),45,161(a)] By treating [Cu

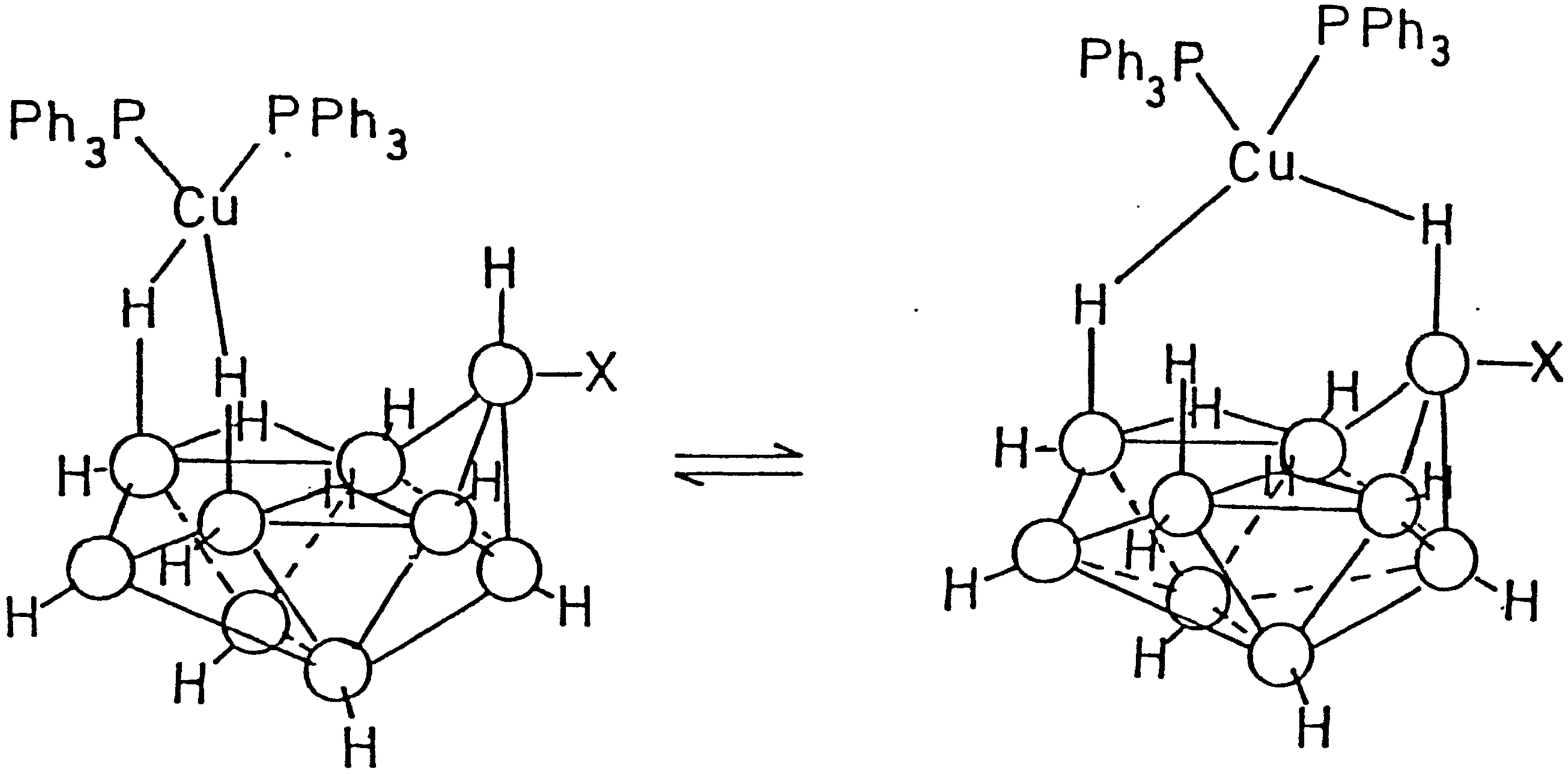

Figure 7.2 The proposed fluxional structures of $Cu(PPh_3)_2(B_9H_{13}X)$ were X=H, NCS, NCSe and $NCBPh_3$.

$(PPh_3)_2]_2B_{10}H_{10}$ and $Cu(PPh_3)_2(B_3H_8)$ with diborane Shore and co-workers[54] were able to extract the labile phosphine ligands to produce $Cu_2B_{10}H_{10}$, CuB_3H_8 and $PPh_3.BH_3$. Preliminary investigations of $Cu(PPh_3)_2(B_9H_{13}NCSe)$ with $BH_3.SMe_2$ in dichloromethane indicate that a similar type of reaction occurs since $PPh_3.BH_3$ is the only soluble product obtained from this reaction. A brown solid is obtained that is insoluble in chlorinated solvents and may, like $Cu_2B_{10}H_{10}$,[113,151,162(a)] be polymeric.

The 115.5 MH_z ^{11}B n.m.r. spectrum (Fig. 7.3) of $Cu(PPh_3)_2(B_9H_{13}NCBH_2NCBH_3)$ is virtually identical to that of the free anion. However, on complexation the resonance due to the $[BH_3]$ moiety of the substituent is shifted 6.3 p.p.m. to higher frequency (lower field). This chemical shift difference is comparable to the large chemical shift difference of 5 p.p.m. that is observed in the base boron nuclei when $Cu(PPh_3)_2(B_5H_8)$[168] is prepared from the $[B_5H_8]^-$ anion.[169] In this complex the $Cu(PPh_3)_2$ moiety occupies a bridge position in the base of the $[B_5H_8]$ cage.[170] The large chemical shift observed for the $[BH_3]$ moiety of the substituent on formation of complexes (v) and (vi) indicates that copper complexation is through the substituent.

The 360 MH_z ^1H n.m.r. spectra of complexes (v) and (vi) showed that the copper is tetrahedrally bound to two PPh_3 ligands and to the nonaborane fragment via two Cu-H-B bridge bonds. Specific frequency decoupling experiments showed conclusively that copper complexation

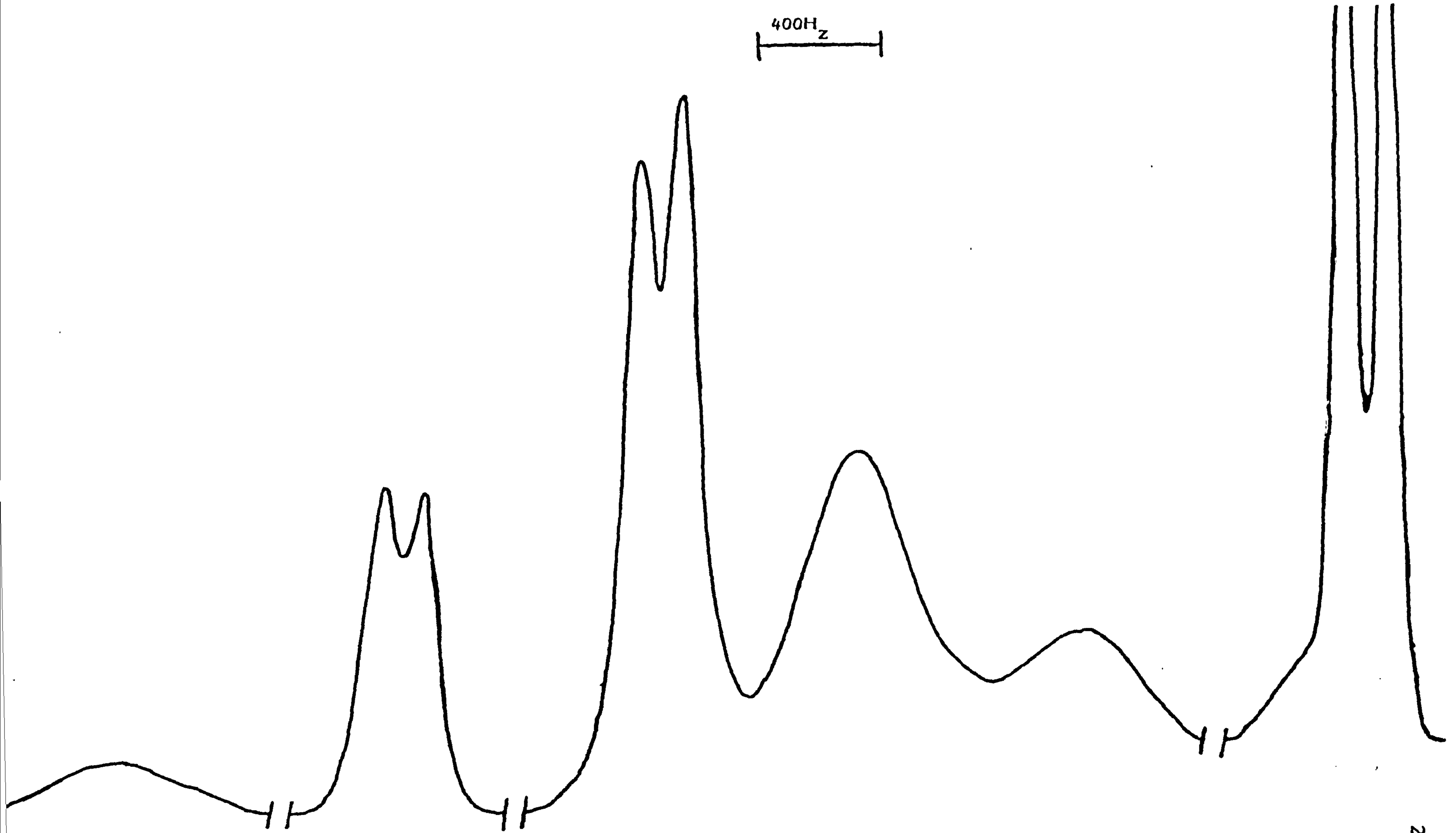

Figure 7.3 The 115.5MHz ^{11}B n.m.r. spectrum of $Cu(PPh_3)_2(B_9H_{13}NCBH_2NCBH_3)$ in $CDCl_3$

was not through the cage since both the exo and the endo hydrogen atoms associated with B(6) and B(8) were observed. Therefore, copper complexation is through the $[BH_3]$ moiety of the substituent.

In contrast to the 145.7 MH_z ^{31}P n.m.r. spectra obtained for complexes (ii) and (iv), the ^{31}P n.m.r. spectrum of (vi) remained a singlet at all temperatures down to 171K, consistent with a complex whose fluxional behaviour resulted from a much lower energy barrier.

The ^{31}P, ^{11}B and ^{1}H n.m.r. data of complexes (v) and (vi) indicate a structure that is static at room temperature, on the n.m.r. time scale. Interaction of the copper occurred through the $[BH_3]$ moiety of the substituent, hence structures (v) and (vi) can be considered as complexes of substituted tetrahydroborate (1-) derivatives (Fig.7.4).

In addition to complexes (v) and (vi), it was found that reaction of $Cu(PPh_3)_2(BH_4)$ and $[B_9H_{13}(NCBH_2CN)B_9H_{13}]^-$ also resulted in displacement of the borohydride ligand, by the larger anion, to produce a copper complex. In this copper complex the copper centre is tetrahedrally bound to the $[BH_2]$ moiety of the bridging substituent via two Cu-H-B bridge bonds.

The ^{11}B n.m.r. of the complex, $Cu(PPh_3)_2(B_9H_{13}NCBH_2CNB_9H_{13})$, is similar to that of the free anion. The only difference in the ^{11}B n.m.r. spectrum on complexation is that the resonance due to the $[BH_2]$ moiety shifts 3.6 p.p.m. to higher frequency. This chemical

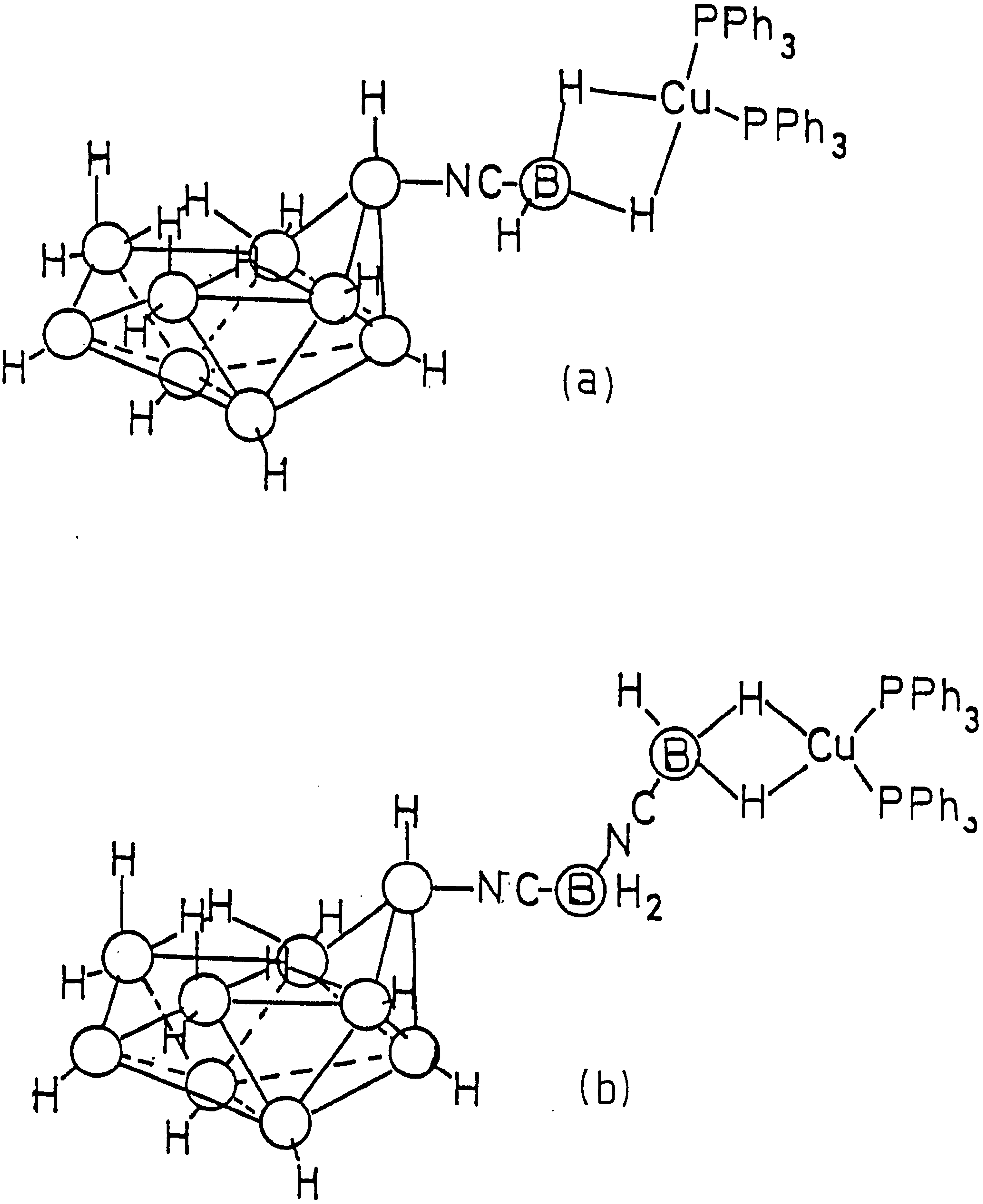

Figure 7.4(a) The proposed structures of $Cu(PPh_3)_2(B_9H_{13}NCBH_3)$ and (b) $Cu(PPh_3)_2(B_9H_{13}NCBH_2NCBH_3)$.

shift difference represents a direct interaction between the $[BH_2]$ moiety and the copper centre.

The ^1H n.m.r. spectrum of the complex showed both <u>exo</u> and <u>endo</u> terminal hydrogen atoms on B(6) and B(8) of each $[B_9H_{13}]$ fragment, and two bridge hydrogen atoms in each cage. The resonance that appears at $\delta 0.45$ p.p.m. in the $^1H\{^{11}B.C.W.\}$n.m.r. spectra attributed to the hydrogen atoms of the $[BH_2]$ moiety are broadened with respect to the free anion. These data are consistent with a static complex in which complexation occurs via two Cu-H-B hydrogen bridge bonds to the $[BH_2]$ moiety of the bridging substituent, (Fig. 7.5).

It has been reported[158(c),165] that the copper complex formed with the cyanotrihydroborate (1-) anion has the molecular configuration, $[Cu(PPh_3)_2(NCBH_3)]_2$, consisting of dimeric units in which each copper atom is four coordinate. The coordination geometry is that of a distorted tetrahedron defined by the two phosphorus atoms of the phosphine ligands and a nitrogen and hydrogen atom from two different $[BH_3(CN)]^-$ ligands, (Fig. 7.6).

The nonaborane (1-) anion, $[B_9H_{13}(NCBH_2CN)]^-$, can be viewed as a substituted derivative of $[BH_3(CN)]^-$ It has been found that the reaction of $Cu(PPh_3)_2(BH_4)$ and $[B_9H_{13}(NCBH_2CN)]^-$ results in the borohydride being eliminated by the larger anion to produce the dimeric complex, $[Cu(PPh_3)_2(B_9H_{13}NCBH_2CN)]_2$. The copper occupies a tetrahedral environment and is coordinated to two different borane ligands via a Cu-N bond and a single Cu-H-B bridge bond.

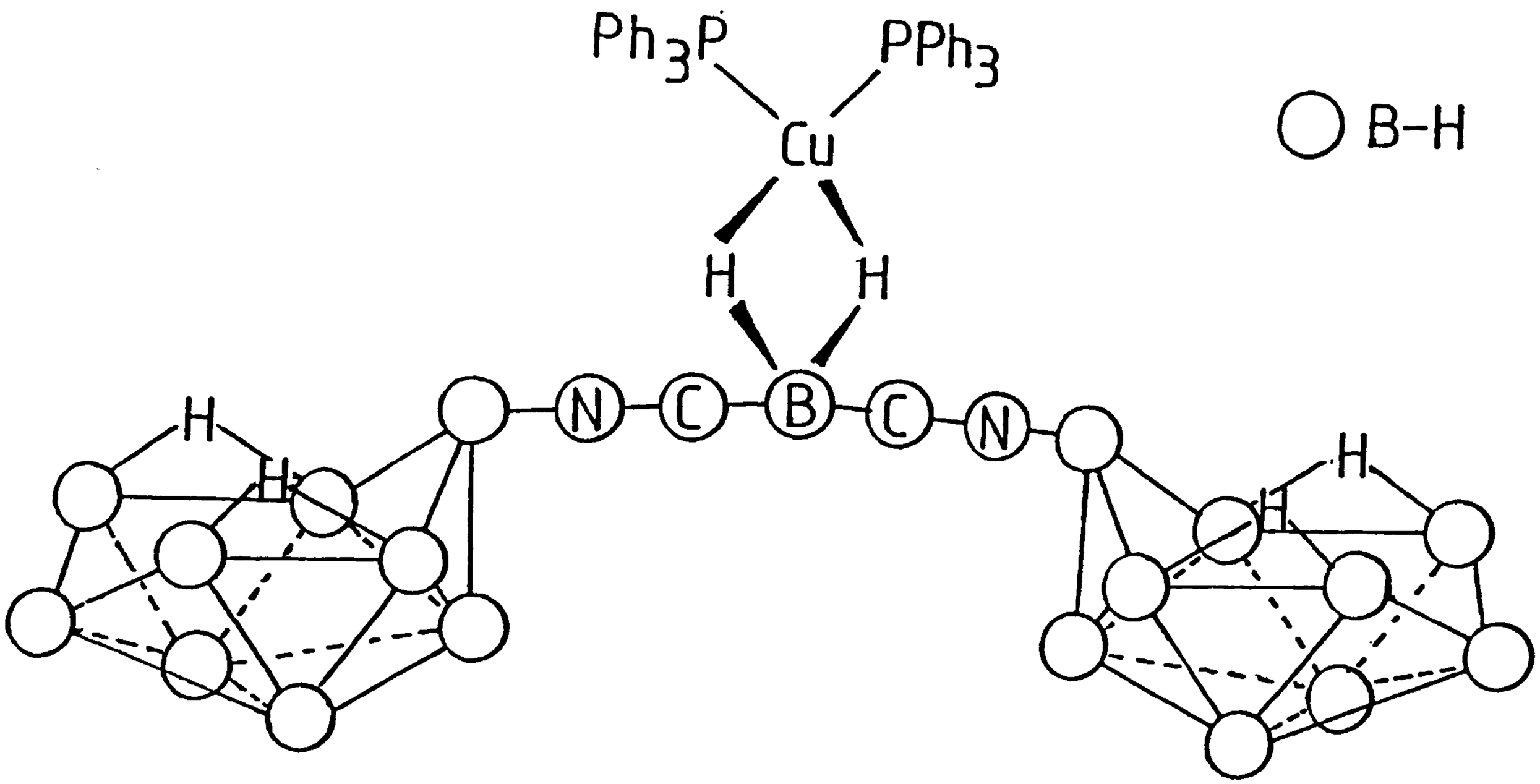

Figure 7.5 The proposed structure of $Cu(PPh_3)_2(B_9H_{13}NCBH_2CNB_9H_{13})$

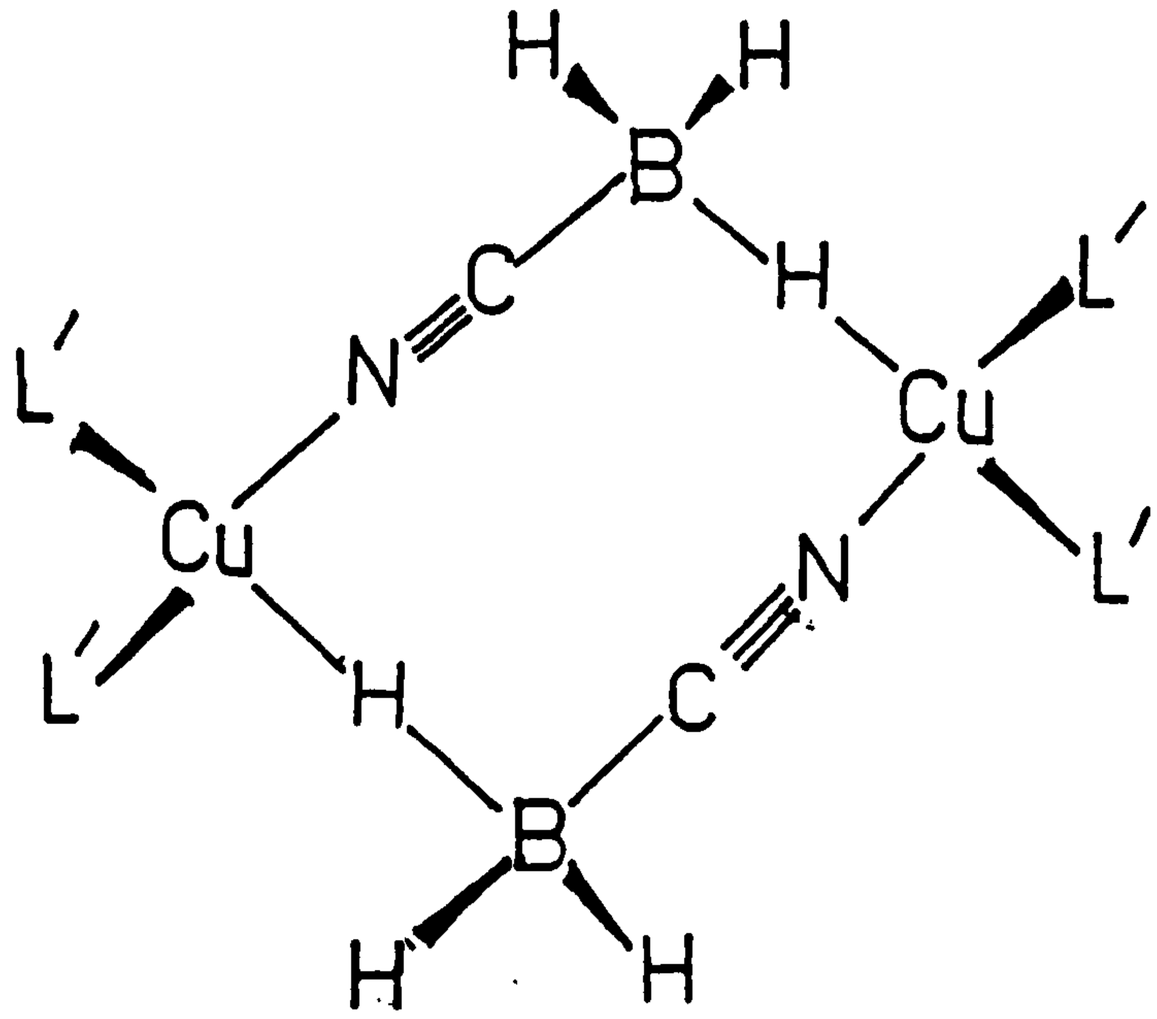

$L' = P(Ph)_3$

Figure 7.6 The structure of $[Cu(PPh_3)_2(NCBH_3)]_2$

The ^{11}B n.m.r. spectrum of the complex, $[Cu(PPh_3)_2(B_9H_{13}NCBH_2CN)]_2$ is virtually identical with that of the free anion. The only difference being that in the complex the resonance due to the $[BH_2]$ moiety of the substituent is broadened due to the quadrupolar effect of the copper.

The ^1H n.m.r. spectrum showed both <u>exo</u> and <u>endo</u> terminal hydrogen atoms on B(6) and B(8) in each nonaborane fragment indicating that again the complex is static and that the copper is bonded through the substituent. However, specific irradiation of the boron frequency that corresponds to the $[BH_2]$ moiety results in two proton resonances being observed, one which is sharp at $\delta 1.44$ p.p.m. and one which is broadened at δ 0.49 p.p.m. The proton resonance at $\delta 0.49$ p.p.m. is broadened due to the quadrupolar effect of the copper, hence the

copper is bonded via a single hydrogen bridge to the ligand, the remaining coordination site is occupied by the N from the cyano group on another borane ligand, (Fig. 7.7).

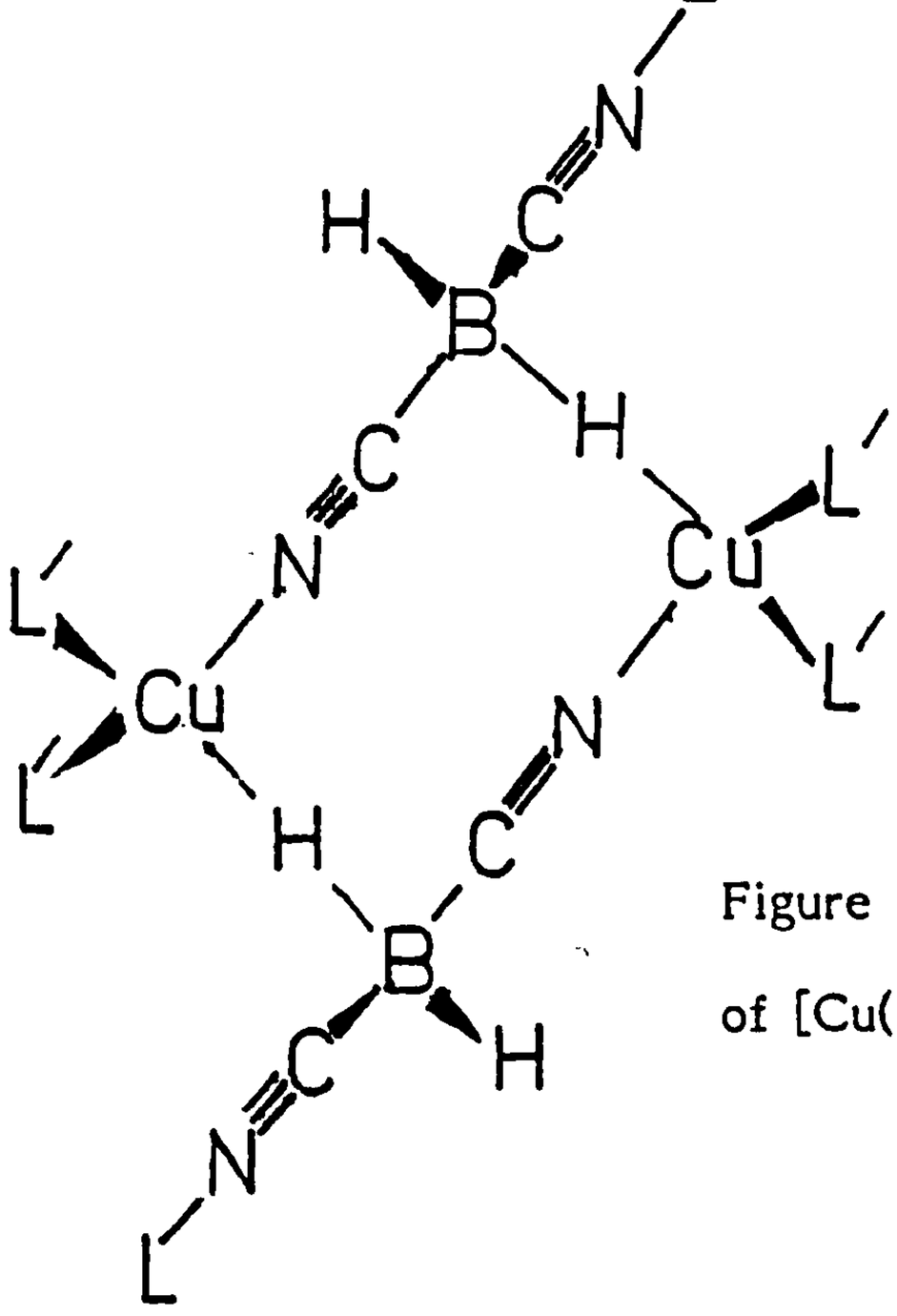

Figure 7.7 Proposed structure of $[Cu(PPh_3)_2(B_9H_{13}NCBH_2CN)]_2$

The infra-red spectra of complexes (i) - (viii),(Table 7.3), in general were similar to those of the free anions in the region 2600 - 2800cm.$^{-1}$ However, the BH str. modes of the $[BH_3]$ and $[BH_2]$ moieties in complexes (v), (vi) and (vii) are less well defined than those of the free anions. The band that is attributed to the stretching frequency of the terminal CN of the substituent in $[B_9H_{13}(NCBH_2CN)]^-$ is not observed in the copper complex. Presumably this is due to the fact that in the dimeric complex the terminal CN of the free anion is now bridging between the boron atom of the substituent and a copper centre.

Table 7.3 Infra-red Absorption Frequencies for $Cu(PPh_3)_2(B_9H_{13}X)$ Complexes as HCBD and Nujol mulls

	Substituent	2600 - 1800cm^{-1}		Assignment
(i)	H	2565s, 2380s, 2365sh		B-H_t
		1965m, 1946m, 1915m		B-H_b
(ii)	NCS	2520s,		B-H_t
		2180s		CNstr.
		1815w, 1895w, 1960w		B-H_b
(iii)	NCSe	2540s		B-H_t
		2170s		CNstr
(iv)	$NCBPh_3$	2540s		B-H_t
		2180s		CNstr
(v)	$NCBH_3$	2540s, 2440m, 2390m		B-H_t
		2273s	bridge	CNstr
		2170w, 2120m		B-H_b
		1815w, 1893w, 1963w		B-H_b
(vi)	$NCBH_2NCBH_3$	2545s, 2420sh, 2370s		B-H_t
		2250s, 2200w	bridge	CNstr.
(vii)	$NCBH_2CN$	2140s,2390m		B-H_t
		2275m	bridge	CNstr.
(viii)	$NCBH_2CNB_9H_{13}$	2250s,2400m		B-H_t
		2280s	bridge	CNstr.

t - terminal, b - bridge

7.1.3 Electrochemical Studies of $Cu(PPh_3)_2(B_9H_{13}X)$ Complexes

The complexes were studied by cyclic voltammetry and a.c.voltammetry. In dichloromethane the complex, $Cu(PPh_3)_2(B_9H_{14})$ showed a broad irreversible oxidation at Ep. 1.5V but failed to show clearly defined oxidation or reduction waves. However, the substituted derivatives showed irreversible oxidations or reductions approaching the potential limits of the solvent (CH_2Cl_2). For $Cu(PPh_3)_2(B_9H_{13}NCS)$ an irreversible oxidation was observed at Ep 1.75V, and is shown in Figure 7.8, the free anion exhibits an irreversible oxidation at Ep 1.67V in CH_2Cl_2. $Cu(PPh_3)_2(B_9H_{13}NCSe)$ also showed an irreversible oxidation that appeared at Ep 1.67V, in addition a clearly defined irreversible reduction appeared at Ep -1.40V which was the only reduction observed for any of the complexes examined in dichloromethane. The free anion $[N(PPh_3)_2][B_9H_{13}(NCSe)]$ shows an irreversible oxidation at Ep 1.62V in CH_2Cl_2. The complexes $Cu(PPh_3)_2(B_9H_{13}NCBH_2NCBH_3)$ and $[Cu(PPh_3)_2(B_9H_{13}NCBH_2CN)]_2$ each showed irreversible oxidations at Ep 1.52V and Ep 1.48V respectively, the free anions in this case show irreversible oxidations at Ep 1.64V and Ep 1.58V respectively.

The data available indicate that on complex formation the complexes in which the copper is bound to the cage become oxidatively more stable than the anion. Conversely when the copper is bound through the ligand the complexes become less stable to oxidation than the free anion.

It was previously reported[97] that voltammetric investigations of Cu

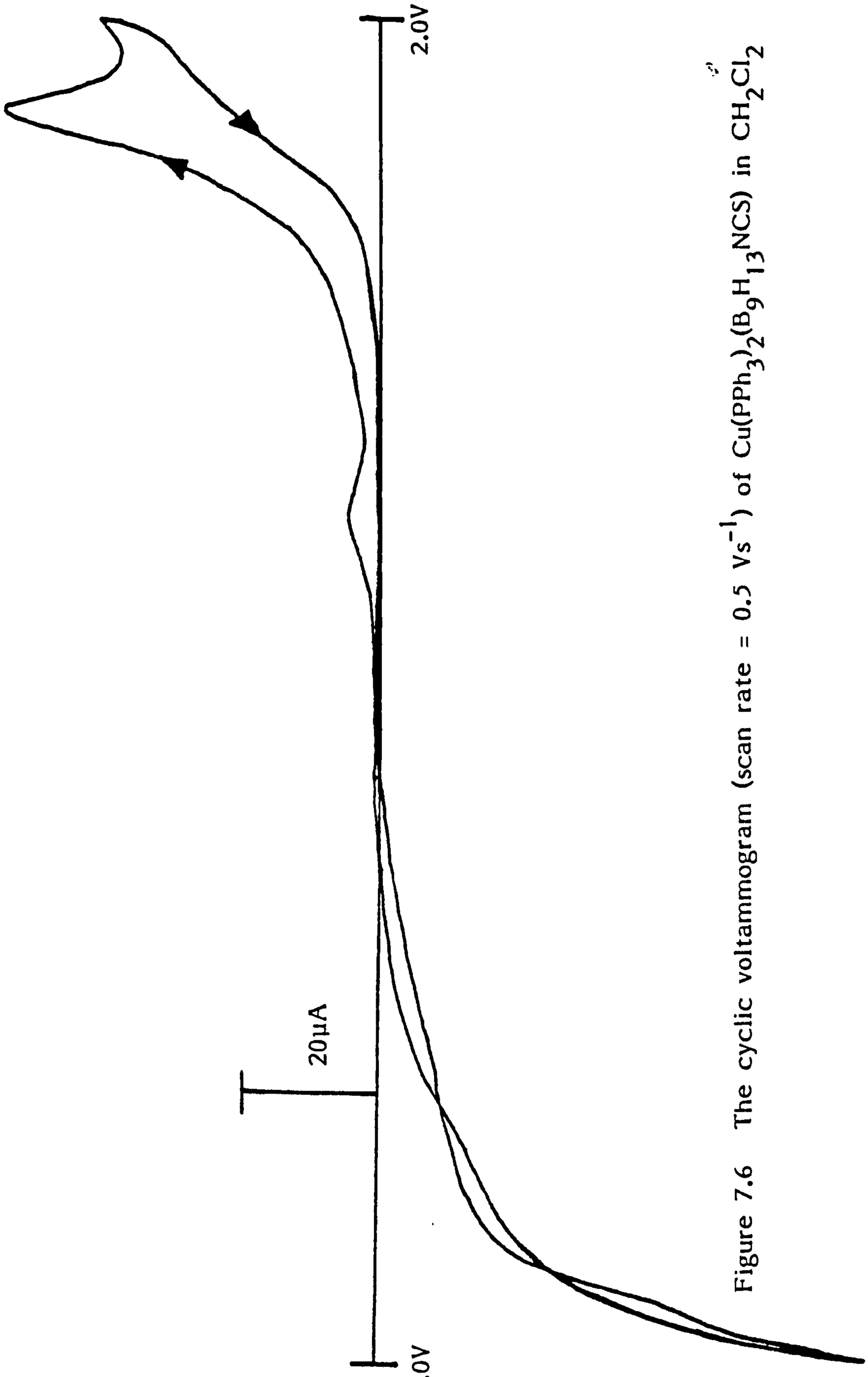

Figure 7.6 The cyclic voltammogram (scan rate = 0.5 Vs^{-1}) of $Cu(PPh_3)_2(B_9H_{13}NCS)$ in CH_2Cl_2

$(PPh_3)_2(B_3H_8)$ and $Cu(PPh_3)_2(BH_4)$ in acetonitrile, produced irreversible reductions which were attributed to disruption of the complexes.

$$Cu(PPh_3)_2(B_3H_8) \rightarrow Cu^{\circ} + [B_3H_8]^- + 2PPh_3 \qquad (7\text{-}2)$$

However in acetonitrile the substituted complexes have been shown to dissociate to form solvated ions. Cyclic voltammetry and cyclic a.c. voltammetry of the complexes $Cu(PPh_3)_2(B_9H_{14})$, $Cu(PPh_3)_2(B_9H_{13}NCS)$ and $Cu(PPh_3)_2(B_9H_{13}NCBH_2NCBH_3)$ in acetonitrile show clearly defined irreversible reductions at Ep-0.54V, Ep-0.61V and Ep-0.64V respectively attributed to Cu(I) →Cu(O). Copper metal is plated on to the cathode in each case. In addition several irreversible oxidations were observed in each case which could be attributed to: re-oxidation of Cu°, oxidation of ligands or oxidation of the borane fragment. It is evident that in acetonitrile the complexes dissociate to form, $[Cu(PPh_3)_2(CH_3CN)_2][B_9H_{13}(X)](X=H,NCS,NCBH_2NCBH_3)$,in which Cu^{I} undergoes reduction readily. Since $Cu(PPh_3)_2(B_9H_{13}NCSe)$ exhibits an irreversible reduction in dichloromethane, then, in this case, the copper may only be weakly bound to the cage. This may be a useful method for measuring the degree of dissociation when going from a less polar solvent to a more polar solvent.

The reaction of $Cu(PPh_3)_2(BH_4)$ and the 2,5:6,10:8,10-Tri-μ-hydro-nonahydro-nido-nonaborate (1-) anion, $[B_9H_{12}]^-$ yields a brown solid. However, unlike the reactions with the arachno- nonaborane anions, the exact nature of the complex is not known. The ^{11}B n.m.r. spectrum of the complex retains the general symmetry of the anion. (Table 7.4).

However in the complex all the resonances are broadened.

Table 7.4 115.5MH$_z$ ^{11}B N.M.R. Data for Cu(PPh$_3$)$_2$(B$_9$H$_{12}$) in CDCl$_3$

δ^{11}B (p.p.m.)	J_{B-H}(H$_z$)	Int	Assignment
6.0	-	2	
4.8	-	1	
-4.4	-	2	
-6.4	-	1	
-31.8	-	2	
-36.8	57		Ph_3PBH_3
-47.8	127	1	

Analytical data obtained for the complex indicates that the complex is Cu(PPh$_3$)$_2$(B$_9$H$_{12}$), inferring that the copper centre is bound to the cage via two Cu-H-B bridge bonds. The data indicated that the copper occupied a position in a plane of symmetry in a time averaged environment on the n.m.r. time scale. It is proposed that the copper centre undergoes pseudorotation with the hydrogen bridges on the top face of the [B$_9$H$_{12}$]$^-$ anion. Also present in the ^{11}B n.m.r. at δ -36.8 p.p.m. is a resonance attributed to PPh$_3$BH$_3$ indicating that the phosphine ligands are labile. The presence of PPh$_3$BH$_3$ indicates that a complex where the copper is triply hydrogen bridged to the anion may be present.

$$Cu(PPh_3)_2(B_9H_{12}) \longrightarrow Cu(PPh_3)(B_9H_{12}) + PPh_3BH_3 \quad (7\text{-}3)$$

7.2 Experimental

The substituted derivatives of $[B_9H_{14}]^-$ were prepared as previously described (Chapter 4). $Cu(PPh_3)_2(BH_4)$ was prepared by the literature method.[157,159,160(b)] $[N(PPh_3)_2IB_9H_{12}]$ was prepared as described in Chapter 6.

7.2.1 Preparation of Bis(triphenylphosphine)Copper Complexes Derived from the $[B_9H_{14}]^-$ Ion

Equimolar mixtures of $Cu(PPh_3)_2(BH_4)$ (1 mmol) and $[N(PPh_3)_2IB_9H_{13}X]$ (X = H, NCS, NCSe, $NCBPh_3$, $NCBH_3$, $NCBH_2NCBH_3$, $NCBH_2CN$ and $NCBH_2CNB_9H_{13}$) (1 mmol) were placed in a 250cm³ round-bottomed flask fitted with a stopcock adaptor. Dried, degassed dichloromethane (ca.30cm³) was condensed into the system under vacuum, and the mixture was warmed to room temperature. After stirring the solution for 4 hr. the solvent was removed under reduced pressure to yield a brown solid for the H, NCS, NCSe, $NCBH_2CN$ and $NCBH_2CNB_9H_{13}$ substituted complexes, and a white solid for the $NCBPh_3$, $NCBH_3$ and $NCBH_2NCBH_3$ substituted complexes. Thin-layer chromatography on silica gel using 100% CH_2Cl_2 as eluant in each case indicated the presence of a single major component, (Table 7.5). Purification by chromatography on silica gel using 100% CH_2Cl_2 as eluant gave the copper complexes in good yield (35 - 75%). Analytical data are presented in Table 7.5.

Table 7.5 Analytical Data for Substituted Nine-Vertex Metallaboranes

	Compound	T.l.c	C%		H%	
		Rf	Found	Requires	Found	Requires
(i)	$Cu(PPh_3)_2(B_9H_{14})$	0.81	61.93	61.78	6.63	6.34
(ii)	$Cu(PPh_3)_2(B_9H_{13}NCSe)$	0.80	54.78	55.28	6.26	5.39
(iii)	$Cu(PPh_3)_2(B_9H_{13}NCS)$	0.81	55.16	58.70	5.87	5.73
(iv)	$Cu(PPh_3)_2(B_9H_{13}NCBPh_3)$	0.83	67.82	68.31	7.80	6.05
(v)	$Cu(PPh_3)_2(B_9H_{13}NCBH_3)$	0.82	-	-	-	-
(vi)	$Cu(PPh_3)_2(B_9H_{13}NCBH_2NCBH_3)$	0.85	58.22	58.69	6.56	6.23
(vii)	$[Cu(PPh_3)_2(B_9H_{13}NCBH_2CN)]_2$	0.84	59.91	59.75	5.62	5.93
(viii)	$Cu(PPh_3)_2(B_9H_{13}NCBH_2CNB_9H_{13})$	0.82	-	-	-	-

	N%		P%	
	Found	Requires	Found	Requires
(i)	-	-	8.08	8.85
(ii)	1.90	1.74	6.37	7.71
(iii)	1.62	1.85	8.27	8.19
(iv)	0.95	1.44	5.56	6.41
(v)	-	-	-	-
(vi)	3.60	3.60	6.96	7.17
(vii)	2.91	3.66	8.00	8.11
(viii)	-	-	-	-

7.2.2 Preparation of $Cu(PPh_3)_2(B_9H_{12})$

Equimolar mixtures of $Cu(PPh_3)_2(BH_4)$ (1 mmol) and $[N(PPh_3)_2]B_9H_{12}]$ (1 mmol) were placed in a 250cm³ round-bottomed flask fitted with a stopcock adaptor. Dried, degassed dichloromethane (ca.30cm³) was condensed in under reduced pressure, and the mixture was warmed to room temperature. After stirring for 4 hr. the solvent was removed under vacuum to yield a brown solid. Thin-layer chromatography on silica gel using 100% CH_2Cl_2 as eluant indicated a single major product (Rf = 0.81). Purification by column chromatography on silica gel using 100% CH_2Cl_2 as eluant gave a brown solid in good yield (0.44g, 63%) identified as $Cu(PPh_3)_2(B_9H_{12})$ from analytical and spectroscopic results.

(Found: C,63.39; H,6.10; P,8.21%. Calculated for $C_{36}H_{42}B_9CuP_2$: C,61.96; H,6.07; P,8.85%).

7.2.3 Electrochemistry

Cyclic and cyclic a.c. voltammetry were carried out as previously described, (Chapter 3). Platinum cathodes and anodes were used. Solutions in CH_3CN were referenced to $Ag/AgNO_3$ (0.1 mol dm^{-3}), and solutions in CH_2Cl_2 were referenced to Ag/AgCl ($[N(PPh_3)_2]Cl$ 0.1 mol dm^{-3}).

7.3 Copper Metallaboranes Derived from Substituted Derivatives of $[B_3H_8]^-$

7.3.1 Introduction

It is known that the octahydrotriborate (1-) ion, $[B_3H_8]^-$, forms metal complexes by displacement of coordinated ligands[3,40] as described in Chapter 1. In this section a convenient and versatile route to metallaborane complexes of substituted derivatives of the octahydrotriborate (1-) ion is described. It has been found that reaction of $Cu(PPh_3)_2(BH_4)$ with the salts $[N(PPh_3)_2][B_3H_7(X)]$(X = Cl, NCS, NCSe, $NCBPh_3$,NCB_3H_7,$NCBH_3$ and $NCBH_2NCBH_3$) results in the substituted triborane anion displacing the coordinated tetrahydroborate (1-) ion $[BH_4]^-$, to produce the complexes $Cu(PPh_3)_2(B_3H_7X)$ (X = Cl(i), NCS(ii), NCSe(iii), $NCBPh_3$(iv), NCB_3H_7(v), $NCBH_3$(vi) and $NCBH_2NCBH_3$ (vii)). The 115.5 MH_z ^{11}B n.m.r. spectra obtained indicate that two types of complex are formed. For complexes (i) - (v) the copper is bound in a bidentate manner to the triborane cage via two Cu-H-B bridge bonds. For complexes (vi) and (vii) the copper preferentially bonds via two Cu-H-B bonds through the $[BH_3]$ moiety of the ligand.

7.3.2 Results and Discussion

The reaction of $Cu(PPh_3)_2(BH_4)$ and $[N(PPh_3)_2][B_3H_7(X)]$ (X = Cl, NCS, NCSe, $NCBPh_3$, NCB_3H_7, $NCBH_3$ and $NCBH_2NCBH_3$) in dichloromethane resulted in displacement of $[BH_4]^-$ from the copper borohydride complex by the larger triborane anion to produce complexes of the type $Cu(PPh_3)_2(B_3H_7X)$. In all cases the final purified complex was

contaminated to some extent with $Ph_3P.BH_3$ which reflects the instability of the complexes and the relative lability of the phosphine ligands.

(a) N.m.r. Discussion

The 115.5 MH_z ^{11}B n.m.r. spectra of all the complexes, (Table 7.6), resembled those of the free anions indicating that on complexation symmetry is retained. In addition the resonance due to $Ph_3P.BH_3$ was present as a 1:3:3:1 quartet of doublets (δ =-37.8 p.p.m.; J_{BH} = $98H_z$; J_{PB} = $56H_z$).[23] In the complexes the resonances due to the unsubstituted and substituted boron atoms of the triborane fragments were considerably broadened by the quadrupolar effect of the copper nucleus.[166] This broadening is typical of phosphine substituted metallaboranes. In the complexes (iii) - (vii) the chemical shifts of the complexed ^{11}B resonances are virtually identical with those of the free anion. This indicates that the perturbation of the borane cage on complexation is minimal in these complexes. However, in the complex $Cu(PPh_3)_2(B_3H_7Cl)$ the B_2,B_3 and B_1 resonances are respectively shifted 15.1 p.p.m. and 22.4 p.p.m. to lower frequency. This effect may be due to an interaction between the copper and the chloride substituent. The ^{11}B n.m.r. spectrum of $Cu(PPh_3)_2(B_3H_7NCS)$ appears as a very broad singlet centred at δ-29.0 p.p.m. The fluxional protons, of relative area 7, in $Cu(PPh_3)_2(B_3H_7NCS)$ appear at δ 1.11 p.p.m.

The ^{11}B n.m.r. spectra of the complexes in CD_3CN showed that dissociation to form the free ion had occurred as has previously been reported with $[L_3Cu(NCBH_3)]$ and $[L_2Cu(NCBH_3)]_2$,[165] (reaction 7-1).

(b) Infra-red Discussion

The infra-red spectra of the complexes are very similar to those of the free anions in the region 2600 - 1800 cm^{-1}. However, the BH str. modes of the $[BH_3]$ moiety in the complexes, $Cu(PPh_3)_2(B_3H_7NCBH_3)$ and $Cu(PPh_3)_2(B_3H_7NCBH_2NCBH_3)$, are less well defined than those of the free ions. The BH str. modes due to the $[B_3H_7]$ moiety in both complexes and anions are virtually identical. The relevant i.r. absorption frequencies of the complexes are presented in Table 7.7.

7.3.3 Conclusions

Previously the copper complex $Cu(PPh_3)_2(H_3BCNB_3H_7)$ has been prepared electrochemically.[97] In this complex it was shown that the copper of the $Cu(PPh_3)_2$ moiety achieves four coordination by bonding in a bidentate manner through two Cu-H-B bridge bonds to the $[BH_3]$ moiety of the substituent.

Comparison of the ^{11}B n.m.r. and infra-red spectra of the complex obtained via the reaction of $Cu(PPh_3)_2(BH_4)$ with the anion indicates that both complexes are identical. Similarly, in $Cu(PPh_3)_2(B_3H_7NCBH_2NCBH_3)$ the copper is attached through the ligand rather than the cage,as was also observed in the copper complexes of the corresponding substituted nonaborate (1-) ions,$[B_9H_{13}(X)](X = NCBH_3, NCBH_2NCBH_3)$.

The complexes (i) - (v) can be viewed as substituted bidentate metal derivatives in which the metal fragment formally replaces a "wing tip" BH_2^+ in the B_4H_{10} butterfly,[41] in which the exo/endo geometry is retained. The ^{11}B and ^{1}H n.m.r. spectra are consistent with a structure that undergoes pseudorotation in the same way as $Cu(PPh_3)_2(B_3H_8)$ (Chapter 1, page 14). It has been found that in the ^{11}B n.m.r. spectrum of the $Cu(PPh_3)_2(B_3H_7NCB_3H_7)$ complex the resonances due to the N-coordinated cage are broadened to a much greater extent than those of the C-coordinated cage, indicating that complexation is preferentially through the N-coordinated cage. This effect may be due to the enhanced electron density donation from the nitrogen of the cyano group into the N-coordinated cage.

Table 7.6. ^{11}B N.M.R. Data for $Cu(PPh_3)_2(B_3H_7X)$ in $CDCl_3$ at 115.5 MH_z

Substituent	δB(2), B(3)ppm.	δB(1)p.p.m.	Other
Cl	-32.0	-44.0	
NCS	-29.0	-29.0	
$NCBPh_3$	-17.3	-30.4	-11.6 (BPh_3)
NCB_3H_7	-10.0,-14.3*	-33.6,-49.3*	
$NCBH_3$	-12.8	-34.3	-39.9 (BH_3)
$NCBH_2NCBH_3$	-10.0	-34.6	-27.1 (BH_2) -41.4 (BH_3)

*carbon-coordinated cage resonances

Table 7.7 Infra-red Absorption Frequencies for $Cu(PPh_3)_2(B_3H_7X)$

Substituent	2600 - 1900cm^{-1}	Assignment
Cl	2475s 2420m	BHstr.
	2380s	BHstr.
	2120w	BH_b
NCS	2500s 2435sh 2385m	BH str.
	2190s	NC str.
	2120s	BH_b
NCSe	2500s 2470sh 2430m	BH str.
	2180s	NC str.
$NCBPh_3$	2490s 2450sh 2430m	BH str.
	2180s	NC str.
NCB_3H_7	2500s 2440s	BH str.
	2275s	bridge CN str.
$NCBH_3$	2505s 2435s 2380sh	BH str.
	2255m	bridge CN str.
	2160m	BH_B
$NCBH_2NCBH_3$	2500s 2440s 2370s	BH str
	2260s	bridge CN str.
	2160m	BH_b

7.4 Experimental

The substituted derivatives of $[B_3H_8]^-$ were prepared as previously described (Chapter 2).

7.4.1 Preparation of Bis (triphenylphosphine) Copper Complexes Derived from the $[B_3H_8]^-$ ion

Equimolar mixtures of $Cu(PPh_3)_2(BH_4)$ (1 mmol) and $[N(PPh_3)_2][B_3H_7(X)]$(X = Cl, NCS, NCSe, $NCBPh_3$, NCB_3H_7, $NCBH_3$ and $NCBH_2$ $NCBH_3$), (1 mmol), were placed in a 250cm^3 round-bottomed flask fitted with a stopcock adaptor. Dried, degassed dichloromethane (ca.30cm^3) was condensed in under vacuum, and the mixture was warmed to room temperature. After stirring for 4 hr. the solvent was removed under reduced pressure to yield a brown solid when the substituent is Cl, NCS or NCSe and a white solid when the substituent is $NCBPh_3$, NCB_3H_7, $NCBH_3$ or $NCBH_2NCBH_3$. T.l.c. on silica gel using 100% dichloromethane as eluant in each case, indicated the presence of a single major component (Rf = 0.80 - 0.85). Purification by chromatography on silica gel using 100% CH_2Cl_2 as eluant gave the complexes (i) - (vii) in good yield (43 - 85%). The ^{11}B n.m.r. spectra and the analytical data obtained indicated complexes of the type $Cu(PPh_3)_2(B_3H_7X)$ that are contaminated with $PPh_3.BH_3$.

7.5 Manganese Metallaboranes Derived from Substituted Derivatives of $[B_9H_{14}]^-$

7.5.1 Introduction

The reaction between arachno- $[B_9H_{14}]^-$ and $Mn(CO)_5Br$ in tetrahydrofuran has been shown to yield the ten atom nido - [6 - $(CO)_3$ - 6

-$MnB_9H_{13}]^-$ anion with small amounts of {2-[THF]-6-$(CO)_3$-6-MnB_9H_{12}} also being produced.[77] Two equivalents of $Mn(CO)_5Br$ reacted with $[B_9H_{14}]^-$ to form the structural isomer{7-[THF]-6-$(CO)_3$-6-MnB_9H_{12}}.[77] In an earlier work[99] the reactions between $Mn(CO)_5Br$ and the substituted nonaborane anions, $[B_9H_{13}(NCS)]^-$ and $[B_9H_{13}(NCBH_3)]^-$, were investigated. The reaction with $[B_9H_{13}(NCS)]^-$ gave the substituted <u>nido-</u> anion{7-[NCS]-6-$(CO)_3$-6-MnB_9H_{12}}$^-$ which is the structural analogue of{7-[THF]-6-$(CO)_3$-6-MnB_9H_{12}}.[78]

In this work the reactions between $Mn(CO)_5Br$ and the other substituted higher borane anions, $[B_9H_{13}(NCBPh_3)]^-$,$[B_9H_{13}(NCSe)]^-$ and $[B_9H_{13}(NCBH_2NCBH_3)]^-$ have also been investigated. It was of interest to discover if these reactions would occur with retention of the substituent. The position of the substituent on the borane cage relative to the metal in the metallaborane product was also of interest.

7.5.2 Results and Discussion

The reaction between $[B_9H_{13}(NCBH_2NCBH_3)]^-$ and $Mn(CO)_5Br$ in refluxing tetrahydrofuran produced a yellow crystalline solid. The ^{11}B n.m.r. spectrum (Table 7.8) of the solid revealed the presence of a nonaborane derivative that retained the C_s symmetry of the anion. The quartet exhibited by the $[BH_3]$ moiety of the anion was not present in the metalla derivative. However, close examination of the relative intensities of the resonances in the ^{11}B n.m.r. spectrum

of the yellow solid revealed that the $[BH_2]$ moiety of the substituent was present. The infra-red spectrum (Table 7.9) indicated that the compound obtained was a $[N(PPh_3)_2]^+$ salt, bands were also observed in the region $1900cm^{-1}$ to $2200cm^{-1}$ which were attributable to the carbonyl ligands attached to manganese.

The $[B_9H_{13}(NCBH_2NCBH_3)]^-$ anion can be visualised as a substituted derivative of $[BH_4]^-$. Relatively little is known about manganese tetrahydroborate $Mn(CO)_5BH_4$ due to the instability[171,172] of the species. The compound decomposes at 25°C to yield other carbonyl borane species such as $Mn_3(CO)_{10}(BH_3)_2H$.[172] It is proposed that in the reaction of $[B_9H_{13}(NCBH_2NCBH_3)]^-$ with $Mn(CO)_5Br$ a cleavage reaction takes place to produce $[B_9H_{13}(NCBH_2NC)]^-$ and some carbonyl borane species such as $Mn_3(CO)_{10}(BH_3)_2H$ or BH_3CO. The isocyanide of the nonaborane anion then attacks any available $Mn(CO)_5Br$ replacing the bromide with isocyanide to produce $[B_9H_{13}(NCBH_2NC)Mn(CO)_5]^-$ or alternatively, replacing carbonyl with isocyanide to produce $[B_9H_{13}(NCBH_2NC)Mn(CO)_4Br]$. Similar behaviour was observed with the anion $[B_9H_{13}(NCBH_3)]^-$.[99]

The ^{11}B n.m.r. spectrum (Table 7.8) of the product obtained from the reaction between $[B_9H_{13}(NCBPh_3)]^-$ and $Mn(CO)_5Br$ in refluxing T.H.F. showed that the C_s symmetry exhibited by the anion is retained on formation of the complex in solution. The infra-red spectrum (Table 7.9) of the complex indicated that the complex was a $[N(PPh_3)_2]^+$ salt. Bands attributable to carbonyl ligands on the manganese centre

Table 7.8 ^{11}B N.M.R. Spectral Data for Manganese Complexes at 115.5 MH_z in $CDCl_3$

Derivative	$\delta^{11}B$ (p.p.m.)	$J_{B-H}(H_z)$	Int	Assignment
$[B_9H_{13}(NCBH_2NC)]^-$	17.41	-	1	7
	5.11	138.6	1	1
	14.8	-	2	5,9
	-20.07	-	2	6,8
	-27.04	-	2	4,BH_2
	-38.59	142.1	2	2,3
$[B_9H_{13}(NCBPh_3)]^-$	15.74	-	1	7
	5.22	-	1	1
	-10.57	-	1	BPh_3
	-15.04	134.0	2	5,9
	-19.49	-	2	6,8
	-25.29	-	1	4
	-38.52	146.1	2	2,3
$[B_9H_{13}(NCSe)]^-$	16.4	-	1	7
	5.4	138.0	1	1
	-15.2	-	2	5,9
	-18.8	-	2	6,8
	-24.8	-	1	4
	-38.8	138.0	2	2,3

are observed between 1800cm^{-1} and 2100cm.$^{-1}$ In this case the cleavage reaction cannot occur since the hydrogen atoms on the BH_3 moiety, which would bridge to Mn, have been replaced by the relatively large phenyl rings. The manganese centre therefore must complex through the nonaborane cage in the same way as [6 - $(CO)_3$ - 6 - $MnB_9H_{13}]^{-77}$ i.e., with an $[Mn(CO)_3]^+$ unit formally replacing a $[BH_2]^+$ unit at the six position in $B_{10}H_{14}$ to give [6 - $(CO)_3$ - Mn - $B_9H_{12}(NCBPh_3)]^-$. The proposed structure is shown in Figure 7.9.

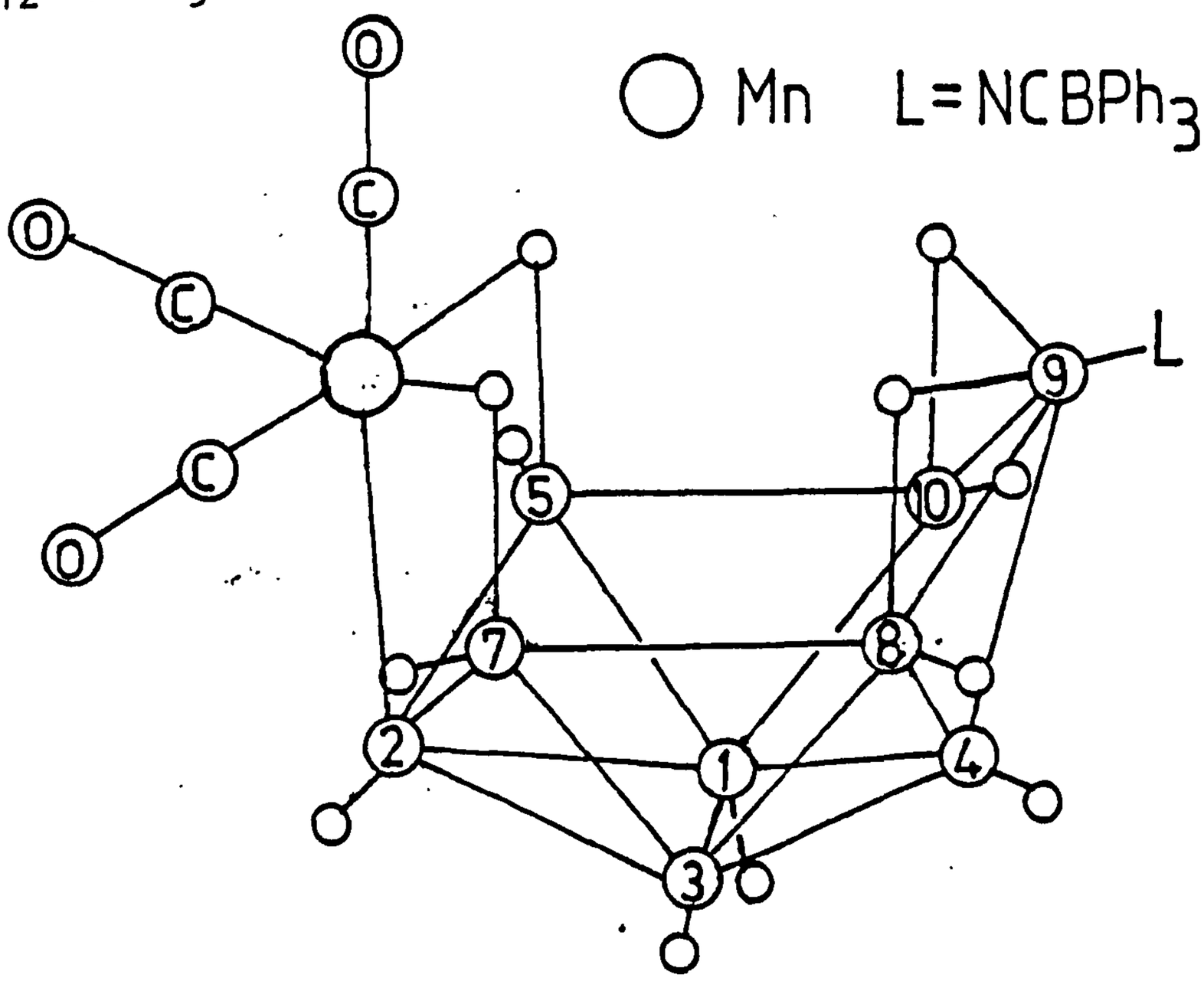

Figure 7.9

In addition to $[B_9H_{13}(NCS)]^{-99}$ it was thought that the reaction of $[B_9H_{13}(NCSe)]^-$ and $Mn(CO)_5Br$ in refluxing T.H.F. would produce the asymmetrically substituted metallaborane [7-(NCSe)-6-$Mn(CO_3)$ $B_9H_{12}]^-$. However, the ^{11}B n.m.r. spectrum (Table 7.8) of the complex formed with $[B_9H_{13}(NCSe)]^-$ indicated retention of the C_s symmetry of the cage in the complex. The infra-red spectra (Table 7.9) again

Table 7.9 Infra-red Absorption Frequencies of Manganese Derivatives as Nujol Mulls

Derivative	Absorption	Assignment
$[B_9H_{13}(NCBH_2NC)]^-$	2540s	BH_t of B_9H_{13}
	2420s	BH_t of BH_2
	2255s	bridge CN
	2190s, 2170sh	
	2120w, 2070sh	Carbonyl bands
	1960s	
$[B_9H_{13}(NCBPh_3)]^-$	2540s	BH_t of B_9H_{13}
	2250s	bridge CN
	2190s 2100s	
	2050sh 2020s	Carbonyl bands
	1960s	
$[B_9H_{13}(NCSe)]^-$	2540s	BH_t of B_9H_{13}
	2180s	CNstr.
	2190s 2120s	
	2050sh 2020s	Carbonyl bands

indicated that the complex was a $[N(PPh_3)_2]^+$ salt with bands attributable to the carbonyl ligands attached to the Mn centre between $1800cm^{-1}$ and $2100cm^{-1}$. Since there is no evidence of the formation of manganese selenide, MnSe, by cleavage of SeCN by manganese it is proposed that the manganese is again bonded through the nonaborane cage to produce $[6\text{-}(CO)_3\text{-}Mn\text{-}B_9H_{12}(NCSe)]^-$.

7.5.3 Experimental

$[N(PPh_3)_2][B_9H_{13}(NCBH_2NCBH_3)]$, $[N(PPh_3)_2][B_9H_{13}(NCBPh_3)]$ and $[N(PPh_3)_2][B_9H_{13}(NCSe)]$ were prepared as described in Chapter 4. $Mn(CO)_5Br$ was a gift from Professor D F Gaines, Wisconsin.

7.5.4 Reaction between $[B_9H_{13}(NCBH_2NCBH_3)]^-$ and $Mn(CO)_5Br$

$[N(PPh_3)_2][B_9H_{13}(NCBH_2NCBH_3)]$ (1.18g, 1.62 mmol) and $Mn(CO)_5Br$ (0.61g, 2.22 mmol) were placed in a three-necked, round-bottomed, flask flushed with dry nitrogen. THF (ca. 40cm^3) was added and the solution was heated to reflux for 4 hr. after which time a white precipitate had formed. The precipitate was filtered and the orange filtrate was collected and the solvent was removed under reduced pressure to yield an orange solid. T.l.c. analysis on silica gel using 100% CH_2Cl_2 as eluant indicated the presence of a single major component (Rf = 0.62), and other minor components (Rf = 0.47). The residue was purified by chromatography on silica gel using 100% CH_2Cl_2 as eluant. The single major component was collected and the solvent was removed under vacuum to yield a yellow crystalline solid in low yield which was examined by ^{11}B n.m.r. spectroscopy.

7.5.6 Reaction Between $[B_9H_{13}(NCBPh_3)]^-$ and $Mn(CO)_5Br$

$[N(PPh_3)_2][B_9H_{13}(NCBPh_3)]$ (1.87g, 2 mmol) and $Mn(CO)_5Br$ (0.56g, 2 mmol) were charged to a nitrogen flushed three-necked, round-bottomed, flask. Dry THF (ca. 40cm^3) was added and the solution was heated to reflux for 3 hr. The resulting pale yellow solution was cooled and the solvent was removed under reduced pressure to

yield a pale yellow oil. T.l.c. analysis of the oil on silica gel using 100% CH_2Cl_2 as eluant indicated two major products (Rf = 0.71, 0.51). Purification by column chromatography on silica gel using 100% CH_2Cl_2 as eluant yields unreacted starting material (Rf = 0.71) and a yellow oil (Rf = 0.51) in low yield that was examined by i.r. and ^{11}B n.m.r. spectroscopy.

7.5.7 Reaction Between $[B_9H_{13}(NCSe)]^-$ and $Mn(CO)_5Br$

$[N(PPh_3)_2][B_9H_{13}(NCSe)]$ (0.75g, 1 mmol) and $Mn(CO)_5Br$ (0.30g, 1.1 mmol) are charged to a nitrogen flushed three-necked, round-bottomed, flask. Dry THF (ca. $40cm^3$), was introduced and the solution was refluxed for 1.5 hr. The resulting red solution was cooled to room temperature and the solvent was removed under reduced pressure to yield a red oil. T.l.c. analysis of the red oil on silica gel using 100% CH_2Cl_2 as eluant indicated a single major component (Rf = 0.70). The oil was purified by chromatography on silica gel using 100% CH_2Cl_2 as eluant. The solvent was removed under reduced pressure to give a red solid in low yield which was examined by i.r. and ^{11}B n.m.r. spectroscopy.

CHAPTER EIGHT

EXPERIMENTAL TECHNIQUES

8.1 Experimental Techniques

8.1.1 General

All reactions were carried out under vacuum or in an inert atmosphere of dry nitrogen. No rigorous attention was paid to maintaining anaerobic or anhydrous conditions during work up unless stated. Most crystalline solids were reasonably air-stable. Less stable solids were stored under nitrogen.

8.1.2 Vacuum Line and Glove Box

Standard vacuum line, inert atmosphere and glove box techniques were employed and these have been described previously.[177]

8.1.3 Chromatographic Techniques

Thin layer chromatography (t.l.c.) was carried out on plates made in the laboratory as required from silica gel [Kieselgel 60G (Merck)]. The dimensions of the columns and the quantity of silica gel used for liquid chromatography were determined by the quantity of material to be separated, and the Rf values of individual components. The eluant from the columns was monitored by t.l.c. Solvents used in liquid chromatography were reagent grade and were used without further purification.

8.1.4 Solvents

Most solvents were dried and purified before use.

Dichloromethane and 1,2-dichloroethane	Dried over CaH_2 and distilled before use.

Diethylether and Tetrahydrofuran	Dried over Na and distilled from Na/benzophenone before use.
n-hexane	Dried over Na and distilled before use.
Acetonitrile	For non-electrochemical use, dried over CaH_2 and distilled before use.

8.2 Spectroscopic Techniques

8.2.1 Infra-red Spectroscopy

The infra-red spectra were obtained as nujol or hexachloro-1,3-butadiene mulls or as thin films between KBr plates. Spectra were recorded on a Perkin-Elmer 457 Grating Infra-red Spectrometer.

8.2.2 Nuclear Magnetic Resonance Spectroscopy

250 MH_z ^{1}H and 80.24 MH_z ^{11}B n.m.r. spectra were recorded on a Bruker WH-250 spectrometer. 360 MH_z ^{1}H and 115.5 MH_z ^{11}B n.m.r. spectra were recorded on a Bruker WH-360 spectrometer. Lock was achieved in these cases by the use of a deuterated solvent. Chemical shifts are quoted as being negative to low frequency of the reference standards which were tetramethylsilane for ^{1}H n.m.r. and $BF_3O(Et)_2$ for ^{11}B n.m.r. All spectra were recorded at ambient temperature unless otherwise stated.

8.3 Electrochemical Techniques

8.3.1 Equipment

The equipment for cyclic voltammetry consisted of a Hi-Tek Instruments Potentiostat Type DT 2101, and a Wave-form Generator Type PPR1. The voltammograms were recorded on a Bryans Southern Instruments Ltd. Model 25000 XY-t recorder. Scan rates were usually $0.5Vs^{-1}$ for cyclic voltammetry and $0.05Vs^{-1}$ for cyclic a.c. volta-mmetry. A signal averager (Hi-Tek Type AAI) was used for cyclic voltammetry at high scan rates.

In addition, for cyclic a.c. voltammetric studies a home built variable frequency a.c. generator and phase sensitive detector with associated reference phase shifter and amplifiers was also used.

For preparative controlled potential electrolysis experiments a Hi-Tek Instruments Gated Digital Integrator and D.V.M. recorded the total current passed. The current was also monitored on a Servoscribe Chart Recorder measuring the voltage drop across a Decade resistance box in series with the cell.

8.3.2 Cell Design

(a) Cyclic Voltammetry and A.C. Voltammetry

The cell was of a simple one compartment design. The working electrode was generally the metal wire under examination and it was coated in Teflon tape or mounted in a glass tube to expose only a small area to the solution. The secondary electrode was a coil of platinum wire. The reference electrode was constructed from a capillary tube, which was mounted close to the working electrode.

The reference solution, [Ag/$AgNO_3$(0.1mol dm^{-3}; CH_3CN)] or Ag/[$N(PPh_3)_2$]Cl (0.1 mol dm^{-3}; CH_2Cl_2)] was separated from the bulk solution by a porous ceramic sinter. The reference electrode potential was found to be +0.366 ± 0.005V vs the S.C.E. for the acetonitrile solution. A stream of dry nitrogen was passed over the solution under examination.

(b) Controlled Potential Electrolysis

The cell for preparative scale controlled potential electrolysis experiments was a two compartment U-shaped design. The anode and cathode compartments were separated by a cation exchange membrane (Nafion 427). This was generally exchanged to the appropriate cation form by soaking in a solution of a salt containing that cation. The working electrode was the metal under examination and the secondary electrode was usually platinum foil. The reference electrode was identical to that described in sect. 8.3.2(a). The anolyte was stirred magnetically and nitrogen was passed over both the anode and the cathode solutions. The passage of current in the cell was improved by increasing the surface area of the electrodes and optimising the electrode positions.

8.3.3 Metals, Solvents and Reagents

The metal wires were the purest supplied by Koch-Light, i.e., Co, Cu, Au, Zn, Ni, Fe (better than 99.997%), Pd(99.99%), Ta, Ti, W, (99.9%), Nb, Zr (99.5%), Goodfellow metals, V(99.8%) and Fisons, Pt, Ag (99.9%).

Acetonitrile for electrochemistry, Fisons H.P.L.C. (Far U.V. grade) was stored under nitrogen and was used without further purification.

Supporting electrolytes included $[NBu^n_4][BF_4]$ and $[N(PPh_3)_2]Cl$. Solutions were generally prepared in acetonitrile or dichloromethane (0.1 mol dm^{-3}) and their purities were conveniently monitored by cyclic voltammetry at an inert electrode (e.g. platinum).

REFERENCES

1 (a) R. Schaeffer and F. Tebbe, J.Am.Chem.Soc., 1962, 84, 3974.

(b) D.F. Gaines and R. Schaeffer, Inorg.Chem., 1964, 3, 438.

(c) J. Dobson, D.F. Gaines and R. Schaeffer, J.Am.Chem.Soc., 1965, 87, 4072.

2 (a) I.A. Ellis, D.F. Gaines and R. Schaeffer, J.Am.Chem.Soc., 1963, 85, 3885.

(b) G.B. Dunks and K.P. Ordonez, Inorg.Chem., 1978, 17, 1514.

(c) H.C. Miller, N.E. Miller and E.L. Muetterties, Inorg.Chem., 1964, 3, 1456.

3 (a) S.J. Lippard and D.A. Ucko, Inorg.Chem., 1968, 7, 1051.

(b) F. Klanberg, E.L. Muetterties and L.J. Guggenberger, Inorg. Chem., 1968, 7, 2272.

4 (a) L.J. Edwards, W.V. Hough and A.D. McElroy, J.Am.Chem. Soc., 1956, 78, 689.

(b) L.J. Edwards, W.V. Hough and A.D. McElroy, J.Am.Chem. Soc., 1958, 80, 1828.

5 (a) K.C. Nainan and G.E. Ryschkewitsch. Inorg.Nucl.Chem.Lett., 1970, 6, 765.

(b) K.C. Nainan and G.E. Ryschkewitsch, Inorg.Synth., 1974, 15, 113.

6 D.F. Gaines, R. Schaeffer and F. Tebbe, Inorg.Chem., 1963, 2, 526.

7 H.C. Miller and E.L. Muetterties, Inorg.Synth., 1967, 10, 81.

8 W.J. Dewkett, M. Grace and H. Beall, J.Inorg.Nucl.Chem., 1971, 33, 1279.

9 E.B. Baker, R.B. Ellis and W.S. Wilcox, J.Inorg.Nucl.Chem., 1961, 23, 41.

10 D.F. Gaines, Inorg.Chem., 1963, 2, 523.

11 G. Kodama and R.W. Parry, J.Am.Chem.Soc., 1960, 82, 6250.

12 L.J. Edwards, M.D. Ford and W.V. Hough, Callery Chemical Company under Contract No. Noa(s) 52-1024-TR-214[cited as reference 320 in Holzmann et al, "Production of the Boranes and Related Research," p.252, Academic Press, New York, 1967].

13 B.M. Graybill, J.K. Ruff and M.F. Hawthorne, J.Am.Chem. Soc., 1961, 83, 2669.

14 R.B. Cruickshank, W.V. Hough, M.D. Marshall and A.D. McElroy, Callery Chemical Company Final Report No. NOw 60 - 0168-c, 1962 [cited as reference 404 in Holzmann et al ., (P.252)].

15 C.R. Peters and C.E. Nordman, J.Am.Chem.Soc., 1960, 82, 5758.

16 W.N. Lipscomb "Boron Hydrides," W.A. Benjamin, New York, N.Y., 1963, pp 43-49.

17 (a) W.N. Lipscomb, Advan.Inorg.Chem.Radiochem., 1959, 1, 117.

(b) W.N. Lipscomb, "Boron Hydrides," W.A. Benjamin, New York, N.Y., 1963, pp 127-128.

(c) H.C. Miller, E.L. Muetterties and W.D. Phillips,J.Am.Chem. Soc., 1959, 81, 4496.

(d) A. Norman and R. Schaeffer, J.Phys.Chem., 1966, 70, 1662.

(e) H. Beall, C.H. Bushweller, W.J. Dewkett and M. Grace, J.Am.Chem.Soc., 1970, 92, 3484.

(f) D. Marynick and T. Onak, J.Chem.Soc.A., 1970, 1160.

18 (a) L.J. Edwards and W.V. Hough, Abstr.Pap.Congr.Int.Chem.Pure Appl., 16th, Phys.Inorg.Div., 1957, p 158.

(b) L.J. Edwards, M.D. Ford and W.V. Hough, Abstr.132nd. Meet.Amer.Chem.Soc., New York, 1957, p 15N.

(c) W.V. Hough, M.D. Ford and L.J. Edwards, Callery Chemical Company under Contract No. Noa (s) 52-1024-TR-199 [cited as reference 311 in Holzmann et al., (p.254)].

(d) W.V. Hough, M.D. Ford and A.D. McElroy, Callery Chemical Company under Contract No. Noa(s) 52-1024-TR-274 [cited as reference 348 in Holzmann et al., (p 254)].

(e) L.J. Edwards, W.V. Hough and M.D. Ford,Z.Angew.Chem., 1957, 69, 678.

19 E.R. Lory and D.M. Ritter, Inorg.Chem., 1971, 10, 939.

20 (a) M.A. Fleming, Diss.Abstr., 1963, 24, 1385.

20 (b) S. Fleming and R.W. Parry, Inorg.Chem., 1972, 11, 1

21 R.W. Parry and L.J. Edwards, J.Am.Chem.Soc., 1959, 81,3554.

22 (a) W. R. Deever and D.M. Ritter, Inorg.Chem., 1968, 7, 1036.

(b) R.W. Parry, R.W. Rudolph and D.M. Shriver, Inorg.Chem., 1964, 3, 1479.

23 B.M. Graybill and J.K. Ruff, J.Am.Chem.Soc., 1962, 84, 1062.

24 (a) G. Kodama, R.W. Parry and J.C. Carter, J.Am.Chem.Soc., 1959, 81, 3534.

(b) N.E. Levitin, E.F. Westrum Jr. and J.C. Carter, J.Am.Chem. Soc., 1959, 81, 3547.

25 J. Spielman and A.B. Burg, Inorg.Chem., 1963, 2, 1139.

26 W.R. Deever and D.M. Ritter, J.Am.Chem.Soc., 1967,89, 5073.

27 (a) R.T. Paine and R.W. Parry, Inorg.Chem., 1972, 11, 268.

(b) J.D. Glore, J. Rathke and R. Schaeffer, Inorg.Chem., 1973, 12, 2175.

28 (a) M.A. Ring, E. Witucki and R.C. Greenough, Inorg.Chem., 1967, 6, 695.

(b) W.J. Dewkett, H. Beall and C.H. Bushweller, Inorg.Nucl. Chem.Lett., 1971, 7, 633.

29 V.L. Bishop and G. Kodama, Inorg.Chem., 1981, 20, 2724.

30 G. Kodama,. Inorg.Chem., 1975, 14, 452.

31 L.D. Brown and W.N. Lipscomb, Inorg.Chem., 1977, 16, 1.

32 V.R. Miller and G.E. Ryschkewitsch, J.Am.Chem.Soc., 1975, 97, 6258.

33 V.R. Miller and G.E. Ryschkewitsch, Inorg.Synth., 1974, 15, 118.

34 V.D. Aftandilian, H.C. Miller and E.L. Muetterties, J.Am. Chem.Soc., 1961, 83, 2471.

35. W.L. Jolly, J.W. Reed and F.T. Wang, Inorg.Chem., 1979, 18, 377.

36 G.B. Jacobsen and J.H. Morris, Inorg.Chim.Acta., 1982, 59, 207.

37 M. Arunchaiya, J.H. Morris, S.J. Andrews, D.A. Welch and A.J. Welch, J.Chem.Soc. Dalton Trans., 1984,2525.

38 S.J. Andrews, A.J. Welch, G.B. Jacobsen and J.H. Morris, J.Chem.Soc.Chem.Commun., 1982, 749.

39 C.E. Nordman and C. Reimann, J.Am.Chem.Soc., 1959, 81, 3538.

40 J. Borlin and D.F. Gaines, J.Am.Chem.Soc., 1972, 94, 1367.

41 P.A. Wegner in "Boron Hydride Chemistry" (E.L. Muetterties, ed.) p 431, Academic Press, New York, 1975.

42 L.J. Guggenberger, Inorg.Chem., 1970, 9, 367.

43 F. Klanberg and L.J. Guggenberger, J.Chem.Soc.Chem. Commun., 1967, 1293.

44 S.J. Lippard and K.M. Melmed, Inorg.Chem., 1969, 8, 2755.

45 E.L. Muetterties, W.G. Peet, P.A. Wegner and C.W.Alegranti Inorg.Chem., 1970, 9, 2447.

46 C.H. Bushweller, H. Beall, M. Grace, W.J. Dewkett and H.S. Bilofsky, J.Am.Chem.Soc., 1971, 93, 2145.

47 D.F. Gaines and S.J. Hildebrandt, Inorg.Chem., 1978, 17, 794.

48 D.F. Gaines and J.H. Morris, J.Chem.Soc.Chem.Commun., 1975, 626.

49 J.C. Calabrese, D.F. Gaines, S.J. Hildebrandt and J.H., Morris, J.Am.Chem.Soc, 1976, 98, 5489.

50 J.C.Calabrese, D.F. Gaines and S.J. Hildebrandt, Inorg.Chem. 1978, 17, 790.

51 J.C. Calabrese, M.B. Fischer, D.F. Gaines and J.W. Lott, J.Am.Chem.Soc., 1974, 96, 6318.

52 M.W. Chen, D.F. Gaines and L.G. Hoard, Inorg.Chem.,1980, 19, 2989.

53 H.D. Kaesz, W. Fellman, G.R. Wilkes and L.F. Dahl, J.Am. Chem.Soc., 1965, 87, 2753.

54 R.K. Hertz, R. Goetze and S.G. Shore, Inorg.Chem., 1979, 18, 2813.

55 A.R. Kane and E.L. Muetterties, J.Am.Chem.Soc., 1971, 18, 2813.

56 L.J. Guggenberger, A.R. Kane and E.L. Muetterties, J.Am. Chem.Soc., 1972, 94, 5665.

57 L.E. Benjamin, S.F. Stafiej and E.A. Takacs, J.Am.Chem. Soc., 1963, 85, 2674.

58 S.K. Boocock, N.N. Greenwood, M.J. Hails, J.D. Kennedy and W.S. McDonald, J.Chem.Soc.Dalton Trans., 1981, 1415.

59 C.G. Savory and M.G.H. Wallbridge, Inorg.Chem., 1971, 10, 419.

60 C.G. Savory and M.G.H. Wallbridge, J.Chem.Soc., A,1973,179.

61 N.N. Greenwood, J.A. McGinnety and J.D. Owen, J.Chem. Soc., A, 1972, 1963.

62 N.N. Greenwood, H.J. Gysling J.A. McGinnety and J.D. Owen, J.Chem.Soc.Chem.Commun., 1970, 505.

63 P.C. Keller, Inorg.Chem., 1970, 9, 75.

64 J. Dobson, P.C. Keller and R. Schaeffer, Inorg.Chem., 1968, 7, 399.

65 F.E. Wang, P.G. Simpson and W.N. Lipscomb, J.Chem.Phys., 1961, 35, 1335.

66 (a) E.L. Muetterties and F. Klanberg, Inorg.Chem., 1966, 5, 315.

(b) B.M. Graybill, A.R. Pitochelli and M.F. Hawthorne, Inorg. Chem., 1962, 1, 626.

67 S. Hermanek, J. Plesek, B. Stibr and F. Hanousek, Collect. Czech.Chem.Commun., 1968, 33, 2177.

68 E.L. Muetterties and W.H. Knoth, Inorg.Chem., 1965, 4, 1498.

69 E.L. Muetterties and V.D. Aftandilian, Inorg.Chem., 1962, 1, 731.

70 B. Stibr, J. Plesek and S. Hermanek, Collect.Czech.Chem. Commun., 1969, 34, 3241.

71 G.M. Bodner, F.R. Scholer, L.J. Todd, L.E. Senor and J.C. Carter, Inorg.Chem., 1971, 10, 942.

72 (a) V. Subrtova, Collect.Czech.Chem.Commun., 1971, 36, 4034.

72 (b) J. Plesek, S. Hermanek and B. Stibr, Collect.Czech.Chem. Commun., 1970, 35, 344.

73 J. Plesek, S. Hermanek, B. Stibr and F. Hanousek, Collect. Czech.Chem.Commun., 1967, 32, 1095.

74 J. Plesek, S. Hermanek and F. Hanousek, Collect.Czech. Chem.Commun., 1968, 33, 699.

75 R. Schaeffer and E. Walter, Inorg.Chem., 1973, 12, 2209.

76 R.R. Rietz, R. Schaeffer and L.G. Sneddon, J.Am.Chem.Soc., 1970, 92, 3514.

77 J.W. Lott and D.F. Gaines, Inorg.Chem., 1974, 13, 2261.

78 D.F. Gaines, J.W. Lott and J.C. Calabrese, Inorg.Chem., 1974, 13, 2419.

79 (a) V.R. Miller and R.N. Grimes, J.Am.Chem.Soc., 1973,95, 5078.

(b) J.R. Pipal and R.N. Grimes, Inorg.Chem., 1977, 16, 3251.

80 W.N. Lipscomb, "Boron Hydrides", W.A. Benjamin, New York, N.Y., 1963, p 187.

81 A.R. Siedle, G.M. Bodner, A.R. Garber and L.J. Todd, Inorg.Chem., 1974, 13, 1756.

82 L.J. Todd and A.R. Siedle, Prog.N.M.R. Spectrosc., 1979, 13, 87.

83 C.K. Nelson (Ph.D.Thesis), Diss.Abs.Int., 1983,43, 2549.

84 A.J. Bard and L.R. Faulkner, "Electrochemical Methods Fundamentals and Applications," John Wiley and Sons, New York, 1980.

85 W.H. Schechter, U.S. patent, 1962, 3,033,766

86 H.R. Hoekstra, U.S. Atomic Energy Commission Report, A.E.C.D., 1949, 2144.

87 R.K. Birdwhistell, H.E. Ulmer and L.L. Quill, U.S. patent 2,876,179 March 3, 1959.

88 W.H. Schechter, R.M. Adams and G.F. Ruff, British patent 826,558, January 13, 1960.

89 L.A. Melcher, I.A. Boenig and K. Niedenzu, Inorg.Chem., 1973, 12, 487.

90 J.H. Morris and D. Reed, J.Chem.Res., 1980, (S) 282; (M) 3567.

91 A. Drummond, J.F. Kay, J.H. Morris and D. Reed, J.Chem. Soc.Dalton Trans., 1980, 284.

92 (a) J.H. Morris and D. Reed, J.Chem.Res., 1980, (S) 378; (M) 4522,

(b) J.H. Morris and D. Reed, Inorg.Chim.Acta, 1981, 54, L7.

93 J.F. Kay, J.H. Morris and D. Reed, J.Chem.Soc.Dalton Trans., 1980, 1917.

94 B.Gyori, J. Emri and I. Feher, J.Organomet.Chem., 1983, 255, 17.

95 P.J. Dolan, J.H. Kindsvater and D.G. Peters, Inorg.Chem., 1976, 15, 2170.

96 B.G. Cooksey, J.D. Gorham, J.H. Morris and L. Kane, J. Chem.Soc.Dalton Trans., 1978, 141.

97 G.B. Jacobsen, J.H. Morris and D. Reed, J.Chem.Res., 1982, (M), 3601.

98 N.N. Greenwood and H.J. Gysling, unpublished results.

99 G.B. Jacobsen, Ph.D. Thesis, Strathclyde University, 1982.

100 E.B. Rupp, D.E. Smith and D.F. Shriver, J.Am.Chem.Soc., 1967, 89, 5562.

101 D.E. Smith, E.B. Rupp and D.F. Shriver, J.Am.Chem.Soc., 1967, 89, 5568.

102 J.Q. Chambers, A.D. Norman, M.R. Bickell and S.H. Cadle, J.Am.Chem.Soc., 1968, 90, 6056.

103 R.H. Toeniskoetter, Ph.D. Thesis, St. Louis University, 1958.

104 R.M. Adams, Adv.Chem.Ser., 1961, 32, 184.

105 J.H. Morris and D. Reed, J.Chem.Research, 1980, (S), 380.

106 F. Klanberg, D.R. Eaton, J.J. Guggenberger and E.L. Muetterties, Inorg.Chem., 1967, 6, 1271.

107 E.L. Muetterties, J.H. Balthis, Y.T. Chia, W.H. Knoth and H.C. Miller, Inorg.Chem., 1964, 3, 444.

108 F.Klanberg and E.L. Muetterties, Inorg.Chem., 1966, 5, 1955.

109 E.L. Muetterties and W.H. Knoth, "Polyhedral Boranes", Marcel Dekker, Inc., New York, 1968, p 103.

110 W.H. Knoth, H.C. Miller, J.C. Sauer, J.H. Balthis, Y.T. Chia and E.L. Muetterties, Inorg.Chem., 1964, 3, 159.

111 W.H. Knoth, J.C. Sauer, D.C. England, W.R. Hertler and E.L. Muetterties J.Am.Chem.Soc., 1964, 86, 3973.

112 R.L. Middaugh and F. Farha Jr., J.Am.Chem.Soc., 1966, 88, 4147.

113 A. Kaczmarczyk, R.D. Dobrott and W.N. Lipscomb, Proc. Natl.Acad.Sci.U.S., 1962, 48, 729.

114 A.R. Pitochelli, W.N. Lipscomb and M.F. Hawthorne, J.Am. Chem.Soc., 1962, 84, 3026.

115 M.F. Hawthorne, R.L. Pilling, P.F. Stokely and P.M. Garret, J.Am.Chem.Soc., 1963, 85, 3704.

116 B.L. Chamberland and E.L. Muetterties, Inorg.Chem., 1964, 3, 1450.

117 M.F. Hawthorne, R.L. Pilling and P.F. Stokely, J.Am.Chem. Soc., 1965, 87, 1893.

118 R.J. Wiersma and R.L. Middaugh, J.Am.Chem.Soc., 1967, 89, 5078.

119 R.J. Wiersma and R.L. Middaugh, Inorg.Chem., 1969, 8, 2074.

120 R.J. Wiersma and R.L. Middaugh, J.Am.Chem.Soc., 1970, 92, 223.

121 (a) J.D. Baldeschwieler and E.W. Randall, Chem.Rev., 1963, 63, 81.

(b) R.A. Hoffman and S. Forsen, Nucl.Magn.Reson., 1966, 1, 15.

122 (a) J.Jeener, Ampere International Summer School, Basko Polje, Yugoslavia, unpublished results.

(b) A. Bax, R. Freeman and G. Morris, J.Magn.Reson., 1981, 42, 164.

(c) A.D. Bain, R.A. Bell, J.R. Everett and D.W. Hughes, Can. J.Chem., 1980, 58, 1947.

122 (d) K. Nagayama, K. Wuthrich and B.R. Ernst, Biochem.Biophys. Res.Commun., 1970, 90, 305.

(e) A. Kumar, G. Wagner, R.R. Ernst and K. Wuthrich, Biochem. Biophys. Res. Commun., 1980, 96, 1156.

(f) G. Wagner, A. Kumar and K. Wuthrich, Eur.J.Biochem., 1981, 114, 375.

123 (a) G.R. Eaton and W.N. Lipscomb "N.M.R. Studies of Boron Hydrides and Related Compounds", Benjamin, New York, 1969.

(b) L.J. Todd and A.R. Siedle, Prog.Nucl.Magn.Reson.Spectrosc., 1979, 13, 87.

(c) A.R. Siedle, Ann.Rep.N.M.R.Spectrosc., 1982, 12, 177.

124 R.Weiss and R.N. Grimes, J.Am.Chem.Soc., 1978, 100, 1401.

125 A.O. Clouse, D.C. Moody, R.R. Rietz, T. Roseberry and R. Schaeffer, J.Am.Chem.Soc., 1973, 95, 2496.

126 (a) N.F. Ramsey, Phys.Rev., 1950, 78, 699.

(b) N.F. Ramsey, Phys.Rev. 1953, 90, 232.

127 (a) T.L. Venable, W.C. Hutton and R.N. Grimes, J.Am.Chem. Soc., 1984, 106, 29.

(b) T.L. Venable, W.C. Hutton and R.N. Grimes, J.Am.Chem. Soc., 1982, 104, 4716.

128 (a) D.C. Finster, W.C. Hutton and R.N. Grimes, J.Am.Chem. Soc., 1980, 102, 400.

(b) I.J. Colquhoun and W. McFarlane, J.Chem.Soc. Dalton Trans., 1981, 2014.

129 (a) T.C. Farrar and E.D. Becker "Pulse and Fourier Transform N.M.R.", Academic Press, New York, 1971.

(b) D. Shaw, "Fourier Transform N.M.R. Spectroscopy", Elsevier, Amsterdam, 1976.

(c) H. Gunther, "N.M.R. Spectroscopy", Wiley, Chichester, 1980.

130 H.C. Torrey, Phys.Rev. 1949, 76, 1059.

131 (a) W.P. Aue, E. Bartholdi and R.R. Ernst, J.Magn.Reson., 1981, 43, 259.

(b) S. Macura, Y. Huang, D. Suter and R.R. Ernst, J.Magn. Reson., 1981, 43, 259.

132 (a) A. Bax, "Two-Dimensional Nuclear Magnetic Resonance in Liquids," Delft University Press, Delft, Holland, 1982.

(b) D.I. Hoult and R.E. Richards, Proc.R.Soc.London,Ser.A., 1975, 344, 311.

133 (a) E. Switkes, R.M. Stevens and W.N. Lipscomb, J.Chem.Phys., 1969, 51, 2085.

(b) E. Switkes, I.R. Epstein, J.A. Tossell, R.M. Stevens and W.N. Lipscomb, J.Am.Chem.Soc., 1970, 92, 3837.

(c) E.A. Laws, R.M. Stevens and W.N. Lipscomb, J.Am. Chem. Soc., 1972, 94, 4467.

(d) R.F. Sprecher and J.C. Carter, J.Am.Chem.Soc., 1973, 95, 2369.

134 R.G. Swisher, E. Sinn and R.N. Grimes, Organometallics, 1983, 2, 506.

135 V.R. Miller, R. Weiss and R.N. Grimes, J.Am.Chem.Soc., 1977, 99, 5646.

136 P. Brint and T.R. Spalding, J.Chem.Soc.Dalton Trans., 1980, 1236.

137 R.L. DeKock and T.P. Fehlner, Polyhedron, 1982, 1, 521.

138 A. Drummond and J.H. Morris, Inorg.Chim.Acta, 1978, 24, 191.

139 D.S. Kendall and W.N. Lipscomb, Inorg.Chem., 1973, 12, 2915.

140 D.S. Kendall and W.N. Lipscomb, Inorg.Chem., 1973, 12, 2920.

141 R.C. Wade, E.A. Sullivan, J.C. Berschied and K.F. Purcell, Inorg.Chem., 1969, 8, 1262.

142 S.J. Andrews and A.J. Welch, Inorg.Chim.Acta, 1984, 88, 153.

143 G.B. Jacobsen, J.H. Morris and D. Reed, J.Chem.Soc.Dalton Trans., 1984, 415.

144 M. Kubo, H. Watanabe, T. Totani and M. Ohtsuru Molec. Phys., 1968, 14, 367.

145 (a) B.S. Krumgal'z and V.V. Trofimova, Zh.Fiz.Khim., 1976, 50, 146.

(b) J.W. Dewitte and A.I. Popov, J.Solution Chem., 1976, 5, 231.

146 M. Suzuki and R. Kubo, Molec.Phys., 1964, 7, 201.

147 S.J. Andrews and A.J. Welch, submitted to Inorg.Chim.Acta, 1985.

148 J. Emri and B. Gyori, J.Chem.Soc.Chem.Commun., 1983,1303.

149 J. Bould, N.N. Greenwood and J.D. Kennedy, J.Chem.Soc. Dalton Trans., (in press).

150 (a) L. Barton, Top.Curr.Chem., 1982, 100, 169.

(b) L. Barton, Top.Curr.Chem., 1982, 100, 184.

151 R.D. Dobrott and W.N. Lipscomb, J.Chem.Phys., 1962, 37, 1779.

152 K. Wade, J.Chem.Soc.Chem.Commun., 1971, 792.

153 D. Reed, J.Chem.Research, (in press).

154 J. Bould, N.N. Greenwood and J.D. Kennedy, Polyhedron, 1983, 2, 1401.

155 W.N. Lipscomb, Inorg.Chem., 1964, 3, 1683.

156 F.S. Swicker, Diss.Abstr.Int.B. 1972, 32, 4474.

157 T.J. Marks and R.J. Kolb, Chem.Revs., 1977, 77, 263, and references therein.

158 (a) J.C. Bommer and K.W. Morse, J.Chem.Soc.Chem.Commun., 1977, 137.

(b) J.L. Atwood, R.D. Rogers, C. Kutal and P.A. Grutsch, J.Chem.Soc.Chem.Commun., 1977, 593.

(c) K.M. Melmed, T.Li, J.J. Mayerle and S.J. Lippard, J.Am. Chem.Soc., 1974, 96, 69.

(d) J.C. Bommer and K.W. Morse, J.Am.Chem.Soc., 1974, 96, 6222.

(e) J.C. Bommer and K.W. Morse, Inorg.Chem., 1979, 18, 531.

159 F. Cariati and L. Naldini, J.Inorg.Nucl.Chem., 1966, 28, 2243.

160 (a) F. Cariati and L. Naldini, Gazz..Chim.Ital., 1965, 95, 3.

(b) J.M. Davidson, Chem. and Ind., 1964, 2021.

(c) S.J. Lippard and K.M. Melmed, J.Am.Chem.Soc., 1967, 89, 3929.

(d) S.J. Lippard and K.M. Melmed, Inorg.Chem., 1967, 6, 2223.

(e) M. Grace, H. Beall and C.H. Bushweller, Chem.Commun., 1970, 701.

161 (a) E.L. Muetterties and C.W. Alegranti, J.Am.Chem.Soc., 1970, 92, 4114.

(b) H. Beall, C.H. Bushweller and M. Grace, Inorg.Nucl.Chem. Lett., 1971, 7, 641.

(c) H. Beall, C.H. Bushweller, W.J. Dewkett and M. Grace, J.Am.Chem.Soc., 1970, 92, 1384.

162 (a) T.E. Paxson, M.F. Hawthorne, L.D. Brown and W.N. Lipscomb, Inorg.Chem., 1974, 13, 2772.

(b) J.T. Gill and S.J. Lippard, Inorg.Chem., 1975, 14, 751.

(c) G.G. Outterson, Jr., V.T. Brice and S.G. Shore,Inorg.Chem., 1976, 15, 1456.

163 (a) F.K. Klanberg, E.I. dupont de Nemours, U.S. Pat. 3,450,733, June 17, 1969.

(b) F.K. Klanberg, E.I. du pont de Nemours, U.S. Pat. Re. 27,465, Aug. 22, 1972.

164 (a) N.N. Greenwood and I.M. Ward, Chem.Soc.Revs., 1974, 3, 231.

(b) N.N. Greenwood, Pure Appl.Chem., 1977, 49, 791.

165 S.J. Lippard and P.S. Welker, Inorg.Chem., 1972, 11, 6.

166 A. Marker and M.J. Gunter, J.Magn.Reson., 1982, 47, 118.

167 D.A.T. Young, R.J. Wiersma and M.F. Hawthorne, J.An. Chem.Soc., 1971, 93, 5687.

168 V.T. Brice and S.G. Shore, J.Chem.Soc.Chem.Commun., 1970, 1312.

169 V.T. Brice and S.G. Shore, Inorg.Chem. 1973, 12, 309.

170 N.N. Greenwood, J.A. Howard and W.S. McDonald, J.Chem. Soc.Dalton Trans., 1977, 37.

171 G. Monnier, Ann.Chim., (Paris), 1957, 12, 309.

172 P.H. Bird and M.G.H. Wallbridge, Chem.Commun., 1968,687.

173 W.H. Knoth and E.L. Muetterties, J.Inorg.Nucl.Chem., 1961, 20, 66.

174 S.J. Andrews and A.J. Welch, submitted to Acta Crystallogr., Section C, 1984.

175 R.H. Cragg, M.S. Fortuin and N.N. Greenwood, J.Chem. Soc. (A)., 1970, 1817.

176 D.E. Hyatt, F.R. Scholer and L.J. Todd, Inorg.Chem., 1967, 6, 630.

177 D.F. Shriver, "The Manipulation of Air-sensitive Compounds", McGraw-Hill, New York, 1969.

178 A.P.Schmitt and R.L. Middaugh, Inorg.Chem.,1974, 13, 163.

179 R.L. Middaugh and R.J. Wiersma, Inorg.Chem., 1971, 10, 423.